N2

PROBABILITY AND CONSEQUENCES OF THE NEXT ALPINE FAULT EARTHQUAKE

GEOTECH CONSULTING LTD

EQC

Frontispiece: The Alpine Fault shear zone at Gaunt Creek showing pale blue and green fault gouge and cataclasite sheared over young fan gravels

Cover Photo: Satellite photo of the central and north section of the Alpine Fault from the Karangarua River in the south to the Robinson River in the north. Note the very obvious fault trace forming the western boundary to the Southern Alps (photo courtesy of Landcare Research (NZ) Ltd).

THE PROBABILITY AND CONSEQUENCES OF THE NEXT ALPINE FAULT EARTHQUAKE

Research undertaken by:

Mark D. Yetton

Geotech Consulting Ltd

with

Andrew Wells

Nick J. Traylen

March 1998

2nd Printing July 1998

Funded in part by EQC and NZNSEE

EQC Research Report 95/193

(Refer to Acknowledgments section for the numerous local authorities and infrastructure providers who also supported this project)

Technical Abstract

The probability and consequences of the next Alpine Fault earthquake

Yetton, M.D; Wells, A.; Traylen, N.J.

EQC research project 95/193, March 1998.

We have carried out paleoseismic investigation of the central and northern sections of the Alpine Fault. Trenching of the fault at five locations between Hokitika and the Ahaura River indicates the last rupture south of the Haupiri River occurred after 1660 AD and probably between 1700 and 1750 AD. An earlier event in the central section at around 1600 AD is the most recent event at the more northern locations. An updated record of landslide and aggradation terrace ages is consistent with two earthquakes in the last 500 years but does not significantly refine the date estimates.

Analysis of forest age in Westland from the Paringa River to Springs Junction reveals two periods of synchronous regional forest disturbance and re-establishment at 1625 ± 15 AD and 1715 ± 15 AD which we infer was the result of the two most recent earthquakes. Analysis of tree rings in trees which have survived these earthquakes allow estimates of event timing to be narrowed to 1620 ± 10 AD for the penultimate event. The most recent event occurred in 1717 AD and appears to have been a synchronous rupture from Milford Sound to the Haupiri River, a distance of approximately 375 kilometres.

The paleoseismic history can be used in conjunction with typical recurrence data from other plate boundary faults to predict the probability of the next earthquake using the method of Nishenko & Buland (1987). This indicates a probability over the next fifty years of 65 ± 15 % increasing to 85 ± 10 % over the next 100 years.

Based on the previous events the next rupture is likely to produce a earthquake of Magnitude 8 ± 0.25 with an epicentral area displaced slightly east of the fault trace. Very strong shaking will occur close to the epicentral area and for most locations the next Alpine Fault earthquake will be larger than any previous earthquake in the last 100 years. Landslides and liquefaction are likely to cause the greatest immediate impact but longer term the increased sediment loads will cause strong aggradation in major rivers with increased channel avulsion and flooding.

PROBABILITY AND CONSEQUENCES OF THE NEXT ALPINE FAULT EARTHQUAKE

Executive Summary

This three year project has been funded by the Earthquake Commission, the New Zealand National Society of Earthquake Engineering, and numerous local authority and infrastructure providers. It evaluates the probability and consequences of a future earthquake on the Alpine Fault in the central South Island. The Alpine Fault is the largest active fault in New Zealand and extends over 650 kilometres from Milford Sound to Blenheim. The Southern Alps are a consequence of uplift along the fault, but by far the greatest component of fault movement is horizontal, with an estimated total offset of matching strata of around 470 kilometres. The evidence suggests the offset is episodic and each movement of several metres is accompanied by a large earthquake.

The most active part of the fault is the central section which forms the western boundary of the Southern Alps from Haast to the Taramakau River at Inchbonnie. Further north the fault becomes progressively less active as movement is transferred to numerous branch faults within Marlborough. This project has focussed on the seismic hazard associated with the central and north section.

To evaluate the probability of a future earthquake the history of past earthquakes must first be established. This has been done by a combination of four methods, many of which have been applied to the Alpine Fault for the first time. The first and most direct method is the excavation of trenches and pits across the most recent area of fault rupture. By defining and dating older sheared strata, and overlying younger post earthquake sediments, the timing of past fault ruptures and associated earthquakes can be estimated. Dating requires the presence of organic material to allow the use of ^{14}C radiocarbon methods but fortunately organic material is relatively common in the forested areas of Westland. The resolution possible with radiocarbon dating is limited but the timing of the last earthquakes can be bracketed within broad date bands.

Previous earthquakes in rugged forested terrain in New Zealand and overseas have demonstrated the profound effects of earthquakes on forests in the epicentral area. Earthquakes can damage forest by triggering landslides on sloping ground, causing

liquefaction of alluvial areas, and by shaking the trees until some fall. Much of the dead vegetation is either buried in the landslide debris or enters the river systems as these aggrade in response to the earthquake debris. Radiocarbon dates from numerous landslides and aggradation terraces in Westland match the trench date ranges of the past earthquakes but do not significantly improve the estimates of timing.

Following a large earthquake new forest will simultaneously re-establish in the clear areas of the landslide scars and along uplifted flood plains leaving a potential record of the timing of the disturbance in the age structure of the forest. Forest age can be estimated by carrying out ring counts on large numbers of living trees, a more precise dating method than radiocarbon dating, and by combining the data it is possible to define narrow modes of forest age coinciding with each of the earthquake date ranges.

Some trees also survive the earthquake but still suffer root damage, broken branches and tilting. This is often recorded in their growth rings which potentially provide a very accurate way to estimate the precise timing of earthquake disturbance.

All four of these methods have been applied to the Alpine Fault between the Paringa River (south of Mount Cook) and the Rahu Saddle near Reefton. They produce a consistent record from which we infer two recent earthquakes on the Alpine Fault in the last 500 years. Figure A summarises the data for the two most recent earthquakes.

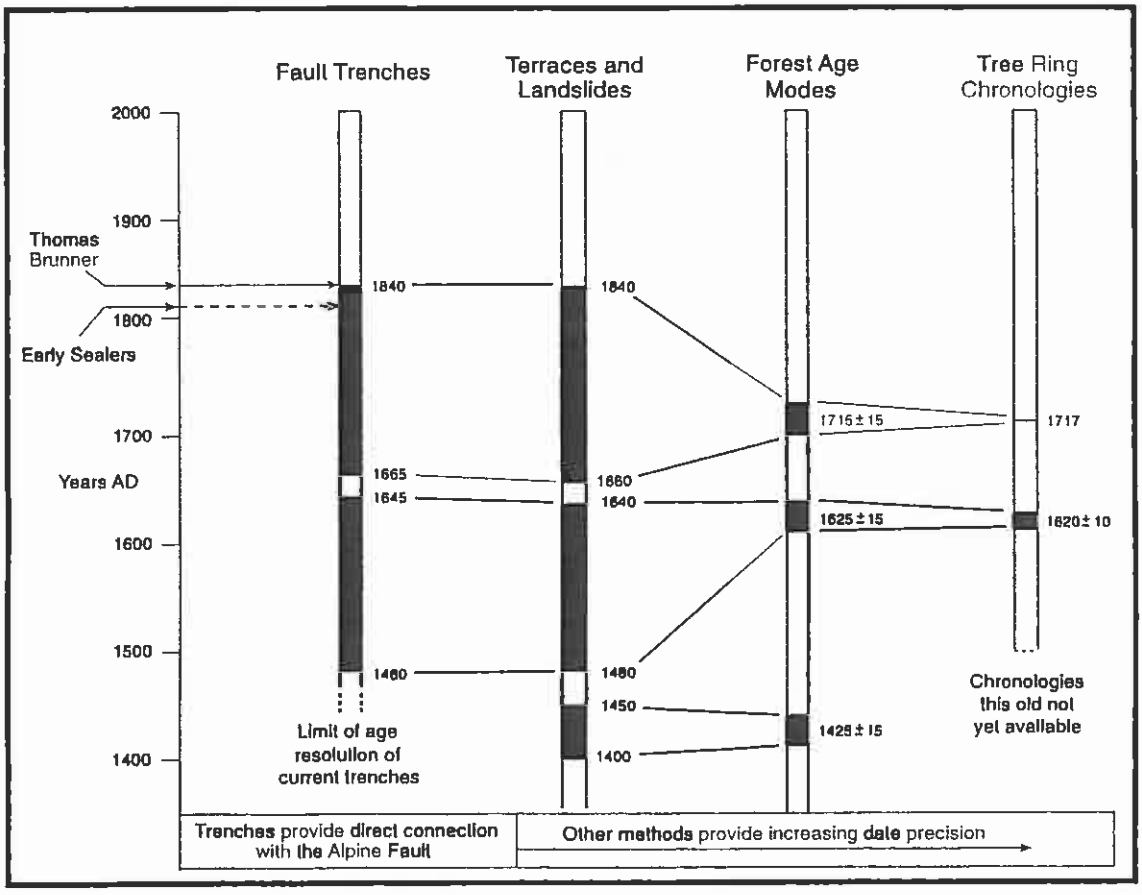

Figure A: Summary of the four methods used to establish the timing and extent of the last two Alpine Fault earthquakes.

The most recent event appears to have taken place in 1717 AD and the surface fault rupture extended in length from Milford Sound to the Haupiri River, a distance of at least 375 kilometres. Approximately 100 years earlier, at around 1620 AD, another earthquake occurred in the north section of the fault and extended at least as far south as the Paringa River. Prior to this, another earthquake at around 1450 AD is suggested by the data, but this has not yet been recognised in trenches.

The implied pattern of earthquake recurrence is not regular but averages around 200 years and varies from 100 years to at least 280 years, which is the lapsed time since the last earthquake. Probability estimates can be made using the record of Alpine Fault earthquake recurrence and a combined analysis of earthquake timing on other plate boundary faults around the world. Other faults also exhibit a wide range in recurrence behaviour, but for the Alpine Fault the probability estimates of the next earthquake are consistently high, with a probability of 65 ± 15 % over the next 50 years increasing to 85 ± 10 % over the next 100 years (refer Table A)

Years Hence from 1998	**Probability of an earthquake event (%)**	
	Average	**Range**
5	10	6-14
15	27	12-26
20	35	20-45
30	45	30-60
40	55	40-70
50	65	50-75
70	75	60-90
100	85	75-95

Table A: Probability estimates for the next Alpine Fault earthquake on the central section of the Alpine Fault using an updated version of the method of Nishenko & Buland (1987).

Based on the rupture length we estimate both of the most recent earthquakes were around Magnitude 8 and reconstructions can be made of the most likely pattern of earthquake shaking intensity. Those earthquakes which also rupture the more northern portion of the fault, like the one around 1620 AD, have generally more impact on the main population centres and Figure B shows the estimated shaking pattern.

The next Alpine Fault earthquake is likely to produce very strong shaking in locations close to the Southern Alps. In particular locations such as Arthurs Pass, Otira, Mount Cook and Franz Josef will be seriously affected. Hokitika and Greymouth will also be strongly shaken. Predicted intensities are generally less on the east coast but in virtually all central South Island locations the next Alpine Fault earthquake will be stronger than any other earthquake experienced there in the last 100 years. Figure C summarises the predicted intensities and compares these to other recent earthquakes.

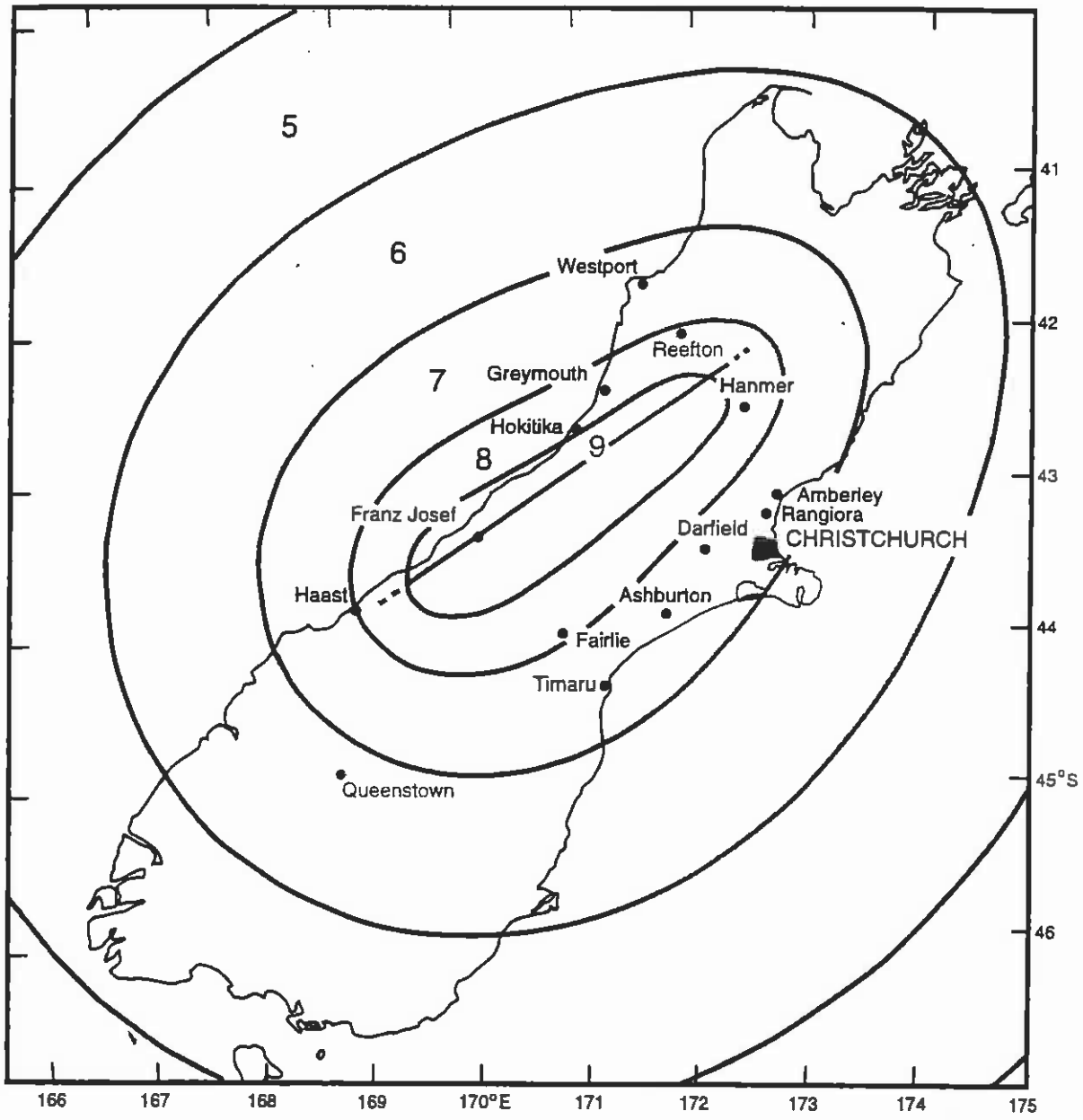

Figure B: Estimated Modified Mercalli Intensity isoseismals (lines defining equal shaking intensity) for the Alpine Fault earthquake around 1620 AD. Modelled using the method of Smith (1995a & 1995b) and reproduced courtesy of Warwick Smith, Seismological Observatory (pers. comm., 1997).

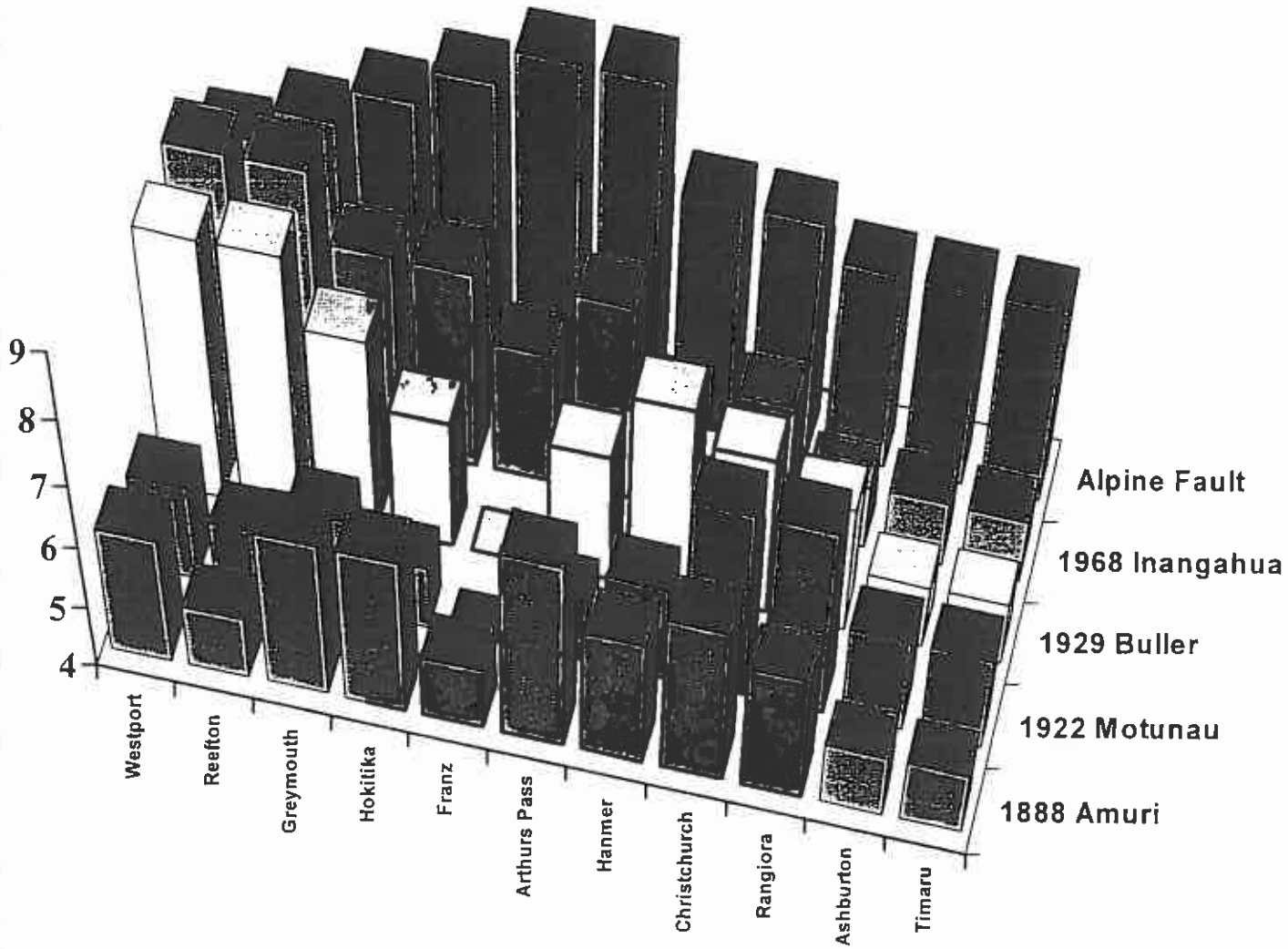

Figure C: A comparison of predicted shaking intensities for the next Alpine Fault earthquake with those experienced in other large earthquakes this century for a range of locations. The vertical scale shown here from 4 - 9 is the Modified Mercalli Intensity and has a highest possible value of 12.

Direct effects of the next earthquake will include landslides and liquefaction. Landslides will be most severe in and around the Southern Alps. It is likely some large rock and debris avalanches will be triggered but the majority of landslides will be relatively shallow failures of weathered soil and rock. Temporary landslide dams are

likely to be created. Landslides will also be triggered in sloping ground in Greymouth and the east coast foothills. They are unlikely to be serious as far away as the Port Hills of Christchurch however the greater density of housing in this area may still result in significant property damage.

In general liquefaction in Christchurch is likely to cause more damage than landslides, because the city it is known to have susceptible soils, and it is well within the likely range of liquefaction. Liquefaction will also be widespread in Westland.

One of the most profound long term impacts will be to the river regimes of catchments which drain the Southern Alps. Increased sediment load from landslide material entering the rivers will result in river aggradation and channel shifting, particularly in the upper catchments. This has potential implications for river control, bridging and hydro-electric generation.

TABLE OF CONTENTS

Executive Summary

Chapter 6 - Estimates of probability

Chapter 7 - Likely characteristics of the next earthquake

Chapter 8 - Likely effects of an Alpine Fault earthquake

Chapter 8 continued

Chapter 9 - Conclusions and Recommendations

Chapter 1

INTRODUCTION

1.1 Project Objectives

This project has the following aims:

- definition of the past record of earthquakes on the central and northern Alpine Fault using a range of paleoseismic indicators.
- estimation of the probability of the next Alpine earthquake
- bracketing of the likely range of magnitude and intensity of the next event
- consideration of the probable consequences

The most time consuming part of the project has been to first establish a reliable paleoseismic record and the report content reflects the large amount of effort this task has required. Predicting the consequences of the next earthquake is one of the most important project outcomes however the limitations in accuracy inherent with any forecasting limits the extent of this section. Despite this the likely consequences have been addressed comprehensively, and at a level of detail compatible with the precision of the input data. We are confident this will fulfil the primary requirements of the end - users who have generously supported this project. For the various territorial authorities and infrastructure providers an additional report has been prepared which summarises the main report and addresses specific relevant issues.

This chapter is an introduction to the Alpine Fault describing it and outlining previous work relevant to the fault's potential as an earthquake source. An outline of the contents of the other chapters is included at the end of this chapter as section 1.4.

1.2 Introduction to the Alpine Fault

1.2.1 Definition and division into sections

The Alpine Fault is part of a transform fault zone through continental crust linking the west dipping subduction zones of the eastern North Island with the east dipping subduction zones of southern Fiordland. Figure 1, from Berryman et al (1992), shows the major plates of the south west Pacific and the plate tectonic setting of the Alpine Fault.

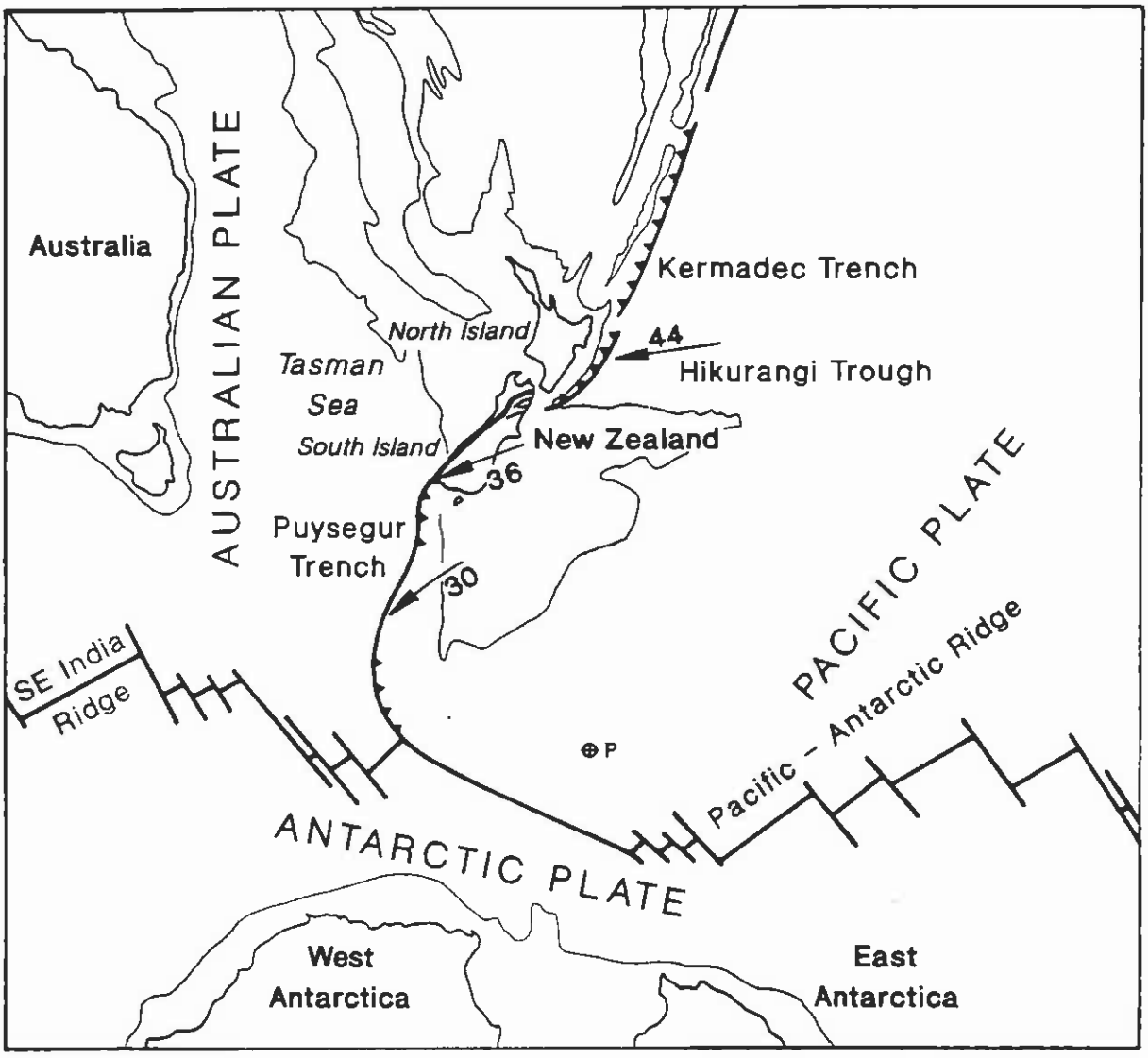

Figure 1.1 - The plate tectonic setting of New Zealand and the Alpine Fault (from Berryman et al, 1992). The orientation and relative velocity of the Pacific plate with respect to the Australian plate is given in mm/yr and the pole of rotation according to De Mets at al (1990) is shown as "P".

The fault is 650 km long and extends from Milford Sound on the Tasman coast to Blenhiem on the Pacific coast. Berryman et al (1992) include in their definition of the Alpine fault the section along the Wairau valley, sometimes referred to as the Wairau Fault, which begins at the Tophouse Saddle near Lake Rotoiti. The fault appears clearly on satellite images of the South Island (refer report cover photo) with an very distinct, apparently straight trace from Milford to the so called "big bend" near Springs Junction. This double bend is complete by the Matakitaki River, from where the fault is again straight until the Tophouse Saddle. The transition to the Wairau valley is marked by a slight change to a more easterly strike.

Berryman et al (1992) divide the fault into the most north - eastern Wairau section, the north Westland section from Tophouse to the Taramakau River, the central Westland section from Taramakau to Haast, and the most southern Westland section extending to Milford Sound (refer Figure 2). These sections have been defined on the basis of geomorphology and structural style. The authors propose these sections may also be fault rupture segments but note the data available at that time to make this inference was very limited.

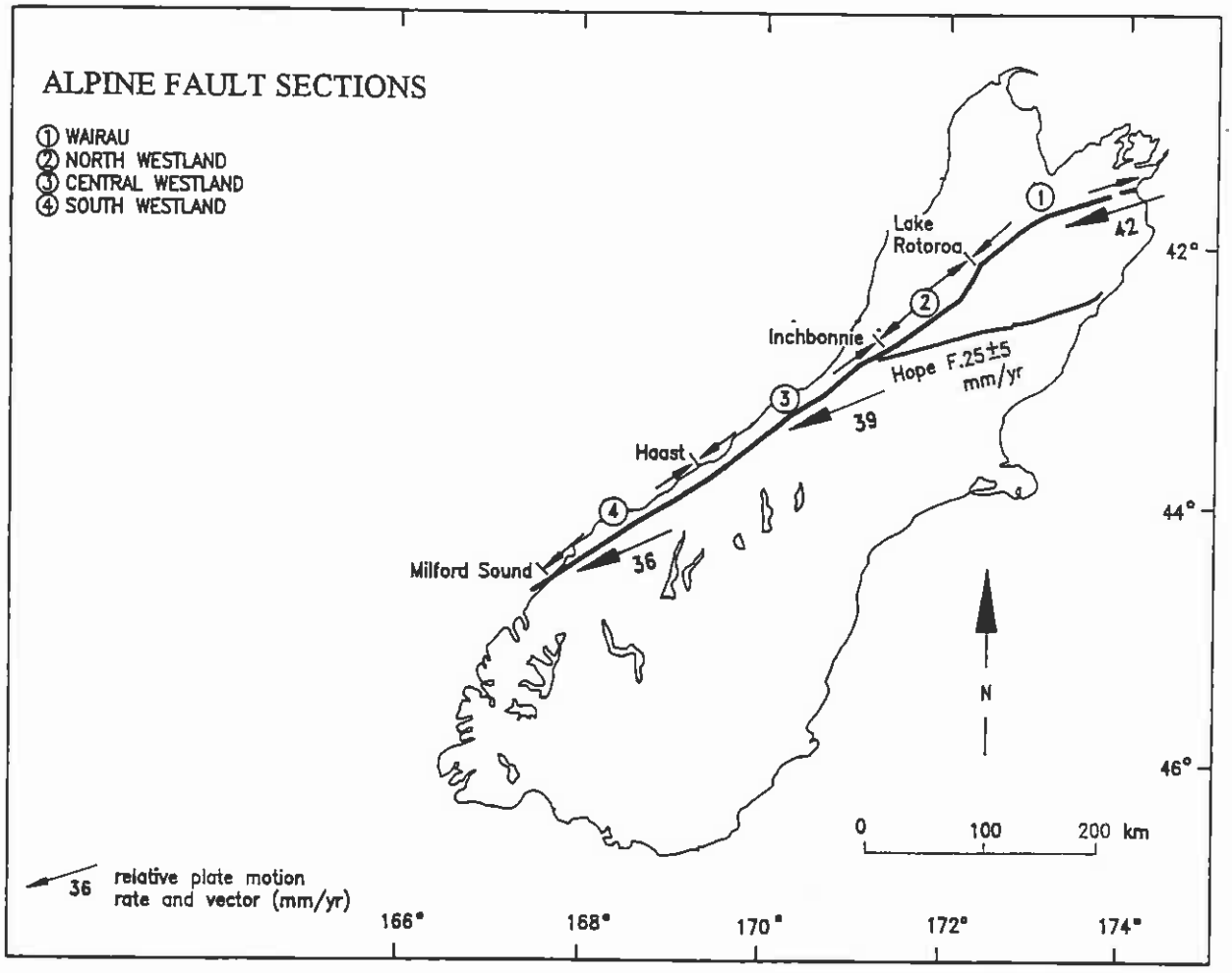

Figure 1.2 - Division of the Alpine Fault into four sections after Berryman et al (1992) but these sections are not necessarily fault rupture boundaries. Figure adapted from Berryman et al (1992).

Bull (1996) inferred segment boundaries occur at the Taramakau River, where the Hope Fault splays off the Alpine Fault, and again at the beginning of the "big bend" of the Alpine Fault. He proposed the names "Cook segment" for the straight central section, and "Brunner segment" for the much shorter section to Springs Junction. The evidence on which these proposed segment boundaries are inferred is limited to the most obvious structural discontinuities ie the splaying at the Hope Fault junction and the curve in strike at the big bend.

This report adopts the geographic division into sections as outlined by Berryman et al (1992) in preference to inferred rupture segments. One of the conclusions of this project is that the last Alpine Fault earthquake rupture extended past the Taramakau River, and the Hope Fault splay, and that the rupture length has probably varied between each event (refer Chapter 5).

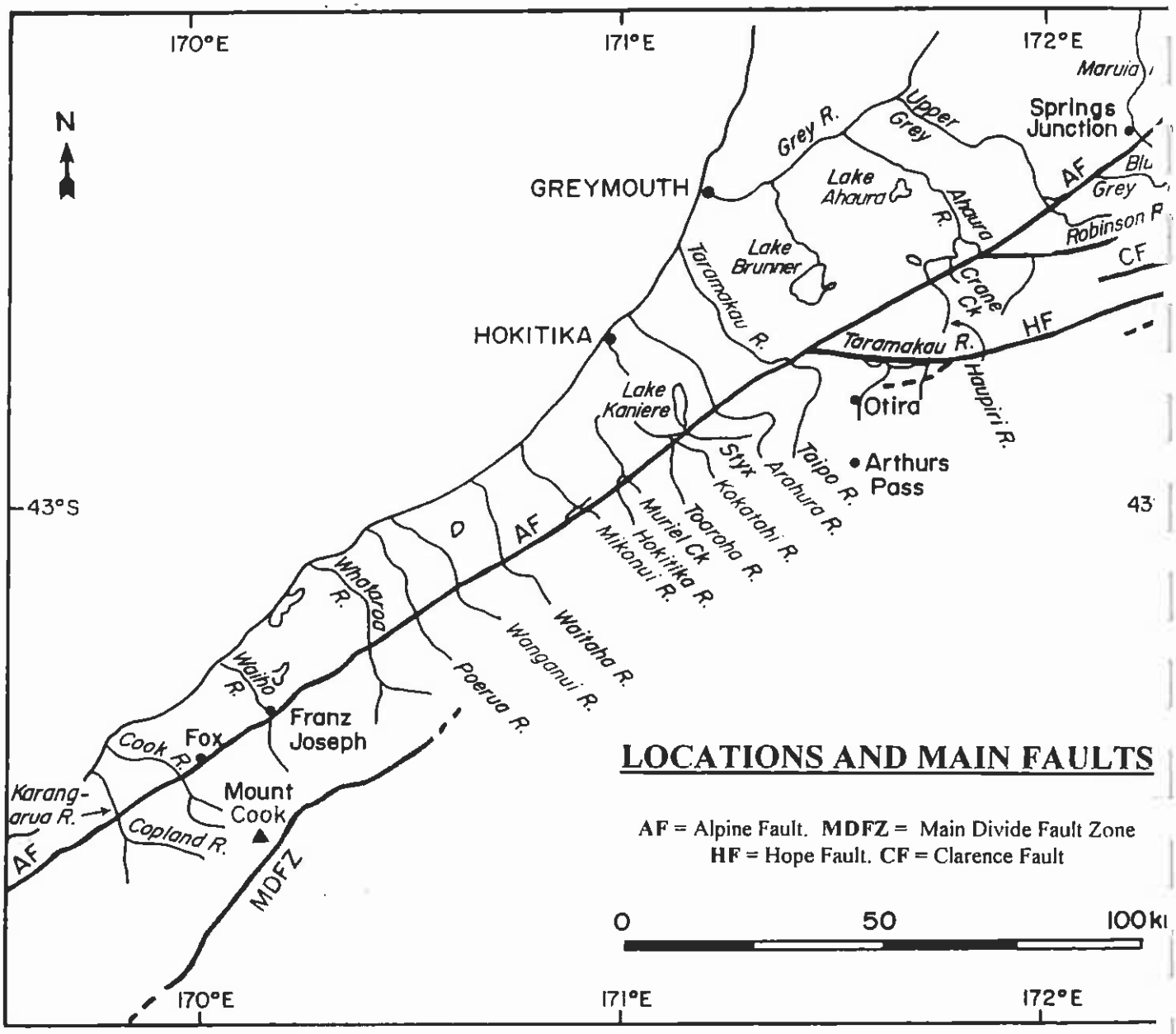

Figure 1.3 - Location diagram of Westland showing the main faults, rivers and locations referred to in the report.

The work outlined in this report has been carried out mainly in the northern and north central section of the Alpine Fault, extending from the Hokitika River to the Ahaura River. However some specific investigations, generally to follow up on earlier work by others, has extended to sites as far south as the Karangarua River and further north up to Springs Junction. Figure 1.3 shows the area in which the work has taken place and the main rivers which have provided most of the information.

1.2.2 Plate vectors, slip rates and the sense of fault movement

De Mets et al (1990) provides the most recent estimate of current plate pole position and the orientation and relative velocity of the Pacific plate (Figure 1.1). They estimate rates ranging from 36 - 39 mm/yr at an azimuth of 071 °. For most of the central section this can be resolved into components of 37 mm/yr parallel to average strike of the Alpine Fault and 11 mm/yr perpendicular to it (Norris & Cooper, 1995).

The dominantly fault parallel plate movement, in combination with a significant compression perpendicular to the fault, results in a oblique transpressive sense of fault movement. A combination of dextral strike slip movement and oblique thrusting develops near the surface where the relative amounts of each vary slightly with subtle changes in fault strike. For example Norris & Cooper (1995) show segmentation of the fault on the scale of several kilometres, into dominantly strike slip segments with a more northerly strike, and relatively east west aligned oblique thrust segments. They suggest this is a near surface phenomena resulting from perturbations in the stress field in the upper 1 - 4 km created by valley incision (Figure 1.4).

Horizontal Rates

The rate of horizontal slip parallel to the Alpine Fault is not well constrained. This reflects the absence of suitable offset reference points which can still be recognised on both sides of the fault. Either deposition on the relatively downthrown western side, or erosion on the uplifted eastern side, tends to remove one or other part of the matching offset. Plate tectonics implies the rate cannot be much more than 35 mm/yr at the most active central section and this maximum assumes all the horizontal plate motion is focussed on the Alpine Fault. This appears a reasonable assumption but the rugged area 5 - 30 km east of the fault may contain other active faults of which we are currently unaware.

There are a number of minimum rate estimates which suggest at least c. 25 mm/yr in the central section (for example Berryman et al, 1992; Cooper & Norris, 1995). More recently Norris & Cooper have derived a slip rate over the last 20,000 years of 22 - 30 mm/yr at Waikukupa near Franz Josef (Norris & Cooper, 1997). Combined with the earlier minimums the errors reduce to 25 - 30 mm/yr.

The other way to estimate the slip rate for the central section of the fault is sum the average slip on the Hope Fault with estimates of the slip on the north Alpine Fault. Estimates of total slip for the Hope Fault zone are c. 25 ± 10 mm/yr (Cowan, 1989; Cowan, 1990; Van Dissen & Yeats, 1991) and all of this appears to transfer to the Alpine Fault between the Taramakau River and the Toaroha River.

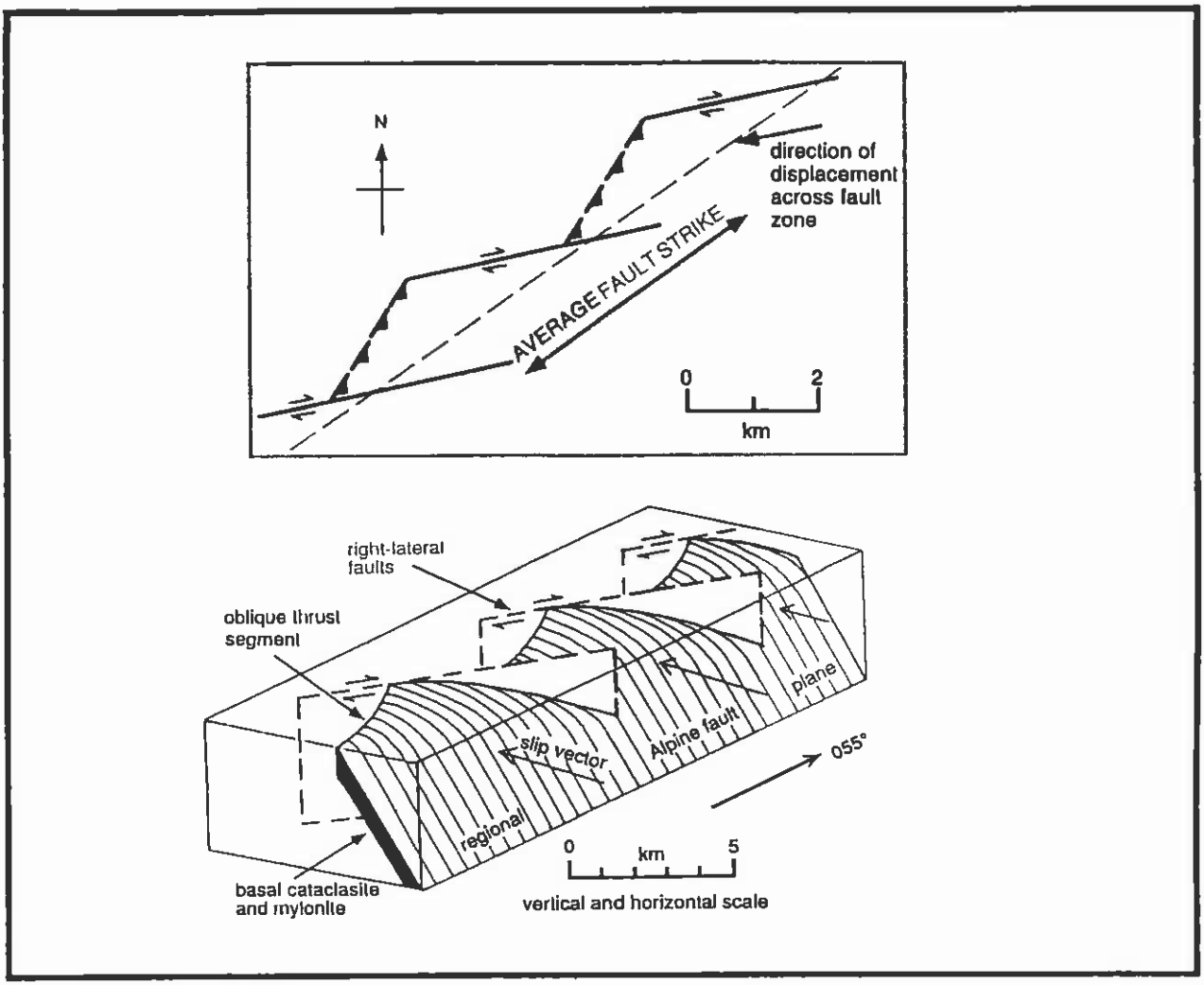

Figure 1.4 - Conceptual view of near surface segmentation of the Alpine Fault into alternating right lateral strike slip fault traces and oblique thrust traces typical of the fault near Franz Josef (after Norris & Cooper, 1995).

The north Alpine Fault average slip is estimated by Berryman et al 1992 to be 10 ± 2 mm/yr at Inchbonnie which is at the extreme southern end of this section. We have obtained an average slip rate of 6 ± 2.5 mm/yr for this section of fault at the Haupiri River, 25 km further north, but where more Alpine Fault movement may have transferred to parts of the Marlborough fault system. The sum of these is 35 ± 12 mm/yr and 31 ± 12.5 mm/yr respectively. The large errors associated with the Hope Fault estimates limit the value of this approach, but in light of the plate tectonic upper limit of 37 mm, this suggests the Hope Fault estimates may be on the high side but the upper limit of 30 mm/yr for the Alpine Fault is the most likely end of the range.

The field evidence collected over the last few years indicating that the Alpine Fault accounts for 75 - 100 % of the plate motion rate refutes a line of reasoning first proposed by Walcott (1979). Walcott suggested that the Alpine Fault accommodates

less than one third of the plate motion, the remainder being taken up by aseismic permanent strain in the Southern Alps. Walcott discounted regular earthquakes on the Alpine Fault on the basis that the observed fault offsets of young surfaces were not high enough. At that time only 6 - 13 mm /yr of horizontal fault parallel slip could be demonstrated (Berryman, 1979).

Despite the progressive recognition by field workers that the slip rate is actually much higher (see for example the discussion in Berryman et al, 1992) the notion that insufficient strain accumulates at the fault to produce large earthquakes persists in the thinking of some geologists.

Vertical Rates

The Southern Alps are the consequence of the compressive component of plate motion operating across the fault and there have been a number of models of uplift proposed (see for example Walcott, 1979; Wellman, 1979; Norris et al, 1990). The rate of uplift of the Southern Alps has been estimated by Walcott (1979) and Wellman (1979) at 22 mm/yr and 17 mm/yr respectively although these estimates were based on the early estimates of a more northern plate pole of rotation. Uplift along the Alpine Fault plays a major part in Southern Alps uplift rate, and probably the largest part, but estimates of vertical uplift rates at the fault itself have been consistently less than 10 mm/yr (for example Suggate, 1968; Bull & Cooper, 1986; Berryman et al, 1992; Simpson et al, 1994; Yetton & Nobes, in press), and typically around 6 - 7 mm/yr for the central section. Our work in the north section of the fault at Haupiri indicates vertical uplift of only 2.5 ± 0.5 mm/yr which implies a rapid drop in relative uplift north of the Hope Fault splay

1.2.3 Geodetic and GPS Surveys

Resurveys of the 100 year old geodetic survey networks (Walcott, 1978; Walcott, 1984; Wood & Blick, 1986) indicate elastic strain is accumulating over a broad zone in the rocks on each side of the Alpine Fault at rates consistent with the plate tectonic predictions. It is most likely this accumulated elastic strain represents potential energy in storage for the next Alpine Fault earthquake. Berryman et al, 1992 highlight the surprising consistency of the magnitude of the strain rate across the fault from south Westland to the Wairau section, despite the implied reduction in slip rate to the north. They also note that these rates alone, in conjunction with the definite absence of Alpine Fault earthquakes since at least 1840, suggests the observed strains can only continue to accumulate for one or two hundred more years before rock strength is exceeded and an earthquake occurs.

More recently the first GPS resurveys of the original triangulation network have been carried out between Christchurch and Hokitika utilising the benefits of the modern navigation satellite network (Pearson et al, in prep.). The observed strain rates over a period from 1978 to 1992 are once again consistent with the De Mets et al, 1990 plate velocities, and indicate about two thirds of the plate motion is being taken up as elastic strain in the vicinity of the Alpine Fault. Further strain is accumulating east of the Alpine Fault in the Porters Pass - Amberley fault zone (Cowan et al, 1996) but this in

turn may ultimately join the Alpine Fault, possibly in the vicinity of the Whataroa River (Anderson & Webb, 1994).

1.2.4 Historical seismicity

Historic (pre - instrumental) seismicity

There has definitely been no rupture on any section of the Alpine Fault in the 160 year record since 1840. While it is possible an Alpine Fault earthquake may have gone unrecognised between 1800 and 1840, sealers and whalers were regularly working in the region and this is unlikely. Sealers did record a series of strong earthquakes in Dusky Sound, Fiordland, in 1826 - 1827 (McNab,1907). These are generally attributed to events in the offshore Fiordland area and not the Alpine Fault (Norris, pers. comm. 1996).

Enquires through the Ngai Tahu liaison officer with D.O.C in Hokitika indicate no known oral tradition of a large earthquake in the Arahura area near Hokitika, despite the importance of the area for Pounamu gathering. There may have been early tribes in the area from the sixteenth century (eg the Waitaha) but Ngai Tahu became progressively established from the seventeenth to eighteenth century (Belich, 1996).

The absence of an oral tradition of earthquakes does not preclude an event having occurred after Ngai Tahu began using the area, because it possible the impact was minor for the early gathering parties, and a permanent local population may not have established for some time. The oral record may also be incomplete, particularly for events well before 1800 AD. Potton (1987) notes that Brunner's census of 1847 recorded a total of only 99 Maori living north of latitude 44N (Cascade Point, south of Jackson Bay and 50 km south of Haast). Raids by northern tribes a generation earlier had decimated the local inhabitants which may also have wiped out many oral traditions. However, the absence of oral tradition does tend to suggest the last large earthquake did not occur within the 2 - 3 generations immediately prior to the first European contact in the 1840's.

Aseismic Creep

In very rare cases faults can move by aseismic creep. This has so far only been recognised occurring on modern faults in two cases, both of which are in California. The best example is a segment of the San Andreas Fault near Hollister which has deformed a wine cellar built across the trace at between 10 and 20 mm/yr (Eiby, 1989). The other example has been the progressive shearing of drillholes crossing the Buena Vista Fault in Kern County (op. cit.)

Aseismic creep has not been observed for the Alpine Fault, or any New Zealand fault. This is despite the Alpine Fault trace crossing sealed roads in at least 10 locations and the construction of a concrete monitoring wall across the trace at Springs Junction in 1964 (Beanland, 1987). There were early reports in the New Zealand Geological Survey files (Bowen, 1957) of power lines requiring loosening over a 20 year period in the vicinity of the fault trace at Rocky Point, near Inchbonnie.

No deformation of the two adjacent roads each side of this site which cross the fault was recorded. The poles concerned are in the active bed of the Taramakau River and it is also possible gravel movement was causing this. More recent enquires with TransPower, who have inherited the transmission network, indicate no further problems have been noted. However it should always be recognised that in many locations aseismic movement of the fault would not be recognised due to the actively changing landforms and the extensive forest cover.

Instrumental seismicity

The traditional view of recorded seismicity along the Alpine Fault has been of anomalously low levels in relation to the importance of the structure. This led to the term " seismic gap" (for example Adams, 1980) to describe the pattern of shallow seismicity in the central fault region. Recent improvements in the seismograph network indicate more seismicity is occurring than was being recorded in the old network(Eberhart-Phillips, 1995).

Figure 1.5 overleaf shows the recorded seismicity over the three years between 1991 and 1994 for which published data is available. In this time range there were 9 earthquakes per year along the fault in the magnitude 2.5 - 3.6 range. The observed seismicity extends to around 10 km depth and the impression is gained of an east dipping fault plane. While the level of recorded seismicity is still relatively low it is comparable to the Mojave section of the San Andreas Fault which last ruptured in 1857 and is estimated to have had at least 10 large earthquakes in the last 1400 years (Sieh et al, 1989).

1.2.5 Evidence that Alpine Fault ruptures are accompanied by earthquakes

While it is universally accepted that earthquakes are produced by fault rupture there has persisted a view, based mainly on the absence of historic earthquakes and the early views of Walcott (1979) regards aseismic permanent strain, that the Alpine Fault moves in some way which does not cause earthquakes. We have outlined above the historic evidence against aseismic fault creep, which is the only known alternative to seismic slip. However there are also two strong additional arguments indicating that when movement does occur it is associated with earthquakes.

The first is the abundance of pseudotachylyte, a dark glassy material produced by friction melt during seismic slip. Wallace (1976) first recorded this in the Alpine Fault zone and later Sibson et al (1979) described the distribution in more detail, noting it as " the product of seismic slip on discrete planes". It is particularly abundant in the fault rocks of the central section of the fault.

The second argument for past seismic events is the presence of liquefaction induced features in the trenches which cross the fault. This has been recognised for the first time in a trench in this study (the Kokatahi 2 trench, refer section 2.2.2) but Wright (1994) notes probably liquefaction induced folding and clastic dykes in tilted terrace gravels 500m from the fault at this same location. Liquefaction is caused by an abrupt increase in pore water pressure associated with shear stress loading at a rate which

does not allow drainage. As such it is a very good indicator of earthquake, as opposed to slow aseismic deformation during which drainage is possible.

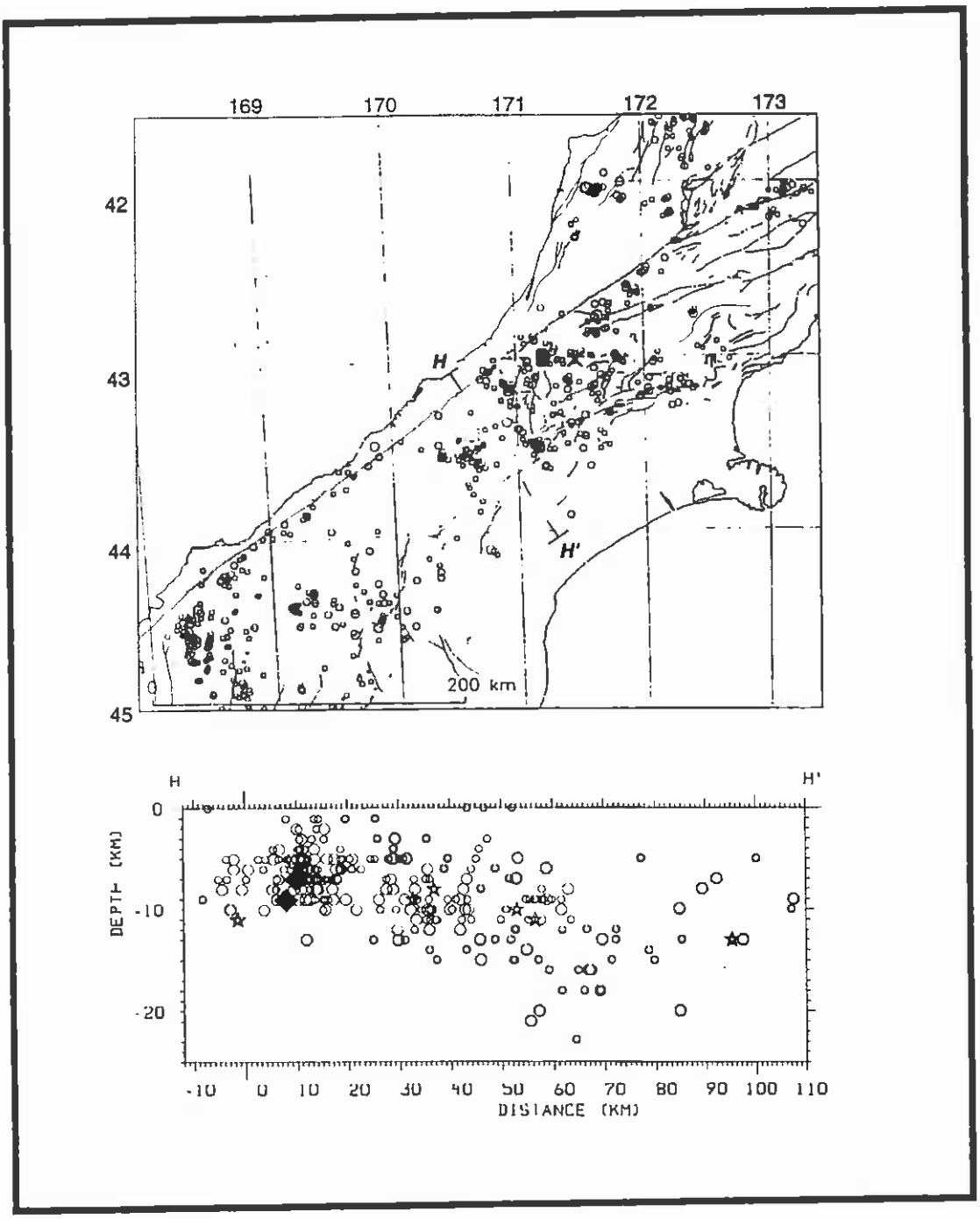

Figure 1.5 - Three years of seismicity with a range in magnitude from M = 2 to M >5 for the period March 22 1991 to April 30 1994 for events with depths less than 40 km. Note the occurrence of small earthquakes along the fault. The crossection H - H' shows the depths of events of various magnitudes (circles = M 2-3.9; stars = M 4-4.9; filled diamonds = M $\geq$ 5. The Alpine Fault is at zero on this section and the impression is gained of a fault plane dipping east at around 45 degrees. Figure from Eberhart - Phillips (1995).

Many of the trenches presented later in Chapter 2 show intense deformation (folding), and truncation of the sedimentary units. While this is strongly suggestive of sudden rupture, as opposed to slow progressive deformation, this is not as definitive as the presence of liquefaction structures.

1.2.6 Total fault offset

The Alpine Fault was recognised as one of the major strike slip faults in the world when Wellman noted the lateral shift of the Permian rocks by the fault from Fiordland up to North West Nelson (Wellman, 1955). This is an apparent offset along the fault of approximately 460 - 480 km. While there has been some disagreement over this estimate (see for example Suggate, 1963), and others have proposed alternative oblique slip models resulting in some apparent offset rather than a pure strike slip separation (Campbell & Rose, 1996), most geologists accept at least 350 km of strike slip movement has occurred along the fault.

Wesnousky (1989,1990) introduced the concept of cumulative geologic offset as the major control on the evolution of strike slip faults. In summary he demonstrates from California and Turkish examples that seismological evolution takes place as the fault plane is smoothed by successive offsets (Table 1.1).

Fault and location. (California, USA unless noted otherwise).	**Cumulative offset** (Kilometres)	**Total fault length** (Kilometres)
Newport - Inglewood	1 -10	60
Whittier - Elsinore	10 - 40	330
San Jacinto	25	230
Garlock	64	240
Calaveras	24	220
San Andreas	approx. 250	1000
N. Anatolia Turkey	25 - 45	900
Porters Pass Fault Zone, New Zealand *	< 2	100
Hope Fault, New Zealand *	20	200
Alpine Fault, New Zealand	> 350, probably 460 - 480	650

Table 1.1: A comparison of cumulative offset for major strike slip faults in California, Turkey and New Zealand. (data from Wesnousky,1989; * denotes data from Cowan & Nichols ,1996).

As a result of this structural and seismic evolution the size of major earthquakes increases but the relative frequency of intervening smaller earthquakes decreases. It is important to note that the Alpine Fault has the greatest cumulative offset of the faults for which this data is known. We suggest the extremely large cumulative offset of the Alpine Fault is the explanation of the relatively low instrumental seismicity along it.

This also explains why the Alpine Fault seismicity most closely resembles sections of the San Andreas fault, the fault with the next largest known offset (Eberhart - Phillips, 1995). This also implies that when Alpine Fault earthquakes do occur they will have longer rupture lengths than might be expected for other faults and that segmentation may play a relatively minor role in arresting rupture propagation.

1.2.7 Deeper crustal structure

Current views of crustal structure in the South Island (for example Norris et al, 1990) view the Alpine Fault as the westward boundary of a zone of distributed deformation formed by the oblique convergence of continental crust of the Pacific and Australian plates. A critical wedge model has been proposed which views the Alpine Fault as dipping east under the Southern Alps and Canterbury, accommodating delamination of the upper 20 - 25 km of the Pacific plate on a ductile detachment. Figure 1.6 shows the model as proposed by Norris et al, 1990.

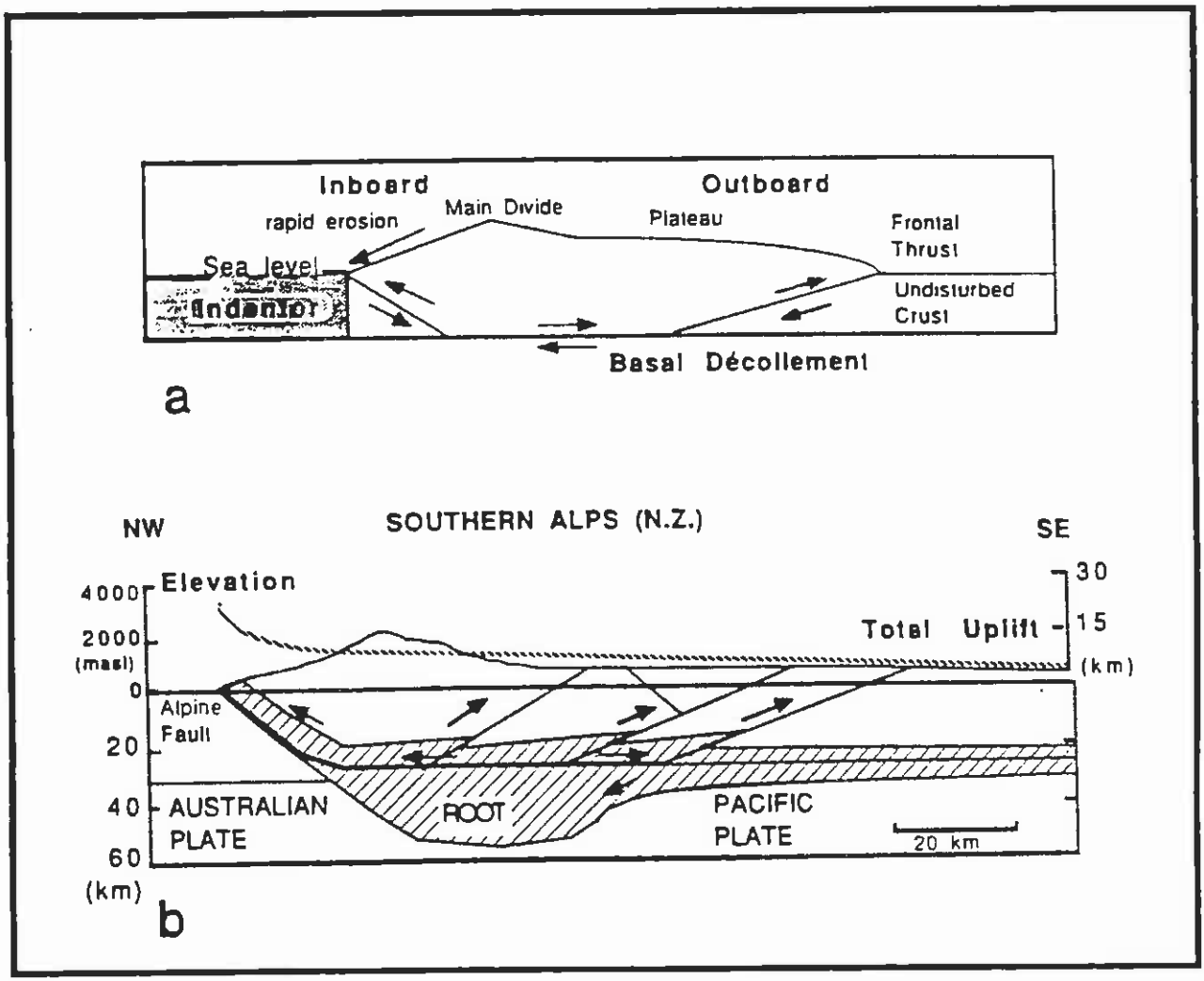

Figure 1.6 - Inferred deeper crustal structure of the central South Island after Norris et al, 1990. (a) shows a schematic representation of a two sided deforming orogen area based on critical wedge mechanics with erosional constraints. (B) applies this model to the Southern Alps with a lower crustal detachment

Support for this model comes from recorded microseismicity under the Southern Alps (for example Reyners, 1987) and the existence of gravity anomalies (Allis, 1986; Woodward, 1979).

More recently two comprehensive geophysical transects have been completed across the central South Island near Mt Cook and the Rangitata River. At present the data gathered is still being analysed but initial indications confirm a crustal thickening of the Pacific plate across the Alpine Fault of approximately 20 km (Stern et al, 1997; Wilson & Eberhart-Phillips, 1997) and a probable dip for the Alpine Fault of around 45 degrees. A dip for the fault of around 45 degrees on geological grounds has already been proposed by Sibson et al, 1979 and Norris et al, 1990.

The implications of this dip for future earthquakes generated by the Alpine Fault includes a likely offset in epicentre eastward and away from the fault trace by what ever depth of focus the event may have. In addition the surface area of the fault above the brittle - ductile transition involved in the release of earthquake energy is increased by the dip, thereby increasing the seismic moment and corresponding earthquake magnitude.

Most estimates would put the likely depth of focus for crustal earthquakes in the South Island at around 10 - 12 km (Smith pers. comm., 1997) but this is not well defined. One line of reasoning is that with thicker crust on the Pacific plate the seismogenic depth may be more than this. This is supported to some extent by Reyners (1987) who describes microearthquake activity to depths around 70 km under the crest of the Southern Alps (about 30 km east of the Alpine Fault trace) which is presumed to be in the upper mantle. More recently Eberhart-Phillips (1995) recorded microseismicity across the Alpine Fault with an improved instrument array which ranged in depth from 10 km to more than 20 km at distances up to 60 km from the fault (refer again Figure 1.5).

The alternative view to suggestions that the focal depth for Alpine Fault earthquakes is likely to exceed 10 km relates to the high heat flow associated with rapid uplift along the fault (see for example Allis et al, 1979; Koons, 1987; Holm et al. 1989). This raises the brittle/ductile transition to depths as shallow as 6 - 8 km, and thereby reducing the area of crust which is available to shear coseismically.

At this stage it is not possible to resolve the question of the likely focus depth for large Alpine Fault earthquakes and a focal depth of around 10 km is adopted in the later modelling in Chapter 7 as a reasonable compromise between the conflicting views.

1.3 Previous paleoseismic investigations

Paleoseismic investigation of the central and north Alpine Fault has been relatively neglected to date considering the fundamental importance of the fault to the seismology and geological structure in the South Island. This reflects the poor exposure of the fault, the very rapid modern processes which tend to mask it, and the difficulty of working in such heavily forested terrain. We discuss briefly here the work

which has been done by others and compare their conclusions with the results of this project in later section 5.3.

Adams (1980)

The earliest research on paleoseismology of the Alpine Fault was the work of Adams (1980). He gathers together ten ^{14}C dates from landslides and aggradation terraces in central and south Westland and uses dates which coincide as indirect evidence of the timing of large earthquakes on the Alpine Fault (Figure 1.7).

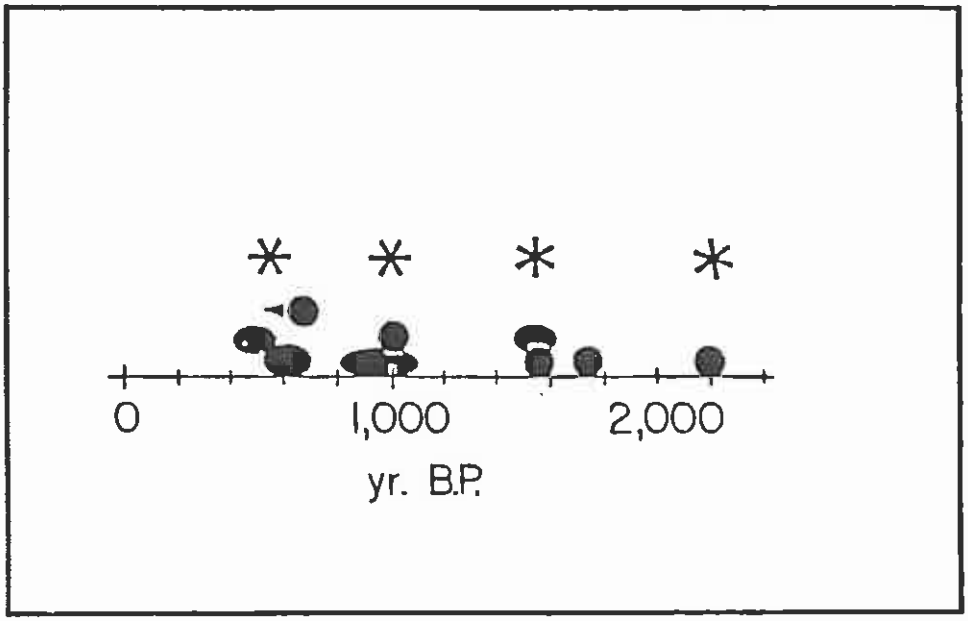

Figure 1.7 - Adams (1980) radiocarbon date distribution from aggradation terraces and landslides in Westland over the last approximately 2000 years. Note the relatively small number of dates and the inferred earthquakes (*) on the central Alpine Fault at around 500 year intervals with the most recent around 550 years ago (1450 AD).

Two or more dates which coincide are considered by Adams to be sufficient evidence to infer a series of earthquakes at approximately 500 year intervals over the last 2000 years with the most recent event around 550 years ago. However Adams noted that the record may still be incomplete and that future dating may reveal intermediate age earthquakes.

Bull (1996)

The only other work on paleoseismicity in the central Alpine Fault is that of Bull (1996). Bull inferred a quite different pattern of past earthquakes on the Alpine Fault

based on lichenometric dating of rockfalls. These rockfall sites were all well east of the fault, the closest being approximately 18 km away, and the majority more than 25 km. The dating method is based on assumptions regards uniform lichen growth rates on new rock surfaces created during rock falls. Lichens of the genus *Rhizocarpon* subgenus *Rhizocarpous* apparently grow in the Southern Alps at the same uniform growth rate of c. 0.17 mm/yr in the altitude range between 400 and 1600m, independent of substrate, microclimate or aspect.

While the dating technique has been criticised (refer for example McAlpin, 1996; Oelfke and Butler, 1985) Bull is able to demonstrate a correlation with the historical earthquake record for the Hope and Kakapo faults.

He infers regional peaks in lichen size modes of 43 mm, 84 mm and 125 mm are the result of earthquakes on the Alpine Fault at 1748 ± 10 yrs AD, 1489 ± 10 yrs AD and 1226 ± 10 yrs AD respectively. A less distinct size mode at 166 mm also suggests an event around 967 ± 10 yrs AD. The implied recurrence interval is a remarkably constant 261 ± 14 years (Bull, 1996).

Cooper & Norris (1990)

The only other significant paleoseismic investigation of any other part of the Alpine Fault is the work of Cooper & Norris (1990) in south Westland. This involved the ^{14}C dating of material excavated from sag ponds near the fault scarp and estimates of the age of trees which appear to have lost their crowns as a result of earthquake shaking. The tree age estimates are based on circumference as opposed to the more reliable increment corer method which samples actual tree rings.

They conclude that the last large earthquake in the area due to movement of the Alpine Fault occurred in the period between 1650 AD and 1725 AD. An incomplete record suggests a possible earlier event around 2000 years ago (conventional ^{14}C date of 1980 ± 60 yr: Wk 1478). This work of Cooper & Norris (1990) has the important advantage of being a more direct investigation than the previous work in the central area of Adams (1980) and Bull (1996) and represents the most reliable published estimate of previous earthquake timing on any part of the Alpine Fault to date.

Other current work

No other work has been completed on the central and north Alpine Fault to date but Wright (pers. comm. 1997; Wright, 1997) is currently involved in the excavation of sag ponds and analysis of tilted rimu trees along the fault scarp at the Waitaha River (central Westland). His preliminary conclusions are included in Chapter 5. At the time of writing there are also plans to trench the fault at Haast (south Westland) in early 1998 in a joint University of Otago and I.G.N.S. project (Norris, pers. comm. 1997).

1.4 Outline of report framework

This report outlines the conclusions reached by examination of four independent potential paleoseismic indicators in central and northern Westland. These are:

a) Radiocarbon ages obtained from 7 trenches and pits excavated across the fault.

b) Radiocarbon ages of aggradation terraces and mass movement deposits.

c) Forest stand ages which indicate periods of synchronous regional forest disturbance and re-establishment.

d) Synchronous tree ring disturbance in long living tree species which have survived previous Alpine Fault earthquakes.

These four independent indicators are discussed individually in chapters 2 - 4. They reveal a consistent paleoseismic record for the last 750 years, which is summarised in chapter 5, along with the available information on the locations and lengths of rupture in previous events. The paleoseismic record is then used to calculate the probability of the next Alpine fault earthquake in chapter 6. Inferences are made regards the magnitude and shaking intensity of the previous earthquakes in chapter 7, and these are used to bracket the likely seismic characteristics of the next earthquake. In the final chapter 8 the general consequences of the next earthquake are discussed. Chapter 9 outlines the conclusions and general recommendations.

This report is a largely a technical document. The work it outlines forms the basis of more specific considerations of the consequences of the next earthquake which have been prepared as series of less technical supplementary reports for the various local authorities and infrastructure providers. We have still endeavoured to keep the report as simple as possible while demonstrating the rigorous standards of the work undertaken. For those not wishing to read all of the report we recommend reading the summaries at the end of Chapters 2 - 7, then most of Chapter 8 (Consequences) and Chapter 9 (Conclusions and recommendations).

Chapter 2

EVIDENCE FROM TRENCHING THE FAULT

2.1 Trench evidence for a penultimate earthquake around 1600 AD - The Crane Creek event.

2.1.1 Crane Creek

Crane Creek (Figure 1.3) is a small river draining the Mt Rochfort basin in the Haupiri Range (GR K32/098465). It is north of the Hope Fault junction with the Alpine Fault and located in the north Westland section of the Alpine Fault. The only geological investigation of the area was carried out in the late 1940's by the former New Zealand Geological Survey and the conclusions summarised by Munden (1952).

The Alpine Fault crosses Crane Creek approximately 1 km upstream from the Haupiri Road bridge and the creek has formed a bend along the fault strike. Figure 2.1 is a locality map showing the location of the trench site on a high terrace above Crane Creek. Figure 2.2 is a more detailed map of the fault trace at the trench site.

The scarp at this location is 22m high with a 20 - 30 degree slope angle. The scarp slope is covered in a dense forest of mature red beech (*Nothofagus fusca*) and the occasional member of the podocarp family. There is no bare or eroding ground above the trench and a thick forest floor litter covers the entire scarp slope. The trench, which was dug by hand and of limited depth and extent, was located across a small swampy furrow at the base of the scarp marking the most recent rupture at this location.

The trench log is presented in Figure 2.3 with the soil descriptions and interpretation. The stratigraphic relationships are relatively simple in the trench. The scarp has formed in fluvial silty gravels overlying moraine. A shear zone can be defined which contains green - grey silty fault gouge mixed with dense clayey peat. Overlying this is

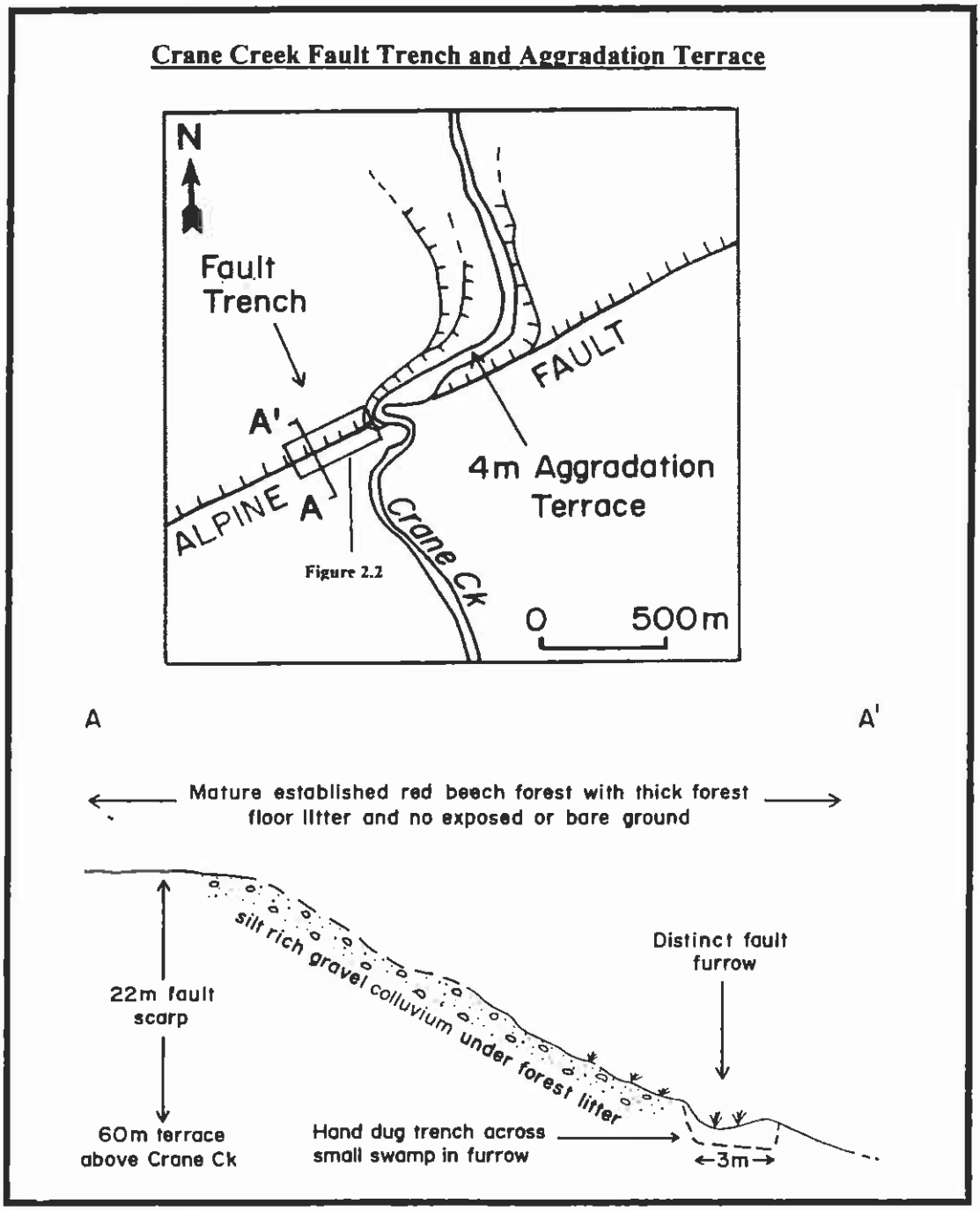

Figure 2.1 - General location of the trench on a 60m terrace at Crane Creek and the 4m aggradation terrace exposed down in the current river channel.

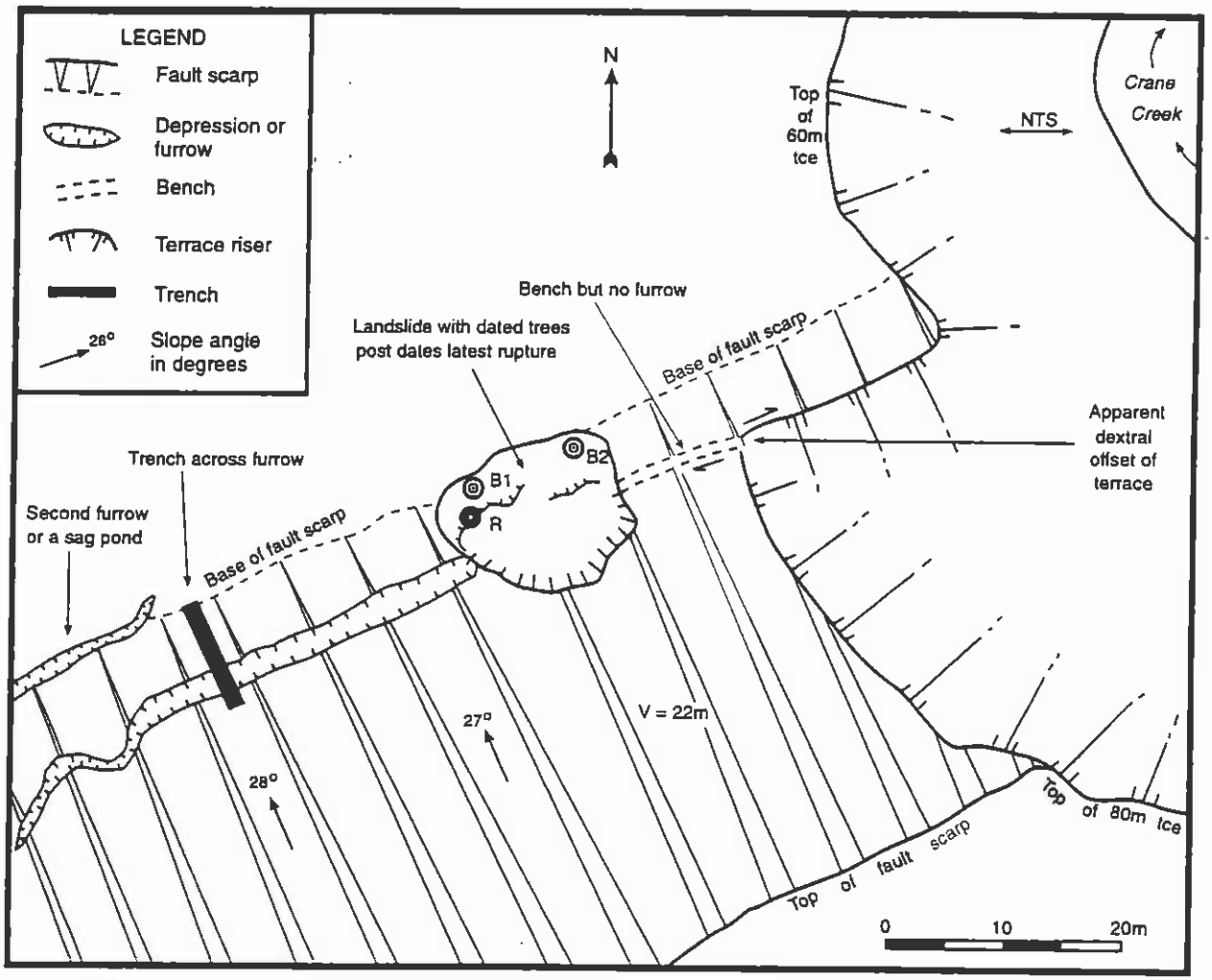

Figure 2.2 - Detailed plan of the fault scarp in the vicinity of the Crane Creek fault trench. The furrow through which the trench has been excavated has been covered over by a landslide that post dates the last rupture. Red beech trees growing on the landslide (B1 and B2) have estimated ages of 236 and 295 years respectively indicating no rupture at this location since approximately 1700 AD. An 540 year old tilted rimu (R) predates the shallow landslide, which may have been earthquake triggered.

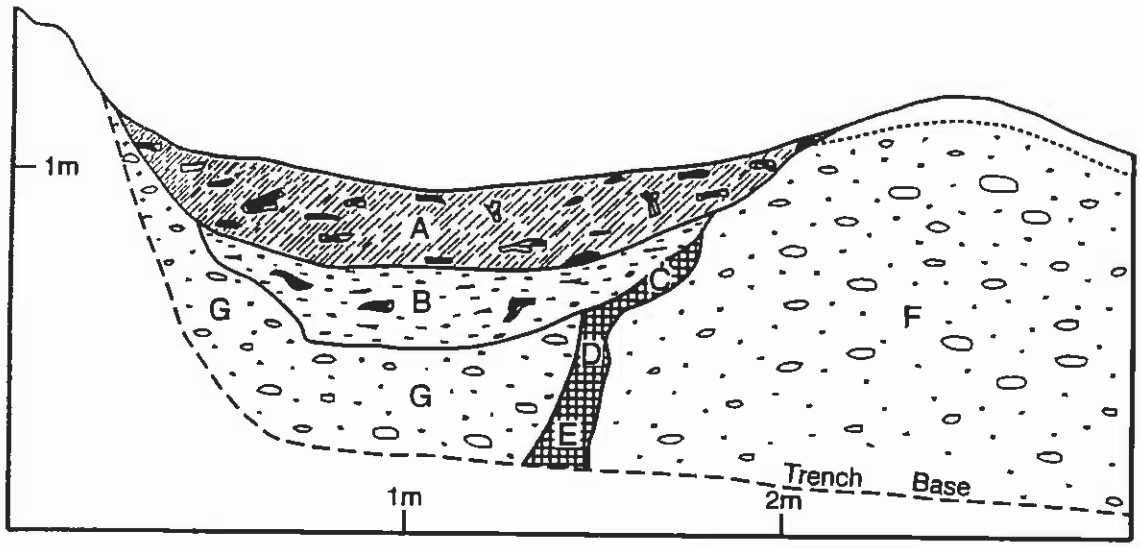

Horizon	Soil Description	Interpretation	^{14}C Dates
A	Soft brown peat and twigs	Forest litter since the last earthquake	Not dated
B	Firm white sandy silt and rare fine schist gravel and twigs	Coseismic scarp erosion sediment from last earthquake	Wk 4489 360 ± 50 BP Wk 5263 380 ± 25 BP
C, D & E	Hard dark brown clayey peat grading down into green silty clay with some peat	Old peat caught in fault plane mixed with fault gouge	Wk 4490 5430 ± 60 BP Wk 5030 5030 ± 60 BP
F & G	Light grey and white grey silty sandy schist gravel	Post glacial terrace gravels	No datable material

Figure 2.3 - Log of the pit across the fault furrow shown in Figure 2.2. Inferred coseismic and immediately post seismic sediment yields dates of 360 ± 50 BP *and 380 ± 25 BP *. The peat above this contains no sign of a more recent coseismic sediment pulse.

* Through out this report we report radiocarbon dates as BP, indicating radiocarbon years prior to 1950. Radiocarbon years do not equate simply with calendar years (years AD) and the relationship is shown graphically in Appendix 1. The error quoted with the radiocarbon date is only one standard deviation but when converting dates to calendar years we have adopted two standard deviations for greater reliability but with a corresponding drop in calendar age resolution.

We infer the pebbly silt formed as a coseismic and immediately post seismic scarp erosion sediment which has rapidly filled the furrow in the first few rains following the earthquake. The scarp has then settled back down to it's normal stable and well vegetated state, and subsequently purely organic detritus filled the furrow to the present day.

Material was collected for dating from the inferred coseismic silt, and two locations in the gouge. Conventional ^{14}C dates (refer footnote page 20) were obtained of 360 ± 50 BP for the silt and 5430 ± 60 BP and 5030 ± 60 BP for the peaty gouge. The gouge dates appear to reflect local ingestion of organics in a strongly dilatant rupture event around 5000 - 6000 years ago. Since then this material has probably been intermittently mixed and intruded by younger organics. Little can be gained from further dating of this mixed gouge.

A second twig sample from the silt was submitted for high precision dating of extracted cellulose to refine the age estimate and has yielded a date of 380 ± 25 BP. Calibration of this high resolution date adopting the southern hemisphere offset of Vogel et al, 1993 and the calibration curve of Stuiver & Reimer, 1993, indicates an age somewhere between 1480 and 1645 AD (full two sigma limits).

There is no evidence of a more recent event at this location in the north section of the fault, for example marked by renewed detrital sedimentation or the deformation of the existing scarp erosion sediment. There is also no obvious evidence of older scarp erosion sediments, suggesting the furrow at this location may only be one event old.

A small landslide which clearly post dates the fault furrow has several large beech trees growing on it (Figure 2.2). We have cored these with an increment corer, which is a 10 mm diameter hollow tube corer able to extract a "straw" of cross grain timber without causing significant damage to the living tree. The oldest beech tree is approximately 300 years old and indicates no rupture along this furrow since around 1700 AD. An older rimu predates the landslide with landslide material piled up around it and evidence of new root growth at a higher level following burial. This tree is approximately 540 years old. Given the gentle scarp slope angle, and the thick forest cover adding to the slope stability, the landslide may well have been triggered during aftershocks or the final moments of the last earthquake but this cannot be demonstrated.

Several other old rimu and miro trees (*Dacrydium cupressinum* and *Prumnopitys ferruginea* respectively) grow amongst the younger red beech along the fault scarp. Seven have been cored and analysis of the growth rings of all seven trees indicates a period of either growth suppression or acceleration 380 ± 10 years before present (Wells, pers. comm. 1997). This is a common pattern in a forest strongly disturbed by earthquake, where some trees experience root disturbance and a slowing in growth, while others benefit from increased light as their neighbours fall (see for example Kitzberger et al, 1995; Jacoby, 1997; Allen et al, in press). Figure 2.4 shows the ring width count for several of the trees cored. However there is also a change in growth patterns in 5 of these trees at 420 ± 10 years ago. The 380 ± 10 year estimate is the preferred (1620 ±10 yrs AD) because it is present in all trees and is the best fit to the regional patterns discussed later.

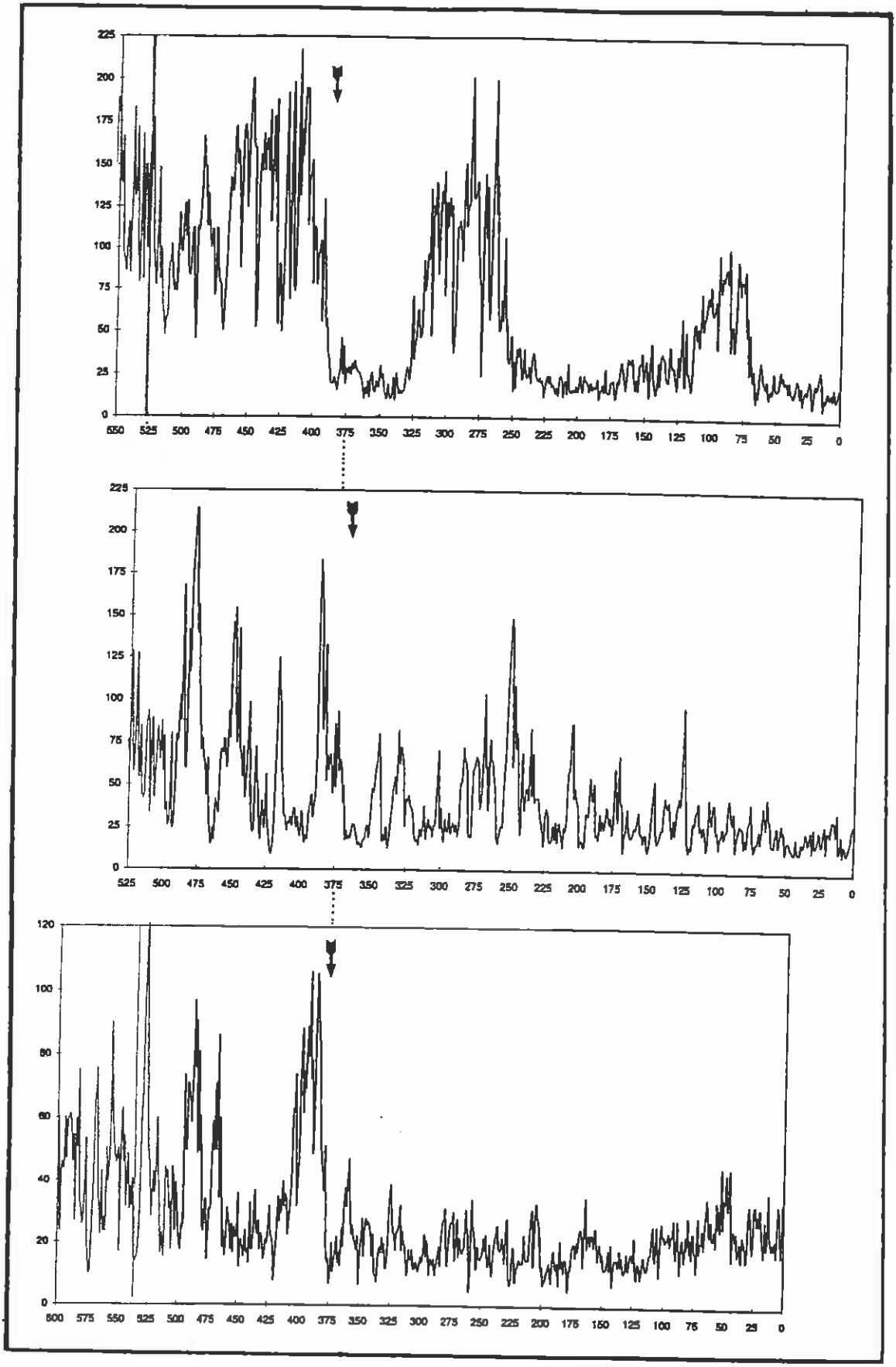

Figure 2.4 - Tree ring width counts (in microns) for three trees growing on the fault scarp at Crane Creek. A total of seven old podocarp trees growing on the scarp all show ring disturbance at 380 ± 10 years before present (approximately 1620 AD).

Matching aggradation terrace

In Crane Creek itself, 600m downstream from the trench site, there is a low aggradation terrace 4m above the modern river. The coarse gravel forming this is loose, sandy and poorly imbricated. In one location several large red beech trunks protrude and the sapwood of one of these has a conventional radiocarbon age of 390 ± 50 yrs BP (WK 4343, refer later Table 3.1 for details). Figure 3.1 in the next chapter is a photo of the terrace at this locality.

Growing on the surface of the aggradation terrace is a dense stand of red beech (*Nothofagus fusca*) which has an even age structure typical of a colonising stand. Unfortunately many of the largest beech trees are now rotten and have fallen relatively recently with a new generation of younger beech replacing them. Coring of the largest of the remaining trees indicates the oldest tree still surviving is 295 years. To this age must be added a period to establish and grow to the height of the corer. This is normally estimated to be 30 to 50 years. This data alone suggests a minimum age of formation of the aggradation surface of around 330 years before present. When some allowance is made for the probable loss of the oldest trees, and also the time needed for the river to cut back down and regularly abandon the surface after forming it, a range of 350 - 400 years is indicated. The age of the colonising trees at this location is a better fit to the 1620 AD earthquake estimate, as opposed to the alternative of 1580 AD.

In summary the ^{14}C dates at the Crane Creek site indicate the last Alpine Fault earthquake at this location was between 1480 and 1645 AD. This estimate can be further refined by the minimum age of the aggradation terrace and the ring disturbance in the podocarps which suggests a date of 1620 AD ± 10 years of this event.

We refer to this earthquake as the **Crane Creek event**. The adoption of a name for this event, as opposed to a date, recognises the likelihood of further improvements in estimates of the exact timing of this earthquake. This name does not imply an epicentre at or near Crane Creek, or suggest that this was an event restricted to only this area (the inferred regional extent of the earthquake is discussed in section 2.1.3).

As well as demonstrating that the Alpine Fault ruptured at this time the excellent match between the dated aggradation terrace and the fault trench date at this location provides support for the use of dates from aggradation terraces in this type of indirect paleoseismic analysis in other areas of Westland (Chapter 3).

2.1.2 Ahaura River

Approximately 6 km further north - east along strike the Alpine Fault crosses the dominantly greywacke alluvium of the Ahaura River. This is a large river system draining the Amuri Pass area and the postulated continuation of the Clarence Fault to join the Alpine Fault. Very little geological investigation on the Alpine Fault has been carried out in this area and nothing has been published. Earth Deformation Section of the former New Zealand Geological Survey briefly inspected the trace in 1975 and 1985 (Officers of the Geological Survey, 1975;1985).

The Alpine Fault at this location has formed a double trace, with the youngest trace the most westward of the pair. Figure 2.5 shows the traces and the location of a small machine dug trench across a subsiding furrow on the west side of the youngest trace.

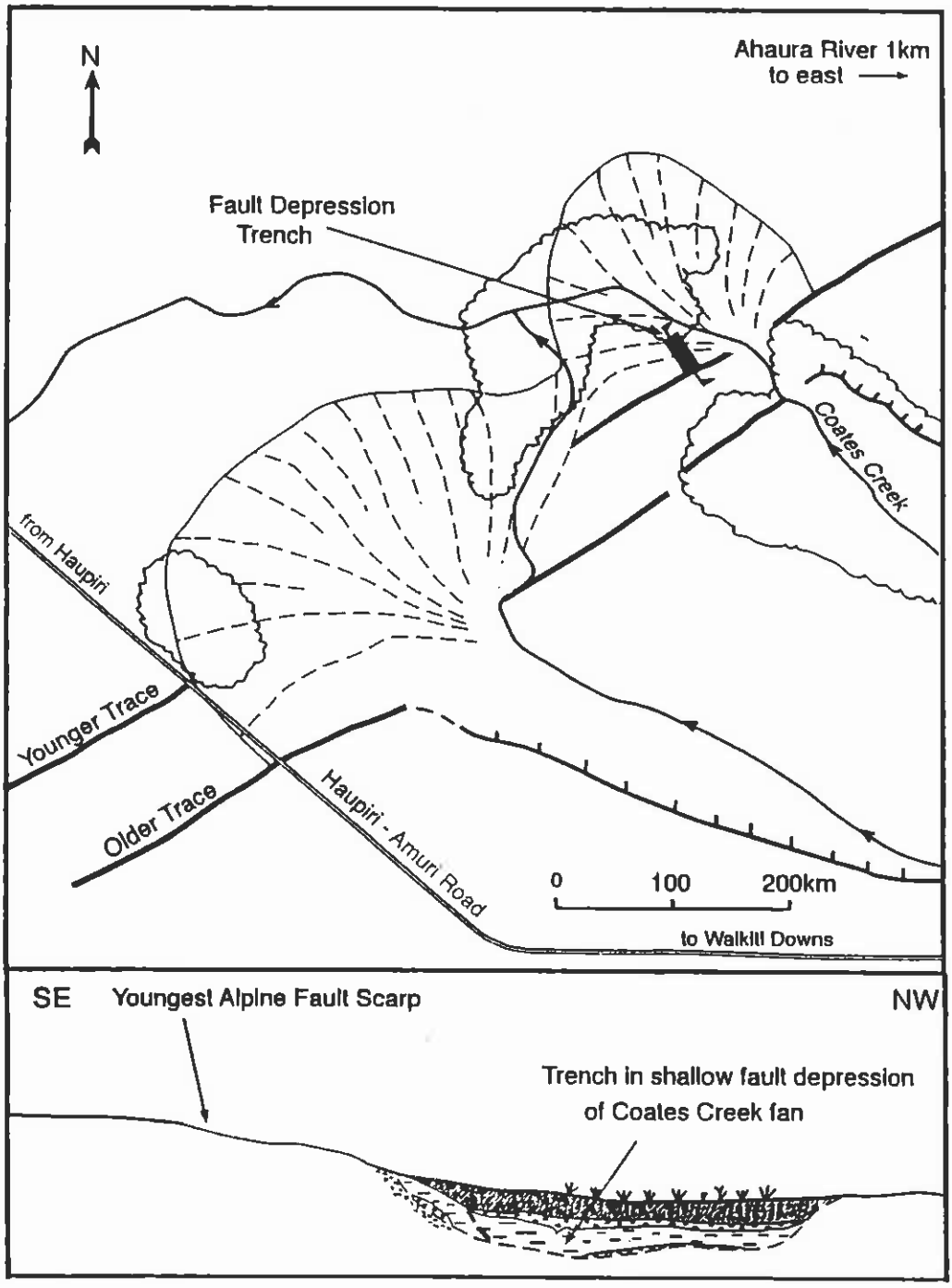

Figure 2.5 - The Alpine Fault trace at the Ahaura River showing the location of a trench excavated across a shallow depression at the base of the youngest scarp.

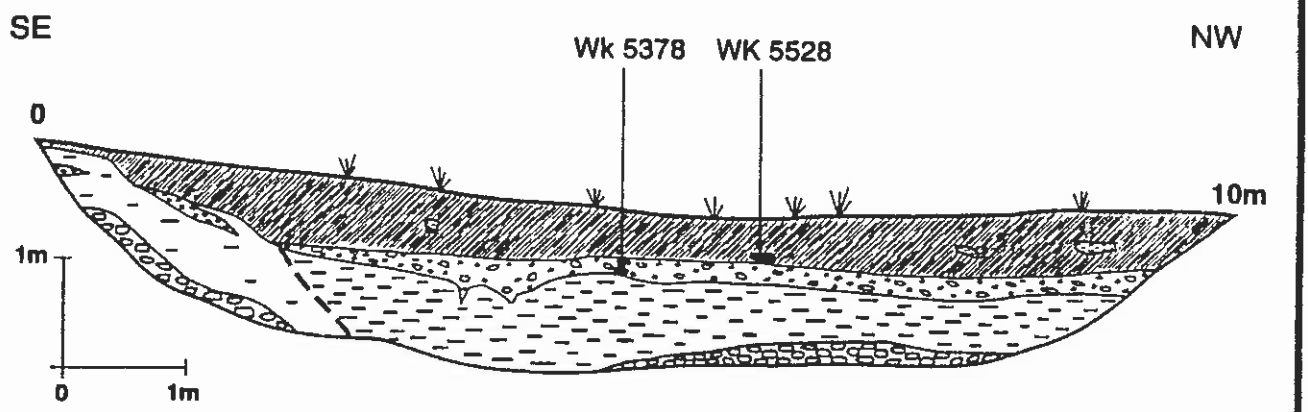

Horizon	Soil Description	Interpretation	Age
	Soft brown peat and branches with minor sand and schist gravel	Post seismic swamp accumulation. Dated wood from near base	Wk 5528 "Modern" (Post 1750)
	Loose blue grey silty sandy angular fine schist gravel	Immediately post seismic creek aggradation gravel in fissured depression	Wk 5378 380 ± 60 yrs
	Firm blue grey uniform silt	Young overbank silts partly burying scarp and fissured in last earthquake	No datable material
	Firm grey brown silt with coarse sand lenses	Older overbank silts in scarp	No datable material
	Tight grey well rounded medium - coarse greywacke gravel	Ahaura River gravels	No datable material

Figure 2.6 - Log of the trench at the location shown in Figure 2.5. The last event is marked by the influx of schist derived aggradation material which has infilled fissures in the underlying deformed silts. A radiocarbon date of 380 ± 60 BP has been obtained from the gravel matching the dates from the Crane Creek trench..

The log for the trench is presented in Figure 2.6. The scarp has formed in the Ahaura gravels and overbank silt terrace cap. The critical feature is the sudden influx of schist derived angular alluvium on to the fissured silt which has accumulated below the scarp. We infer the most recent earthquake at this location has down faulted and fissured the silt. It has also triggered landslides in the steep schist catchment of the small creek near the trench. This fine angular schist gravel has created aggradation in the creek and the sediment has swept south west around the scarp base and in-filled the down faulted area. A small branch in the base of this schist gravel has yielded a ^{14}C date of 380 ± 60 BP which matches the timing of the Crane Creek event. After a period of

schist gravel deposition, which may have lasted some considerable time as the steep slopes settled down, mainly organic deposition commenced. A "modern" date (indicating a post 1700 AD age) has been obtained for twigs 100 mm above the base of the mainly organic top unit.

There is no evidence of a more recent aggradational pulse in the uniform organic top unit and no evidence of rupture or folding of the 380 yr ± 60 yr BP lower unit. The absence of both features once again suggests the Crane Creek event was the most recent at this most northern location.

The Crane Creek event can therefore be recognised in Alpine Fault trenches at two localities in the northern section of the fault. There is no evidence in either trench to suggest a more recent earthquake event at these sites.

2.1.3 The geographic extent of the Crane Creek event based on ^{14}C dating

At present the Crane Creek event is represented south of Crane Creek only by landscape damage. As well as aggradation terraces these include a schist rockfall on the fault scarp at the Styx River (420 ± 60 BP); a rock avalanche in the Cropp River catchment of the Hokitika River (363 ± 56 BP; NZ 5252; Basher, 1986); and fan building at Parker Creek fan in the Whataroa (433 ± 53 BP; NZ 6684C; date from T. Chinn, pers. comm, 1996). This indirect information is presented in Chapter 3.

The location furthest south which has yielded ^{14}C dates in this range is the Karangarua River, south of Franz Josef. P. Wardle obtained a date of 370 ± 60 yr BP on buried stumps exposed in the main river near the McTaggert Creek tributary (NZ 1292; reported in Adams, 1980). This location was recently revisited and samples for high resolution dating collected for a direct comparison with Crane Creek. This work has been carried out in conjunction with Andrew Wells who has been working on forest age patterns in this catchment (Wells and Yetton, in prep.).

Figure 2.7 shows the McTaggert Creek location and sample details. The site is 6 km from the Alpine Fault and it appears the stumps at river level have been buried by a debris avalanche of angular schist debris and fan gravels which have swept into the original forest area breaking and burying the stumps. The distal end of this debris avalanche is approximately 2 km from the steep valley slopes from which it has been derived. This type of debris avalanche is commonly triggered by a large earthquake.

An extensive fan surface has then developed over this debris avalanche. The change to finer sediments immediately above the avalanche debris in the fan suggests there may have been a temporary landslide dam behind the avalanche deposit with silting up prior to dam burst and the resumption of normal fan sedimentation. The Karangarua River has subsequently cut back down through all this to expose the basal stumps in the main river at the McTaggart Creek confluence. Meanwhile up on the fan surface a new forest has re - established.

Figures 2.8 and 2.9 show one of the stumps in the modern river and typical angular schist exposed in the river trimmed end of the debris avalanche. Broken wood can also be found mixed with the debris in many locations.

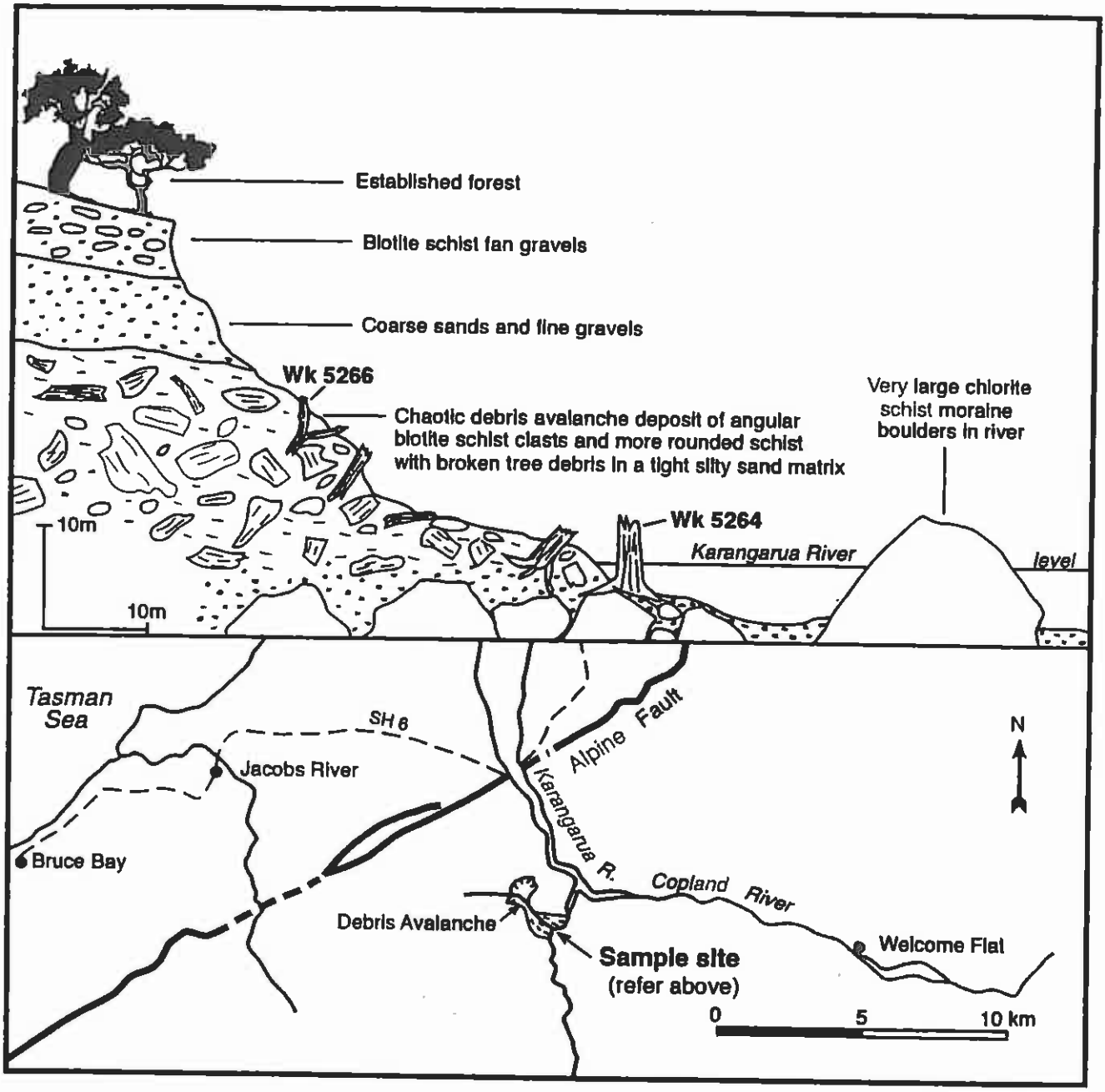

Figure 2.7 - The exposure in the Karangarua River, south of Fox and Franz Josef, of the toe of the McTaggert Creek debris avalanche. Wood is present both in the angular debris and as broken tilted stumps in growth position. Radiocarbon dates on the stumps have yielded ages of 360 ± 60 BP and 420 ± 25 BP, while wood in the debris has provided a date of 320 ± 60 BP. Trees on top of the fan began establishing around 1620 AD and all the radiocarbon dates can be reconciled to approximately this time.

Figure 2.8 - A rimu stump protruding from the modern Karangarua River. Note the large moraine boulders further upstream on to which the debris avalanche has fallen.

Figure 2.9 - Typical angular chaotic schist debris making up the main basal section of the debris avalanche.

Sapwood averaging 10 years of age was collected from a different buried stump to that dated by Wardle. The date obtained was 430 ± 25 yrs BP (effectively 420 ± 25 years with the sap wood adjustment and reconcilable with Wardle's earlier 360 ± 60 yrs BP date). Sapwood from a broken branch 10m further up in the debris avalanche gave a date of 320 ± 60 yrs BP.

The age of living trees on the fan can also be used at this location to provide a minimum age of the fan surface. The oldest tree growing on the fan based on increment coring is 330 years old and assuming a 30 - 50 year forest establishment time this suggests that fan formation was complete by 360 - 380 years ago.

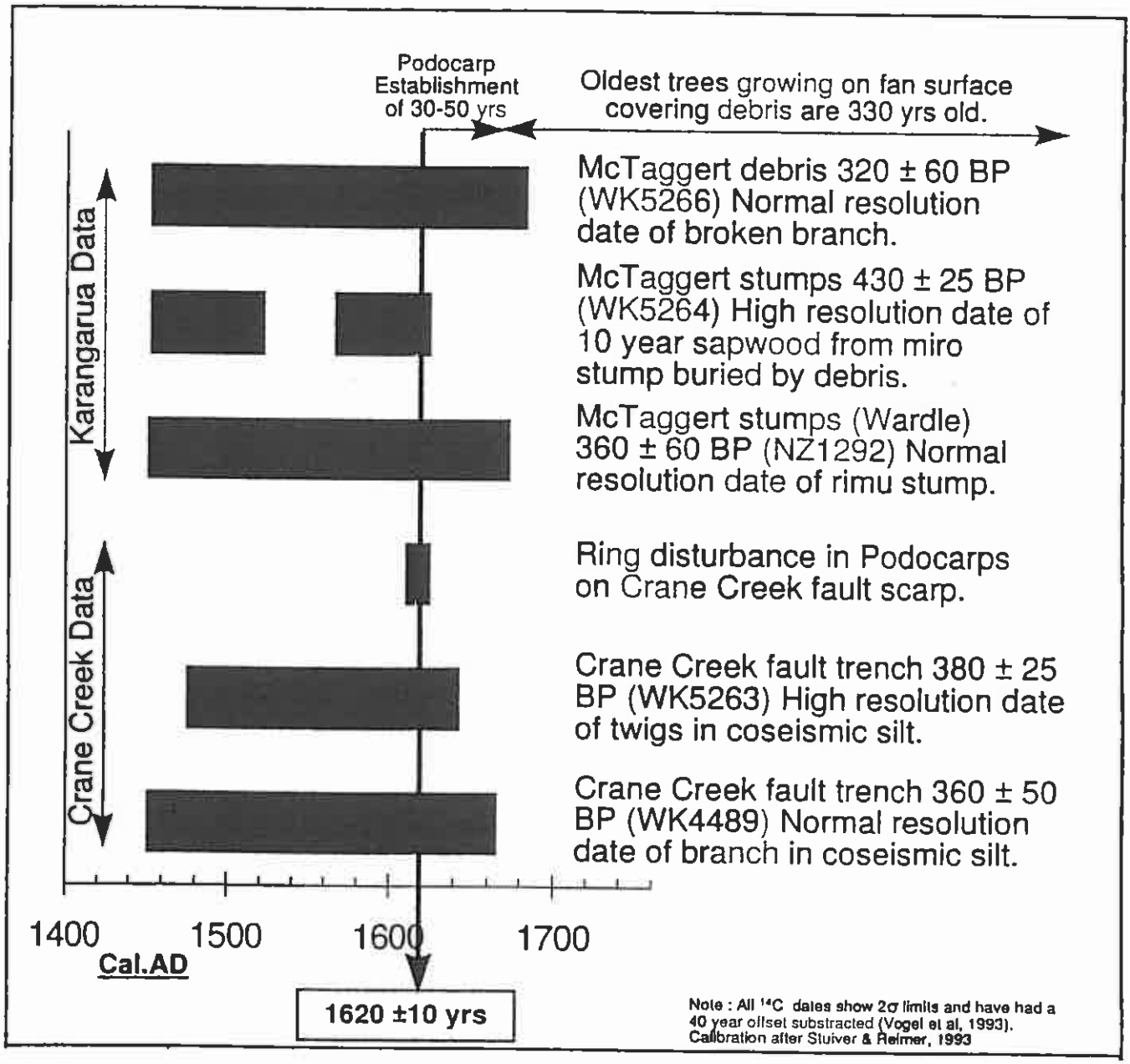

Figure 2.10 - Summary and comparison of the date information from Crane Creek and the debris avalanche in the Karangarua River.

This date information is plotted along with the Crane Creek data in Figure 2.10. The best fit for the McTaggert data is a date of formation around 1620 AD, which matches the Crane Creek event very well, and suggests the Crane Creek event may have extended at least as far south as the Karangarua River. This is a distance along the fault of approximately 200 km.

2.2 Trench evidence for a more recent earthquake around 1700 AD - 1750 AD - The Toaroha River event.

2.2.1 Toaroha River

The Toaroha River crosses the Alpine Fault very close to the Kokatahi and Styx Rivers near the south end of Lake Kaniere (Figure 1.3). This area was first inspected by Wellman (1955) and later by the New Zealand Geological Survey (Officers of the Geological Survey, 1975; 1985). Wright (1994) included the area in his mapping work along the range front.

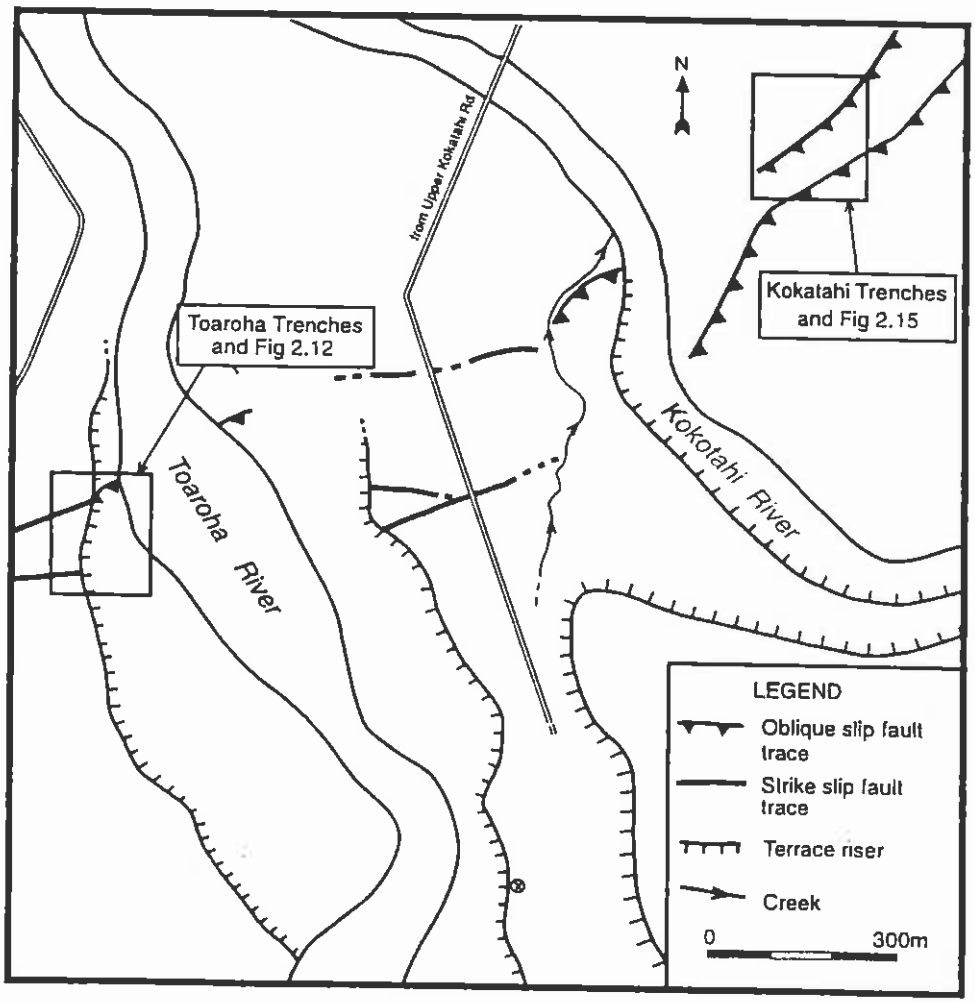

Figure 2.11 - The Alpine Fault in the vicinity of the Toaroha and Kokatahi Rivers (near Hokitika). Refer Figure 1.3 for the general location.

Our work at the site shows the Alpine Fault has a complex pattern of segmentation and multiple traces in this area where it changes from a predominantly strike slip segment on the south west side of the Toaroha River to a more north striking oblique thrust near the Kokatahi River. Figure 2.11 shows a simplified map of the fault in the vicinity of the Toaroha River trench sites. The Kokatahi River trench sites, which are only 1 km further to the north west, are also shown.

Given the possible existence of a branch fault in this general area (inferred by Warren, 1967 and supported by the local geology) the trench was located on the most westerly Alpine Fault trace, which has also been the most active in displacing the alluvial channels and risers. Figure 2.12 shows the location of the two trenches at the Toaroha River in detail.

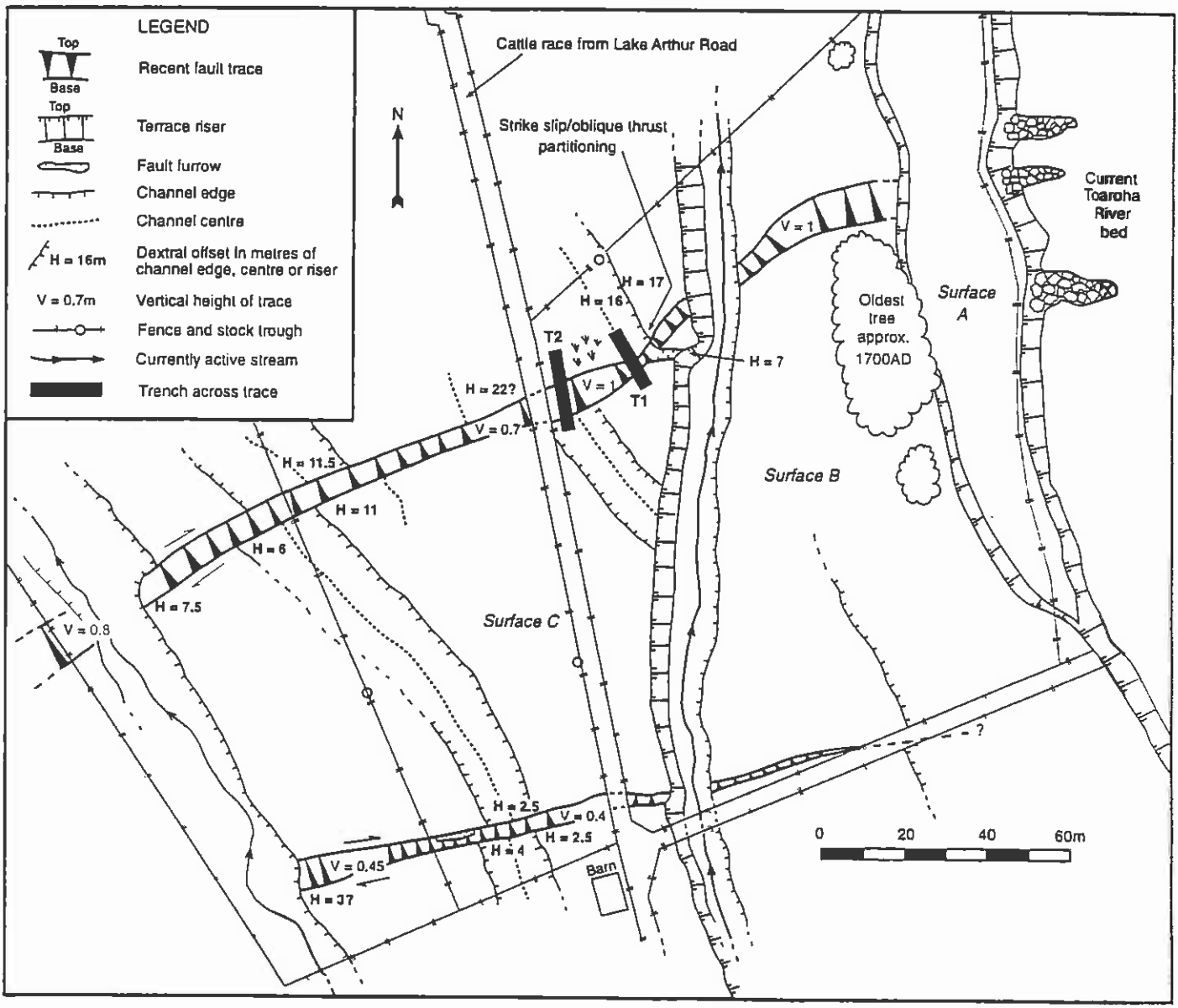

Figure 2.12 - Trench location details for the two trenches on the true left of the Toaroha River. The trenches were located on the third terrace tread (Surface C) where the N-W fault trace has ruptured at least twice.

They were located close together on a terrace approximately 6 metres above current average river level. This terrace surface (Surface C) is the third tread above the current river flood plain and the fault trace across it has a subdued surface expression with approximately 1m of current vertical relief.

The trench log for the Toaroha 1 trench is presented with the key and summary box as Figure 2.13. The Toaroha 1 trench reveals a steeply dipping fault zone with evidence of earthquake associated rupture of several finer grained fluvial units at the fault which are continuos on the north - west side. Coarser fluvial sandy gravels and gravelly sands underlay these units on the downthrown side but are continuous to the surface on the relatively up-thrown south-east side.

Wood and charcoal was collected for dating. Sample Wk 5510 was from very near the ground surface in a peaty matrix. Unfortunately the area had been first logged around 1880, and then fully cleared later with grazing and some minor cropping continuing to the present. At least some disturbance of the original ground surface is inevitable in these operations and the date for this shallow sample indicates an origin post 1950 (ie post the first influence of atomic bombs in the New Zealand area).

Wk 5512 was from the outside of a buried branch, very close to the fault which appeared at this location to extend close to surface. This returned a "modern" date which indicates an calendric age anywhere between around 1700 AD and 1950 AD (but not post 1950 AD). It is possible that this branch was not original and was somehow related to timber milling however this did not appear to be the case.

The final date from this trench was Wk 5511 from a root in apparent growth position in the coarse sand unit. Finer roots could be traced from this which were all confined to the sand and did not extend down from the gravel or overbank silts above it. We infer these roots belonged to vegetation killed by the subsequent gravel inundation but root intrusion from the surface cannot be discounted. This returned a date of 250 ± 50 yr BP which only provides a minimum age for this faulted sand unit. Unfortunately it does not constrain any particular event timing.

The Toaroha 1 trench is therefore inconclusive. There is a suggestion of a faulting event between 1700 and 1950 AD but contamination associated with logging cannot be ruled out as the alternative explanation of this date.

Fortunately the Toaroha 2 trench shown in Figure 2.14 is more definitive. It was only 15m from the first trench and all the same units are represented although the coarse sand on the north- west side is thinner here. The critical date is Wk 5513 in the overbank silt unit. This was obtained by dating the outer 20 rings of a small, slightly abraded, fragment of silver pine branch (*Lagarostrobos colensoi*) which was broken and completely encased in undisturbed overbank silt. Silt had been deposited in the broken ends and there were signs of minor fluvial abrasion which had removed the bark and at least some sap wood.

The conventional radiocarbon age for the outer twenty rings was 210 ± 50 yr BP which represents the oldest possible radiocarbon age for the overbank silt. Some sap

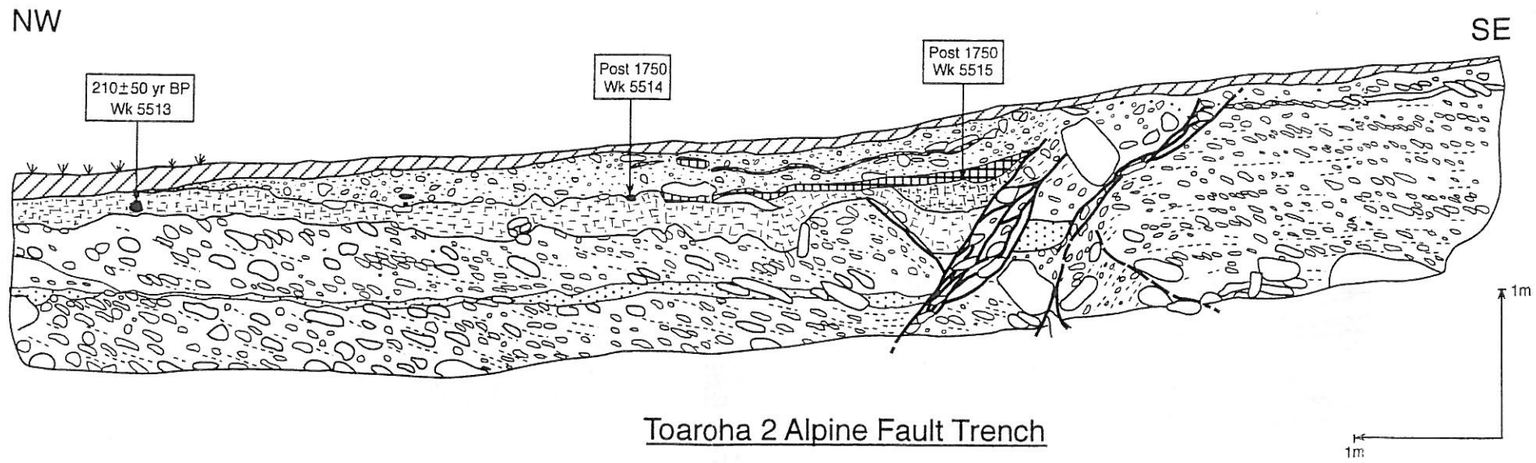

Toaroha 2 Alpine Fault Trench

Stratigraphic key for Toaroha trenches

Symbol	Description	Interpretation
	Soft brown organic clayey silt.	Topsoil
	Soft black brown charcoal and sandy peat.	Buried soil from forest clearing and local swamp accumulations.
	Grey silty sandy fine - medium gravel with no fluvial structure.	Scarp derived colluvium and/or regrading from forest clearing.
	Grey slightly gravelly sandy silt with no fluvial structure.	Finer scarp derived colluvium.
	Grey blue gleyed slightly sandy silt with some clay. Charcoal, wood and fine gravel locally abundant. Minor stratification.	Overbank fluvial silts, aged around 210 ± 50 yr BP from sapwood of transported branch.
	Grey coarse sand and fine schist gravel with local lenses of silty sand. Stratification common.	Flood channel fluvial sands and fine gravels. Age > 250 ± 50 yr BP date on an old root.
	Grey sandy medium to coarse, subangular to rounded, schist gravels with clast alignment and imbrication shown diagrammatically.	Fluvial gravels showing various degrees of disruption by faulting.

Summary

- Predominantly steeply dipping strike slip (068° strike)
- Earthquake associated rupture (not aseismic deformation)
- At least two ruptures represented
- Last event post 210 ± 50 yr BP

Figure 2.14 - Log, key and summary of the main features of the Toaroha 2 trench

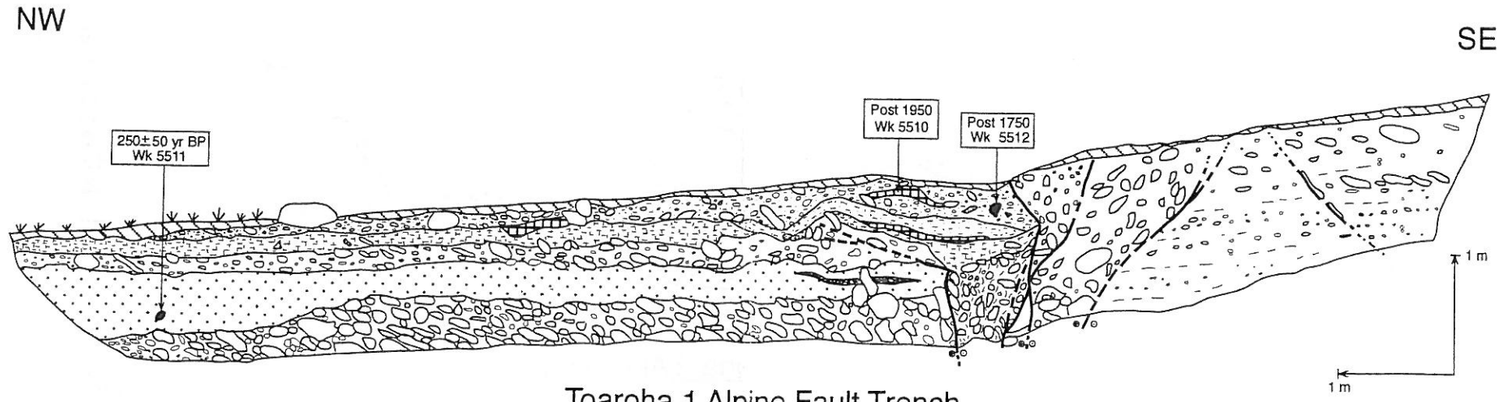

Toaroha 1 Alpine Fault Trench

Stratigraphic key for Toaroha trenches

Symbol	Description	Interpretation
	Soft brown organic clayey silt.	Topsoil
	Soft black brown charcoal and sandy peat.	Buried soil from forest clearing and local swamp accumulations.
	Grey silty sandy fine - medium gravel with no fluvial structure.	Scarp derived colluvium and/or regrading from forest clearing.
	Grey slightly gravelly sandy silt with no fluvial structure.	Finer scarp derived colluvium.
	Grey blue gleyed slightly sandy silt with some clay. Charcoal, wood and fine gravel locally abundant. Minor stratification.	Overbank fluvial silts, aged around 210 ± 50 yr BP from sapwood of transported branch.
	Grey coarse sand and fine schist gravel with local lenses of silty sand. Stratification common.	Flood channel fluvial sands and fine gravels. Age > 250 ± 50 yr BP date on an old root.
	Grey sandy medium to coarse, subangular to rounded, schist gravels with clast alignment and imbrication shown diagrammatically.	Fluvial gravels showing various degrees of disruption by faulting.

Summary

- Predominantly steeply dipping strike slip faults (068 ^{o} strike)
- Earthquake associated rupture (not aseismic deformation)
- At least two ruptures represented
- Last event post 250 ± 50 yr BP

Figure 2.13 - Log, key and summary of the main features of the Toaroha 1 trench.

wood younger than this was missing off the sample due to fluvial abrasion so this may have removed 5 - 10 years of time. In addition the branch had to break and fragment after death, make its way into the river system, and later accumulate during a flood in the overbank silt. This silt has then been subsequently faulted as the trench clearly shows.

The oldest possible calendric age for the wood itself is 1660 AD, indicating deposition and faulting post 1660 AD, possibly by some tens of years. Ignoring the likely time for lost abraded wood and the subsequent deposition and faulting, even the oldest possible age of the wood as dated (1660 AD) cannot be reconciled with the Crane Creek high precision radiocarbon date of 380 ± 25 yr BP (corresponding to a youngest possible calendric age for this material of 1645 AD). 1660 AD is also more than 40 years after the preferred date of the Crane Creek event based on tree ring disturbance at 1620 ± 10 yr AD. This Toaroha 2 trench therefore provides the first unequivocal evidence of a rupture of the central Alpine Fault some time after the Crane Creek event and post 1660 AD.

Two other inconclusive dates come from this trench. Both Wk 5514 and Wk 5515 are from immediately above the overbank silt from charcoal in peaty soil. Both returned "modern" dates suggesting post 1700 AD but pre 1950. Wk 5515 in particular appeared to be faulted at the south-east end but once again both dates could be from ground disturbed and burnt during logging of the site.

Indirect evidence of a more recent earthquake event than the Crane Creek event in this area is also provided by the radiocarbon date on the outside of a punga trunk of 200 ± 50 yr BP (Wk 4919, Table 3.1) obtained from within the debris of a moderately large granite mylonite rock fall from the east side of Mt Harry. This is only 300m from the Toaroha trenches and rainfall triggered rockfalls in the relatively hard and resistant granite derived mylonites of this area are not common. We suggest this could also have been triggered by the recent rupture revealed in the nearby Toaroha 2 trench but there is no way to confirm this.

2.2.2 Kokatahi River

The true right bank of the Kokatahi river has young fault traces with a generally more east-west strike and which frequently exhibit back tilt to the east on the relatively up-thrown side. This is a surface feature typical of an oblique fault zone containing more low angle east dipping shallow faults. Figure 2.11 shows the area in relation to the fault zone structure and the Toaroha trenches. Figure 2.15 is a detailed map of the trench sites.
Two adjacent scarps were selected for trenching. The first is the more eastern and is around 1m high with a similar general appearance to the Toaroha scarp. An abandoned channel crosses the fault 50m south-east of the trench, and there is no surface trace of the fault across this, suggesting flow and sedimentation since the last rupture. After crossing the fault this channel swings north along the base of the scarp. The trench was excavated perpendicular to the scarp and with a drain along the scarp base, and within the channel, which extended to the creek approximately 50m away. The log is presented in Figure 2.16 and includes the log for a section of the drain approximately 30m away from the main trench.

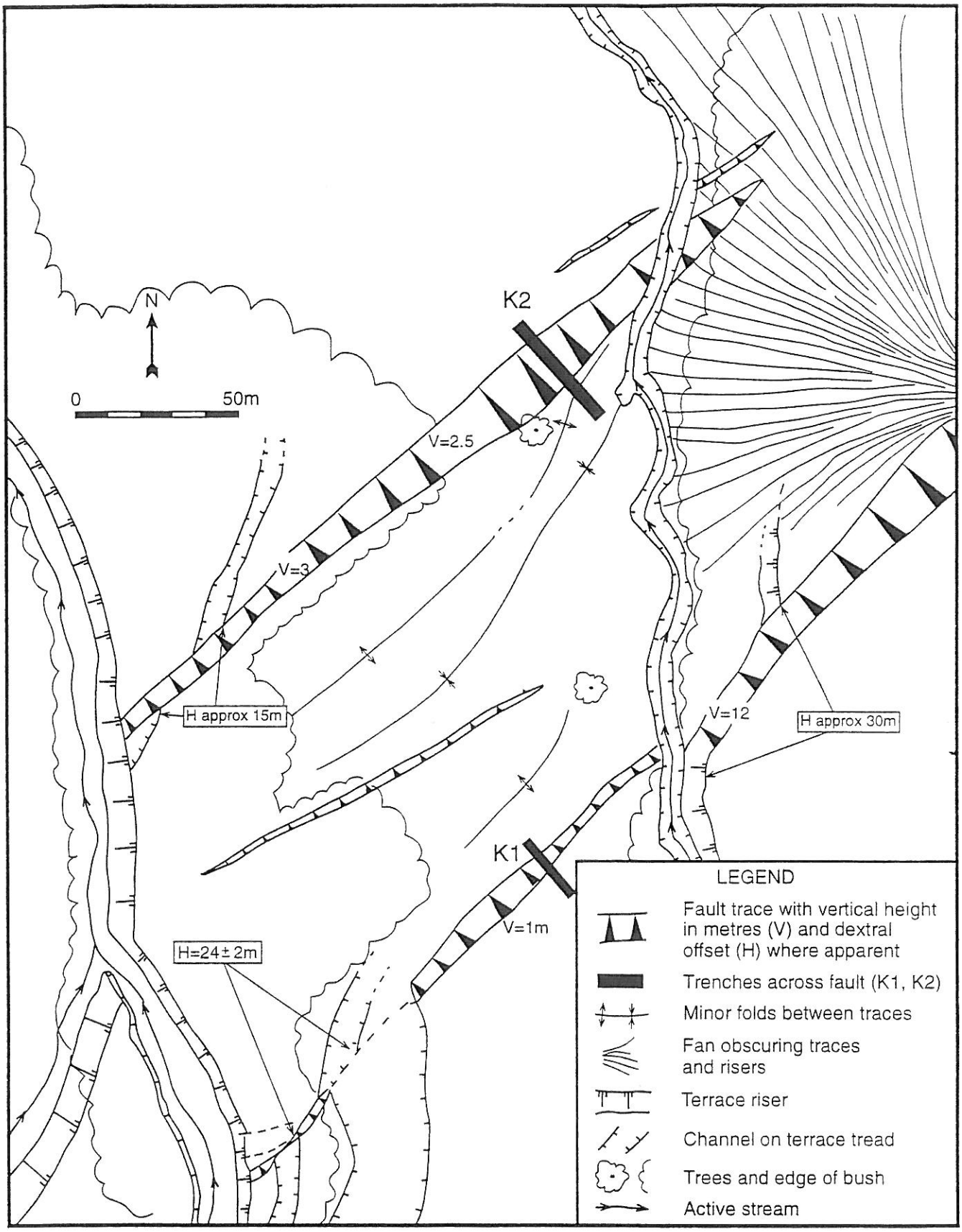

Figure 2.15 - The Alpine fault and the location of the two trenches on the true right of the Kokatahi River. Refer also Figure 2.12 for proximity to the Toaroha trenches and Figure 1.3 for general location.

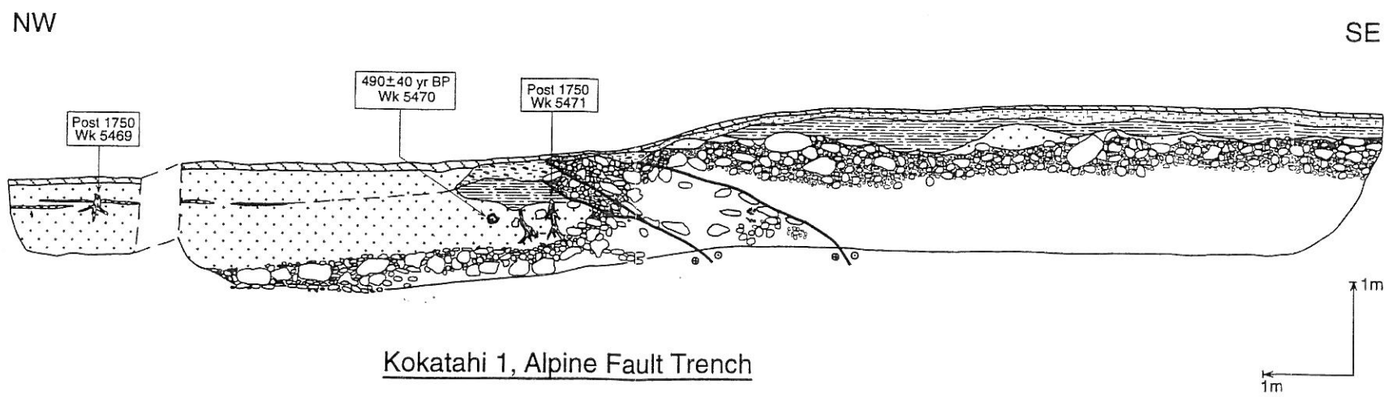

Kokatahi 1, Alpine Fault Trench

Stratigraphic key for Kokatahi 1 trench

Symbol	Description	Interpretation
	Soft brown organic clayey silt	Topsoil
	Grey blue clayey silt with angular coarse sand and fine gravel clasts. No stratification. Clasts aligned parallel to slope.	Scarp derived colluvium.
	Grey blue gleyed slightly sandy silt with minor stratification.	Overbank fluvial silts.
	Grey brown silty fine sand. Minor stratification.	Overbank fluvial silty sands.
	Grey uniform coarse sand with a discontinuous lens of iron stained pebbly sand 50cm below surface. Transported and abraded rata branches near base (Wk 5470) and some broken roots close to fault zone (Wk 5471).	Flood channel fill from around 490 ± 40 yr BP in lower part of unit. Hiatus marked by iron staining, then a much younger flood channel fill, post the last earthquake, burying the stump at the NW end.
	Grey and brown medium to coarse subangular to rounded sandy schist and greywacke gravel.	Main Kokatahi River bed load.

Summary

- Predominantly oblique thrust faulting (045° strike)
- Two events post 490 ± 40 yr BP deposition of the sand unit

Figure 2.16 - Log, key and summary of the main features of the Kokatahi 1 trench.

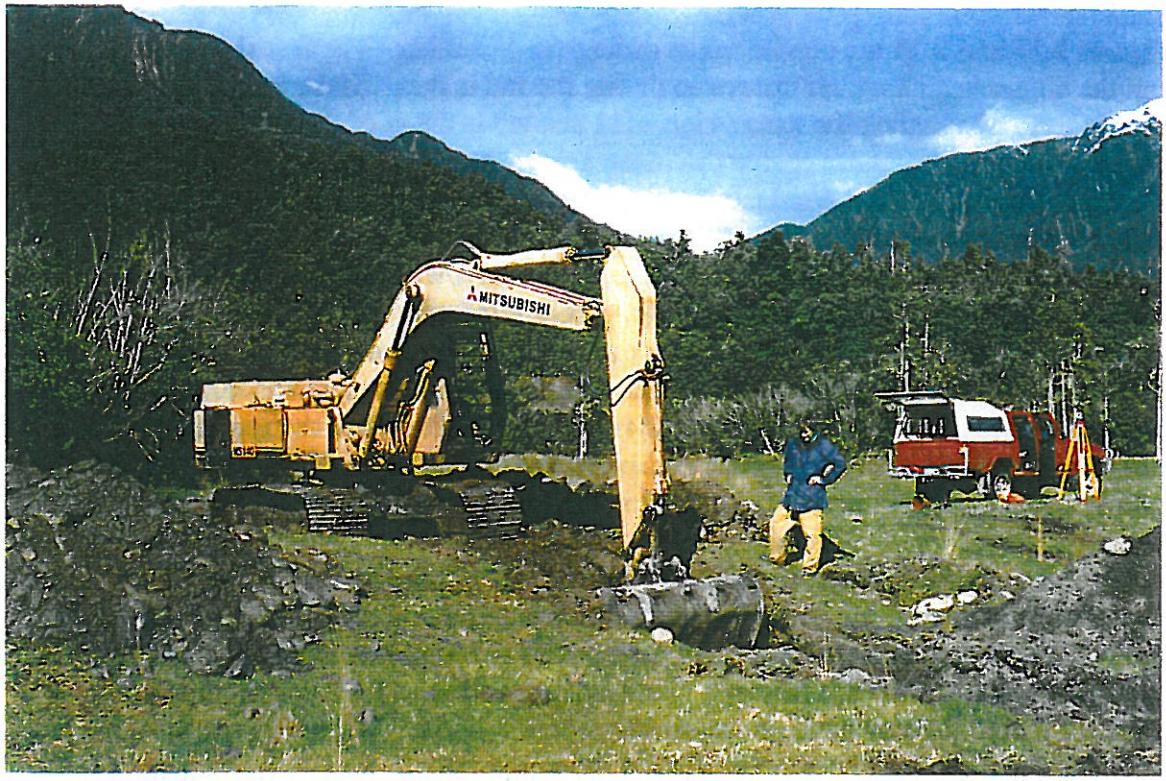

Figure 2.17 - The excavator at work beginning the Kokatahi 1 trench. The bucket is just starting to reach the actual fault rupture and blue grey coarse sand channel fill is visible immediately downhill of the bucket.

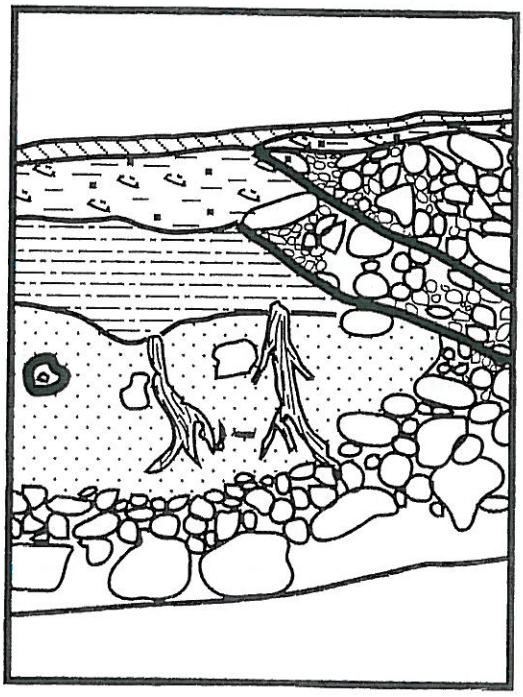

Figure 2.18 - Photo and relevant section of log showing evidence for two rupture events since deposition of the sand containing transported wood from post 1470 AD.

Figures 2.17 and 2.18 are photos taken during the trenching. The first shows the scarp and the digger beginning the excavation. The second is detail of the trench log showing the two successive shears discussed below.

The trench reveals a sand dominated channel fill on the downthrown north-west side which has accumulated in at least two episodes. Wk 5470 was collected from a section of a large rata branch (*Metrosideros umbellata*) which had the sap wood abraded away in virtually all areas. To get sufficient sample volume to allow a date the sample wood was collected from nearer the heart wood between 50 and 60 rings from the outermost remaining ring. This branch was definitely fluvially transported and this older wood yielded a radiocarbon age of 490 ± 40 yrs BP. When the adjustment for sample age is made this represents a maximum age for the basal sand unit of post 1470 AD.

A hiatus in sand deposition is indicated by a thin pebbly horizon approximately 400 mm below the surface on the north-west side. Iron staining was abundant along this horizon and in the drain a stump of an unidentified softwood species was found in growth position. A sample from the sapwood was collected (Wk 5469) which returned a post 1700 AD and pre 1950 AD date. We infer this sand is post the most recent faulting event and the inundation of the stump reflects the late reoccupation of the channel and removal of the surface trace where the channel crosses the fault.

Near the fault itself, and very close to the transported rata branch, several small - kahikitea roots (*Dacrycarpus dacrydiodes*) were found in apparent growth position. which also returned a post 1700 AD and pre 1950 AD date (Wk 5471). These appeared to have had their upward continuation torn out, possibly by shearing, but there is no reason why this could not have been the result of wind throw or forest clearing.

The most definitive aspect of the Kokatahi 1 trench is the pattern of shears and associated colluvial material in relation to the oldest sand unit (refer photo and log detail in Figure 2.18). The western most shear broke up through the basal sand and terminated at an apparently colluvial unit derived from local erosion of the scarp. A similar unit terminated the eastern most shear. Between these a splay from the west shear broke up through the colluvial unit to virtually the ground surface. This was overlain only by thin topsoil. Given that the maximum age of the basal sand unit is post 1470 AD this indicates two separate episodes of shearing since 1470 AD. This is consistent with initial rupture in the Crane Creek event and renewed movement in the later Toaroha event.

This does not rule out the scarp being in existence as the eastern bank of the original channel, in which the basal sand accumulated prior to 1470 AD, or provide any information on the total age of the scarp. A date from the gravels themselves would be required to determine this and unfortunately datable material in the gravels is very rare.

The second trench was excavated 150m north-west of the first across the most westerly scarp which is approximately 2.5m high. The log is presented in Figure 2.19 Once again the shears within the scarp dipped east and more than one event can be recognised.

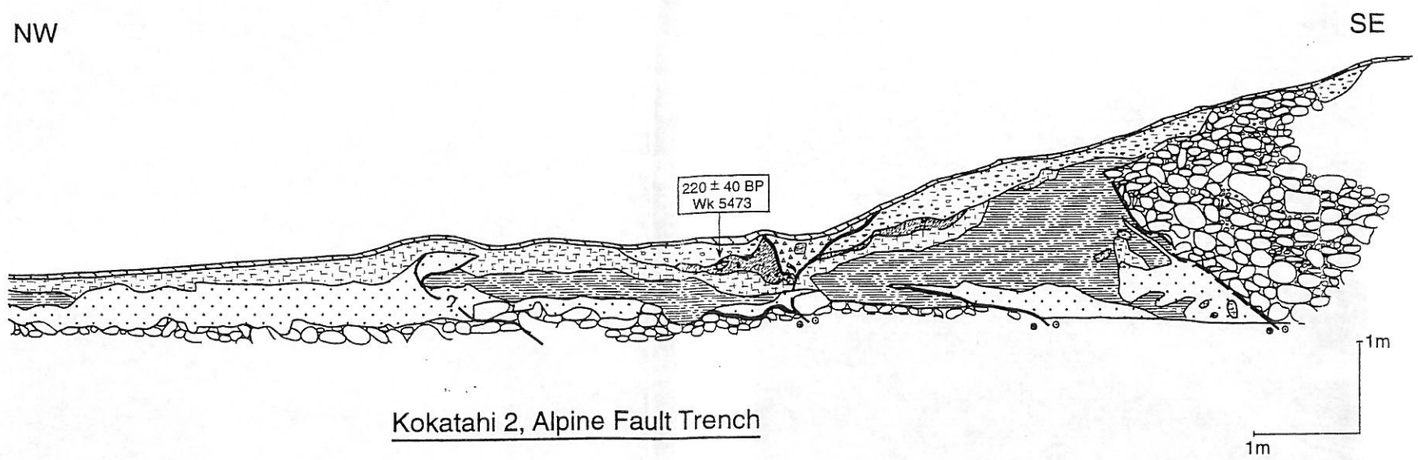

Kokatahi 2, Alpine Fault Trench

Stratigraphic key for Kokatahi 2 trench

Symbol	Description	Interpretation
	Soft brown organic clayey silt.	Topsoil
	Grey blue clayey silt with angular coarse sand and fine gravel clasts. No stratification. Clasts aligned parallel to slope.	Scarp derived colluvium
	Loose grey brown soil "breccia" of clods of all other units in a silty sand matrix.	Rupture induced fragmentation (and probably liquefaction) of existing soil units.
	Soft brown peat and silty peat with abundant wood including twigs and young branches.	Local swamp accumulation in fault depression around 220 ±40 yr BP predating the last rupture and incorporated in " breccia"
	Grey blue gleyed slightly sandy silt with minor stratification.	Overbank fluvial silt.
	Grey brown silty sand with minor stratification.	Overbank fluvial silty sand.
	Grey uniform coarse schist and greywacke sand. No stratification.	Flood channel fill.
	Grey and brown medium to coarse subangular to rounded sandy schist and greywacke gravel.	Main Kokatahi River bed load.

Summary

- Predominantly oblique thrust faulting (045 ^{O} strike)
- Earthquake associated rupture and liquefaction (not aseismic deformation)
- At least two ruptures represented
- Last event post 220 ± 40 yr BP

Figure 2.19 - Log, key and summary of the main features of the Kokatahi 2 trench.

Detail A: The main oblique thrust of sandy gravels sheared over coarse sand which contains fragments of other soils and laminar "flow" bands (both visible in Detail B).

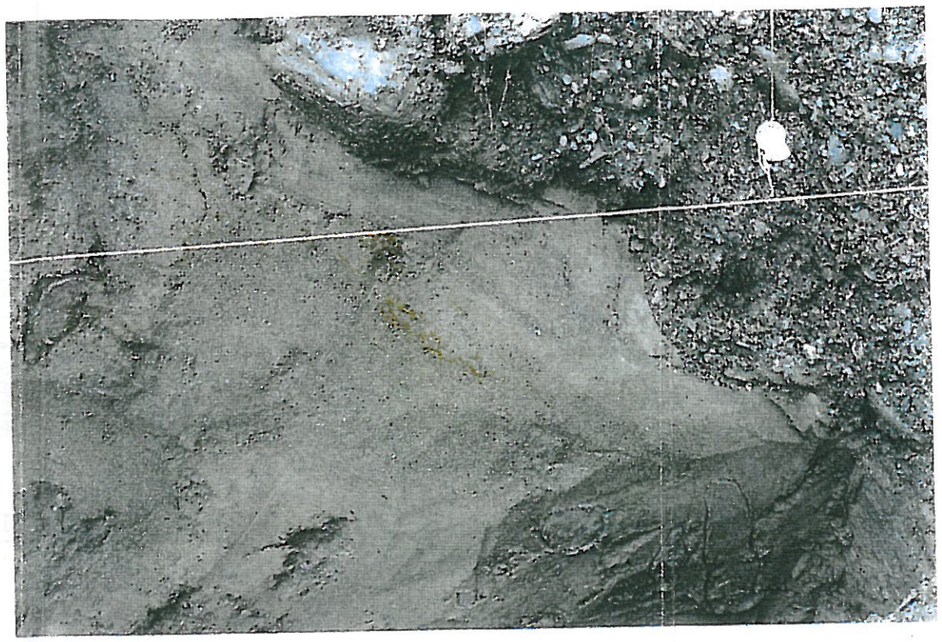

Detail B: Close up showing faint laminar bands parallel to the shear and fragments of blue grey gleyed silts, some of which at the top and bottom have been emphasised for the photo by scratching around their outlines. Both features suggest liquefaction of the sand during shear.

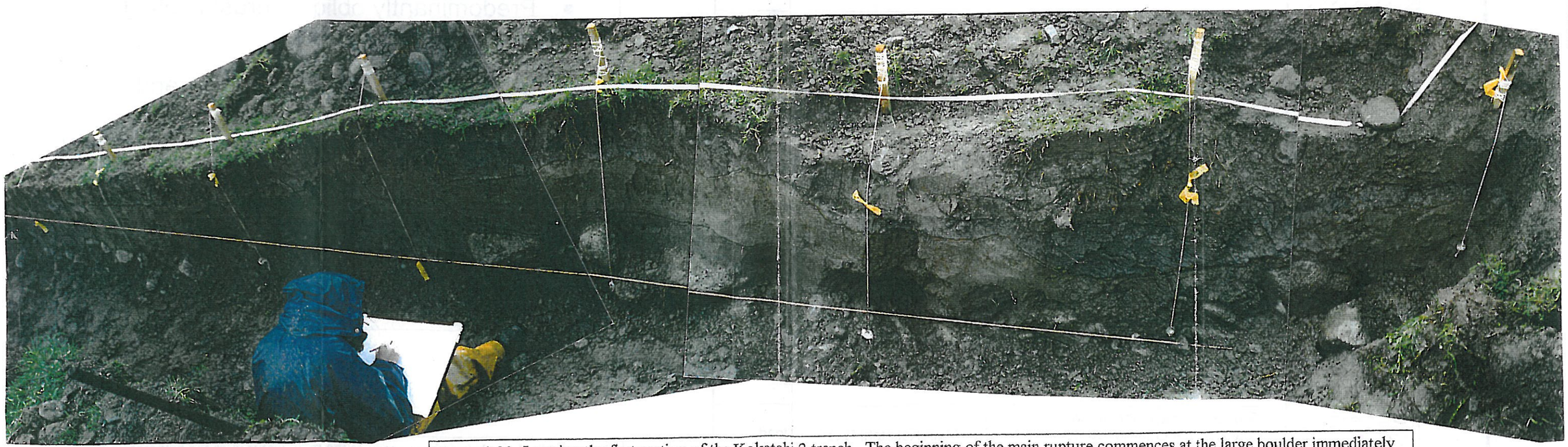

Figure 2.20 -Logging the first section of the Kokatahi 2 trench. The beginning of the main rupture commences at the large boulder immediately uphill of the end of the orange string level line. Disrupted pieces of grey blue silt are visible in the peaty soils 300 mm above the boulder. Details A and B are from the subsequent extension of the trench further into the scarp.

Unfortunately only one date could be obtained in this trench however this once again indicates a rupture since the Crane Creek event. Wk 5473 was obtained from a piece of partly rotted rata branch (*Metrosideros umbellata)*, with only the heart wood preserved, which was in peaty soil which appears to have accumulated in a small depression at the bottom of the scarp. This depression may have originally been a linear furrow similar to Crane Creek.

The peaty material and wood had been sheared and "intruded" with a loose assemblage of angular pieces of soil from all the other fine grained nearby lithology's in a silty sand matrix. These pieces of other soil within the silty sand where angular and broken, resembling a "soil breccia". We interpret this material as having formed as the product of liquefaction in the last earthquake. Figure 2.20 are a series of photographs from this trench. The close up photo of the fault plane also shows similar pieces of blue grey soil within a coarse sand which itself exhibits evidence of flow along the shear. This is the first direct evidence of liquefaction at the fault trace and this can only be the result of earthquake rupture, not aseismic creep.

The radiocarbon date for the sample was 220 ± 40 yrs BP and this came from heart wood with at least an estimated 15 rings missing but possibly more. This estimate is based on the average ring density of the heart wood and the typical minimum thickness of sap wood expected on a branch of this diameter. The corresponding oldest possible calendric age for this wood is 1665 AD. This is once again too young to be reconcilable with the Crane Creek event and indicates a younger episode of rupture and liquefaction.

2.2.3 Haupiri River

The Haupiri River is 25 kilometres north east along fault strike from the Hope Fault junction at Inchbonnie (Figure 1.3). Figure 2.21 shows the general trace details at the Haupiri River. This location was also described in Munden (1952) and Wellman (1955) and was visited in the later reconnaissance trips made by the New Zealand Geological Survey (Officers of the Geological Survey, 1975;1985).

Relatively early in our work several young indirect radiocarbon dates were obtained in the Haupiri River area near the fault. An aggradation terrace was apparent 3m above modern average river level which yielded dates of 260 ± 50 yrs BP (Wk 4874, Table 1) for sapwood on a red beech log (*Nothofagus fusca*), and 270 ± 50 yrs BP (Wk 4873) for some rata heartwood (*Metrosideros umbellata*) of unknown self age.

An old debris flow was also apparent in an unnamed small stream near the Haupiri River (GR K32/060435 and referred to here informally as Moss Creek, Table 3.1) which drains a section of the range front near the fault zone. This debris flow had buried a once large area of trees in growth position. The trees have subsequently died and the projecting trunks fallen so that the currently grazed paddock has several short trunk sections broken at grass level. Moss creek has cut back through the debris and exhumed several of the stumps re-exposing the root plates and the paleosol.

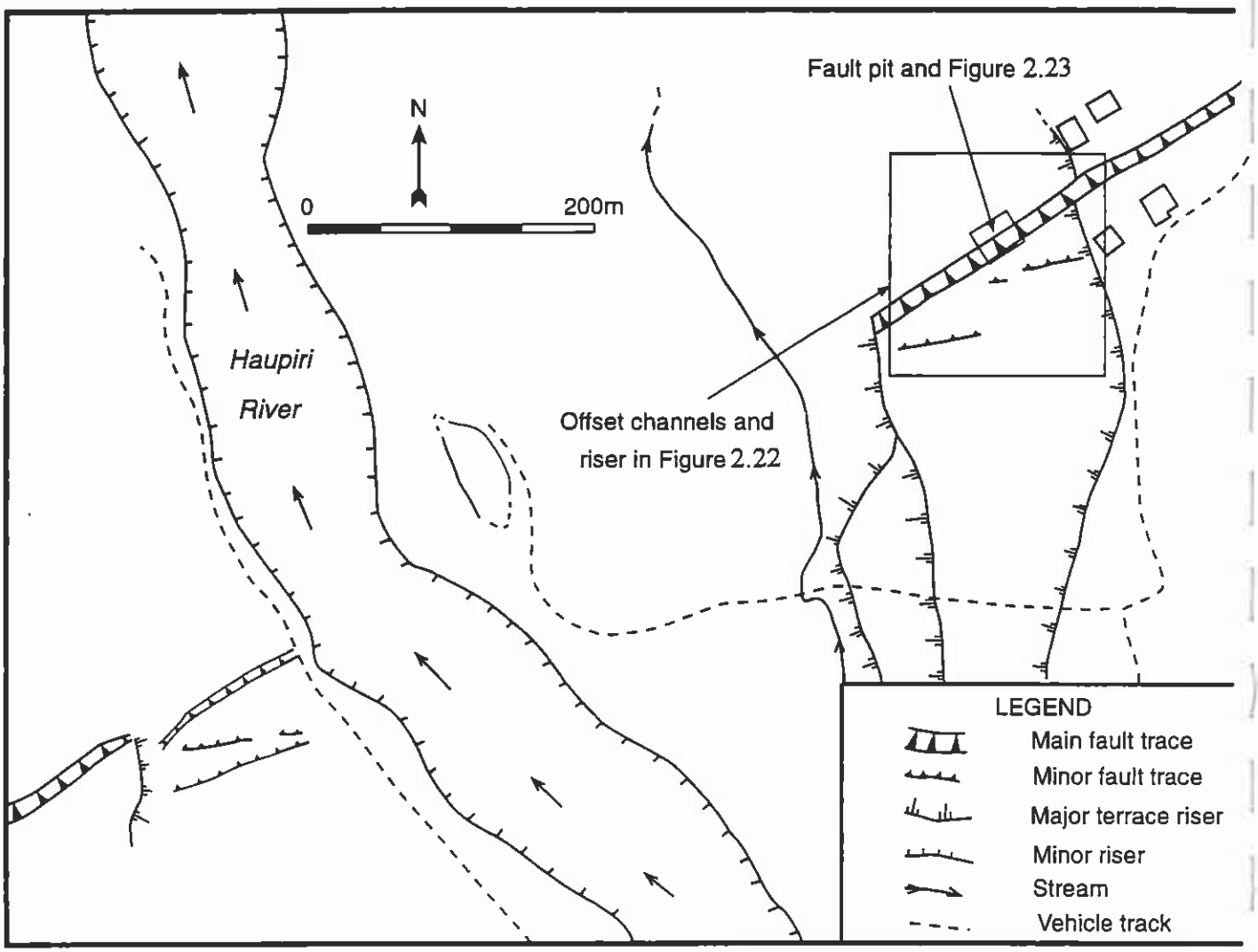

Figure 2.21 - The Alpine Fault at the Haupiri River. Initial trenches on the true left did not provide any material for dating which could constrain rupture timing. A had dug pit at the location shown on the true right was more successful.

Sapwood was collected from a totara stump exposed in Moss Creek (*Podocarpus cunninghamii*) and submitted for dating. Wk 4876 returned a radiocarbon age of 210 ± 50 yr BP which matches the date from the Toaroha 2 trench and is very similar to the Kokatahi 2 trench and the Mt Harry rockfall dates (220 ± 50 yr BP and 200 ± 50 yr BP respectively).

Although the Haupiri River is only 5 km south-west along the Alpine Fault strike from Crane Creek, this indirect evidence suggested that this catchment may have been subjected to a younger event than Crane Creek and Ahaura River. For this reason two attempts were made at trenching the fault at Haupiri. The first was a large machine dug trench on the true left bank where the trace forms a low scarp across cleared paddocks. Despite careful logging this trench only yielded wood from a young channel fill deposit on the downthrown side which was not present at the shear itself. The relationship between the channel fill and the age of last rupture was therefore

ambiguous and the wood was not submitted for dating. There was also abundant evidence of surface disturbance of the upper soil horizons from timber clearing, river protection works, and farm improvement.

A second area on the true right bank was selected in an area of remaining bush cover (Figure 2.21). Because of access limitations in the bush, and the small scale of the selected feature which had a large risk of inadvertent damage by machine, the decision was made to carry out a small excavation by hand similar to the one at Crane Creek.

Figure 2.22 is a more detailed map of the trench area. The scarp at this location is approximately 5m high and has developed over a period of approximately 2000 years. A long term slip rate can be estimated based on a radiocarbon date obtained in a long shallow pit on the terrace tread 100m east of the trace (age range 250 AD - 385 BC). This age range, in conjunction with the average of the riser and channel offsets, indicates a long term slipe rate of 6.3 ± 2 mm/year.

Figure 2.23 shows the detail of a displaced landslide which has been dextrally offset approximately 5m by the fault creating a small furrow at the base of the scarp The geomorphology indicates the most recent fault shear must be in this furrow. This area resembles the successful trench at Crane Creek and was selected for the excavation.

Figure 2.24 is the log of the small pit. The top 150 mm of material is a saturated soft brown peat containing twigs, leaves, and occasional larger branches. This abruptly changes to a loose horizontally imbricated fine to medium schist and greywacke derived sandy gravel. Minor twigs and wood are scattered through out and twig material was collected for possible dating from near the base of the unit. This material appears to have accumulated as a locally derived alluvium and colluvium associated with nearby spring sapping and slope wash off the scarp. There is no sign of shearing in this unit.

This horizontally bedded unit passes down abruptly into a tight silty medium gravel which has no particular bedding or imbrication on the eastern side of the pit. However the more elongate schist clasts present become progressively more rotated and vertical on the western side. They pass laterally into a dense peat of small twigs and leaves pressed in a fine organic matrix. This appears to be the most recent locus of shearing and the organics have been trapped during coseismic displacement against the large boulders of the distal end of the displaced landslide. Further down the organics progressively become more gritty and gravel derived and disappear. A sample of fine twigs and leaves was extracted from the peat matrix in the inferred shear zone, close to the horizontally imbricated upper unit, and was submitted for dating (Wk 5529). This sample returned a radiocarbon age of 210 ± 50 BP.

This matches the dates for the Toaroha event, as indicated in the Toaroha 2 and Kokatahi 2 trenches. It is also a good fit with the nearby Moss Creek debris flow, the Haupiri River aggradation terrace, and the Mt Harry rock fall. It cannot be reconciled with the Crane Creek event. This date comes from material of virtually no self age, trapped within a shear, and suggests the Toaroha event occurred not very long after deposition of the overbank silt unit in the Toaroha 2 trench.

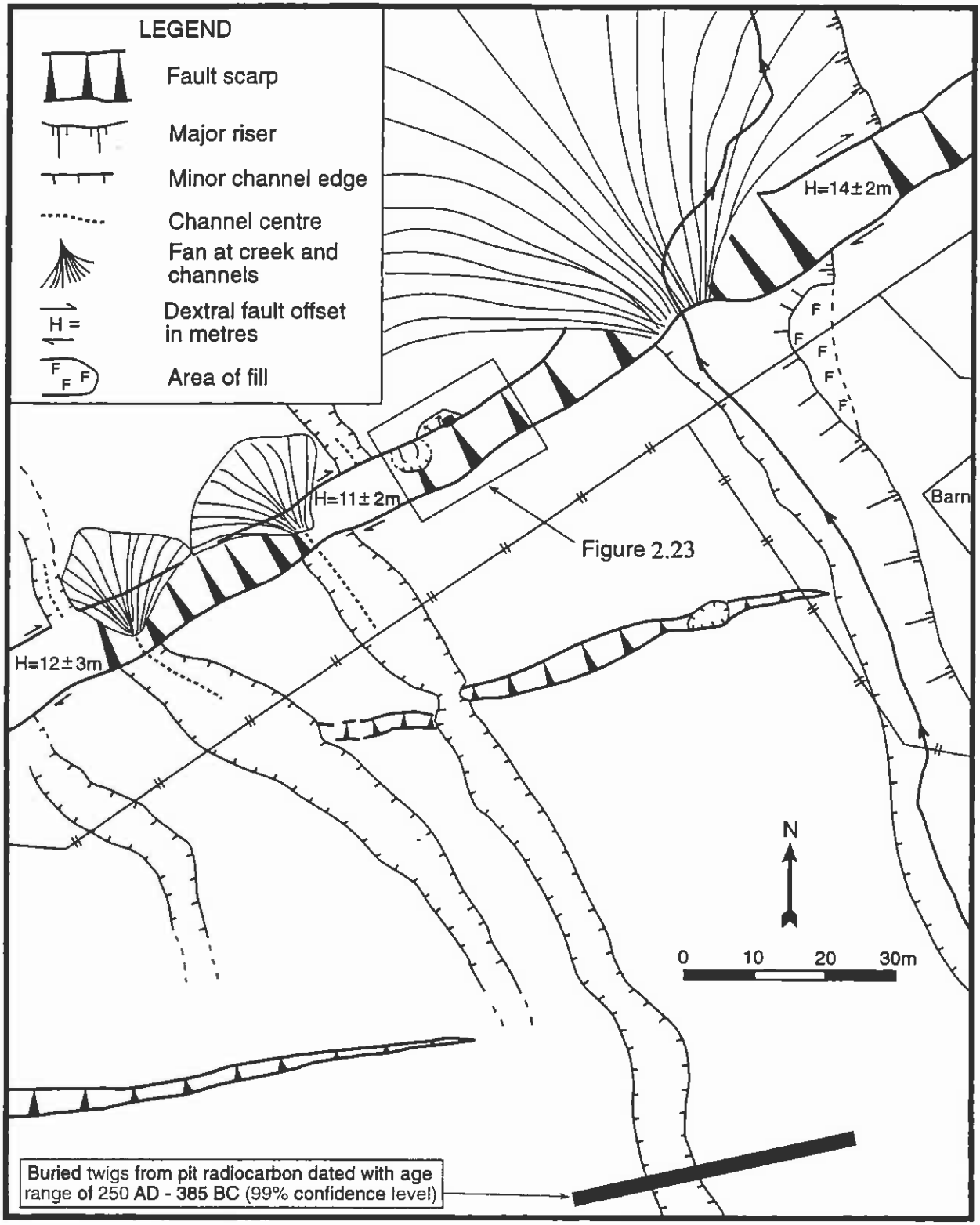

Figure 2.22 - A more detailed map of the trace on the true right of the Haupiri River. A long term slip rate of 6.3 ± 2 mm/yr can be obtained by averaging the channel and riser offsets and adopting an age for the tread obtained from the pit shown at the bottom of the figure.

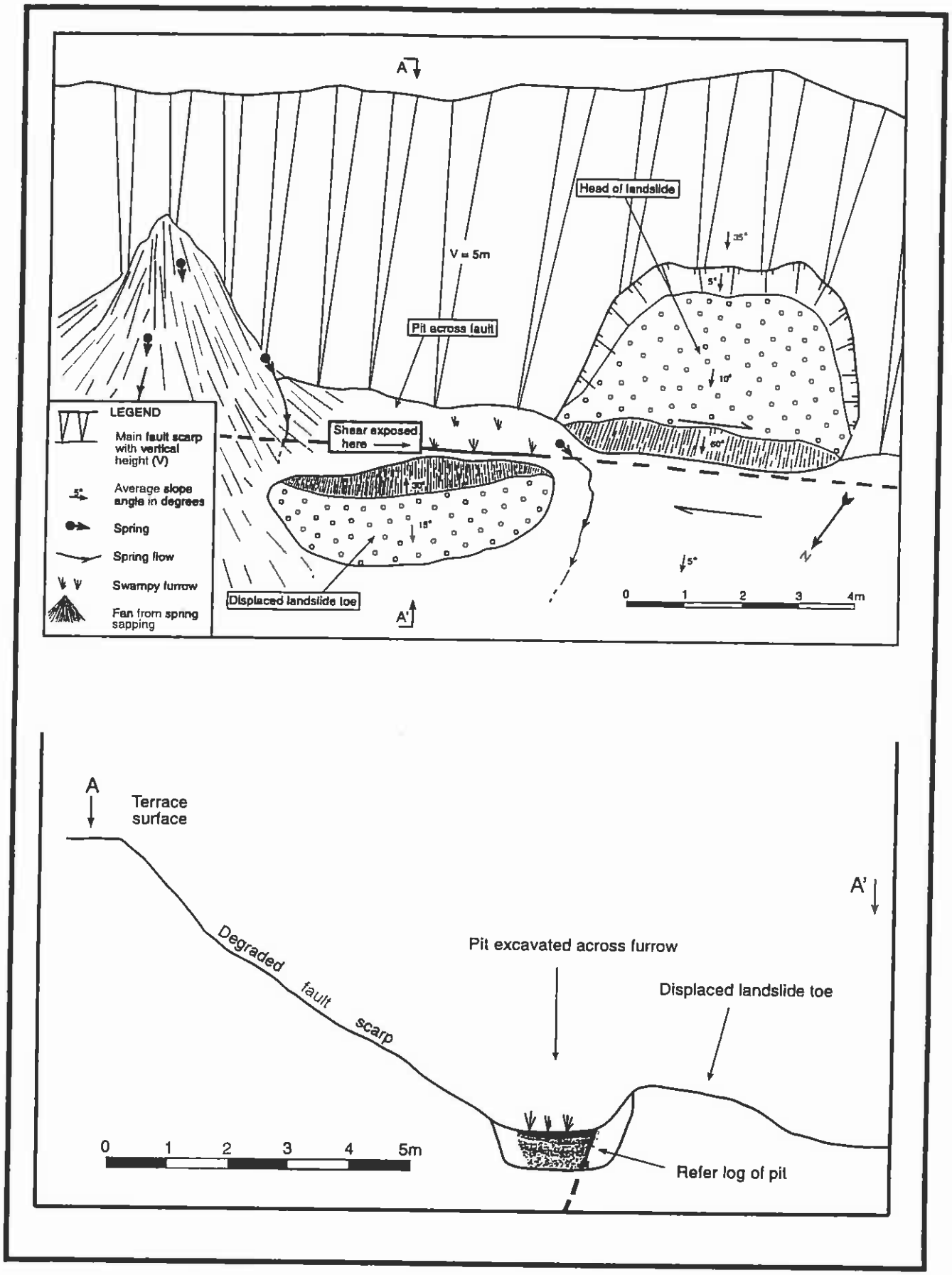

Figure 2.23 - A displaced landslide with associated fault furrow at the base of the scarp shown in Figure 2.22. A small hand dug pit was excavated at the location shown in the plan and section.

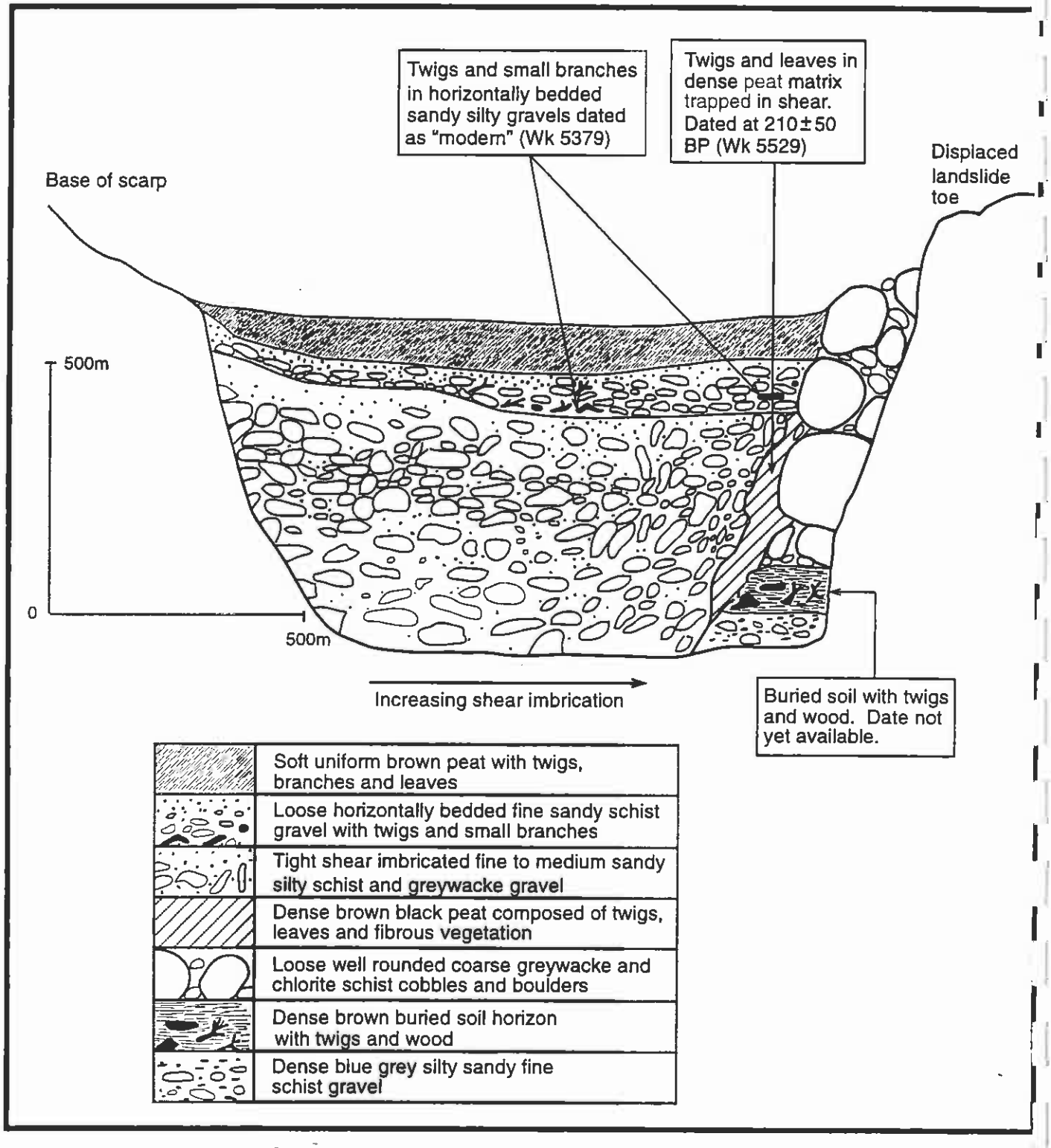

Figure 2.24 - Log of the hand dug pit excavated across the shear displacing the landslide shown in Figure 2.23. A date of 210 ± 50 BP was obtained from twigs and leaves within peat caught in the shear.

This date of 210 ± 50 BP makes it very close to the youngest limit of radiocarbon dating resolution at around 200 BP. This would correspond to a most likely general time period for the Toaroha event at around 1700 - 1750 AD. Organic material of this age will sometimes return a finite conventional age of around 200 - 250 BP but will also sometimes appear as "modern" (A. Hogg, pers. comm. 1998). This may also be the explanation of the apparently anomalous "modern" dates returned for some of the samples in the Toaroha 1 and Toaroha 2 trenches, which were otherwise attributed to logging disturbance.

Further west in the Haupiri pit the large well rounded boulders of the displaced landslide can be traced downwards into a thick peat rich in moderate sized partly rotted branches. This horizontal peat unit continues laterally under the displaced landslide material exposed in the drain and grades progressively out to the current forest floor. Material was recently collected for dating from this buried unit because it potentially dates the landslide which was very likely to be earthquake triggered in this type of location. This date is not yet available.

The Haupiri pit confirms that ground rupture in the Toaroha event extended past the Hope Fault junction at the Taramakua River. This event was not present 5 km further north at the Crane Creek pit, or 11 km further north at the Ahaura River trench. This indicates the northern limit of the rupture in this event was somewhere between the Haupiri River and Crane Creek. It is possible the rupture splayed off to the east of Crane Creek along one of the numerous shear zones striking east from the Alpine Fault zone in this area. Alternatively the rupture at the ground surface along the Alpine Fault trace may have simply decreased to zero over this 5 km.

2.3 Summary

Trenching indicates two rupture events in the last 500 years in the central section of the Alpine Fault. The earliest of these, referred to as the Crane Creek Event, occurred approximately 380 years ago and most probably at 1620 ± 10 yrs AD. The most recent rupture, the Toaroha River event, occurred relatively soon after, post 1660 AD and probably between 1700 and 1750 AD. The rupture for this last event ended just north of the Haupiri River. All five trenches are consistent with one another.

Support for the possible use of aggradation terrace dates as indirect paleoseismic indicators is provided by the excellent correlation between a terrace age and a date for an earthquake in a fault trench at the same site.

Chapter 3

INDIRECT EVIDENCE OF PAST EARTHQUAKES FROM TERRACE AGES AND LANDSLIDES

3.1 Introduction

The trenching described in the previous chapter indicates two Alpine Fault earthquakes in the last 500 years, with one occurring prior to 1640 AD, and the other between 1660 AD and European settlement (most likely 1700 - 1750 AD). Is there indirect evidence to support this in the record of landslides and aggradation terrace ages in Westland ?

As noted in Section 1.3 Adams (1980) assumed the terrace record of rivers draining the Southern Alps range front reflect aggradation following massive sediment pulses created by Alpine Fault earthquakes. In Crane Creek we noted the excellent correlation between the age of an aggradational terrace and the trench record lending support to Adams method (refer page 23). This terrace, and the red beech logs it contains, is shown in Figure 3.1.

The consequences of massive aggradation following historical earthquakes has been noted as early as 1770 by Captain J. Cook in his visit to Jakarta (Hough, 1995). These impacts in steep forested tropical regions are well described in the international literature (Wright & Mella 1963; Pain 1972; Pain & Bowler 1973; Tutton & Browne 1994; Schuster et al 1996). In New Zealand Adams (1980) highlighted the importance of the process in his modelling of Southern Alps erosion. A subsequent more detailed study of the profound geomorphic and botanical impact of the 1929 Buller Earthquake (Magnitude = 7.8, also referred to as the Murchison earthquake) is outlined by Pearce & O'Loughlin (1985) and Pearce & Watson (1986).

Figure 3.1 - The aggradation terrace in Crane Creek 400m downstream of the Alpine Fault discussed on page 23. Red beech logs are visible projecting from the loose sandy gravel of the eroding terrace edge which were dated at 390 ± 60 BP comparing well with the trench dates of 380 ± 25 BP and 360 ± 60 BP.

Figure 3.2 - A rimu log projecting from an aggradation terrace near the Alpine Fault in the Poerua River near Hari Hari (refer Fig. 1.3). Sapwood from this log returned a radiocarbon age of 520 ± 60 BP, similar to Adams (1980) inferred event of c. 550 BP.

The terrain affected in the Buller event is steep, densely forested, and is subject to high rainfall. In these respects it closely resembles the Southern Alps range front. In the Buller event the short term impacts of the sediment supplied by landslides overwhelmed the river system. Aggradation raised the bed levels on average 1 - 3.5 m, inundating standing forest and burying large amounts of wood. Although the rivers have subsequently cut channels into the aggradation surfaces only a negligible proportion of the sediment delivered by the landslides has been removed since the earthquake (Pearce & O'Loughlin 1985).

Past Alpine Fault earthquakes will have had impacts at least as severe as the Buller earthquake and this should be reflected in the ^{14}C ages of aggradation terraces and mass movement deposits. In addition Alpine Fault events change the regional base level along the range front and uplift surfaces thereby creating flights of terraces. This increases the chances of finding wood which may represent individual events by physically separating past aggradation surfaces.

Landslides can also be used as paleoseismic indicators as recently outlined by Jibson (1996). Cowan et al (1996) applied this method of analysis to ten landslides over a 8000 year period in the Porters Pass fault zone. In general landslides can more often be a local feature triggered by some other process, in contrast to a more profound and catchment wide process such as aggradation. However large landslides like rock avalanches or debris avalanches are commonly earthquake triggered. So are landslides on the fault scarp itself where slope angles are moderate and the forest cover extensive (for example the small landslides on the scarp at Haupiri River [Figure 2.] and Crane Creek [Figure].

3.2 Terrace Description

Figure 3.2 shows a typical aggradation terrace near the Alpine Fault containing buried logs in the Poerua River. This type of terrace is now often discontinuous up and down the river valley, due to the lateral river erosion following down-cutting. The gravel making up this type of terrace is generally loose, sandy and poorly imbricated, reflecting the inability of the river to sort and transport the sediment influx. Wood collected for radiocarbon dating at locations such as this provides a method of estimating the approximate time of the earthquake which may have caused the aggradation.

In many terraces an aggradational upper horizon can be recognised capping an older degradation erosion surface. Presumably this occurs as an aggradational pulse fills the existing channel, and the alluvial fill then spills out, to grade over the top of older low level degradational terrace treads. In other locations the same terrace tread in crossection appears to be almost entirely degradational. We interpret this as the consequence of a new section of river bed cutting associated with channel avulsion (ie diversion) during the aggradation. It appears most terrace treads, in both plan and crossectional view, are a complex mix between the two basic terrace types.

3.3 Dating of terraces and landslides - results from an enlarged data-set.

As part of this study a further 14 ^{14}C dates have been obtained from aggradational gravels, fans, and mass movement deposits for the most recent 750 year period. These new dates have been combined with 3 collected by others (T. Chinn pers. comm. 1996, Basher, 1986) and two dates originally used by Adams in this youngest time period. These dates have a geographic spread from Crane Creek to the Karangarua River (more than 200 km, refer Figure 1.3 for location details) and Table 3.1 summarises the site information details. Eleven ^{14}C dates come from terraces and nine from mass movement deposits including rock avalanches, rock falls, landslides, debris avalanches and debris flows.

Feature	Description and location with respect to the Alpine Fault	^{14}C age ± error	Lab. Code	Collector	Grid R
Moss Creek Debris Flow	Youngest sapwood from a Totora stump, buried by the distal end of debris flow from a creek 300m east of the fault.	210 ± 50 BP	WK 4876	M. Yetton	K32/0
Haupiri River 3m Terrace	Youngest sapwood from a Red Beech log in a terrace on the true left of the Haupiri River, 200m upstream of the fault.	260 ± 50 BP	WK 4874	M. Yetton	K32/05
Mt Harry Rockfall	Punga fragment in granitic rockfall debris from the east side of Mt Harry near the Toaroha River, 200m west of the fault.	200 ± 50 BP	WK 4919	M.Yetton	J33/56
Crane Creek 4m Terrace	Youngest sapwood from a Red Beech log in a terrace on the true left of Crane Creek, 100m west of the fault.	390 ± 50 BP	WK 4343	M.Yetton	K32/09
Styx Rockfall	Peat in voids of protomylonite rockfall debris which has fallen into a peat swamp at the base of the 30m high fault scarp.	430 ± 60 BP	WK 4918	M.Yetton	J33/60
Kokatahi River 5m Terrace	Twigs from near the top of the terrace on the true right of the Kokatahi River, 30m downstream of the fault.	330 ± 60 BP	WK 4009	M.Yetton	J33/579
Toaroha River 1m Terrace	Small Rata branch near the top of a terrace in a sandy unit. The terrace is downwarped at this location 25m west of the fault.	320 ± 60 BP	WK 4014	M.Yetton	J33/57
Poerua River 6m Terrace	Sapwood from a Rata branch in a loose sandy gravel terrace on the true left of the river, 1km downstream of the fault.	370 ± 60 BP	WK 4340	M Yetton	I34/083
McTaggart Debris Avalanche	10 year old sapwood from an exhumed Miro stump under a 30m thick schist debris avalanche deposit, 6km east of fault.	420 ± 25 BP	WK 5264	M. Yetton	H36/53
Cropp River Rock Avalanche	Twigs from the base of a mica schist rock avalanche deposit on the true right of the Cropp River, 9km east of the fault.	360 ± 50 BP	NZ 5252	L. Basher	J34/478
Parker Creek Debris Flow	Branch from the base of a schist debris flow and fan deposit overlying Whatoroa River alluvium, 300m west of the fault.	430 ± 50 BP	NZ 6684c	T. Chinn	I35/003
Konini Creek Debris Flow	Twigs and peat from the base of a schist derived debris flow from a side creek of the Haupiri River, 700m west of the fault.	510 ± 60 BP	WK 4875	M. Yetton	K32064
Styx River 2m Terrace	Heart wood of a small rata branch in a low terrace on the true right of the Styx River, 300m upstream of the fault.	680 ± 50 BP	WK 4011	M. Yetton	J33/59512
Toaroha River 3m Terrace	Sapwood of a large Kamahi log in terrace base, true left of Toaroha River, 200m upstream of fault.	650 ± 60 BP	WK 4019	M. Yetton	J33/572
Toaroha River 2.7m Terrace	Sapwood fragment of Rata log in same terrace as above but on the true right of the river and 100m upstream of fault	580 ± 60 BP	WK 4013	M. Yetton	J33/5731
Muriel Creek 4m Terrace	Sapwood for Ribbonwood branch in fine schist gravel terrace on true left of Muriel Creek, 400m upstream of the fault.	540 ± 60 BP	WK 4439	M. Yetton	J33/502
Waitaha Fan	Wood of unknown species and self age buried in fan gravels on true left of Waitaha River, 500m downstream of the fault	680 ± 40 BP	NZ 4629c	J. Adams	I34/2548
Wanganui River 10m Terrace	Heartwood sample with estimated 80 years allowed for missing rings from base of terrace 6km east of fault	610 ± 70 BP	NZ 4628c	J. Adams	I34/210
Geologists Creek Rock Avalanche	Heartwood from small branch in 15m thick mylonite and gouge rock avalanche deposit 300m from fault scarp	550 ± 50 BP	NZ 6471	T. Chinn	J33/6071

Table 3.1 - Sample details for dated aggradation terraces and mass movement deposits less than 750 years old within 10 km of the Alpine Fault in north and central Westland.

Figure 3.3 presents the two sigma calendric conversions for these dates adopting the methods of Stuiver & Reimer (1993) and the 40 year southern hemisphere offset of Vogel et al (1993). All the available dates for this time period are included in Figure 3.3, none have been excluded because of a poor match. Despite this the repetition of common date ranges is immediately apparent, particularly in the middle group.

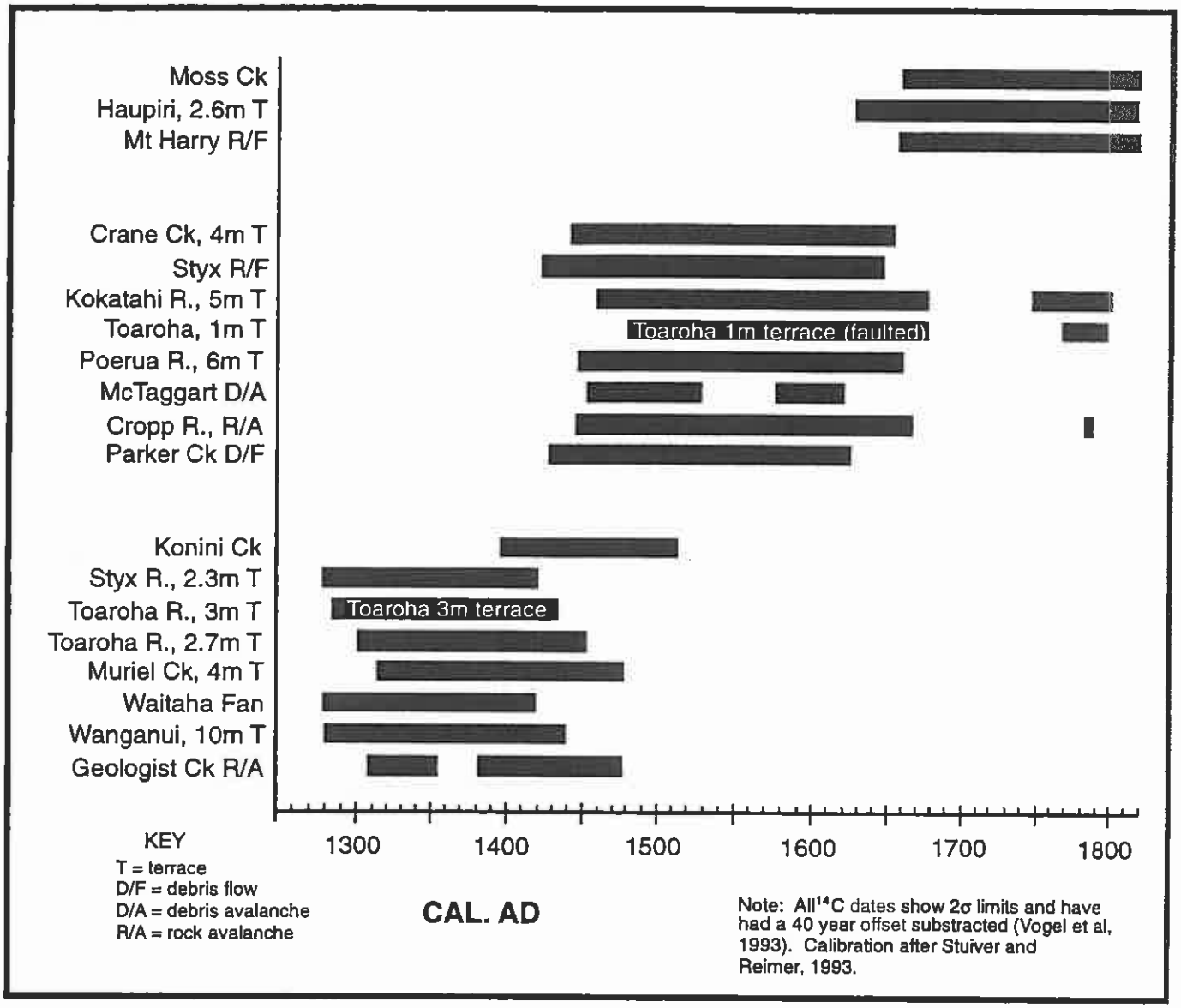

Figure 3.3 - Terrace and landslide age ranges for all dated examples within 10 km of the Alpine Fault in north and central Westland. Refer Table 3.1 for the site information.

Wiggles in the radiocarbon calibration curve (refer Appendix 1) for some dates in the middle group (for example the Kokatahi 5m terrace) produce several discrete possible calendric time ranges for a single dated sample. As a result three of the dates in the middle cluster could belong the youngest cluster, however they have a much higher probability of belonging to the middle group.

The considerable time span for each date is the inevitable result of the radiocarbon dating method and this is particularly the case with dates for the last 500 years. In this age range increased laboratory analysis precision (for example ± 20 or 25 years) offers only a minor increase in resolution. The most important feature to note in Figure 3. 3 is the apparent coincidence of the date ranges, rather than their precise calendric resolution. A series of radiocarbon dates from the same piece of wood from 1620 AD would look exactly like the middle cluster of calendric ranges.

Analysis of the dates using the standard T test for ^{14}C dates of Wilson and Ward (1978,1981) confirms the impression from Figure 3.3 that there are two main clusters of dates with a possible poorly defined third set. The modal calendric age range (ie. that age fitting the most dates in each cluster) is around 1400 - 1420 AD for the oldest group (and referred to here as the 1400 AD group). There is then a middle group of eight dates which appear tightly clustered but have a large calendric range from 1480 - 1640 AD (the 1600 AD group) and which we attribute to the Crane Creek event. This is followed by a more limited younger group with a range from 1675 - post 1800 AD (the 1700 AD group) which may reflect the Toaroha River event.

In most cases it is difficult to use geologic criteria to help in distinguishing and grouping this type of data. However, some limited support for the statistical separation of these dates into three clustered groups is suggested on the true right of the Toaroha River near the fault trace. Here a date of 320 ± 60 years BP (Wk 4014) comes from a down warped terrace at the fault scarp which is now only 1m above river level. This date fits into the middle 1600 AD cluster. The down warping of this terrace tread implies a younger earthquake, possibly the 1700 AD event The next highest terrace above the 1600 AD surface date yields a date of 580 ± 60 yrs BP, which fits in the oldest 1400 AD group, and suggests subsequent uplift during the 1600 AD event.

3.4 Discussion

Aggradation and landslides as earthquake indicators are both indirect and ambiguous. As noted in the introduction they can also be the result of climatic events, vegetation change and fire, or alternatively earthquakes on other nearby faults. While there is no doubt that large Alpine Fault earthquakes would have created regional aggradation and landsliding along the Southern Alps range front, it is also likely other triggers have supplemented the record, at least locally.

Flooding is a short term climatic impact which can lead in some circumstances to aggradation. However there are some important differences between the sedimentary products of earthquake triggered aggradation, and those of flood, which tend to support an earthquake origin for these clustered dates. The earthquake triggered aggradation process responsible for burying and preserving wood in a region of rugged and forested catchments such as central Westland is summarised in Figure 3.4.

An earthquake results in a massive sediment overload relative to carrying capacity for even the largest rivers. The resulting aggradational sediment is typically less sorted and more sandy than normal; is less imbricate and tight; and can be locally rich in

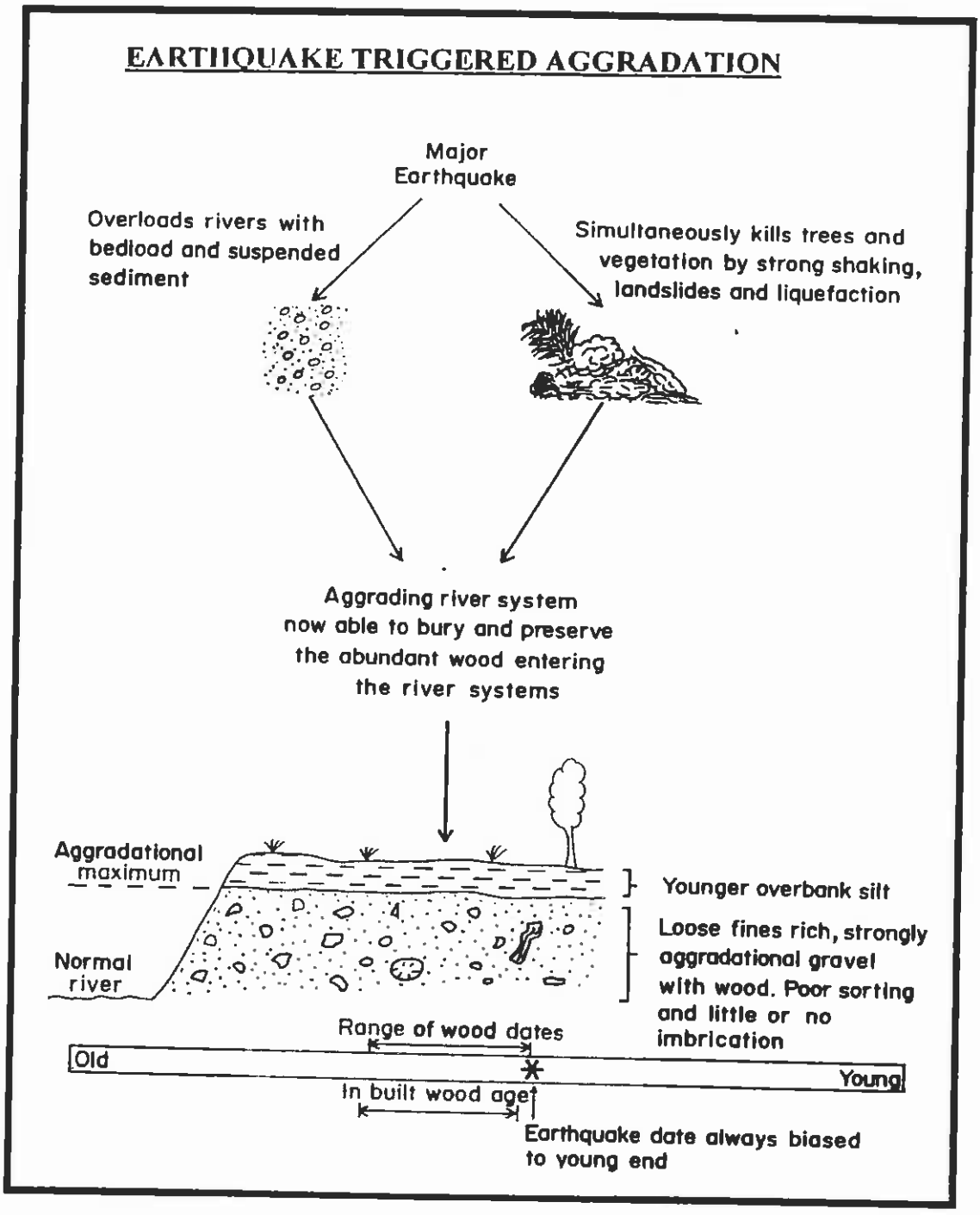

Figure 3.4 - A summary of the aggradation process responsible for burying wood following a large earthquake in a steep forested catchment in Westland.

buoyant material such as wood and plant matter which the rivers would normally float out. It follows that for this reason alone a post earthquake environment of excess sediment favours preservation of a datable record. However, equally as important is the simultaneous impact on an earthquake on tree and plant mortality. Many more trees and plants than usual die in the earthquake and in the immediate post seismic period. This wood enters the river system at the exact time the excess of sediment favours it's burial and preservation.

Figure 3.5 is from Pearce (1986) and shows the burial of fallen and standing forest by aggradation in the Matiri River after the 1929 Buller earthquake. This is a classic example of sediment overload relative to carrying capacity, from which this section of the Matiri River has yet to recover. Presumably the river at this location will ultimately down-cut again, and convert this alluvial fill surface to a corresponding terrace tread and riser. This subsequent process of terrace creation is made much simpler for the Alpine Fault by the component of uplift in each successive earthquake.

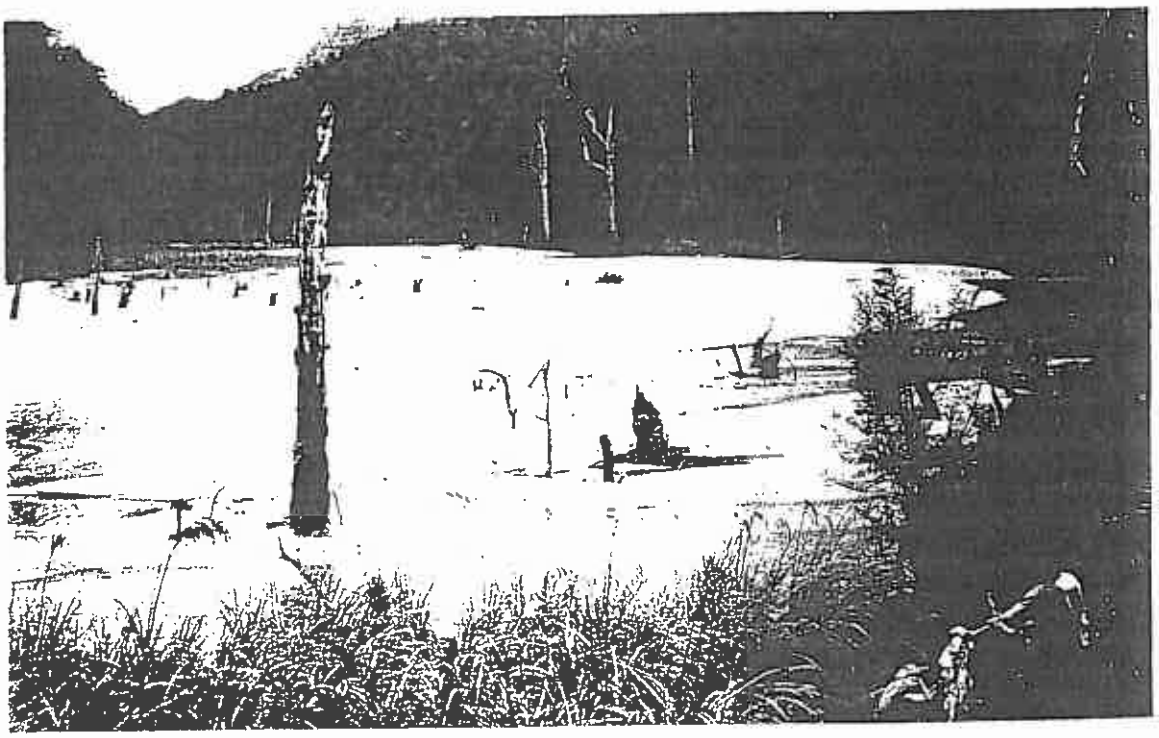

Figure 3.5 - Photo from Pearce & Watson (1986) showing the extent of aggradation in the Matiri River catchment in the epicentral area of the Buller earthquake of 1929. This photo is taken 60 years after the earthquake but aggradation sediment at this location is still yet to be dissected and terraced.

Floods by contrast are the main method the rivers clear themselves of buoyant material. Apart from the wood temporarily stored on high areas by receding floodwaters it is extremely rare for wood to be trapped in the gravel bed load being moved during floods. Floods are characterised by an abnormal increase in carrying capacity, and a corresponding increase in sorting efficiency, so that only the very largest of rain triggered landslides leaves a large volume of organic rich gravel, and then generally only in the second order catchments. The existence in a major river of wood trapped in the poorly sorted and loose bedload of an exposed terrace is a reasonable indication that floods have not been responsible.

Fires can also cause landslides and local aggradation by vegetation disturbance, but these tend to be triggered after the fire in times of heavy rain, and once again when stream power is high. In addition fires are not common in the humid and wet range front of Westland.

The best criteria for assuming the record of aggradation reflects earthquakes as opposed to the alternative explanations outlined above, is the regional extent of the pattern. A check of available records indicates there is no historical precedent for fires or storm induced regional river aggradation in Westland over the past 160 years (Benn, 1990). Westland weather and floods tend to be characterised by localised extremes of rainfall occurring within an overall regional wet cycle. The landscape has generally adapted to these regular wet cycles and widespread damage is not common.

Age Implications

There are also some implications for age interpretations based on the dates from wood in earthquake triggered aggradation gravels. Some of the dated wood and plant material would have been killed synchronously by landsliding associated with the earthquake. The ^{14}C date from such material will then reflect the true event age. However most of the time the highest points in the active river beds of Westland are littered with logs and wood left by receding flood waters. Most of this wood is being progressively floated away in successive floods but some of the more durable wood can survive on surfaces temporarily for many years in these locations. It is likely some of this material would also be buried by an earthquake triggered aggradation pulse thereby distorting the age pattern.

For this reason ^{14}C dates from wood in aggradation gravels when averaged will tend to have an age mode older than the aggradational event responsible for the burial. By concentrating on sampling and dating bedload wood which appears relatively fresh and undecayed potential errors can be minimised.

Limitations of landslides as paleoseimic indicators

Excessive reliance on landslides as earthquake indicators is more problematic. To try to help focus on potential earthquake triggered failures most of the landslides in Figure 3.3 are from either large-scale deep-seated catastrophic failures, for example rock or debris avalanche deposits within 10 km of the Alpine Fault, or smaller rockfalls and debris flows right on the fault scarp. The common association between the larger scale catastrophic features and earthquakes is well documented, for example Keefer (1984a, 1984b, 1994). While it is possible that some of the local scarp failures may be unrelated to past earthquakes, at least the majority are likely to reflect earthquake triggering.

The difficulty with using landslides, as opposed to aggradation terraces from large rivers, is that landslides can more easily occur as local features without seismic triggering, and in the same area of weakened fault zone rocks that coseismic landslides are most abundant. An excellent historical example is "Robinson Slip" on the true right of the Waitaha River (GR I34/ 265875). This is very close to the promising paleoseismic trench site of Wright, 1997.

This old landslide feature is now marked by a prominent fan which has built out of Macgregor Creek, a small second order tributary to the Waitaha River, in which a large landslide occurred in 1903. This was after a period of sustained heavy rain and extreme local flooding (Jim Ferguson, pers. comm. 1996). The tributary drains the

Figure 3.6 - Macgregor Creek on the true right of the Waitaha River near the Alpine Fault. The creek has re-exposed buried forest from a large rainfall triggered landslide which occurred in 1903.

Figure 3.7 - A close up view of the current creek edge where standing trees are being exhumed from the active terrace riser.

Alpine Fault zone and the fan is composed of mylonites, protomylonite, rare gouge (cataclasite) and high grade schist. Apparently the debris flow associated with the landslide formed most of the large fan shape, with the fines extending the greatest distance and flowing onto the upper Waitaha Valley road. Horses got stuck in the "quick sand" and it took many weeks to clear the road. A large area of mature forest was inundated and completely covered by the debris. The fan continued to grow for a period after the landslide, as other smaller failures occurred on the margins of the main landslide, and the upper catchment disgorged the remaining debris.

Figures 3.6 and 3.7 are recent photos taken in Macgregor Creek, which has now incised into the aggradation surface of the original fan. This shows trees buried in growth position which have now been exhumed by the subsequent down-cutting. The height of the trunks conforms to the original aggradation surface where most of the tops of the dying trees have subsequently broken off. This process of trunk trimming at the new ground level is apparently very rapid (often just 1 - 2 years) and assisted by massive infestations of pinhole borer which occur amongst so many dead trees. But not all trees have fallen, and in some areas of the fan surface, the heart wood of dead trunks still protrudes amongst the young forest colonising the surface.

Older examples of this type of non-seismic local burial event no doubt exist in many other places along the Southern Alps range front. The critical difference is that this type of feature will not be synchronous over a very large area. Apparently the rain responsible for Robinson Slip was severe in the Waitaha catchment and areas immediately to the south and north, but was not a widespread regional extreme event. Similarly although the sediment overload was profound for Macgregor Creek there is no obvious equivalent new terrace in the much larger Waitaha River, which was in flood at the time, and this also indicates the essentially local impact.

Robinson's Slip is a good example of the type of sediment overload which would happen synchronously on a much larger scale during an Alpine Fault earthquake. This type of seismic triggered aggradation would be enough to extend into the large rivers and well forward of the range front, and in some areas the impacts of this aggradation would reach the coastline.

Robinson's slip indicates it is possible that some of the landslides (and possibly also some of the aggradation terrace dates) which are included in Figure 3.3 are non seismic in origin. But given that the trenching indicates Alpine Fault earthquakes occurred within the time ranges noted, then for the reasons outlined above, these earthquakes can be reasonably expected to have dominated the record and the modes of the time ranges will approximate to the earthquake event timing.

3.5 Summary

The original data-set of Adams (1980) for the radiocarbon ages of aggradation terraces and landslides in Westland over the last 750 years has been significantly enlarged from three dates to a current total of nineteen. It is probable that apparently clustered regional aggradational and landslide events which occur at around 1400 AD and 1600 AD (and to a lesser extent around 1700 AD) were triggered by rupture on the Alpine

Fault. The limited geological evidence for terrace uplift and deformation of some of these terraces is consistent with three earthquake events in the last 750 years. The timing of the last two clusters is also consistent with the trench data outlined earlier in Chapter 2.

However, without the trenching first indicating rupture events in these time ranges, this type of indirect evidence is not conclusive. It is likely that the paleoseismic signal within this data is being muted to some extent by the self age of the wood and the possible inadvertent inclusion of some dates of a non seismic origin.

Chapter 4

EVIDENCE FROM FOREST AGE PATTERNS AND TREE RING CHRONOLOGIES

4.1 Introduction

Trenching has indicated two earthquakes in the last 500 years, one before 1640 AD and one after 1660 AD and before European colonisation. Where is the evidence in the forest and tree record which can be logically expected for these events ?

New Zealand conifer species regenerate prolifically only on recently created or bared surfaces. A large earthquake creates these surfaces by landsliding and the associated aggradation and flood damage clears forest from existing surfaces. In addition earthquake shaking causes extensive tree fall in forests not directly affected by deposition, floods or landslides. Tree fall can also result from liquefaction of the underlying substrate. In this manner a large earthquake can cause disturbance over a wider range of landforms than a climatic extreme event such as a wind storm or flood. There are several international examples of forest disturbance and stand regrowth episodes in response to large earthquakes (for recent New Zealand and international examples refer Allen et al, in press; Jacoby, 1997; Veblen et al, 1993; Kitzberger et al, 1995).

Figure 4.1 shows the dense forest cover typical of most of the Alpine Fault in Westland. For contrast Figure 4.2 was taken in the Harper Stream following the Magnitude 6.7 earthquake of June 1994. This area was also densely forested below the snowline but the extensive landslides triggered by this relatively small earthquake stripped trees from many areas and deposited them in the rivers. Rupture of the much larger Alpine Fault will cause much greater damage and it is logical to presume this type of disturbance event will be reflected in the distribution of forest age, with modes of tree age corresponding to simultaneous re-establishment after the event.

Figure 4.1 - Extensive mixed red beech forest and podocarp forest typical of the Alpine Fault zone immediately north of Crane Creek.

Figure 4.2 - Damage to beech forest in the Harper River after the 1994 Arthurs Pass earthquake. Note also the large amount of wood in the aggrading channel. Photo courtesy of Chris Chamberlain.

Figure 4.3 - An even age forest stand following forest re-establishment on a relatively young landslide near Goat Creek. An earthquake results in synchronous landslides with many areas of new forest which are all of the same age. Photograph courtesy of Glen Stewart.

Figure 4.4 - Coring a large rimu tree (age greater than 500 years) on Surface C on the true left of the Toaroha River (Figure 2.12, page 31). We are grateful to Professor William Bull (University of Arizona, Tucson) who assisted with this work and can be seen in the background.

4.2 Regional Forest Age Patterns

Even age forest stands can be recognised visually on many slopes in Westland. Figure 4.3 shows a relatively young example from Goat Creek, near Otira. It is possible to obtain the age of trees in this type of location by extracting a thin core of wood revealing the annual rings. Figure 4.4 shows the process in action. This does not kill the tree and it is possible to sample up to 30 trees or more by this method in a days work. The information from individual trees can then be combined into stand age (for the combined population).

Wells *et al* (in press) have compiled all the available information on forest stand age throughout Westland. Figure 4.5 shows the locations of the forests for which the data has been compiled and which extend along approximately 250 km of fault strike. The most southern forest for which data is available is Ohinemaka, near the Paringa River, while the most northern forest is the Rahu forest, near Reefton.

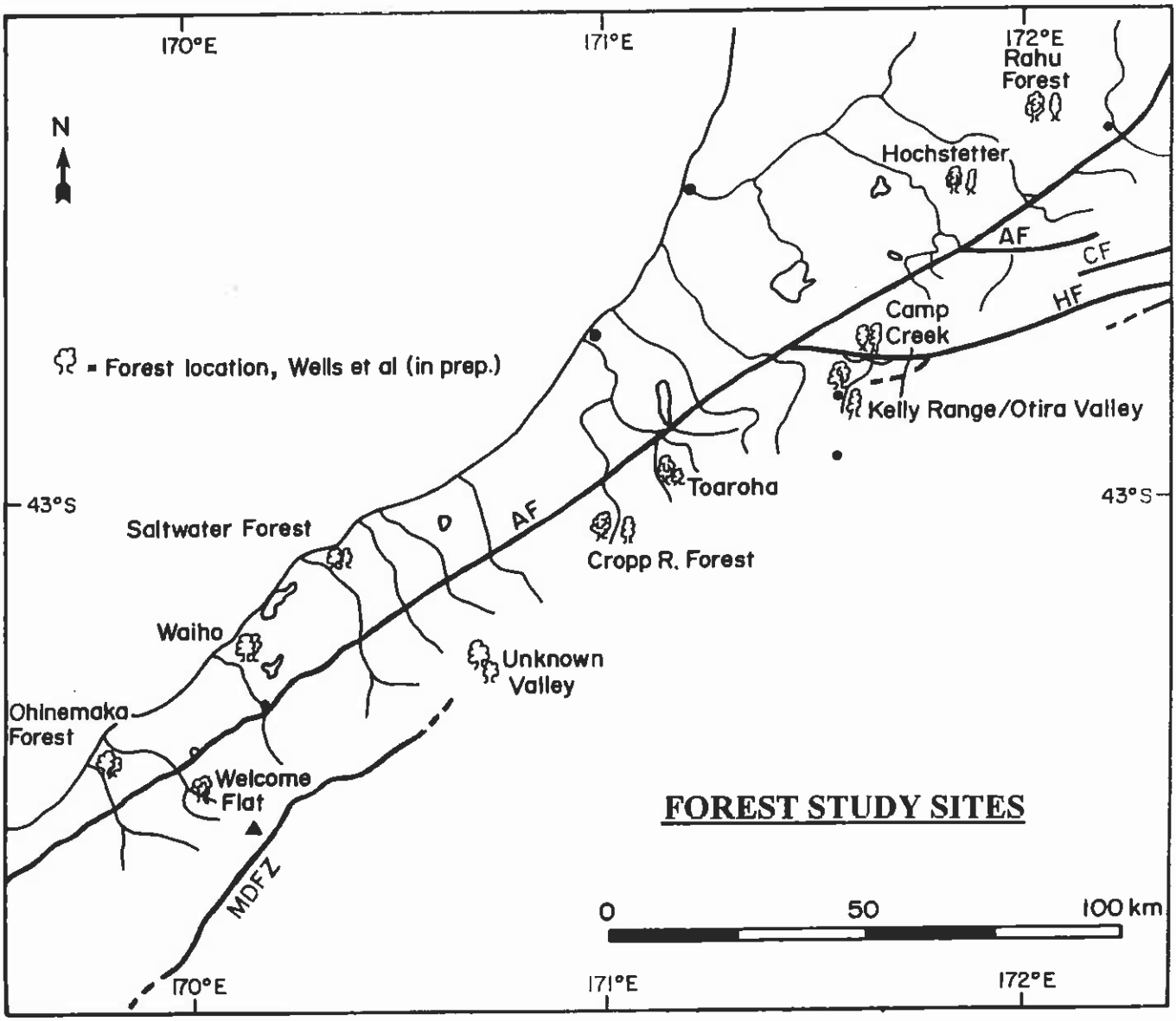

Figure 4.5 - Forest locations in Westland and Southern Alps for which forest stand age information is available for analysis.

Figure 4.6 shows the data with an arbitrary 40 years added to the tree ages to allow for establishment of the first colonisers. This shows two main modes of forest initiation following massive regional disturbance at around 1400 - 1450 AD and 1600 - 1700 AD. The later peak is much broader than the 1400 - 1450 peak and the authors suggest this may reflect two disturbances relatively close together, basing this on more detailed work at the Karangarua River. These modes of common forest age can be recognised across a wide range of landforms from steep uplands to much flatter alluvial and moraine deposits. The authors have independently suggested Alpine Fault earthquakes as a possible explanation of the pattern.

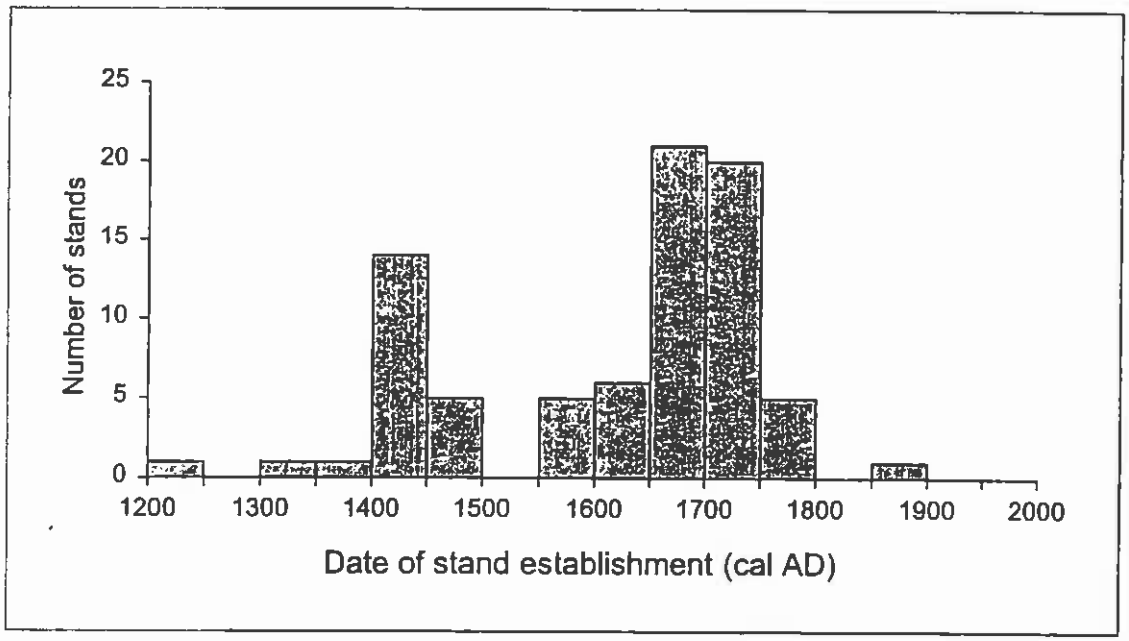

Figure 4.6 - Modes of forest stand establishment from the forests shown in Figure 4.5 from Wells et al (in press). The date of stand establishment has been estimated with an arbitrary 40 year allowance for colonisation and growth to shoulder (corer) height.

The forest disturbance and regrowth pattern fits the date clusters in the aggradation and landslide record well. The disturbance initiated between 1600 and 1650 AD matches the Crane Creek event and connects this forest disturbance with the Alpine Fault. The disturbance record for the Crane Creek event has also been further analysed by Wells to check for any systematic north - south variation in the timing of disturbance. Within the limitations of the 25 year age classes the timing appears synchronous across the region, suggesting the Crane Creek event was a single earthquake responsible for forest damage between Ohinemaka Forest and the Rahu Forest (approximately 250 km). However it is also possible that a progressive rupture over a relatively short time period occurred. Something similar occurred historically in

Turkey with six events of Magnitude 7 - 8 which migrated westward over 750 km of the North Anatolian Fault in the 28 years between 1939 and 1967 (Barka & Kadinsky - Cade, 1988). This pattern may not be recognised in this forest age analysis depending on when the events occur with respect to the 25 year age classes. It is likely cross matched tree ring chronologies will be the only method with sufficient precision to check this possibility.

To investigate the suggestion that the broad forest age peak between 1600 and 1750 is actually two peaks close together Wells *et al* (in prep.) selected only the regional data able to be plotted in 10 year age classes, and combined this with age information obtained from new work in the Karangarua River. The forests selected were also restricted to those clearly colonising new young surfaces created either by landsliding or terrace formation. For this analysis forest on older surfaces such as moraines and high level terraces was excluded.

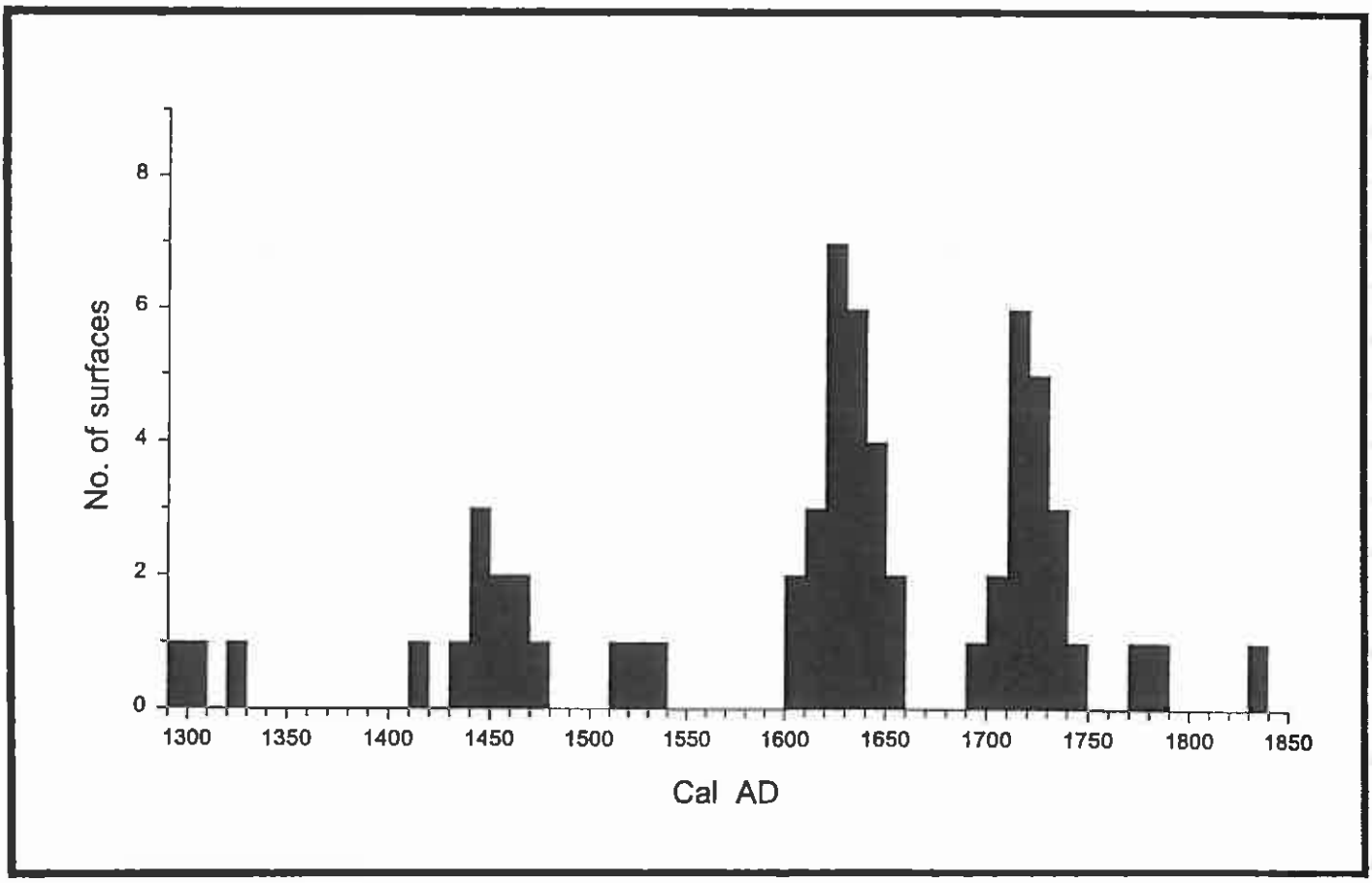

Figure 4.7- Ages of new landslide and terrace surfaces from the Karangarua Valley (37 surfaces) and central and south Westland (24 surfaces) derived from the age of the oldest tree on each surface plus an addition for colonisation time.

In addition the arbitrary 40 year delay added for colonisation time and growth to corer height was refined. New surfaces known to have formed in historical times were investigated and aged separately for the angiosperm species (Kamahi and Rata) and the five conifer species. The mean for the angiosperms was 20 years (range 14 - 27) and for the conifers was 36 years (range 15 - 60). Figure 4.7 presents the new information.

The improved data quality and delay time estimates now clearly delineate two modes of surface formation post 1600 AD. The peak around 1450 AD remains as a single mode. The error on the peaks is much reduced and the disturbance events responsible for the creation of the new surfaces can be more accurately estimated at 1425 ± 15 yr AD, 1625 ± 15 yr AD, 1715 ± 15 yr AD.

4.3 Forest Age on the terrace sequence in the Karangarua River

The three common forest age modes match successive terraces in the Karangarua River upstream of the Alpine Fault (Wells & Yetton, in prep.) Figure 4.8 summarises the terrace sequence. The modern river occupies a broad bed cut within the lowest terrace. The river occasionally floods over this terrace and so strictly speaking this as part of the active flood plain. Vegetation growth on this lowest tread is patchy and flood influenced (approximately 10% forest cover and the rest grass). The few trees that are present indicate river abandonment of some of the more sheltered parts of the terrace between 1820 and 1875 AD.

The next highest terrace tread is the first consistently above modern river flood height and is 80% covered in well developed forest. The oldest trees on this surface indicate river abandonment in the period 1710 - 1720 AD.

The next highest terrace tread has trees established in the period 1610 - 1620 AD matching those growing on McTaggart fan (the debris avalanche described in section 2.2, page 26) which we attribute to earthquake triggering in the Crane Creek event. Amongst this forest, on both the terrace tread and McTaggart fan, there is also evidence of a younger forest disturbance event with areas of trees established at the same time as those on the youngest terrace (ie 1710 - 1720 AD).

The next highest tread has trees of an age indicating abandonment between 1405 - 1445 AD. Once again patches within this forest show signs of subsequent disturbance and representatives of both the 1620 and 1715 disturbances can also be recognised.

Unfortunately river erosion has removed most areas of higher terrace, and the trees on these are so old that many are no longer the first colonisers. In addition coring of large trees becomes less and less accurate because even the largest corer cannot reach the heart and a less reliable estimate for lost rings must be made. However the oldest trees on the next terrace are around 700 years old and the best estimate for the time of abandonment is 1215 - 1245 AD. Because it is less reliable we have not included this terrace in Figure 4.8 but the height (12m) and age does plot on the expected projection of the straight line of the age - height graph in Figure 4.8.

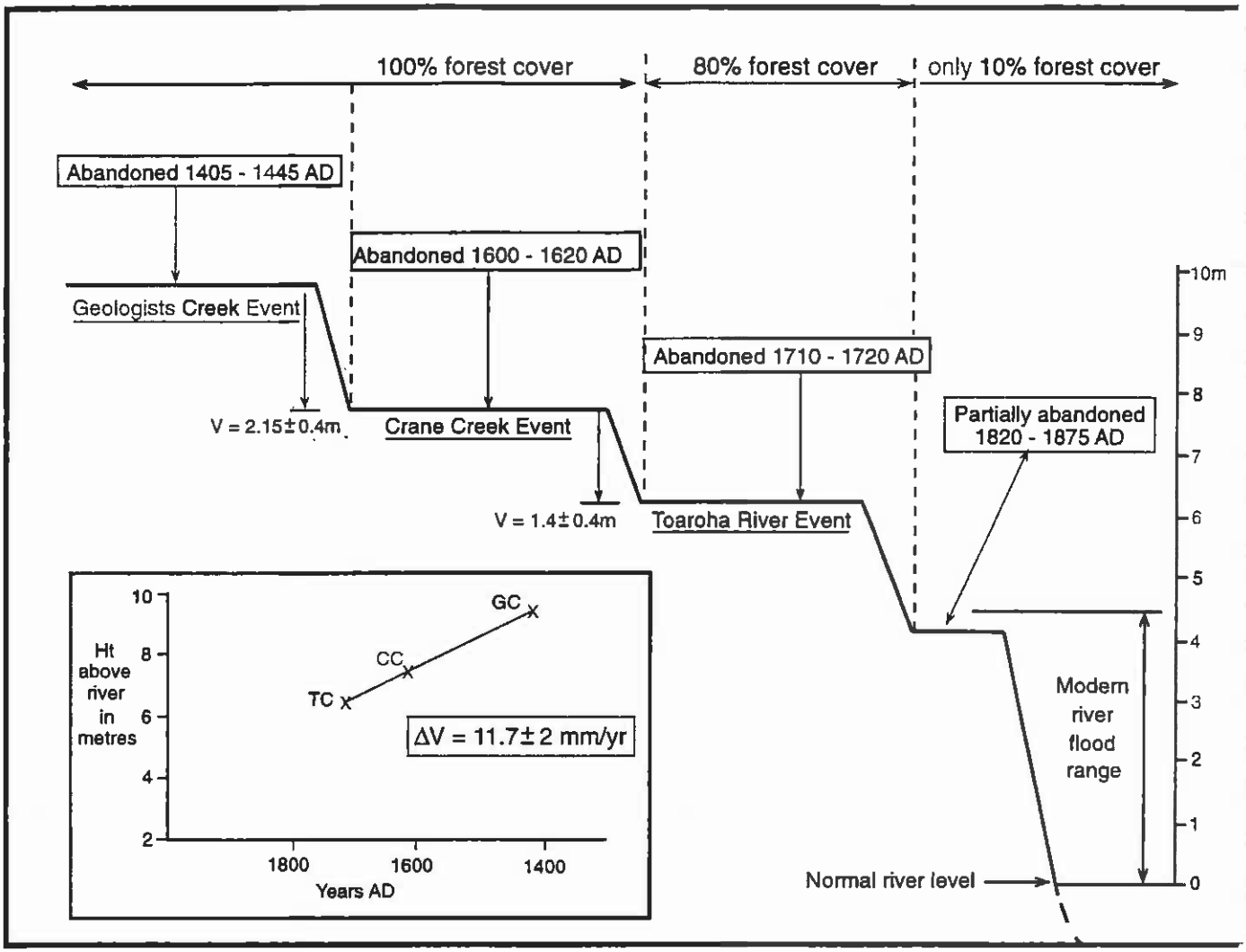

Figure 4.8 - Successive terraces in the Karangarua River which have been abandoned at time ranges matching the modes of forest disturbance in Figure 4.7. An average uplift rate of c. 12 mm/yr can be derived from an age - height graph of the terraces where the three terraces plot as a straight line.

It is generally accepted that the flights of terraces recognisable upstream of the Alpine Fault are the result of episodic uplift by earthquakes along the fault (Adams, 1980). The successive occupation of the new surfaces of uplifted terrace treads by forest conforming to the common forest age modes demonstrates the regional disturbance events are synchronous with new terrace formation. We suggest this is the result of the component of vertical uplift associated with the last three Alpine Fault earthquakes.

By plotting the average terrace height against the time of abandonment an average uplift rate can be obtained (Figure 4.8). The three successive terraces plot as a straight line with a gradient of approximately 12 ± 2 mm/year. This is higher rate than most estimates of uplift at the fault itself which are of the order of 6 - 7 mm/yr (refer section 1.2.2). However the terraces heights have been obtained from averages taken over an 8 km stretch of the river upstream of the fault and some additional broader scale uplift

east of the fault is likely. This estimate of 12 mm/yr is still well below the estimated rates for uplift at the main divide of 17 mm/yr and 22 mm/yr (Wellman, 1979; Walcott, 1979).

There is no possible alternative climatic explanation for a flight of successively younger terraces in this very young age range. A massive storm, or a series of massive storms, may produce aggradation and floods thereby creating or clearing alluvial surfaces. However this will not produce the uplift required to preserve a successive record and each climatic event will work through approximately the same flood and aggradation level range thereby cannibalising the earlier record. Invoking uplift by earthquakes between climatic events to allow preservation is an unnecessary complication of the pattern and in effect the abandonment of the surface by the river still dates to the earthquake.

We have noted that the timing of abandonment is the same as the regional forest age modes (Figure 4.7). The successive terrace sequence in the Karangarua River is the most unambiguous evidence that the regional forest age modes are also the result of earthquakes and not some sort of climatic aberration.

4.4 Evidence from tree ring analysis in NZ Cedar (*Libocedrus bidwillii*)

Disturbance of trees which live through an earthquake is preserved in the pattern of tree ring growth and this can be used to precisely date an prehistoric earthquake. Tree ring dating as a method of dating fault movement in New Zealand was tested by Berryman (1980) on the White Creek fault scarp after the 1929 Buller earthquake. Berryman found red beech (*Nothofagus fusca*) growing on the scarp in 1979 with distinct bends in the trunk. The corresponding asymmetry in growth rings as the trees grew reaction wood precisely dated the tilt to the 1929 event. Tree ring methods have been applied to earthquake dating on the San Andreas fault (for example Jacoby et al, 1988) and other faults in wooded areas of the American west coast (Sheppard and Jacoby, 1989; Jacoby, 1997). Recently another historical earthquake in California (the 1978 Stephens Pass earthquake) demonstrated the reliability of the method (Sheppard and White, 1995). Westland is an ideal location to apply tree ring earthquake dating methods.

In chapter 2 we described tree ring disturbance at around 1620 ± 10 years AD in seven old podocarps growing directly on the fault scarp at Crane Creek. More information has recently been collected in the Karangarua River from 40 old cedars (*Libocedrus bidwillii*) growing on steep slopes at four sites within 12 km of the Alpine Fault in the Karangarua Valley (Wells et al, in prep.). Seismic shaking commonly causes a marked reduction in the radial growth of trees at the fault rupture zone but in steep landscapes at vulnerable locations these impacts can extend to trees over 200 km from the fault (Jacoby et al, 1988; Sheppard & Jacoby, 1989; Kitzberger et al, 1995)

Cedars are particularly well suited to detailed tree ring analysis and are much more reliable than podocarps. Cross matching of several hundred *Libocedrus bidwillii* ring width series shows that this species does not produce false rings, and has less than 1%

absent rings (Norton, 1986). Unfortunately the cedars do not normally grow at the low altitudes typical of the majority of the fault scarp, so sites some distance away were selected. These sites are on steep slopes adjacent to landslide scars with re - established vegetation of an age matching the 1620 and 1720 establishment periods. The trees selected are therefore likely to have been directly affected by seismic shaking but not sufficient to destroy them.

We defined an abrupt suppression in radial growth as a > 100 % decrease in mean ring width between consecutive 10-year means, and identified the starting date of all such suppressions in ring width series by counting in from the outermost ring. The suppression dates are combined into 10-year age classes. Figure 4.9 shows the results of the *Libocedrus bidwillii* suppression analysis.

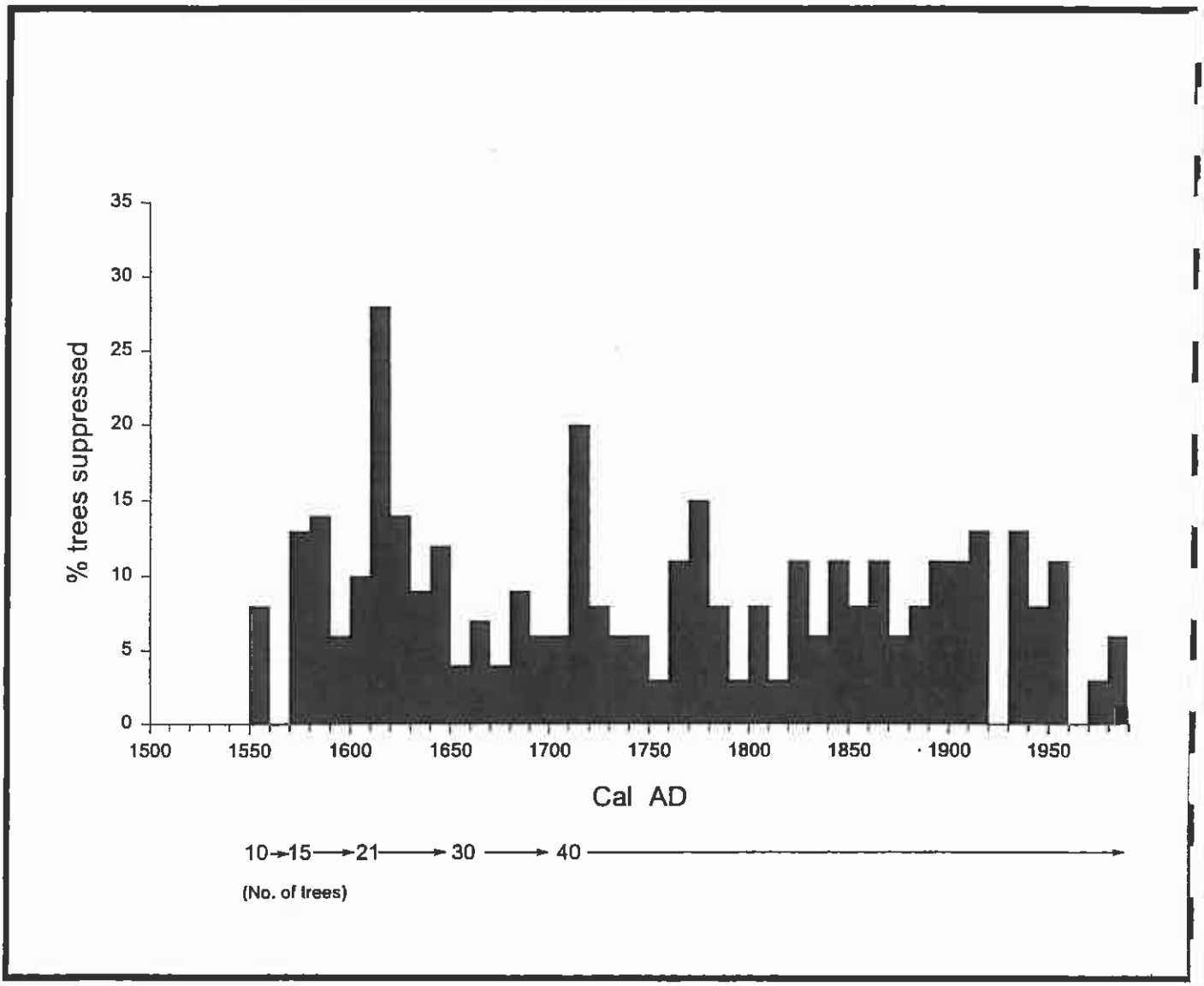

Figure 4.9 - Dates of significant growth suppressions in 40 cedars (Libocedrus bidwillii) in the Karangarua Valley. The criteria for suppression was a greater than 100% difference in mean growth rate between consecutive 10 year means.

Two periods of unusually common growth suppression stand out over the last 450 years where more than 20 % of the trees are affected. These periods (1710 - 1720 AD and 1610 - 1620 AD) match the suggested dates of the Crane Creek and Toaroha River earthquake events deduced from the landslide, trench and forest age evidence presented earlier.

4.5 Precise dating of the Toaroha River event

By matching and combining the tree ring patterns from as many trees as possible a generalised record for a much larger population of trees can be obtained with a reduced dating error (referred to by plant scientists as cross matching).

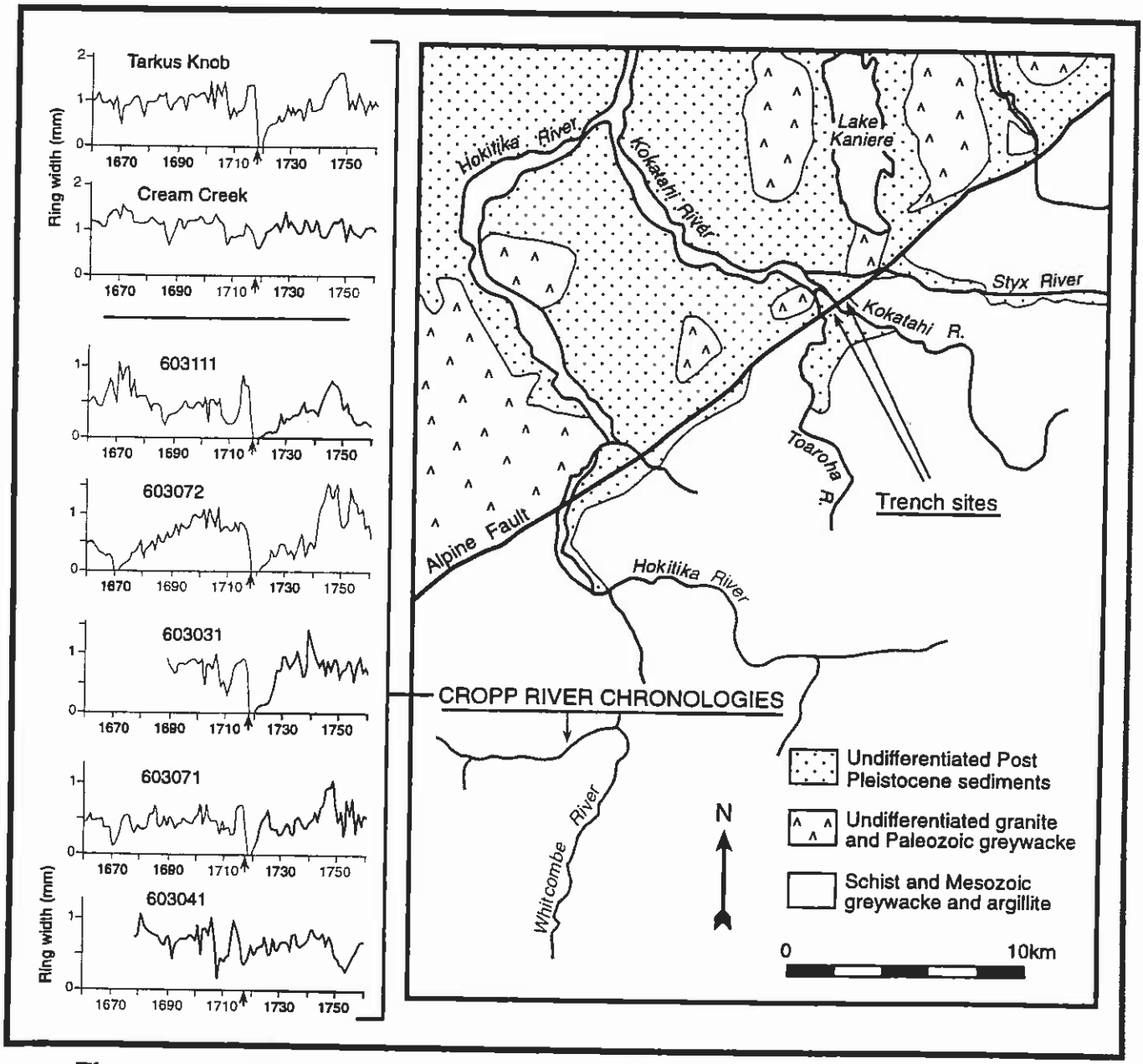

Figure 4.10 - Cross matched chronologies for cedar (Libocedrus Bidwillii) from Norton (1981) for Tarkus Knob and Cream Creek in the Cropp River. Also shown are the plots for five representative individual trees. Note this location is approximately 8 km from the Alpine Fault trace in the expected epicentral area of maximum shaking.

Cross matched cedar tree ring chronologies already exist for the Cropp Valley near the Hokitika River (Norton, 1981). Originally intended for dendroclimatic purposes these chronologies are each based on 19 trees. We have re - examined these in light of the trenching results to look for unusual fluctuations in growth for the period between 1660 and 1840, and in particular the period around 1720 AD as suggested by the forest age and Karangarua data.

The Cropp River sites are 9 km from the Alpine Fault and 25 km from the Toaroha River trench locations. Figure 4.10 shows the location details. Separate chronologies have been constructed for Tarkus knob, a steep south facing slope underlain by schist at shallow depths, and Cream Creek which is a much more gently sloping alluvial surface. The dip of the fault and the likely depth of rupture suggest this area would have been within the zone of maximum earthquake shaking in the Toaroha River event. The cross matched chronologies and a selection of ring width counts from individual trees is presented in Figure 4.10, along with the general location details.

Figure 4.10 shows that abrupt marked growth declines began in both chronologies at 1717 AD and were followed by several years of below average growth. As is expected with earthquake shaking, the steeper Tarkus Knob site shows the greatest impact and this event was the largest growth interruption in 400 years. In four trees the impact began in 1717 with a small suppression but was also followed by a sharp suppression the following year. This pattern suggests that growth was disrupted during the 1717 growing season.

This suppression coincides with that shown in Figure 4.9 for the Karangarua Valley and the regional forest age mode. It also matches the terrace abandonment in the Karangarua River. Six other existing cross matched chronologies (Norton, 1983a & 1983b) were also examined, extending from the Paringa River to the Takahe River near Lake Te Anau, all between 25 and 75 km from the Alpine Fault (Figure 4.11). These chronologies are mainly from silver beech (*Nothofagus menziesii*) with one from mountain beech (*Nothofagus solandri*). All chronologies show a marked growth anomaly at this same time.

Trenching has indicated the northern limit of the Kokatahi event was between Haupiri and Crane Creek. Two cedar chronologies within 10 km of the fault are available for the area further north from sites near the Ahaura River and Rahu Saddle (Limin, 1996). Neither show a growth anomaly at this time, and in fact the Ahaura chronology indicates a period of above average growth. Five other chronologies are available from the central eastern South Island (Limin, 1996 [four *L. bidwillii* chronologies] ; Norton, 1983b [one *N. solandri*]). None of these show a suppression at this time.

Exceptional climatic events such as heavy snowfall or unseasonal frost could cause long - lasting growth suppression in trees at a single site. Historically severe storms in the region have only had a local impact (Benn, 1990). The impacts may extend over many tens of kilometres, but for this type of climatic event to extend for over 300 km from Lake Te Anau to the Cropp River, and yet be suddenly absent in chronologies from north of the Haupiri River, and is extremely unlikely. There is no topographic or other barrier to constrain storms in this area. The absence from eastern South Island chronologies also indicates this was not a national climatic or atmospheric phenomena.

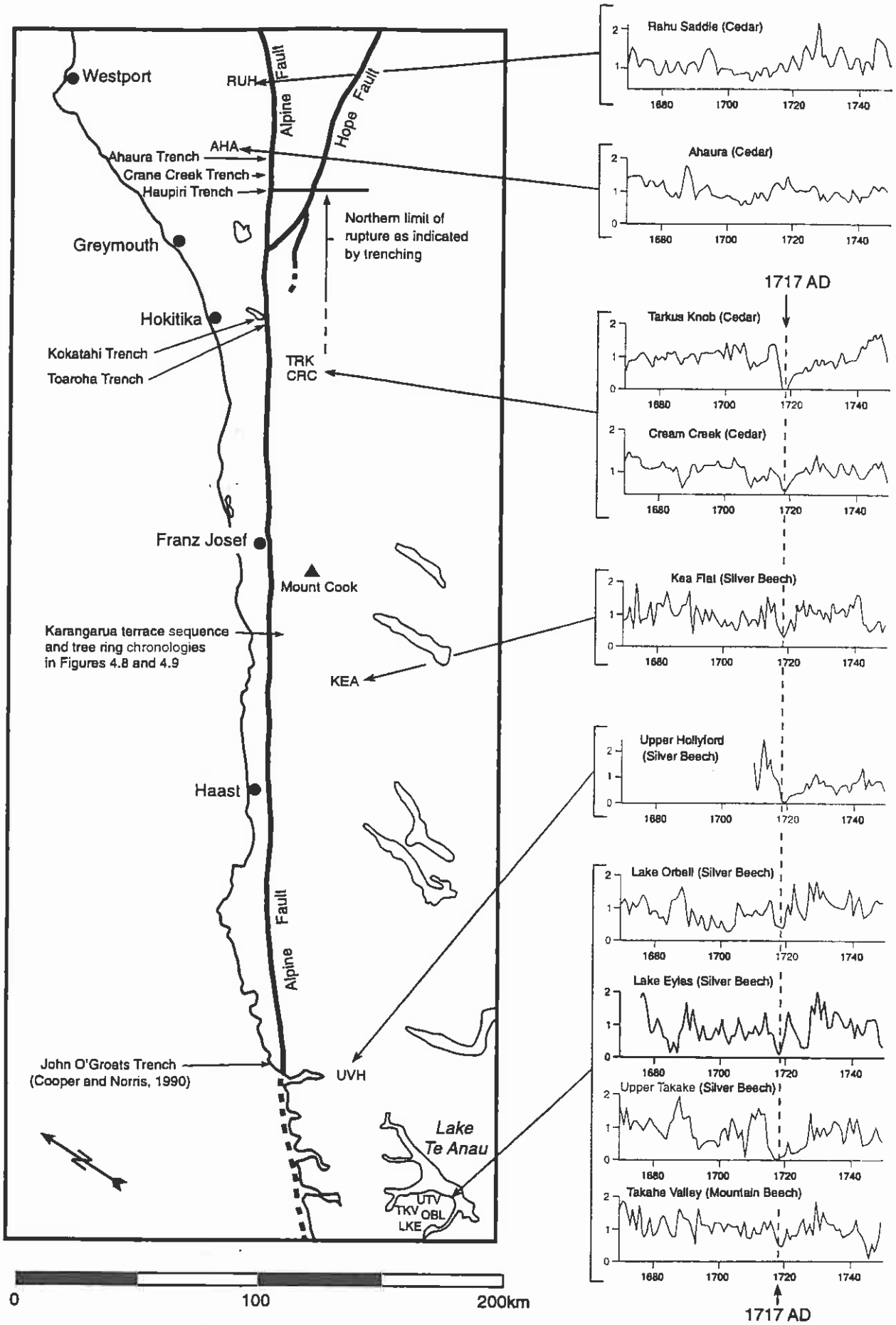

Figure 4.11- Available cross matched tree chronologies along the strike of the Alpine Fault from Lake Te Anau to the Rahu Saddle. The abrupt growth suppression in 1717 AD coincides with the northern limit of the post 1660 AD rupture at the Haupiri River determined by trenching the fault. The Y axis on all the graphs is the ring-width index.

In summary the timing of this event in 1717 AD

- is a very good fit to the inferences from the Kokatahi, Toaroha and Haupiri trenches (1700 - 1750 AD). Wood, leaves and twigs from 1717 AD will sometimes return a conventional radiocarbon age of around 200 yr BP but frequently will appear as "modern"

- it coincides with the timing estimate for the last event in Fiordland, based on pits excavated in sag ponds near the fault and broken beech trees, of between 1650 AD and 1725 AD (Cooper & Norris, 1990)

- it is the most logical explanation of terrace abandonment at this same time in the Karangarua River

- it is the best explanation and an excellent fit to the most recent regional forest age mode (1720 ± 10 years AD)

- and perhaps the most compelling evidence is the coincidence of the northern limit of this growth suppression with that independently determined by trenching.

All the evidence is consistent and indicates the most recent Alpine Fault earthquake (the Toaroha River event) occurred in the 1717 growing season and the shaking impacts were synchronous from Lake Te Anau to the Haupiri River, a distance of approximately 400 km.

4.6 Summary

The forest and tree record in Westland has been examined to better estimate the most likely timing of the last two Alpine Fault earthquakes which have been demonstrated by the trenching and suggested in the landslide and aggradation terrace record. Regional forest age modes can be identified at 1425 ± 15 yr AD, 1625 ± 15 yr AD and 1715 ± 15 yr AD which are consistent with the landslide and terrace record and a good fit to the trench data.

Trees which have survived these disturbances exhibit tree ring fluctuations which more accurately constrain the timing. These suggest the Crane Creek event occurred at 1620 ± 10 yr AD. The more recent Toaroha River event appears to have occurred in 1717 AD and can be traced from Lake Te Anau to the northern limit near the Haupiri River previously identified by trenching.

Chapter 5

PROVISIONAL EARTHQUAKE CHRONOLOGY AND SUMMARY

5.1 Earthquakes in the last 750 years

5.1.1 The Toaroha River Event

This is the best defined of the recent earthquakes due primarily to the excellent tree ring chronologies available for the last 300 years. We summarise the details in Table 5.1 below.

Evidence	Trenching	Landslides and terrace age	Forest Age	Tree ring chronologies
Estimate of Timing	Post 1665 AD, probably 1700 - 1750 AD	Post 1660 AD	1715 AD ± 15 yr	1717 AD
Rupture Length	A minimum length of 375 km is suggested by trenching and the landslide record but a possible length of 450 km is suggested by the tree ring chronologies.			
Magnitude Estimate	For 375 km : M = 8.05 ± 0.15 (Wells & Coppersmith, 1994) M = 8.0 ± 0.26 (Anderson *et al*, 1996) For 450 km: M = 8.15 ± 0.2 (Wells & Coppersmith, 1994). M = 8.05 ± 0.26 (Anderson *et al*, 1996)			

Table 5.1: Summary of key features of the Toaroha River event

Rupture length

The inference regards a rupture length of 375 km is the minimum which the direct fault data indicates. It is based on the northern limit as defined by the trenching at Haupiri River and Crane Creek. The southern limit is taken as the John O'Groats site of Cooper & Norris (1990) in Fiordland. Although the tree ring chronologies indicate impacts continuing much further south to Lake Te Anau the fault surface rupture may not have extended this far. Although this is possible, in many ways it is more likely that the rupture did extend along the section of fault near the coast to at least opposite Lake Te Anau, a total length of approximately 450 km. However the most appropriate approach at this stage is to assume it did not.

Similarly there may ultimately be an case for extending the northern rupture length to include a section of the Hope Fault. Cowan & McGlone (1991) estimate the timing of the penultimate earthquake on the Hope River segment at 1728 AD but with a considerable error of + 53 - 93 years. The Hope Fault may be triggered after a delay of many years but it is also possible the Alpine Fault and Hope Faults rupture together in a pattern similar to the Imperial Valley earthquake in California of 1979 (Archuleta, 1982). Figure 5.1 shows the surface rupture pattern for this event. The continuation of the rupture past the branch to the Brawley Fault zone may be similar to the north section of the Alpine Fault rupturing up to Haupiri.

The last earthquake crossed the Alpine Fault "segment" boundaries proposed by Bull (1996) and Berryman et al (1992). These boundaries had been tentatively proposed on geomorphic and structural grounds. While the division into geographic sections adopted by Berryman et al, 1992 may be still be useful for location description, it appears there may not be persistent segmentation of the Alpine Fault in the normal sense.

Magnitude estimates

The length of surface rupture can be used to estimate the magnitude of the earthquake responsible based on various regression relationships developed over the last 30 years (Bonilla & Buchanan, 1970; Mark & Bonilla, 1977; Sleemons, 1982; Bonilla et al, 1984; Khromovskikh, 1989; Wells & Coppersmith, 1994). These models have improved progressively as more and more data becomes available on the magnitude and rupture length of historic earthquakes from around the world.

The most recent refinement of the method involves the inclusion of average long term slip rate in selecting the appropriate regression line (Anderson *et al.*, 1996). The rationale behind this modification is the observation by the authors that the highest magnitudes for a given rupture length tend to be produced by faults with relatively low long term slip rates. This presumably reflects the more irregular nature of the fault plane resulting in a higher overall residual friction. Greater energy is therefore required to rupture a given length of fault plane and a higher magnitude earthquake results. The converse is likely for the Alpine Fault, particularly given the very large cumulative geologic offset (refer section 1.2.4).

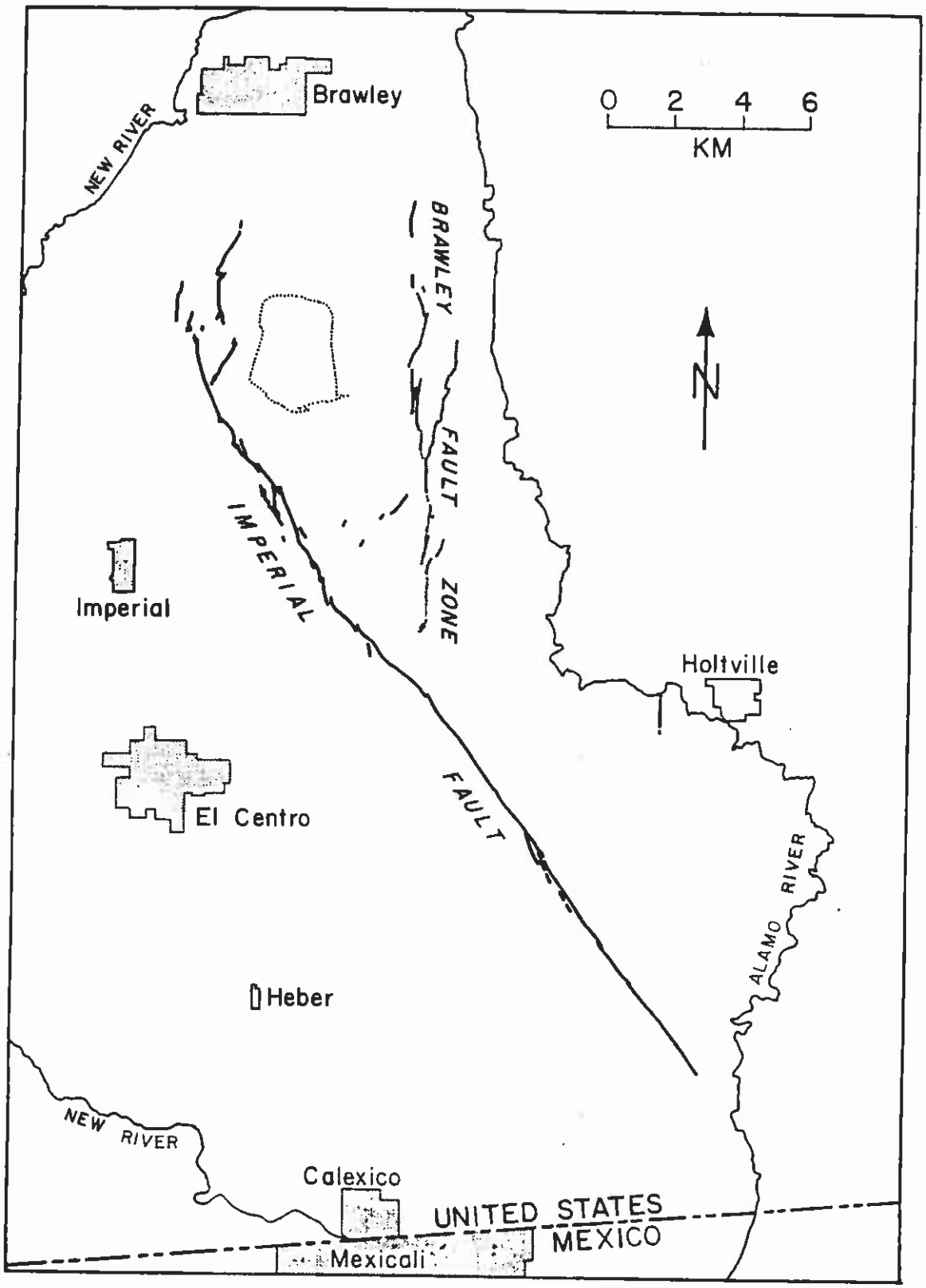

Figure 5.1: Surface rupture pattern in the Imperial Valley earthquake of 1979 in California. The rupture splay into the adjacent Brawley fault zone may be similar to the pattern of rupture at the various Marlborough fault junctions with the Alpine Fault

However, including slip rate in the regression limits the data base to 43 historical earthquakes. This is turn increases the regression error of Anderson *et al* (0.26 M units). For this work both Anderson *et al*, 1996 and Wells and Coppersmith, 1994 give very similar estimates and both are used. Wells & Coppersmith (1994) has a large database of 244 historic examples and a relatively small 95% confidence limits (< 0.2 M units and generally < 0.15). They are also able to demonstrate no systematic variation in the regression relationship for strike slip, normal and reverse faulting. This is an advantage for the Alpine Fault which has components of both strike slip and reverse movement.

One reservation is adopting these international correlations is the small number of New Zealand examples in the data base (one in Anderson *et al*, 1996; four in Wells and Coppersmith, 1994). Where sufficient information is known to include New Zealand examples these all plot well outside the 95 % confidence levels, generally on the high side (ie greater magnitudes for a given rupture length). This suggests the magnitudes estimates for the Alpine Fault events must be viewed with caution and if anything may well be underestimates of the real magnitudes.

It is interesting to note in the 244 historic earthquakes in the Wells & Coppersmith database only one, the San Francisco earthquake of 1902, has a rupture length longer than the 375 km minimum suggested for the Toaroha River event. Table 5.2. summarises the seven historic earthquakes for which magnitude and rupture length is known. The problems with correlating rupture length and magnitude are obvious in that the highest historic magnitude was associated with the shortest rupture length (the Kansu earthquake, China, 1920) and by far the longest rupture resulted in a magnitude in the middle range (the San Francisco earthquake, USA, 1906).

Magnitude	Rupture length	Country	Earthquake Name	Year
8.5	220 km	China	Kansu	1920
8.3	297 km	USA	Fort Tejon	1857
7.9	236 km	Mongolia	Gobi - Altai	1957
7.9	432 km	USA	San Francisco	1906
7.8	360 km	Turkey	Erzihcan	1939
7.5	280 km	Turkey	Kastamonu	1943
7.5	235 km	Guatemala	Motagua	1976

Table 5.2: The magnitudes of the few historic earthquakes for which surface ruptures are known and which exceed 200 km. Data from Wells & Coppersmith, 1994.

Single Event Slip

Single event slip is the horizontal and vertical offset at the surface fault trace caused by a given earthquake. There are major problems in determining this with any reliability.

The difficulties derive in two quite different ways, the first relating the nature of the process and the other to the limitations in field determination.

Many observers have noted it is very rare for a surface offset to remain constant along a fault trace in historical earthquakes. Most earthquakes seem to have subregions that may have greater slip (Lay *et al.*, 1982; Beck & Ruff, 1987; Segall & Du, 1993; Wald & Heaton, 1994). Slip variations of 5 or even 10 to 1 are not uncommon in these historical observations. This phenomena can be replicated in physical models (Das & Aki, 1977; Mikumo & Miyatake, 1978) appears to be a natural consequence of barriers and stiffer regions along the fault plane.

Intuitively it would seem reasonable to assume this variation would be much less for a relatively organised and high slip rate fault such at the Alpine Fault. Further more a lot of the variation may be attributed to measurement across short fault scarp profiles which neglect a subtle far field component. From this point of view the best estimate of slip would be from triangulated geodetic survey. However, work on the 470 km of rupture which occurred along the San Andreas Fault in 1906 casts doubt on both these arguments (Thatcher *et al.*, 1997). This is a fault with a high slip rate, and a relatively large total cumulative offset, yet Thatcher *et al* (1997) observed a variation between 2.3m and 8.6m in the geodetically determined coseismic slip along the 470 km rupture (Figure 5.2).

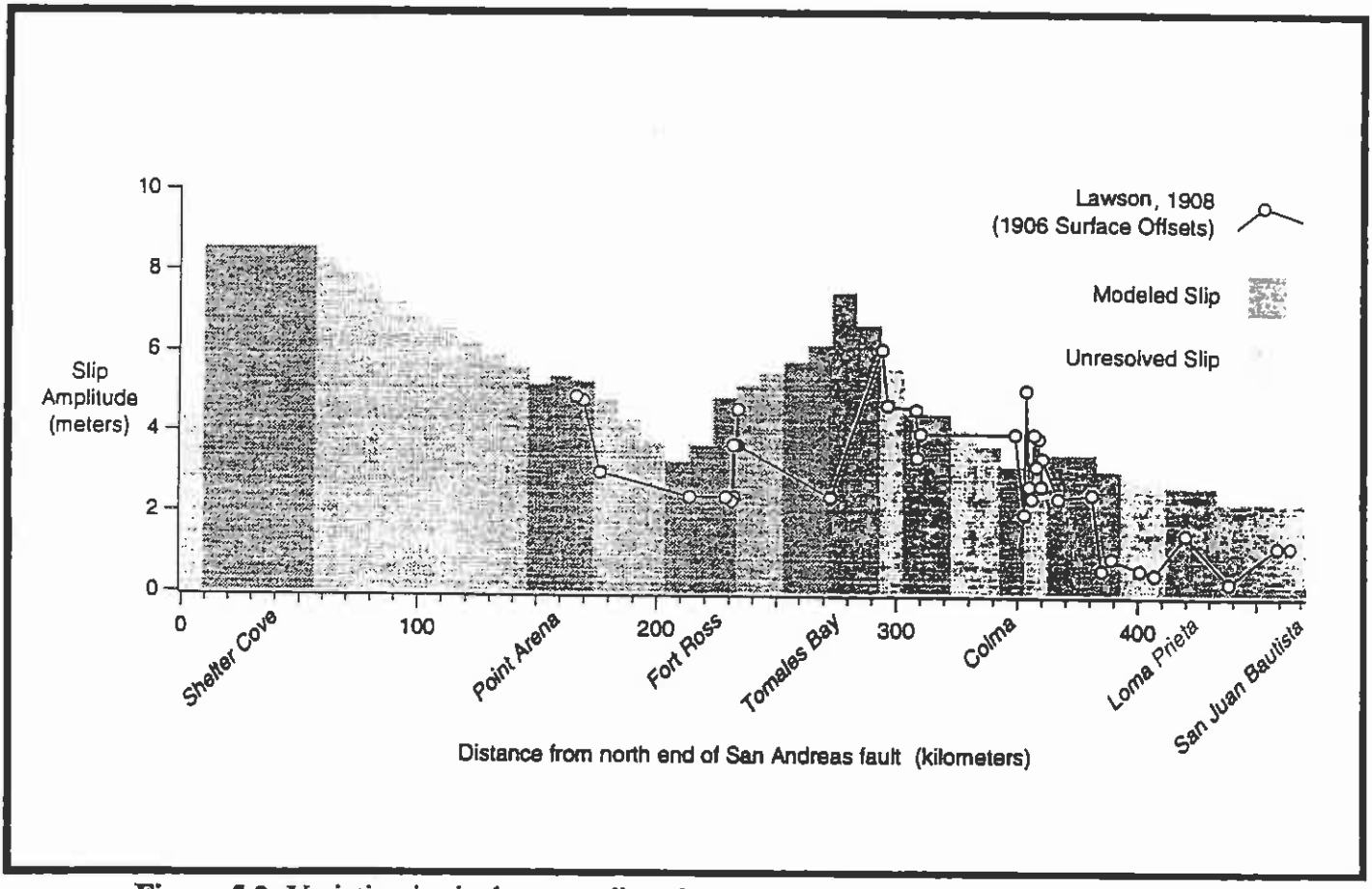

Figure 5.2: Variation in single event slipe along the 470 km of rupture in the 1906 San Francisco earthquake. The lines and circles show variations in actual surface horizontal offsets while the two shades of grey shows variations in geodetic slip.

The concept of average single event slip has also been introduced in an attempt to better utilise slip measurements for magnitude estimates (Kanamori, 1977; Thatcher & Bonilla, 1989; Wells & Coppersmith, 1994). This has been found to be on average 32% lower than the maximum single event slip where sufficient data is available to make a meaningful comparison (Wells & Coppersmith, 1994). However there is no criteria to establish the length of the fault which must be averaged to obtain this value. In the case of the Alpine Fault, where at best there may be on average 2 locations per 100 km of fault length on which to assess single event slip, the limitations drastically restrict the use of this method.

The Alpine Fault may have another source of intrinsic single event slip variation and this relates to variations in trace strike and behaviour. Strike varies by as much as 20 degrees along traces and as a consequence trigonometry indicates horizontal fault parallel slip will vary by approximately 15-25% between the most extreme oblique slip traces (where it is a minimum) and the most extreme strike slip traces (maximum).

There are also very real field difficulties in measuring single event slip in this area of the Alpine Fault. At three of the five trench locations there are multiple traces (Toaroha River, Kokatahi River, Ahaura River). Where two adjacent traces were both trenched (at the Kokatahi River) the results imply both traces moved simultaneously in the last event. There is no way to know how the slip was apportioned between them. At Crane Creek and Haupiri river the fault was a single trace but there has been multiple events and no clear single event offsets.

5.1.2 The Crane Creek Event

Table 5.2 summarises the known information regards the Crane Creek event. The length of rupture is very much a minimum and may seriously underestimate the magnitude. The northern minimum is the Rahu Saddle, based the presence of the Crane Creek event in the forest age record in this area of forest. The Alpine Fault extends another 85 km to Lake Rotoiti and the Tophouse Saddle and nothing is currently known of the earthquake history in this area of the north section.

	Trenching	Landslide and terrace ages	Forest Age	Tree ring chronologies
Estimate of Timing	1480 - 1645 AD	1488 - 1640 AD	1625 AD ± 15 years	1620 AD ± 10 years
Rupture Length	A minimum length of 200 km is suggested by trenching and the landslide record but a minimum of 250 km is indicated by forest age			
Magnitude Estimate	M > 7.8 (both Wells & Coppersmith, 1994 and Anderson *et al*, 1996)			

Table 5.2: Summary of key features of the Crane Creek event

The southern limit is arbitrarily assumed to be just north of the Haast River because the currently available forest and tree ring data does not extend any further south than the Paringa River. This limit north of Haast is also based on the observations of Berryman *et al.*, 1992, who suggest Haast may be fault segment boundary, and who note evidence for just one earthquake event since a radiocarbon date of 860 ± 55 yr BP at the Pyke River near Lake McKerrow in Fiordland. Unfortunately the details of this date are not presented in the paper. The current trenching at Haast will hopefully clarify the situation in this area.

It is not easy to compare magnitudes of the Toaroha River and Crane Creek events based on their relative impact however the impression from both the forest age record (Figure 4.7), and the landslide and aggradation terrace dates (Figure 3.3), suggests the Crane Creek event may have been the larger of the two, at least in the central and north section. This is also suggested by the tree ring chronologies in the Karangarua (Figure 4.9). However this apparent difference could also be the result of the time of the year in which each earthquake occurred. While the tree ring chronologies suggest the Toaroha River event occurred during the growing season, and most likely in late summer, the Crane Creek event may have coincided with a much wetter period. This will make a very large difference to the frequency of landslides and rock avalanches triggered by an earthquake in this terrain and affect the corresponding impact on the forest.

It is possible that the two events were separately biased to the south and north with overlap in the central section. The Toaroha River event may have been triggered in the Fiordland segment and then extended with decreasing severity up to Lake Haupiri. The Crane Creek event may have been the slightly earlier equivalent large earthquake for the north section which also extended down in to the central section. In relation to this it is interesting to note that a series of landslide dams with an age around 1650 AD have been recognised in the area north of Springs Junction (Perrin and Hancox, 1992). These may be related but further work is required in this area to test this possibility.

5.1.3 The Geologists Creek Event

The Geologists Creek event has not been recognised in trenches to date and is the least definite and most poorly defined of the three most recent events. Evidence for this event comes from the landslide and aggradation terrace record and the forest age patterns. The name "Geologists Creek" derives from a large rock avalanche deposit from the fault scarp in Geologists Creek, at the eastern end of Lake Kaniere, first identified by Trevor Chinn (pers. comm, 1996). This deposit has been radiocarbon dated by Chinn at 550 ± 50 yrs (NZ 6471) and this is the best radiocarbon estimate currently available of the precise timing of this inferred earthquake event. Fortunately the radiocarbon time period from 380 - 575 BP corresponds to a relatively steep and unambiguous section of the calendric calibration curve so radiocarbon dates provide much narrower calendric time constraints for this event (see Table 5.3).

	Trenching	Landslide and terrace record	Forest Age	Tree ring chronologies
Estimate of Timing	Not yet recognised	1420 - 1450 AD	1425 AD ± 15 years	Current chronologies not old enough
Rupture Length	A minimum length of 250 km is suggested from the forest age data.			
Magnitude Estimate	M > 7.8 (both Wells & Coppersmith, 1994 and Anderson *et al*, 1996)			

Table 5.3: Summary of key features of the Geologists Creek event

Currently work is continuing by others on a series of recently felled tilted rimu trees (*Dacrydium cupressinum*) growing on the fault scarp at the Waitaha River (Wright, pers. comm., 1997; Wright, 1996). Other trees further from the scarp have remained straight. The logs have been removed by Timberlands for timber milling but discs cut from the tilted stumps are being analysed to determine the exact time of the tilt episode. This approach is similar to that adopted by Berryman (1980) who was able to demonstrate consistent tilting in *Nothofagus fusca* trees growing on the White Creek fault scarp in the 1929 Buller earthquake.

To date the best estimate by Wright for the age of tilt is 1450 AD, which is a good match to the Geologists Creek event as defined in the landslide and forest disturbance record. This preliminary date estimate of 1450 AD may yet extend back as more rings are recognised, and although it is close to the true age, it is effectively a minimum.

The estimate of rupture length is based on the extent of the current forest age record ie Ohinemaka Forest, near the Paringa River, to the Rahu Saddle. This is once again a minimum estimate.

All the available constraints on timing and rupture length are combined below in a space - time diagram of the most recent three events (Figure 5.3).

5.2 Possible earlier events

The evidence for older events becomes less and less conclusive but some patterns appear to emerge. Most dates come from landslide and aggradation terrace ages although the Muriel Creek event has some support from forest age in the Karangarua River. Current work at the Waitaha River site provides some dates for the inferred coseismic creation of sag ponds along the trace at this location (Wright, pers. comm., 1997; Wright, 1997). The date information available to date has been included in Table 5.4 below which summarises the available information.

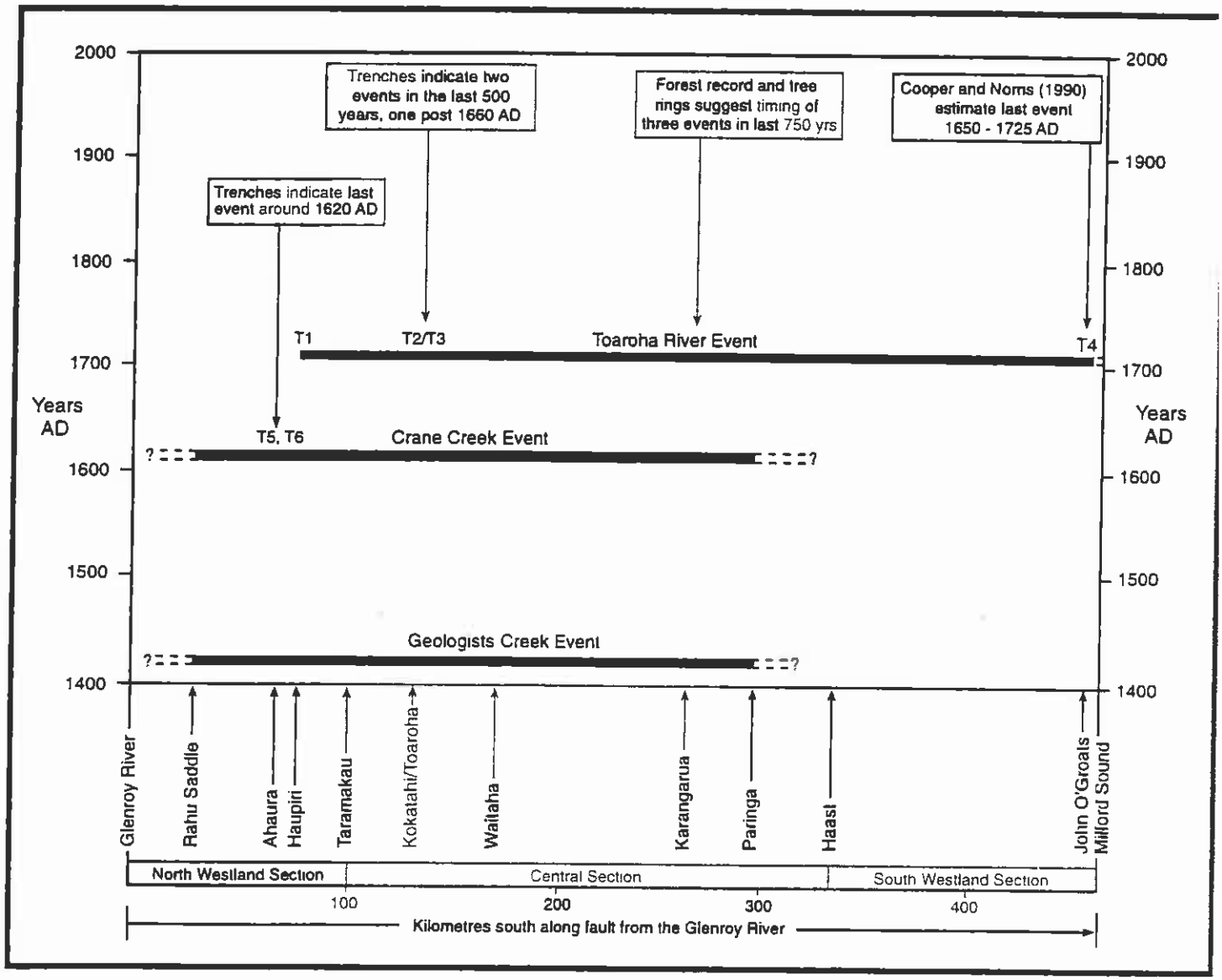

Figure 5.3: Space-time diagram for the most recent three Alpine Fault earthquakes. Note that only the Toaroha event of 1717 AD has a clearly defined rupture limit at the north end. All the other limits are effectively minimums.

Possible event	Supporting evidence
Muriel Creek **1220 AD** **± 50 yrs**	A 6m high terrace in Muriel Creek (GR J33/502032), which is the next highest terrace to a 4m terrace that dated at 540 ± 60 BP (Wk 4439, the inferred Geologists Creek terrace, this project), contains young wood dated at 810 ± 60 BP (Wk 4339, this project). The next most abundant forest age mode prior 1440 AD in the Copland and Karangarua Rivers is around 1200 AD (Wells, pers. comm., 1997). Wright (pers. comm., 1997) has a date for a possible coseismic sediment pulse in the southern sag pond at the Waitaha River site of 910 ± 50 BP (Wk 5424). Bull (1996) also proposes an Alpine Fault event at around this time (1226 ± 10 yrs) based on lichenometry.
Roundtop **940 AD** **± 50 yrs**	The large Roundtop debris avalanche from the fault scarp near the Toaroha River (Wright, submitted; Wright, 1996) has been dated here from radiocarbon dates on two samples of wood, 95 ± 5 rings apart, taken from the same 200 mm diameter kahikatea (*Dacrycarpus dacrydioides*) exposed in the base of the debris in Cunningham Creek (GR J33/535095). The dates were Wk 4877, 1100 ± 45 BP and Wk 4914,1300 ± 40 BP. This method has reduced the error by defining the overlap in ages which corresponds to 940 AD ± 50 yrs. In addition Wright (pers. comm., 1997) has obtained a radiocarbon date of 1160 ± 50 BP (Wk 5426) for the inferred coseismic formation of the central sag pond at the Waitaha River site which is compatible with this date. A large debris flow on the true right of the Karangarua River (GR H36/530311) has been dated at 1210 ± 50 BP (Wk 5268, this project) from the sapwood of a buried ribbonwood branch (*Hoheria lyalli*). Adams (1980) quotes an early radiocarbon date collected by Suggate of 960 ± 150 yrs BP (NZ 9) from a log in a terrace in the Wanganui River which may or may not be related to this inferred event (this is a very large error). In addition Adams quotes a date of 1020 ± 50 BP (NZ 1155) collected by Wardle from a terrace near the Waiho River. Bull (1996) notes the large number of rock avalanche deposits in the Southern Alps dated by weathering rinds which approximate this date (a total of 8, Whitehouse & Griffiths, 1983) and quotes an updated and recalibrated data set which has the highest probability for the combined 8 events at 963 ± 1 AD. Bull (1996) proposes an Alpine Fault event at 967 ± 10 AD based on lichenometry.

Table 5.4 (Part one) : Inferred Alpine Fault earthquakes prior to 1250 AD.

Waitaha River **595 AD ± 60 yrs**	Wright (pers. comm., 1997) has a radiocarbon date from the base of the southern sag pond which he attributes to coseismic formation of 1460 ± 60 BP (Wk 5425). Adams (1980) quotes a radiocarbon age of 1560 ± 55 BP (NZ 1293) collected by Peter Wardle from buried stumps beneath a young aggradation terrace at Welcome Flat in the Copland. In the Cascade Valley, near Jackson Bay, a large rock slide from Mt Delta buries logs dated at 1540 ± 80 BP (NZ 4626C) by Peter Wardle and quoted by Adams (1980).
John O'Groats **BC 25 ± 90**	Cooper & Norris (1990) obtained a date of 1980 ± 60 BP (Wk 1478) from the base of a sag pond at John O'Groats in Fiordland. In Steep Creek (GR K33/ 719226), near the Wainihinihi River, a large debris flow at the fault scarp contains logs dated at 2100 ± 60 BP (Wk 4004, this project). In the Karangarua River, at the junction with the Copland, a large rockfall yields a date of 2150 ± 60 BP (Wk 5269, this project). These three dates can be reconciled within the 95% significance level and the averaged radiocarbon date yields the calendric range noted opposite. Adams (1980) quotes a date from the Okuru River, near Haast, of 2210 ± 90 BP (NZ 1370A, Cooper & Bishop, 1979) which the Ward & Wilson test (Ward & Wilson, 1979) indicates is statistically different, despite it's relatively large error.

Table 5.4 (continued) - Summary of inferred Alpine Fault earthquakes prior to 1250 AD.

This may not be all the events over this period but all of these have at least some evidence other than the coincidence of landslides and terrace ages, and three of the four have direct fault evidence (the exception is the Muriel Creek event).
In addition to the dates noted in the Table 5.4 there are two more dates of which we are aware for the time period this covers. These are 1820 ± 60 BP for a debris flow near the Steep Creek site (Wk 4003, this project) and a date noted by Adams (1980) of 1740 ± 60 BP (NZ 296) for wood from a terrace on the Waiho River. Although these both overlap, and fall into the relatively large time gap between the inferred John O'Groats and Waitaha events, this is currently insufficient evidence to postulate an earthquake.

5.3 Comparison with earlier estimates of earthquake timing

Comparison with Adams (1980)

Figure 1.8 (refer chapter one) is from Adams (1980) This shows the ten dates over the last 2,000 years on which he based his inferences. With this very limited information two or more dates which coincided within the error were considered by Adams to be sufficient evidence to infer an earthquake. The series of inferred earthquakes appeared to be at approximately 500 year intervals with the most recent event around 550 years ago (the Geologists Creek event).

However Adams did note that the record may still be incomplete and that future dating may reveal intermediate age "earthquakes", and noted a single date from the Crane Creek event which he discarded as having no match (NZ 1292, 360 ± 60 BP, collected by Peter Wardle from McTaggerts Creek).

With hindsight there were insufficient dates in the original data set for Adams to make any reliable inference regards earthquake timing. All of the inferences regards earthquakes were based on indirect indicators (landslides and aggradation terraces) which can also result from processes other than earthquake. Furthermore the youngest event at 550 years is supported by just two dates which coincide and one minimum date. The event approximately one thousand years ago (the Roundtop event) is supported by one normal resolution date (NZ 1155; 1,020 ± 42 yr BP) and one with a very large error (NZ 9; 960 ± 150 yr BP).

Although three dates are proposed as supporting the event 1550 years ago only two coincide within the normal error (NZ 1293; 1560 ± 42 yr BP and NZ 4626C; 1540 ± 80 yr BP). The event 2200 years ago is then postulated based on only one date and the previously inferred recurrence interval of 500 years.

However as this project demonstrates it appears that Adams (1980) is broadly correct in inferring earthquake events at around these times, but with some important intermediate and recent events omitted. Furthermore the match between aggradation terrace and landslide ages for the most recent two earthquakes recognised by trenching confirms the fundamental usefulness of the approach he adopted.

Comparison with Cooper & Norris, 1990

There is good agreement between the date of the last earthquake as inferred by Cooper & Norris (1990) in Fiordland and the Toaroha River event. We have adopted their much earlier date of 1980 ± 60 BP from the second pit as direct evidence of an earthquake at around this time which happens to be compatible with our limited number of landslide ages for this period (2).

Comparison with Bull (1996)

Bull (1996) inferred events at 1748 AD, 1489 AD, 1226 AD, and 960 AD (all ± 10 yrs) with a remarkably constant 260 ± 15 yr recurrence interval.

The dates of the most recent two earthquakes are not compatible with three of the four independent lines of evidence on which we base our earthquake chronology for the last 750 years. The broad radiocarbon date bands from the trenches do not highlight the discrepancy. Bull's inferred 1748 event could be the post 1660 Toaroha event. The Crane Creek event (1480 - 1645 AD) could be his 1489 AD earthquake. However if this is the case there is then no equivalent of the Geologists Creek event. The next events coincide well for Muriel Creek (his 1226 AD) and Roundtop (960 AD.).

The main miss match is in the comparison with the forest age record, landslide and terrace dates, and the tree ring chronologies. The sequence of successive terraces in

the Karangarua is also a poor fit. None of these can be reconciled with Bull's dates for his youngest two events.

This may in part be because the lichen method is another indirect method with no unique connection to a single fault. It is essentially a variation on the use of landslides as paleoseimic indicators and is open to the same criticism. Rockfalls can be triggered by processes other than earthquake and even if an earthquake was the trigger it is very difficult to assign a particular fault as being responsible.

In some of the more arid parts of the Hope Fault, Bull has been able to demonstrate a belt of lichen dated rock outcrop damage, in a relatively narrow line along the actual fault (Bull, 1997). This is a much more reasonable approach.

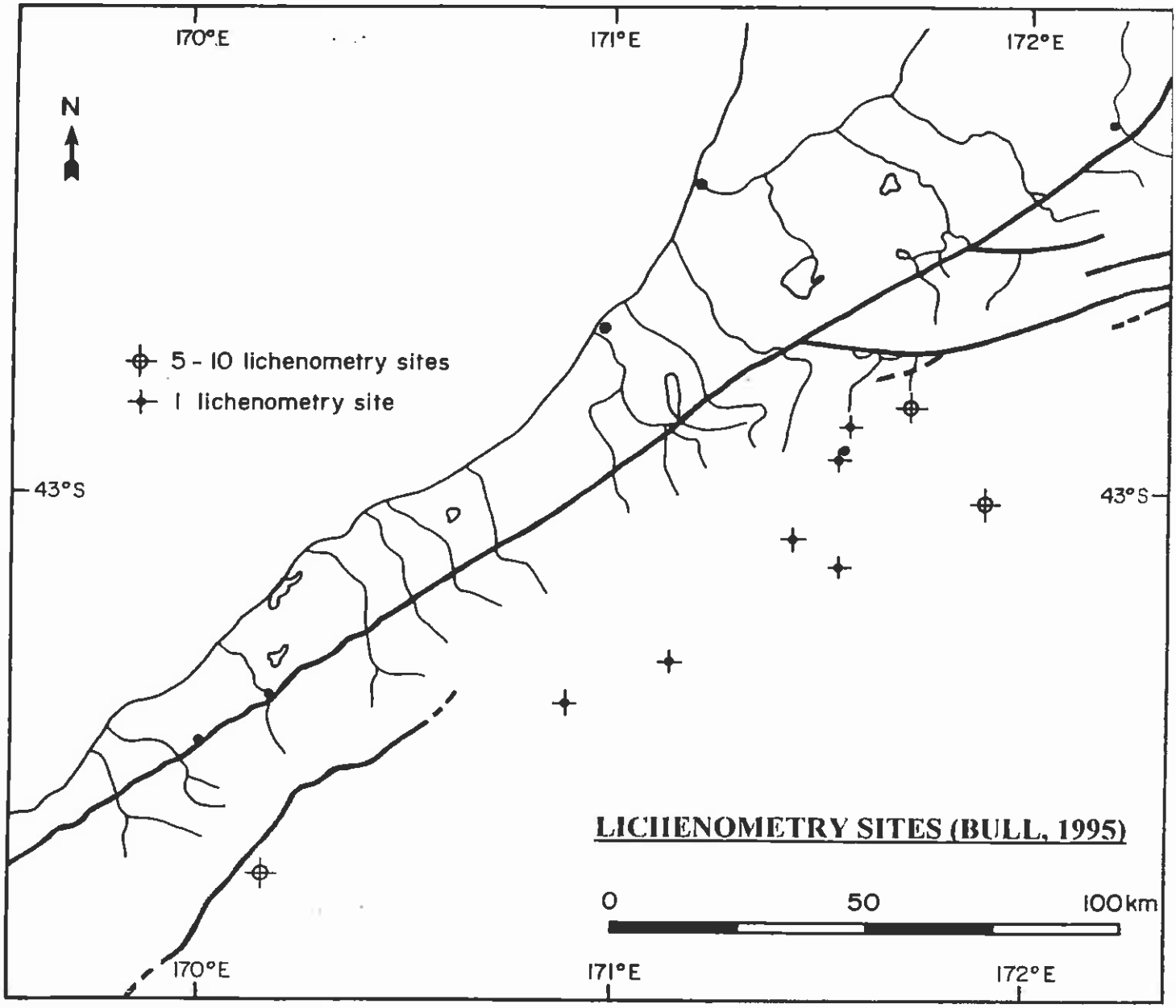

Figure 5.4: Data sites for the lichen analysis of Bull (1996). Note the considerable distance from the Alpine Fault of many of the sites where lichen of the appropriate species flourishes.

The lichen method is not well suited to the area close to the Alpine Fault. Unfortunately it is too wet in most areas of the western range front for growth of the appropriate Rhizocarpon lichen and this is reflected in the eastern bias of the sites which Bull is obliged to use (Figure 5.4).

The closest site is the Otira rock slide at Arthurs Pass, which is still 18 kilometres from the Alpine Fault at Inchbonnie, and is much closer to many other active faults such as the Kelly Fault, the Kakapo Fault and the Hope Fault. Further south other faults, for example the Main Divide Fault zone of Cox (1995), pass right through the main lichen dating areas near Mount Cook which are used by Bull. It is extremely likely that earthquakes on faults other than the Alpine Fault have at least supplemented, and possibly dominated, the lichen record of Bull (1996).

While there are critics of lichenometry as a method (see for example McAlpin, 1996; Oelfke and Bulter, 1985) Bull is able to demonstrate a correlation between historical earthquakes and lichen modes. Furthermore the inferred lichen event dates appear to progressively coincide with the earthquake events inferred in Table 5.4, particularly the Roundtop event. However the lichen method may be better suited to near-fault dating on the arid east coast rather than attempting to extend the inferences to areas where the forest can provide a closer and more reliable record.

Finally it is important to note that the differences between the chronology as defined here, verse that of Bull (1996), makes little difference to the probability of the next earthquake. One implies a remarkable regularity with a lapsed time equal to the average recurrence interval. The other a more irregular recurrence of approximately the same order but a longer lapsed time.

5.4 Summary

Three earthquakes can be recognised on the central section of the Alpine Fault in the area north of the Paringa River. These are summarised in Table 5.4 below.

Toaroha River Event				
Evidence	Trenching	Landslide and terrace ages	Forest Age	Tree ring chronologies
Estimate of Timing	Post 1665 AD, probably 1700 -1750 AD	Post 1660 AD	1715 ± 15 yr	**1717 AD**
Rupture Length	A minimum length of 375 km is suggested by trenching and the landslide record but a possible length of 450 km is suggested by the tree ring chronologies.			
Magnitude Estimate	M = 8.05 ± 0.15 for 375 km and M = 8.15 ± 0.2 for 450 km			

Crane Creek Event				
Evidence	Trenching	Landslide and terrace ages	Forest Age	Tree ring chronologies
Estimate of Timing	1480 - 1645 AD	1488 - 1640 AD	1625 ± 15 yr AD	**1620 ± 10 yr AD**
Rupture Length	A minimum length of 200 km is suggested by trenching and the landslide record but a minimum of 250 km is indicated by forest age			
Magnitude Estimate	M > 7.8 ± 0.1			

Geologists Creek Event				
Evidence	Trenching	Landslide and terrace ages	Forest Age	Tree ring chronologies
Estimate of Timing	Not yet recognised.	1420 - 1450 AD	**1425 ± 15 yr AD**	Current chronologies not old enough
Rupture Length	A minimum length of 250 km is indicated by forest age data			
Magnitude Estimate	M > 7.8 ± 0.1			

Table 5.4: Summary of the key features of the last three inferred Alpine Fault earthquakes. The best date estimate for the timing of each event is shown in bold text.

In addition to these three earthquakes other earlier events can be inferred with generally decreasing data reliability. These are estimated to have been around 1200 AD, 940 AD, 600 AD and 25 BC. It is likely some intermediate events have not been recognised. Promising work currently being undertaken in the Waitaha River (Wright, 1997) seems likely to better define some of these older events.

Chapter 6

Estimates of Probability

6.1 Introduction

Probability estimates have traditionally been used in engineering to quantify risk. If the probability of a given event occurring can be estimated then the relative risk can be balanced against the likely consequences and appropriate action taken. In general a risk with serious consequences will be planned for even if the probability of the event is assessed as being low. For example river engineers and dam builders regular consider floods with annual probabilities as low as 0.2% (the "500 year" flood). The advantage that rivers present is that they are always active, with a flow that can be monitored daily to track the variation over time with respect to the average. Furthermore the basic laws of hydraulics to which they conform are relatively simple and well understood.

Unfortunately earthquake behaviour is episodic, with long periods of relative hiatus, and many of the critical mechanical controls of the physical process are still poorly understood. As a result the application of probability theory to seismic behaviour is at a relatively basic stage. Uncertainty regards the pattern of earthquake recurrence over time leads to most of the difficulty. However in the section below we outline the application of several current methods to the assessment of the probability of the next Alpine Fault earthquake.

In all cases the probabilities apply to the large part of the central section of the fault between the Taramakau River and the Paringa River. This 190 km of the central section has the most data available, in particular the excellent forest disturbance and tree ring record. The probabilities may prove to be broadly similar for the 40 km extension of the central section down to the Haast River, but this is best estimated following the results of planned fault trenching at Haast by University of Otago and I.G.N.S. It is possible the probability of events at Haast is influenced by overlapping ruptures on the central and south Westland sections, if this does prove to be a persistent segment boundary as some have suggested (Berryman et al, 1994).

6.2 The simple Poisson model

The crudest model of conditional probability is the Poisson model. This assumes random fault behaviour and as a result elapsed time has no effect on conditional probability. With this assumption the probability of an earthquake occurring the day after the previous earthquake is the same as the probability of an earthquake occurring after several hundred years of inactivity.

To calculate the Poisson probability for the Alpine Fault for a given period (say 50 years) all that is required is the average recurrence interval for the fault. The date of the last event is not relevant. If we take the event record in Chapter 5, and for this crude exercise ignore the uncertainties in the exact date estimates for the events, the probability can be calculated simply from:

$$P_N = 1 - \exp^{(-t/tr)}$$

where P_N is the probability over 50 years; t = 50 yrs; and tr = the average recurrence interval (in this case 211 years from the recurrence interval of the last five events and the lapsed time since 1717 AD.

$$P_N \text{ for 50 yrs} = \text{approximately 20 \%}$$

The Poisson model defies common sense considerations of stress accumulation and release which suggest that some period of time is required for stress to accumulate after an earthquake before the next earthquake can occur. It tends to overestimate the probability soon after an earthquake but for faults with considerable lapsed time (280 years for the Alpine Fault) it is a serious underestimate. Thus the probability for the Alpine Fault calculated by this method represents the **lowest possible probability** and it is likely to be a substantial underestimation of the true probability.

6.3 The method of Nishenko & Buland (1987)

Early developments in improving on the Poisson model assumed that the variation of recurrence through time was gaussian and could be described by a mean and standard deviation (Sykes & Nishenko, 1984; Bakun and Lindh, 1985). However subsequent examination of sets of historic and prehistoric recurrence data proved this was not the case.

Unfortunately the small number of recurrence intervals available for each fault strongly limits inferences of the correct distribution. Each fault would take thousands of years to define the full variation of recurrence interval which it could possibly exhibit. The largest reliable set of recurrence intervals for a single fault in the historic earthquake record is only nine (from the Miyagi - Oki fault in Japan commencing in 1616 AD). Sieh (1984) defined a possible sequence of 12 prehistoric earthquakes on the Pallet Creek section of the San Andreas fault but only the most recent 5 have been considered reliable enough to use in deriving possible recurrence models (Nishenko & Buland, 1987).

To overcome the problem Nishenko & Buland (1987) adopt an alternative approach. They suggest that if enough recurrence histories are combined from as many plate boundary faults as possible this compilation will be large enough to make some meaningful deductions about the possible diversity of recurrence intervals. This is the so called *"ergodic substitution of space for time"*, as outlined by McAlpin (1996), which is widely used in geology, seismology, geomorphology and hydrology where the time ranges of events are frequently so large. This assumes that under certain circumstances sampling in space can be equivalent to sampling through time at a single location. In effect we may not be able to extend a recurrence history for a single fault much past 10 previous earthquakes, but by combining the past 2 - 4 earthquakes on 20 similar faults, a composite data set of 40 - 80 recurrence intervals becomes available.

Nishenko & Buland (1987) collected data from a number of plate boundary faults where three or more earthquakes have ruptured the same fault. They normalised each recurrence time (T) to the logarithmic mean for that region (T_{ave}), and displayed the result as a histogram of T/T_{ave} (Figure 6.1a.).

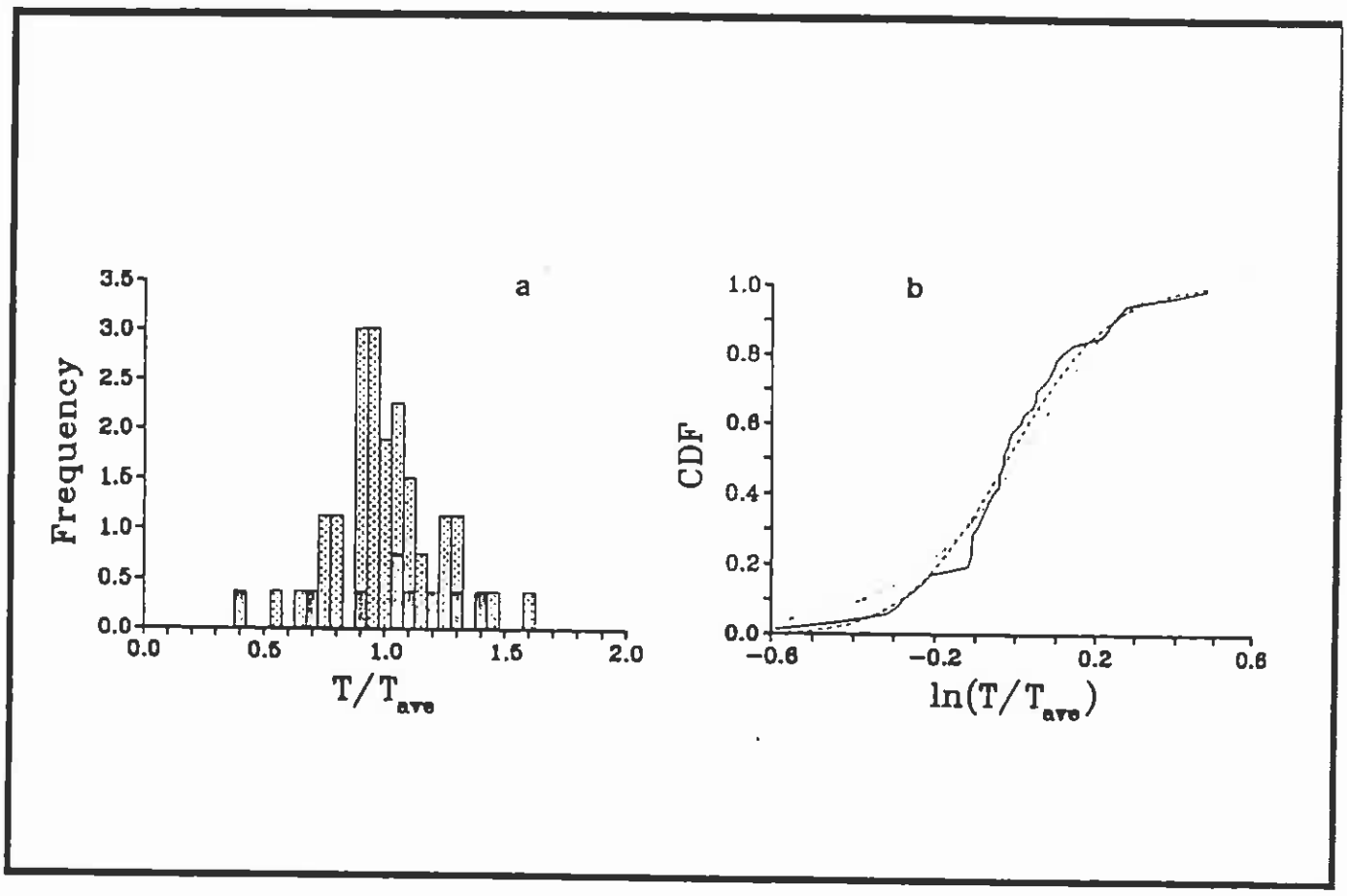

Figure 6.1- Recurrence time data from historic earthquake sequences on plate boundaries with more than three recurrence intervals from Nishenko & Buland (1987). (a) Recurrence time T normalised to the average recurrence time T_{ave} for that segment. (b) Fits of various probability distributions to the data: dashed - lognormal function ;dotted - Weibull function. Lognormal provides the best fit, especially to the tails of the distribution.

If the recurrence behaviour were perfectly periodic, the histogram would be single peak at T_{ave}, but as the figure shows this is not the case. However the behaviour is quasiperiodic with a mean recurrence time which is well defined and a standard deviation which is a measurable function of that mean. They showed a log normal distribution is the best fit to the data (refer Figure 6.1b) and preferable to the alternative of a Weibull distribution. By also defining a recurrence probability function based on this relationship the probability of an earthquakes occurring during a future period of time can also be estimated. Details of their method are included in Appendix two.

The critical parameter in the Nishenko & Buland approach is the standard deviation about the mean ($\sigma_d = 0.21$). The tails of the histogram represent a maximum variation of up to around ± 75% of mean recurrence interval (T_{ave}). Their original dataset included 53 recurrence intervals from both convergent and transform plate boundaries, which spanned a range of two orders of magnitude in recurrence time and six orders of magnitude in seismic moment (ie seismic energy). They include both historic earthquakes and earthquake sequences estimated from paleoseismic investigation, including where necessary the error from C_{14} dating associated with the estimation of these prehistoric events.

The method of Nishenko & Buland (1987) was used for estimates of the probability of earthquake rupture in California (Working Group, 1988, 1990). Savage (1991) criticised the methods of the Working Group, including challenging the adoption of the log normal recurrence interval and the standard deviation ($\sigma_d = 0.21$) of Nishenko & Buland (1987). Savage (1991) considered a standard deviation of $\sigma_d = 0.21$ was too small and suggested that individual standard deviations are likely to apply for each fault.

While this is very likely to be the case we have already outlined the difficulty involved in obtaining enough recurrence intervals to derive statistical parameters from just one fault. We consider the only solution to the problem is to adopt the ergodic approach but accept that in averaging the data some precision for an individual fault will inevitably be lost. But the data available to Nishenko and Buland (1987) can also now be extended to include an improved Pallet Creek paleoearthquake history (Sieh et al, 1989) and data from more recent paleoseismic investigations of other fault segments such as Wrightwood (Fumal et al, 1993; Biasi & Weldon, 1994); Phelan Creek (Sims et al, 1993) and Indio (Sieh, 1986), all of which do exhibit more variability in their recurrence. Furthermore the most reliable recent events in the new Alpine earthquake history as defined in this project can now also be included.

We have added these 16 new recurrence intervals to the 54 in the original Nishenko & Buland dataset and recalculated the critical parameters in their method. This update has the effect of widening the standard deviation to $\sigma_d = 0.34$, which reflects the greater scatter about the mean in the new recurrence data, and which goes some way to answering the criticisms of Savage (1991) that $\sigma_d = 0.21$ is too low. In effect this allows the possibility of a more significant number of recurrence intervals which vary substantially about the mean.

Adopting this wider standard deviation the following probabilities can be calculated for the time periods noted (Table 6.1):

Years Hence from 1998	Probability of an earthquake event (%)	
	Average	Range
1	2	1-3
2	4	3-6
5	10	6-14
15	27	12-26
20	35	20-45
30	45	30-60
40	55	40-70
50	65	50-75
60	70	55-85
70	75	60-90
100	85	75-95

Table 6.1 : Approximate probabilities of an earthquake on the central section of the Alpine Fault (between the Taramakau and Paringa Rivers) using the updated method of Nishenko & Buland (1987). The probabilities for periods of 20 years and longer have been rounded off to the nearest 5%.

The Nishenko and Buland method also allows a time window to be predicted which is defined as the 90% confidence interval about the expected recurrence time. This interval for the Alpine Fault is 1782 AD - 2014 AD.

The Nishenko & Buland method represents the best probability estimate for the Alpine Fault based on the recurrence behaviour pattern of other plate boundary faults around the world. It can be criticised for the same reasons because the recurrence pattern the method assumes has been derived in large part from other plate boundary faults and it is possible the Alpine Fault is some how different.

6.4 The method of Savage (1994)

We noted that Savage (1991) was critical of the Nishenko & Buland approach suggesting that individual faults are likely to have their own standard deviation in recurrence interval which will vary from that derived for the ergodic grouping. Savage (1994) outlines a suggested method of assessing probability which is based on Bayes theorem and requires only the data from an individual fault.

For this method to work at all for the Alpine Fault we need a large data set and have to apply it to the full earthquake sequence suggested in Chapter 5(ie 7 recurrence intervals if all the possible earthquake dates in table 5.4 are included along with their uncertainties). It is quite possible that some earthquake events are missing from this extended sequence while others may be incorrectly inferred. However the resulting probabilities are compared to the Nishenko & Buland (1987) estimates for the same time period (Table 6.2).

Years Hence	Savage (1994) Method		Nishenko & Buland (1987)	
from 1998	Average	Range	Average	Range
30 yr	33	16 - 50	47	33 - 60
50 yr	33	16 - 51	64	50 - 78
100 yr	67	49 - 85	85	76 - 95

Table 6.2: Probabilities using the method of Savage (1994), for all possible Alpine Fault earthquakes listed in Table 5.4, in comparison to probabilities for similar periods adopting the updated Nishenko & Buland (1987) approach.

The method of Savage shows the limitation in the resolution of probabilities in the medium term (ie 30 - 50 years) which follows from a limited data set. Intuitively one suspects the true 30 year value should be lower than the 50 year value, but with the Savage (1994) method and available dataset there is no way to differentiate this. The range about the average is also greater (ie for 50 years , a 34 year range compared to 27 years for Nishenko & Buland). In general the probabilities are lower than those predicted by Nishenko & Buland (1987), in part due to the increased likelihood of missed events in the extended record, but they are still significantly higher than the 20% predicted for 50 years using the crude Poisson distribution.(earlier section 6.2).

6.5 Possible clustering in earthquake recurrence

Part of the difficulty in assessing fault probability is the suggestion that some faults may produce clusters of earthquakes followed by a much longer intercluster time interval. This was first suggested by Sieh et al (1989), when they developed improved precision in their prehistoric dates for the Pallet Creek section of the San Andreas fault. McAlpin (1996) has subsequently developed the idea of bimodal recurrence intervals in relation to possible clustering, one mode representing the intercluster recurrence and the other the longer interval between clusters. Figure 6.2 shows the pattern of inferred earthquakes for Pallet Creek which to date is the best defined example of possible clustering.

The Pallet Creek pattern is characterised by variations in the recurrence interval from 44 years to around 330 years with a mean of 132 years. This equates to a standard deviation of 99 years (ie 75% of the mean recurrence). Sieh et al (1989) point to the longer intervals as defining clusters of earthquakes with a much shorter recurrence interval. This is one interpretation of the data but the difficulty is once again the short time sample. Any particularly long recurrence interval will appear in this type of short

sequence to break the pattern and define "clusters" of a more typical shorter recurrence interval for the periods before and after it.

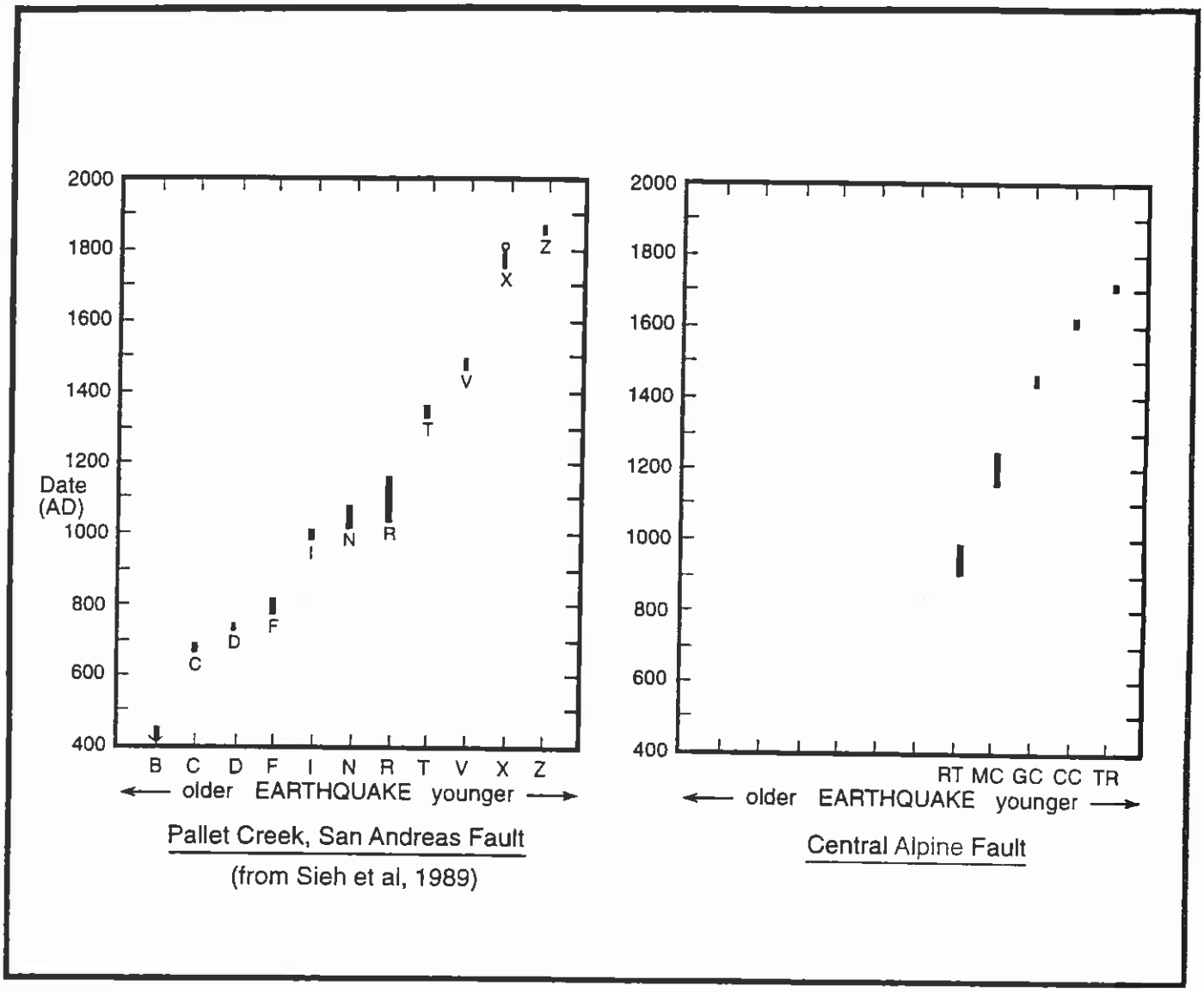

Figure 6.2 Dates from the last 10 earthquakes to have ruptured the San Andreas fault at Pallet Creek obtained by trenching studies. Error bars indicate uncertainties in the radiocarbon dates. Events are assigned alphabetical letters back from Z (the most recent) but with gaps for possible missed events (which have now been discounted). For comparison the most recent events for the Alpine Fault are also shown with appropriate error bars.

These long "intercluster" intervals at Pallet Creek vary in length from 200 years (events F - I) to 332 years (events V - X). The clusters themselves vary in having

either 2 or 3 earthquakes in each one, and the "intracluster" recurrence intervals are not constant (variation from 44 years to 134 years, a standard deviation of 30 years or 44% with respect to the mean).

The alternative explanation of the pattern is that it is simply a random expression of the natural variation in earthquake recurrence as demonstrated by the global analysis of Nishenko & Buland (1987). If another 20 or 30 earthquakes were recorded we may begin to see "clusters" of one earthquake ie two consecutive long intervals, just as we now see three consecutive shorter intervals. We may also start to see "clusters" of more than 3 events.

For comparison the most recent Alpine Fault earthquake record is plotted on the same scale as the Pallet Creek data in Figure 6.2. It must be noted that the events prior to 1440 AD are tentative. If we include the lapsed time of 280 years as a recurrence interval, the standard deviation in recurrence of the last three reliable Alpine Fault intervals is 76 years or 36% of the mean recurrence, and in general the pattern appears a little more regular than for Pallet Creek. If no Alpine Fault earthquake occurs for another 50 years the standard deviation increases to around 60% of the average recurrence and begins to approach the Pallet Creek value of 75% of the mean recurrence.

There are some important geological differences between the Pallet Creek segment of the San Andreas Fault and the Alpine Fault. In general the San Andreas fault is strongly segmented and has a smaller total cumulative offset. These factors may also contribute to a more erratic recurrence pattern.

In conclusion there is apparent evidence for possible clustering of earthquakes on some faults however this may also be the inevitable result of having only short time samples of the recurrence intervals available for analysis. The variation in recurrence exhibited in the best defined example is actually less than would be expected from the results of the ergodic analysis of Nishenko & Buland (1987). In the absence of clear evidence to the contrary the best guide to future Alpine Fault behaviour remains the averaged pattern of recurrence which has been observed globally on other plate boundary faults, including the Pallet Creek segment of the San Andreas Fault which forms part of the updated global dataset.

6.6 Mechanical and slip rate considerations

Some authors have considered the likely mechanical strength of the Alpine Fault in relation to the high strain rates indicated by geodetic networks and the long term slip rates. This cannot be used directly to calculate a probability but does emphasise there is a finite limit to the future time which will elapse before rupture.

Walcott (1978) made several assumptions regards crustal thickness, fault dip, and the rates of plate motion. By calculating the rate of accumulation of seismic moment from this data he demonstrated a return period of 255 years for Magnitude 8 earthquakes. Walcott went on to say that if earthquakes of this magnitude and regularity actually occurred "*we would expect to see features a few thousand years in age or older offset*

across the Alpine Fault at rates comparable to plate motion". At that time (1978) such features had yet to be recognised (eg Berryman, 1978), but since that time the evidence for very high rates of movement of at least 70% of plate motion has been well documented (refer section 1.2.2 for a discussion of average slip rates).

Scholz (1990) emphasises energy balance considerations with respect to the general question of earthquake recurrence. The seismic cycle of stress build up and earthquake release is an energy balance, and even if it is aperiodic it must be characterised by a mean recurrence time because the strength of the fault, though spatially variable, must be a well defined and relatively constant quantity.

Berryman et al (1992) noted that the strain rates are high on the Alpine Fault, going on to note that they "*can only continue to accumulate for one or two hundred years before rock strength of c. 1 - 10 x* 10^{-5} *(units required) is reached*". They based this observation on general estimates of rock strength from Rikitake (1976) and the absence of an Alpine Fault earthquake since 1840 AD. In light of our conclusions that the last Alpine Fault earthquake was much earlier than 1840 (ie 1717 AD) the time available before rock strengths of this order are exceeded is now less than 100 years.

Finally the other indication that we are approaching the time of the next earthquake is the limited information on single event displacement. The largest single event displacements which have ever been reported are from the south end of the fault. These are in the range of 8 - 9 m (Berryman et al, 1992; Sutherland & Norris, 1995) and if anything the single event slip appears to decrease further north. At 30 mm/yr of average horizontal fault slip it would take 270 years to produce 8m of slip. This compares with a lapsed time since the last event of c. 280 years.

6.7 Summary

Estimates of the probability of the next earthquake on the central section of the Alpine Fault between the Paringa and Taramakua Rivers vary with the method adopted. The crudest method of probability assessment assumes a Poisson distribution of earthquake events through time and indicates a 50 year probability of around 20%. However this method disregards the basic mechanical considerations of stress build and release on faults and makes no allowance for the considerable lapsed time since the last earthquake. It is a substantial underestimate of the true probability.

The best guide to the future behaviour of the Alpine Fault is the averaged pattern of recurrence which has been observed globally on other plate boundary faults. This assumes that the Alpine Fault behaves like other plate boundary faults around the world which appears to be a reasonable assumption. Analysis has defined the extent to which previous historic and prehistoric earthquake recurrence intervals have varied about a mean, and how often this variation has occurred. This forms the basis of a method of probability assessment first proposed by Nishenko & Buland (1987) and which has been updated here. Applying this method to the Alpine Fault indicates a 50 year probability averaging around 65% (range 50 - 80%) and a 100 year probability of 85% (range 75 - 95%).

Other methods which rely solely on the recurrence record for an individual fault have also been attempted but resolution in the predictions is severely restricted by the limited number of recurrence intervals for which we have reliable data. However in general the probabilities appear lower (100 year probability of approximately 70%).

It is very unlikely that the Alpine Fault can continue to be stressed at the current rate without rupture in the next 100 years. This time period is the nominal design life of most structures and the time window adopted in most planning and infrastructure development. Mechanical considerations suggest the occurrence of an Alpine Fault earthquake within this longer term time period is virtually certain.

Chapter 7

LIKELY CHARACTERISTICS OF THE NEXT ALPINE FAULT EARTHQUAKE

7.1 Introduction

While there are limitations in accuracy in predicting the characteristics of future earthquake it is generally possible to broadly bracket the most likely range of the seismic parameters. Most of the limitations derive from not knowing how much of a fault will rupture. For the Alpine Fault the last two earthquakes provide some guide to this in that both appear to have ruptured all, or most, of the central section. This makes sense in that the central section has the highest long term slip rates.

However the main questions relate to how much more of the fault will rupture. Will the south Westland section, extending from Haast to Milford Sound and possibly offshore, be included again as it appears to have been in 1717 ? The long term slip rate is estimated to be not much less for this section than the central section. And will the event be once again limited at the north end to somewhere around the Haupiri River ? Given that the area further north did not rupture in the last event could it be ready next time to also rupture ?

The answers to these questions require more investigation work, and the trenching at Haast planned by University of Otago and I.G.N.S., should ultimately assist in assessing the rupture history in south Westland. In the interim the best guide to the next event are primarily the last two events, the most recent of which offers the added advantage of being well defined with respect to rupture limits.

This earthquake came relatively quickly after the Crane Creek event (approximately 100 years), and arguably should have been a smaller earthquake in comparison, at least in the main portion of the central section of the fault which had also ruptured 100 years earlier. Despite this it is an appropriate scenario for the central section where if

anything it may be an underestimate of the next earthquake, given at least 280 years of lapsed time. Slip rates in south Westland are rapid enough for the section of fault from Haast to Milford to once again be approaching the rupture point in the seismic cycle, and we consider a scenario based on the last event is appropriate here. Only in the north section do significant questions remain and more work, preferably extending up to Lake Rotoroa, is a high priority.

We have included for comparison the magnitude and intensity predictions for the earlier Crane Creek event to check how much different this was at representative locations. We base the rupture lengths on the available forest disturbance record which extends from the Paringa River to the Rahu Saddle. However this is inevitably an underestimate and this rupture length remains a minimum until further work extends the record.

7.2 Magnitude Range

The magnitude of the next event can be estimated by two methods. The crudest is to utilise the lapsed time (280 years) and the estimates of average slip rate (Section 1.2.2). This gives an estimate of the average slip in the central section in the next event which ranges from around 7.0 m to 8.4 m if it were to happen very soon. If another 25 years were to elapse the expected slip would increase from around 7.6 to 9.1 m. From Wells & Coppersmith (1994) regression relationships between average slip and magnitude these equate to magnitudes ranging from M = 7.5 to M = 8.4.

The preferably approach, for the reasons outlined in Section 5.1.1 is to use the more reliable rupture length estimates. As noted in this section this suggests the Toaroha River event of 1717 had a magnitude range of M = 8.05 ± 0.15 (Wells & Coppersmith, 1994) to 8.0 ± 0.26 (Anderson et al, 1996). This assumes the minimum of no offshore rupture of the fault south of Milford.
For the purposes of this evaluation it is sufficient to work with M = 8 as a general guide but to note the possibility of the magnitude being either higher or lower (say a range of $7.75 < M > 8.25$). In general the possible variations become more important at greater epicentral distances.

7.3 Typical Intensities

The Modified Mercalli Scale is the most suitable general measure of the effects of earthquake shaking and provides sufficient guide to the impact of future earthquakes for most purposes. This scale can also be broadly correlated with ground accelerations and velocities if required, as is outlined in the next section.

Intensity attenuation relationships were first proposed for New Zealand conditions by Smith (1978). This relationship was used with only minor variations in Smith & Berryman (1983,1986) and Elder et al (1991). Dowrick (1991,1994) proposed a revised attenuation relationship which uniformly reduced the expected intensities at a given distance basing this on the analysis of 30 New Zealand earthquakes. Smith (1995a, 1995b) presents an updated model based on over a hundred earthquakes and proposes a more sophisticated modelling method. This allows the construction of synthetic isoseismals for specific locations and faults in New Zealand.

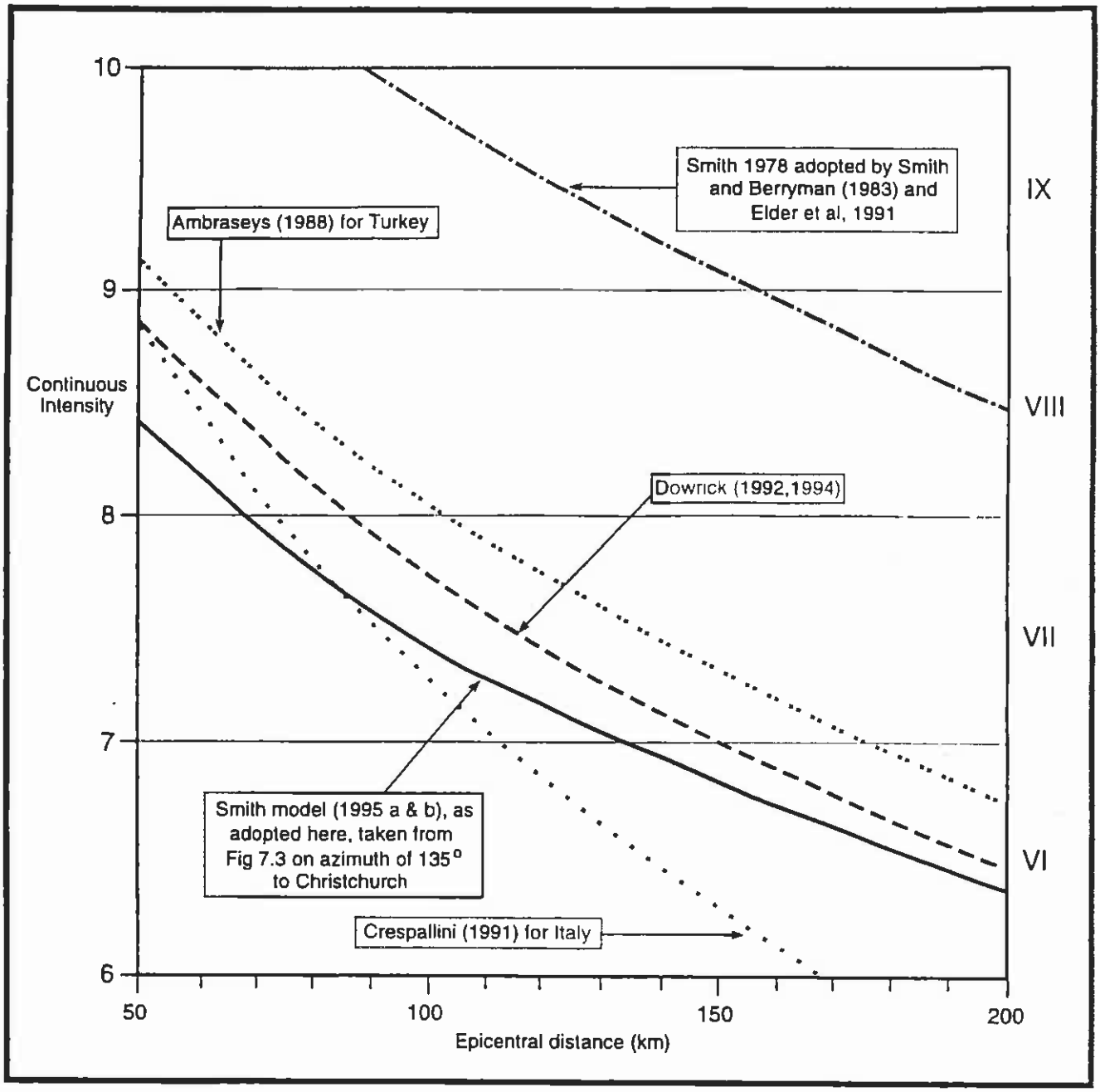

Figure 7.1 - A comparison of various New Zealand and international intensity attenuation relationships at moderate epicentral distances. Note the very conservative early relationship of Smith (1978) which has been substantially revised (Smith, 1995) and now compares well with Dowrick (1992,1994). Dowrick's model tends to predict greater intensities at a given distance than the model adopted here for later Figure 7.2 and 7.3.

Figure 7.1 provides a comparison of the attenuation relationships for New Zealand conditions and some from overseas. It is immediately apparent how conservative the original Smith (1978) model was, but there is now converging agreement between the various more recent attenuation relationships.
Smith (Seismological Observatory, pers. comm., 1997) has provided synthetic isoseismals for the most recent two Alpine Fault earthquakes. For the most recent Toaroha River event we show the one dimensional Smith attenuation relationship

(from Figure 7.2 on an approximate azimuth of 135 degrees from the fault at the Ahaura River), and compare this to that predicted using the relationship of Dowrick (1991,1992). Figure 7.1 shows that the new Smith model adopted here is now slightly less conservative than Dowrick's (ie Dowrick predicts slightly higher intensities for a given distance) but the differences are not significant.

All the attenuation relationships are for average ground conditions with no allowance for amplification, although Dowrick argues that amplification is already built in his data because most observed intensities in historical earthquakes are from alluvial locations prone to amplification. In the specific reports for Christchurch and Waimakariri District we document the evidence for substantial amplification in historical earthquakes.

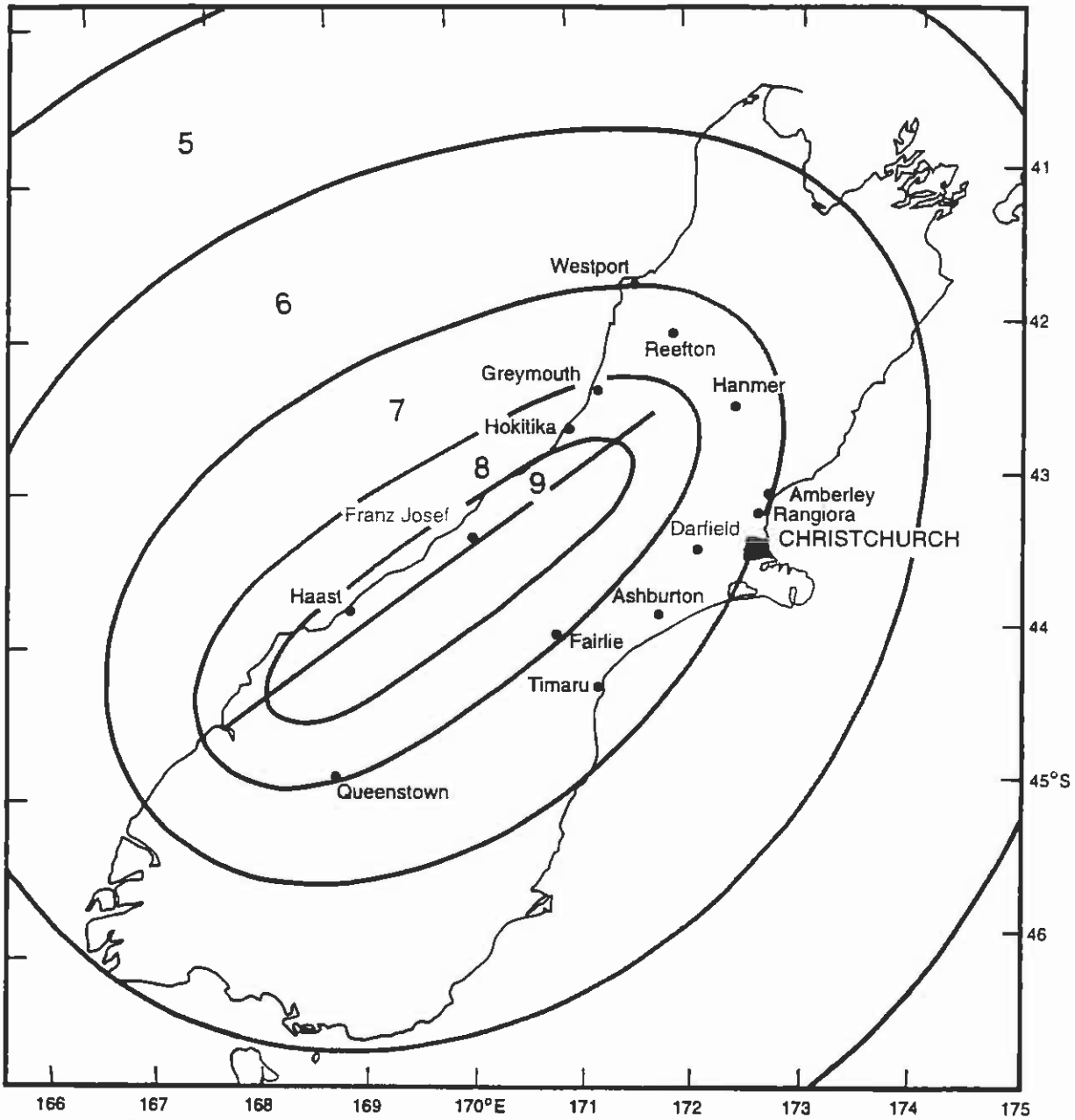

Figure 7.2 Synthetic isoseismals for the Toaroha River event of 1717 AD using the intensity formula and computational methods of Smith (1995a, 1995b). Reproduced courtesy of Warwick Smith, Seismological Observatory (pers. comm., 1997).

Figures 7.2 and 7.3 present modelled isoseismals for the two most recent events based on the rupture length and assuming M = 8. Note that the isoseismals are slightly offset east with respect to the fault trace (by approximately 10 km) to better model the dipping fault plane. The most reliable portions of the isoseismals are in the middle section where assumptions regards the length of rupture are less relevant.

The isoseismal "lines" are drawn as 20 km fuzzy bands to better emphasise the limited accuracy possible in this type of construction. It is also likely there was an MM 10 area closest to the fault trace but this is the most sensitive to local fault effects and has been left off in these models. There are no directivity effects in the modelling and the epicentre and rupture patterns are assumed to be symmetrical.

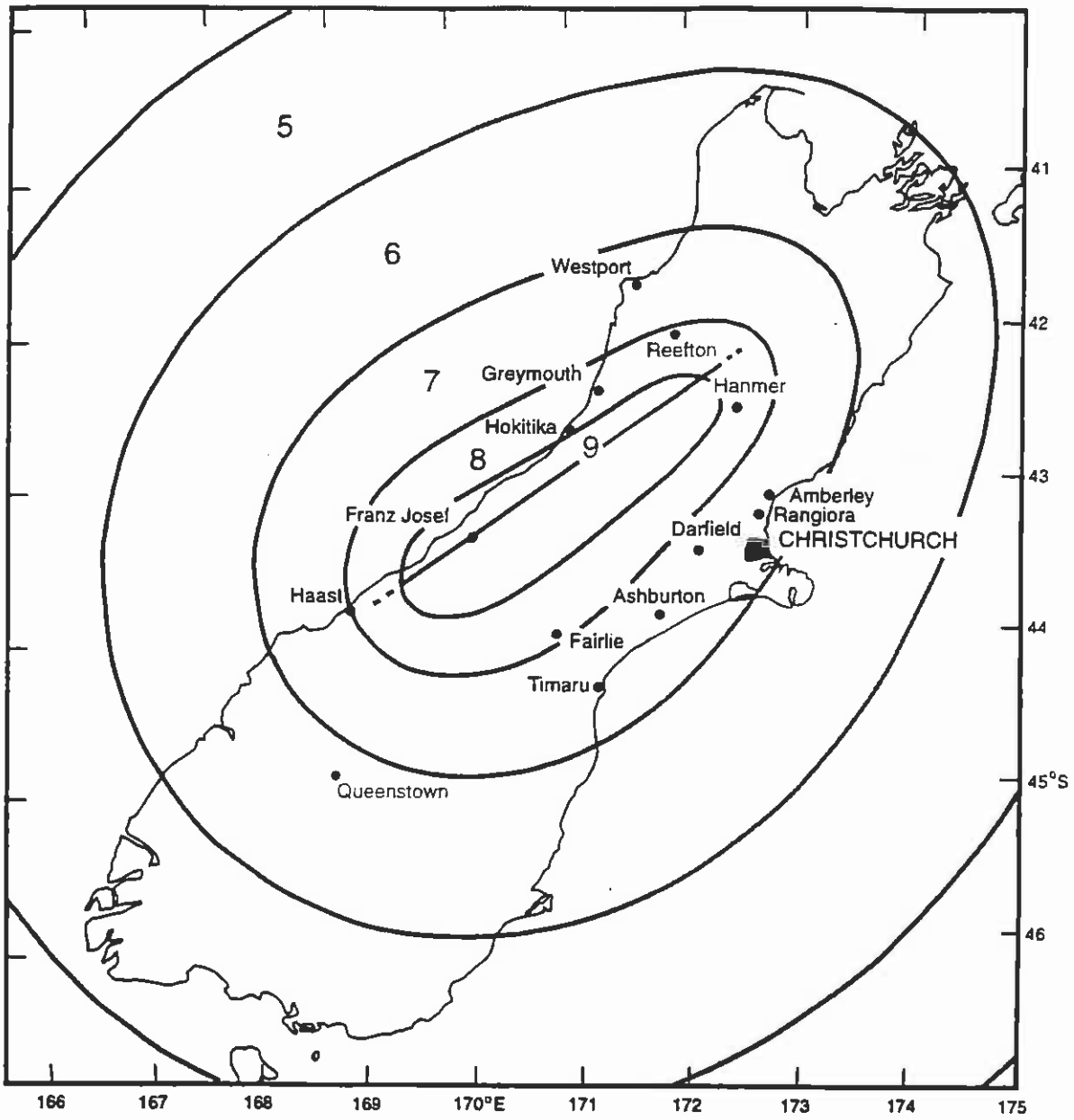

Figure 7. 3 Synthetic isoseismals for the Crane Creek event of 1620 ± 10 AD using the intensity formula and computational methods of Smith (1995a, 1995b) Reproduced courtesy of Warwick Smith, Seismological Observatory (pers. comm., 1997).

In general the Toaroha River event of 1717 resulted in relatively high shaking intensities for locations in the central and southern areas but slightly lower intensities for the northern locations such as Christchurch. This reflects the inferred northern limit of rupture at the Haupiri River, which is approximately perpendicular to Christchurch. In contrast the Crane Creek event, which the forest disturbance record indicates extended north past Haupiri another 50 km to at least the Rahu Saddle, is a more significant event for most northern locations. Unfortunately we have no data from north of the Rahu saddle to provide a basis for the possible extension of the model. However a rupture extending further north that the Rahu starts to also become a significant earthquake for such locations as Nelson and Blenhiem.

Table 7.1 below summarises the intensities which are predicted from Figures 7.1 & 7.2 at a range of locations for both scenarios.

Location	Predicted Intensity (MM units)		
	Crane Creek Event	Toaroha River Event	Modal Intensity
Otira	≥ 9	≥ 9	≥ 9
Arthurs Pass	≥ 9	≥ 9	≥ 9
Franz Josef	≥ 9	≥ 9	≥ 9
Hokitika	9	8	8 - 9
Greymouth	8	8	8
Westport	7	7	7
Reefton	8	7	7 - 8
Queenstown	6	8	7
Fairlie	7	7	7
Timaru	7	7	7
Ashburton	7	7	7
Rangiora	7	7	7
Darfield	7	7	7
Hanmer	8	7	7 - 8
Amberley	7	7	7
Kaipoi	7	6 - 7	6 - 7
Christchurch	7	6 - 7	6 - 7

Table 7.1 Predicted intensities for the two most recent Alpine Fault earthquakes and the most likely modal intensity as a guide to the next. No increase for amplification has been included here.

Figure 7.4 shows graphically a comparison of these predicted intensities with those recorded historically during other significant earthquakes. The recent revision in the intensity attenuation relationship has generally reduced the predicted intensities in the more distant eastern areas (for example Christchurch). However it is still apparent from Figure 7.4 that at most locations the next Alpine Fault earthquake will be significantly larger than any other earthquake experienced this century.

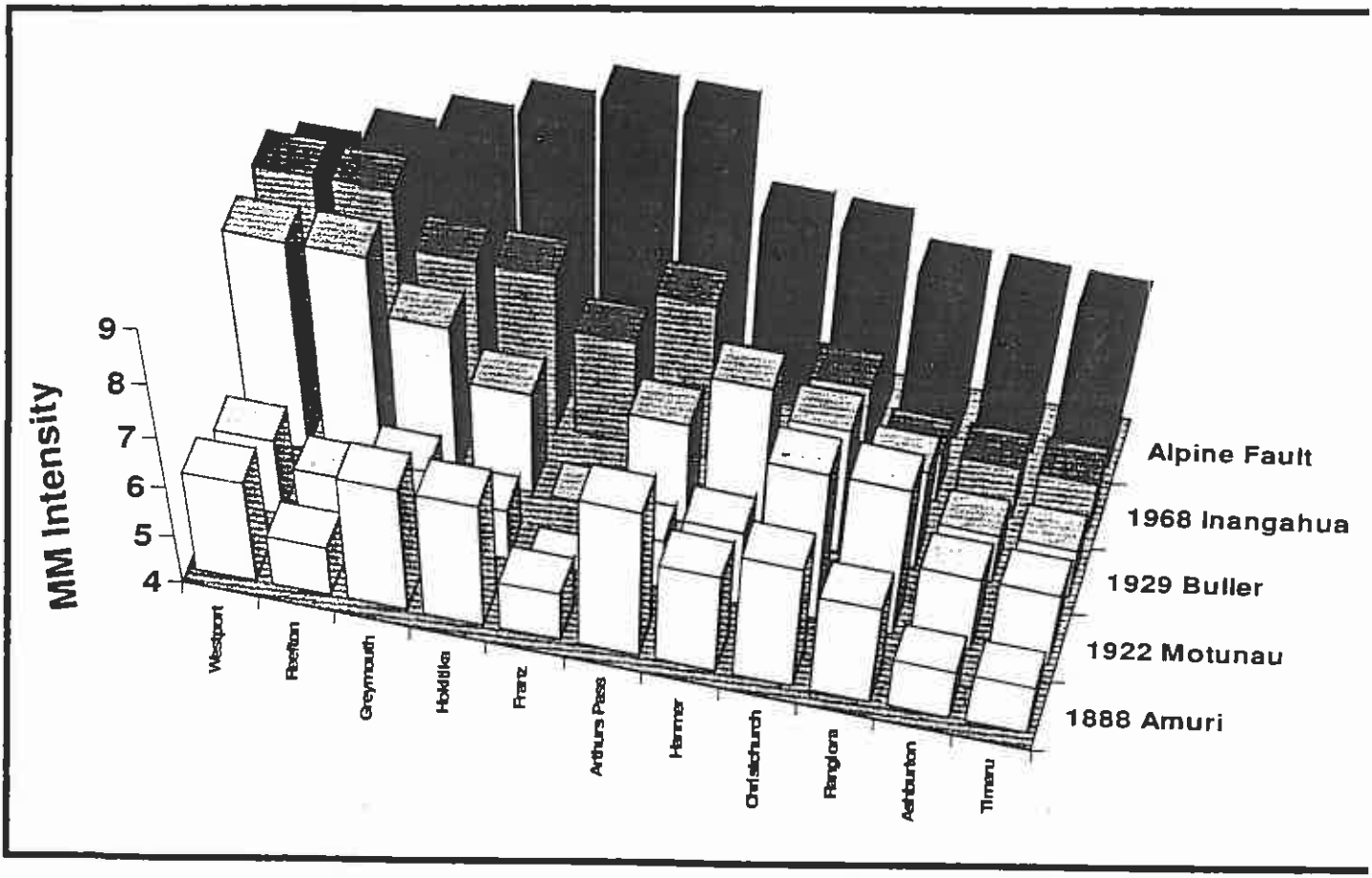

Figure 7.4 - A comparison of predicted intensities associated with the next Alpine Fault earthquake and those experienced in other significant earthquakes this century. For the predicted intensity of the next Alpine Fault earthquake at Christchurch and Kaipoi an arbitrary increase of one MM intensity unit has been added to the value from Table 7.1 to allow for amplification by the soft sediments at these locations which has been observed in historical earthquakes.

7.4 Ground Accelerations, Velocity and Duration

There are numerous published correlations which broadly convert MM Intensity to ground acceleration. Table 7.2 provides a general guide however it should be realised that local amplification and spectral effects will result in considerable variation. The values given assume average ground conditions.

The duration of earthquake shaking is broadly correlated with earthquake magnitude and is an important factor in structural performance because it reflects the number of shear cycles which are imposed on a building or utility. Long duration is also a factor contributing to soil liquefaction because the cyclic loading progressively increases pore water pressures during the time that saturated soils take to drain. In general, for a

given intensity (and associated ground acceleration or velocity), the longer the duration of the strong shaking the greater will be the damage. An Alpine Fault earthquake is likely to have a relatively long duration reflecting the high magnitude of

MM Intensity Unit	Ground Acceleration (cm/sec^2) for periods 0.1 - 0.5 sec	Ground Velocity (cm/sec) for periods 0.5 - 2.0 sec.
5	12 - 25	1.0 - 2.0
6	25 - 50	2.1 - 4.0
7	50 -100	4.1 - 8.0
8	100 - 200	8.1 - 16.0
9	200 - 400	16.1 - 32.0
10	400 - 800	32.1 - 64.0

Table 7.2 Range of ground accelerations and velocities typically associated with each MM Intensity class (taken from "Manual of seismological observatory practice", Report SE -20, World Data Center for a solid earth geophysics, September 1979)

the earthquake and the large area of the rupture surface. Unfortunately it is not possible to predict for example how much longer MM 7 or 8 shaking intensity will last at a given location compared to an equivalent MM 7 or 8 shaking intensity from a lower magnitude earthquake with a source much closer.

7.5 Directional and local effects

There will be complicated near source effects associated with an Alpine Fault earthquake. In particular on such a long fault there are likely to be so called "directivity effects" associated with the propagating rupture front. This tends to focus seismic energy in the direction of rupture. There is no way to be sure of the direction of propagation of a prehistoric earthquake. If a systematic reduction in single event slip can be demonstrated from one end of the fault to the other this may provide some guide. At present this information is lacking for the Alpine Fault.

There is a line of reasoning that the rupture is more readily initiated in relatively stiff brittle crust where the seismicity tends to be deep rather than in thin crust which is widely sheared and disjointed. This would tend to suggest initiation in Fiordland and south Westland with propagation northwards and progressive slip reduction into the Marlborough splay faults. This in turn implies directivity effects focussed around the north central section. If this was the case the isoseismals of at least the MM 9 shaking would tend to be more pear shaped and larger in the north, rather than the symmetrical shape we adopt in Figures 7.2 & 7.3.

The alternative argument is that events can initiate at either end, possibly triggered by movement on one of the Marlborough faults, and we have noted earlier it is possible the Crane Creek event was an earthquake of this type. The central section in this hypothesis is subject to ruptures propagating at different times from both ends. At present this is all conjecture and can not be usefully incorporated in the modelling.

There may also be several "subevents" within the one main earthquake event as the rupture front progresses in a matter of seconds along the range front. This will produce local increases and decreases in shaking intensity and energy release. In addition to these effects there will tend to be topographic amplification on ridge crests and hills which may be a factor in the triggering of rock avalanches and large landslides.

7.6 Foreshocks, aftershocks and triggering

There is still no consensus amongst seismologists regarding foreshock patterns and at present it is unlikely there will be significant warning given of an Alpine Fault earthquake. There is a possibility this could change over the years as more becomes known of the crustal structure of the Southern Alps and the character of foreshocks.

Aftershocks are produced following most significant earthquakes as the crust immediately adjacent to the fault adjusts to the new stress regime. This is a long process, and aftershocks may be detected with sensitive seismographs for many years after a large earthquake. In general the largest aftershock is around 50 - 75% smaller in magnitude than the main event. However because Magnitude is a logarithmic scale the largest aftershock following an Alpine Fault earthquake of M = 8 will probably be approximately M = 7, which still represents a significant earthquake. A series of more moderate magnitude earthquakes of M 5 - 7 is likely to follow over many months.

Triggering is the consequence of stress transferral to other active faults. It is essentially a variation of the aftershock process but at greater distances and involving other discrete fault systems. There has been increasing recognition of the triggering phenomena in the last few years (see for example Lomnitz, 1996). While it is likely that at least some triggering of other faults will occur it is not possible to predict exactly which faults are most likely to trigger, and how long the triggering process may take. If it were to occur to a significant extent, then a period of years to tens of years is the most likely time frame. Much longer than this and triggering becomes difficult to distinguish from normal earthquake recurrence behaviour.

Robinson (1979) noted the cumulative seismic release of energy in the main seismic zone in New Zealand appears to occur in cycles with one cycle occurring around 1850 AD and the most recent in 1930. It is possible an Alpine Fault earthquake will initiate another such cycle by triggering earthquakes on other active faults in the South Island.

7.7 Summary

The next Alpine Fault earthquake is likely to have a Magnitude of approximately 8. It is most likely to rupture the central section of the fault from Haast to Inchbonnie, but the rupture could also extend south to Milford Sound. The extent to which the northern section of the fault ruptures is still difficult to assess.

Attenuation models can be used to estimate the shaking intensity at various locations. The strongest shaking will occur close to the fault where Modified Mercalli Intensities will exceed Intensity 9. At greater distances, for example Christchurch, the intensities are still likely to be relatively strong (Intensity 7 - 8) due in part to the expected amplification by the soft sediments under parts of the city. For most locations in the study area the next Alpine Fault earthquake will be the larger than any earthquake experienced in the last 100 years.

Chapter 8

LIKELY EFFECTS OF AN ALPINE FAULT EARTHQUAKE

8.1 Introduction

In the previous chapter we have outlined the likely range of seismic parameters for the next Alpine Fault earthquake, and in particular the degree of earthquake shaking and ground acceleration which can be expected. This chapter considers the range of direct and indirect effects likely to be caused by surface rupture and shaking associated with this earthquake. Variability in natural material and conditions prevents the prediction of exactly where many of these effects will occur. The exception to this is ground rupture along the fault trace, the location of which can generally be predicted to within approximately 50 m.

This consideration of effects takes as a starting point a description of the type and extent of damage caused by the 1929 Buller earthquake of M = 7.8. We have already noted the similarities between the terrain affected by this event and the Southern Alps range front. While the magnitude of the Buller event is at the low end of the expected range for an Alpine Fault earthquake, the historical analogy is still very useful.

8.2 The Buller Earthquake of 1929

The 1929 Buller earthquake is the largest South Island earthquake this century. Figure 8.1 shows the source region and epicentral area.

The epicentre of this earthquake has traditionally been assigned close to the Buller River, and approximately 10 km west of Murchison. This is the location where reverse vertical movement of 4.5 m could be most clearly seen on the White Creek fault as it crosses State Highway 6. However Adams, 1980b shows a elliptical distribution of landslides with a much more northern bias which would tend to shift the epicentre north east by around 50 km (ie closer to Seddonville and Karamea).

Intensity estimates are hindered by the lack of population in the epicentral area. It is likely MM 10 was reached closest to the fault rupture but isoseismal maps do not show this. Murchison was the most strongly shaken population centre with an estimated intensity of MM = 9, comparable to a peak ground acceleration of 0.5 - 0.9g. Westport was the next most seriously affected large town. Table 8.1 summarises the material damage from the event under several categories.

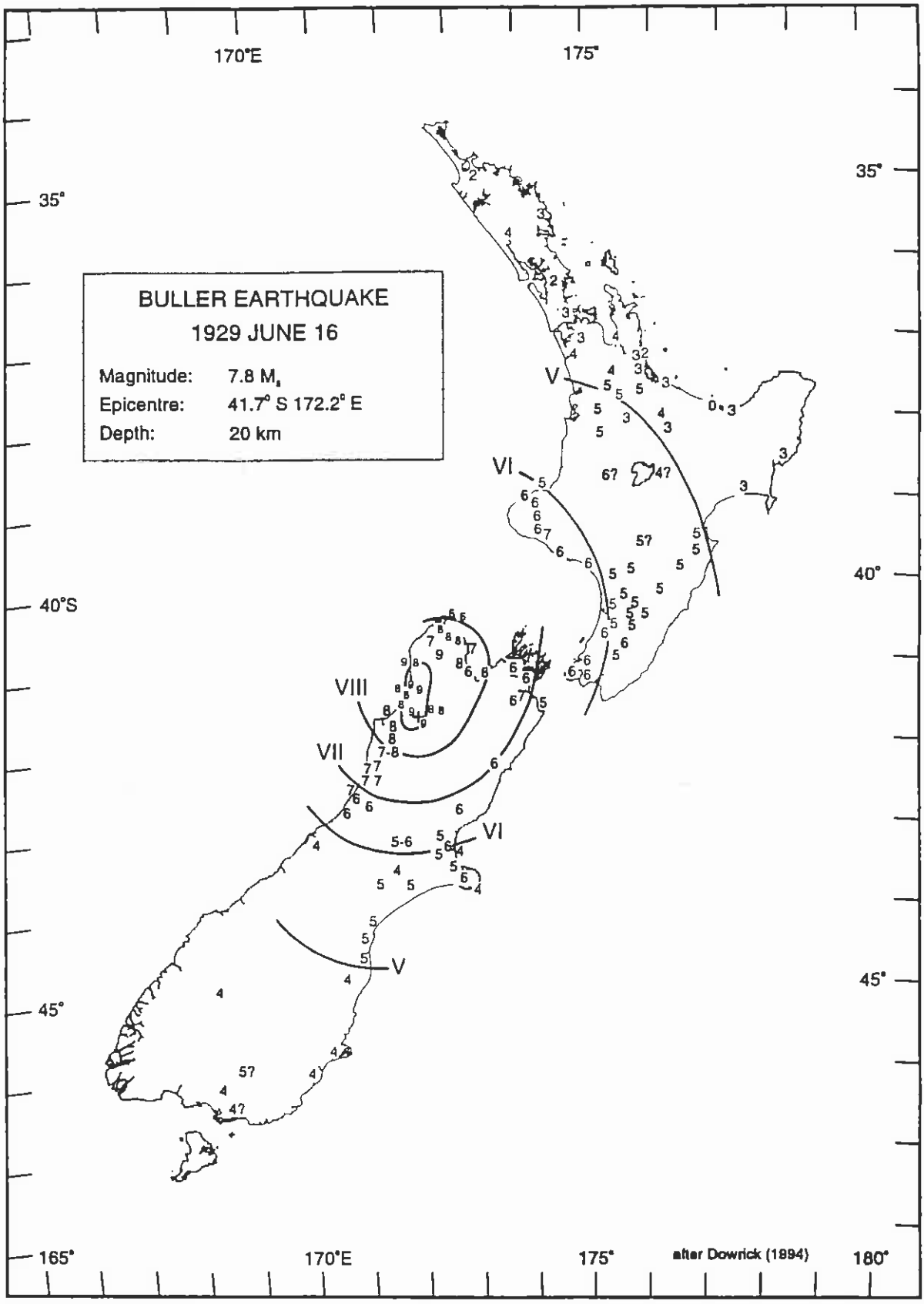

Figure 8.1 - Isoseismals for the 1929 Buller earthquake of M = 7.8. Note the asymmetry of the epicentre with respect to the area of strongest shaking leading to suggestions it should be plotted further north. The MM intensity of 6 at Christchurch is from observatory files and a specific investigation of felt intensities (Dibble et al, 1980) indicates MM 7 in many parts of the city. From Downes, 1995 based on Dowrick, 1994.

Type of Damage	Description
Buildings	Murchison: MM = 9. The main damage to buildings, apart from Hodgsons Store and the BNZ, was practically confined to the universal loss of chimneys. Some houses fell off piles. The BNZ was partly damaged, and the two storey Hodgsons Store was near collapse, due to large sway deflection of the top floor. Westport: MM = 8. Greymouth: MM = 7 Nelson: MM = 8
Services	Not well documented but moderate. Murchison lost it's power station for several months. Westport lost electricity for 13 hours, water for 9 days and the telephone exchange for 3 days. Gas mains broke in 4 places. Various of the smaller communities lost telephone and power for lengthy periods because of landslides sweeping the poles away.
Roads and Bridges	Major damage from landslides occurred within the MM 9 zone, in particular SH 6 between Inangahua and Murchison. This section of road took 22 months to repair and reopen. Landslides also caused major damage to roads in the Matakitaki valley, Maruia saddle and Karamea Bluff (Corbyvale Pass). Subsidence and spreading of embankments and bridge approaches occurred in many local areas as far away as Greymouth (c. 120 km from epicentre) and Takaka and Collingwood (a similar distance). Bridge structural damage was not widespread and generally confined to displacements of the abutments or piers (the Matakitaki bridge at Murchison, the Lyell Creek bridge, the Newton Creek bridge and the Little Wanganui bridge).

Table 8.1 Summary of damage to the built environment during the 1929 Buller earthquake (after Dowrick, 1994; Adams, 1981; Henderson, 1937).

Ground rupture occurred along the White Creek Fault but the only area easily accessed and investigated was adjacent to the Buller River. The trace was followed northwards in the forested and rugged terrain for a total length of around 8 km but the total length

may have been much greater. The main impact of the fault rupture was to SH 6 at White Creek where the road was offset vertically by around 4.5 m.

While damage to buildings, bridges and services was substantial, the epicentral area was very sparsely populated, so that the greatest damage was caused to the natural landscape and the few rural occupants by countless landslides. Pearce & Watson (1986) estimate 410 landslides occurred in just the c. 100 km^2 Matiri catchment. However landslides extended over a total area which was at least 50 times larger, estimated to be more than 5,000 km^2 in total (Adams, 1981). Landslides were more numerous in this earthquake than for any other in New Zealand. This reflects the altitude range and very steep nature of the terrain, with many slopes close to their natural equilibrium.

It was also aggravated by the weather conditions and the high moisture levels prior to the earthquake which occurred in June. Henderson (1937) notes the soil and subsoil were saturated, and Dowrick (1994) demonstrates this was a much wetter June than normal for all the weather stations in the region. While the majority of the landslides were surficial failures of residual soil or thin colluvium sliding on top of deeper harder rocks, the largest landslides more deepseated, and commonly involved failure parallel to bedding planes.

The importance of landslide impacts is reflected in the record of fatalities. Of the 17 people killed as a result of the earthquake, fourteen were killed by landslides. In nearly all cases they were in houses built on relatively flat low ground but near the toe of steep and high slopes. Debris runout from the landslides destroyed the houses and killed or injured their occupants. Henderson (1937) describes landslides in the Matakitaki valley 3 km from Murchison. A deepseated failure in the Tertiary muddy sandstones, which dipped at 30 - 40 degrees towards the valley floor, produced a debris flow which travelled across the river terraces burying these in up to 60 m of debris. Two houses were destroyed at this location with 5 people losing their lives. The Matakitaki River was dammed as result and a 4 km long lake was created which lasted for many years.

Four more people died in a very similar landslide in the nearby Maruia Valley, where slide debris from dipping Tertiary sandstones overwhelmed a homestead. Once again a landslide lake was formed, which was over 5 km long, but in this case the river diverted around it within several days.

Landslide dams were very common in the Buller earthquake. The Buller, Mokihinui, Karamea, Matakitaki, Matiri and Maruia Rivers were all dammed at some stage. Most of these dams have subsequently been removed by river erosion. For example the landslide dams on the Karamea River are now marked by steep, boulder-strewn sections of river rapids, with intervening sandy low gradient reaches (Adams, 1981). The Mokihinui River gorge above Seddonville was also dammed by landslide debris, killing two prospectors on the track, and forming a 11 km long lake (Lake Perrine) up to 20m deep. Three weeks after the earthquake, part of the dam washed out, and the lake suddenly lowered 8m thereby flooding Seddonville. During the flood houses were shifted off their foundations, the hall drifted some tens of meters, and the whole of the Seddonville alluvial flat was deeply covered in water (Henderson, 1937).

Liquefaction was not well understood as a phenomena at the time but Henderson (1937) describes damage to alluvial ground which is very likely to have been liquefaction induced. He notes the earthquake caused:

" numerous sections of river bank to collapse, rents more or less parallel with them to appear - perhaps many chains back - and large masses of poorly consolidated material to move bodily to the unsupported sides. Movements of this kind occurred commonly throughout the region - roads were fissured and depressed; fences were displaced, and railway lines buckled. A good deal of damage was done in Greymouth and Westport, where cracks opened in the streets, water-mains, gas-mains, and sewers were broken, and houses were distorted. At Westport the wharf was slightly damaged. At Karamea a considerable area north of the township moved towards the river, distorting the wharf and training wall and disrupting a tramway. Many fissures opened along the foot of a terrace of older alluvium on the north side of the area, and also on the east side ..... the area sank by 2 ft 3 in. It is the youngest estuarine flat built by the river and is raised but a few feet above sea level.

8.3 Immediate effects of the next Alpine Fault earthquake

8.3.1 Ground rupture and warping

While much of the Alpine Fault trace is also in heavily forested rugged terrain there are number of points where roads and rail routes cross the active trace. We would expect a dextral horizontal offset along the fault trace varying from around 1.8 ± 1 m in the north to around 8 ± 2 m further south. This assumes the range of slip rate of 25 - 30 mm/yr, a lapsed time of approximately 280 years, and a component of natural variance in slip of 30 %. The vertical component will be considerably less, and probably in the range between 0.5 - 1.5 m. Ground distortion and tilting immediately adjacent to the trace is likely to vary in extent with location but will be common within 50 - 100 m of the trace. In some locations (trace step-overs, areas between multiple traces etc) the zone of deformation will be larger.

With the possible exception of Franz Josef (Figure 8.2) no houses are built across the most likely point of next rupture which is generally near the base of the fault scarp. At Haupiri River (and to a lesser extent Inchbonnie) farm houses are built on, or very near, the top of the fault scarp. While these particular houses will be severely shaken, and possibly affected by permanent ground warping, they are unlikely to be physically ruptured by fault offset within their foundation perimeter.

As noted above the main impact of fault rupture at the fault will be to roading and rail where these cross the trace. Table 8.2 below summarises the likely rupture points.

While the locations listed are virtually certain to be rendered at least temporarily impassable, by far the greatest proportion of road and rail disruption will be caused by landsliding, liquefaction and structural damage to bridges. These effects are discussed separately below.

Figure 8.2 - The Alpine Fault trace passing through SH 6 at Franz Josef. The trace is marked by the slight rise in the road immediately in front of the red 4WD. It crosses the road and passes under the service station forecourt.

Figure 8.3 - The Falling Mountain rock avalanche which occurred in the 1929 Arthurs Pass earthquake. This type of large scale rock avalanche is likely to occur in an Alpine Fault earthquake. Photo courtesy of Tim Davies.

Road or rail route	Grid Ref, NZMS 260 Series
SH 7, Lake Daniels rest area	L 31/458725*
Amuri - Haupiri Rd, Ahaura River	L 32/132484*
Inchbonnie - Rotomanu road and rail	approx. only at K32/877323
Inchbonnie - Rotomanu road , Lk Poerua	K32/863314
Jacksons - Inchbonnie Rd, Inchbonnie	K 32/847304
SH 73 Rocky Point	K33/825291
Lake Arthur Road, Kokatahi	J33/588116
SH 6 Whataroa River	I 35/004667
SH 6 Whataroa River	I 35/991658
SH 6 Franz Josef township	H34/818537
SH 6 near Franz Josef	approx. only at H34/811534
SH 6 Paddy Creek	H34/744492
SH 6 Cook Saddle	H34/713463
SH 6 Karangarua	H34/715466
SH 6 Karangarua	H34/524322
SH 6 Haast	

* will only be affected if the far northern section ruptures

Table 8.2: Points of likely fault rupture of existing road and rail routes on the west coast.

8.3.2 Ground shaking

Chapter 7 outlines the likely range of intensity and the typical ground accelerations associated with these intensities which can be reasonably expected in the next event. Ground shaking will cause direct damage to buildings, contents, and services through cyclic vibration at a wide range of frequencies.

Unfortunately even if the exact characteristics of the seismic waves generated by an Alpine Fault earthquake were fully known these waves will be attenuated, reflected and refracted in a complex and largely unpredictable manner by the geological materials they pass through. The geology along every wave path varies, and the final outcome, which is ground shaking at a specific surface location, is subject to the sum of all the variability. Additional to this is the wide variety in building type, building age, and natural period which then governs the response of structures to the shaking. However it is possible to use historical precedent and the current categories of building type to make some general predictions regards damage levels (Table 8.2). The locations which could reasonably expect this intensity of shaking are also noted.

Variations in foundation conditions within a town are likely to result in a range of intensity of at least one intensity unit, and possibly up to two. For cases where amplification has been documented and predicted (for example Christchurch) we discuss this further in the specific reports for the relevant city and regional council. The estimates in Table 8.3 should be viewed as general approximations providing an appropriate scenario to guide relevant district and regional councils and infrastructure providers.

Intensity (& towns likely to experience this)	Impact on People & fittings	Impact on Structures
MM = 7 Part of ChCh Ashburton Timaru Rangiora Amberley Hanmer Darfield Fairlie Queenstown Westport ?	General alarm Difficulty in standing Noticed by drivers of cars Furniture moves on smooth floors and may move on carpeted floors. Some contents disrupted.	Unreinforced stone and brick walls, and poorly built rammed earth and mud houses (Type I) cracked. Some damage to old but well built unreinforced masonry buildings (Type II). Unbraced parapets and architectural ornaments fall. Roofing tiles dislodged. Many chimneys broken. A few instances of damage to brick veneers and plaster or stucco linings. Water cylinders move or leak. Some cracked windows.
MM = 8 Greymouth Reefton Murchison Part of ChCh Westport ?	Alarm may approach panic Steering of cars greatly affected. Furniture and contents damaged.	Well built but old unreinforced masonry buildings (Type II) damaged, some severely. Some cases of damage to Pre 1970 - 1980 buildings (Type III). Monuments and external tanks fall. Brick veneers damaged, some post 1980. Weak piles damaged and houses not secured to foundations may move.
MM = 9 or more Hokitika Ross Hari Hari Whateroa Franz Josef Fox Haast Moana Otira Arthurs Pass	General panic. Furniture and contents greatly damaged.	Well built but old unreinforced masonry buildings (Type II) heavily damaged, some collapsing. Pre 1970 - 1980 buildings damaged, some seriously. Damage and distortion to modern buildings and bridges. Houses not secured to foundations shift off them. Brick veneers fall and expose framing.

Table 8.3: Average intensities for towns and cities which could experience significant ground shaking in the next Alpine Fault earthquake. The method of intensity prediction is outlined in Chapter 7. Correlations between intensity and damage etc from Downes (1995).

As noted in section 8.1, shaking of MM = 9 has already been experienced on the West coast in the epicentral area of the Buller earthquake. Other New Zealand earthquakes which have produced MM = 9 shaking affecting towns include the Wairapa earthquake (1855, MM = 10 in Wellington and MM = 9 in the Wairapa); the Inangahua earthquake (1968, MM = 10 at Inangahua Junction) and the Edgecumbe earthquake (1987, MM = 9 in Te Teko and parts of Kawerua and Edgecumbe).

It is likely a considerable area of MM = 10 shaking will also result from a Magnitude 8 Alpine Fault earthquake but this can not be modelled with any confidence because of the sensitivity of this narrowest isoseismal area to assumptions regards fault rupture depth, rupture propagation direction and the total length of rupture. In general it is most likely to be centred slightly east of the fault trace, and coincide with the highest altitude areas of the western Southern Alps.

8.3.3 Landslides

As occurred in the Buller earthquake, landslides are likely to be the main direct impact on the natural environment, and these will affect roading, services and property located close to the range front or other areas of steep slope. The expected abundance of landslides is the inevitable result of the juxtaposition of the steepest and most elevated area of relief in New Zealand with the epicentral region of strongest earthquake shaking.

Keefer (1989, 1984) noted the relative abundance of relatively shallow rock falls and disrupted soil slides during earthquakes. This type of failure will dominate, as it did in the Buller earthquake. The least common type of failure on a numerical basis is rock avalanches but ironically, when these do occur, they are most frequently triggered by an earthquake (Voight & Pariseau, 1978; Whitehouse & Griffiths, 1983).

The best known New Zealand historical example of a rock avalanche is Falling Mountain triggered during the 1929 Arthurs Pass earthquake (Figure 8.3). This rock avalanche flowed 3 kilometres down the west branch of the Otehake River producing an estimated 100 million tonnes of debris (Cave, 1987). However rainfall and removal of slope support are also possible non-seismic triggers for this type of failure as was recently demonstrated by the Mt Cook rock avalanche.

Whitehouse (1983) compiled information on 46 Holocene rock avalanche deposits in the Southern Alps between Mount Cook and Arthurs Pass. The age estimates for these rock avalanches are based mainly on the weathering rind dating technique for greywacke (Chinn, 1981) which has recently been recalibrated (McSaveny, 1992). Cowan et al (1996) used a recalibrated data set to demonstrate that in general these rock avalanche ages do not coincide with inferred earthquakes in the Porters Pass - Amberley fault zone and they attribute these to possible earthquakes on faults further to the west. Figure 8.4 shows the distribution of all known rock avalanches between Mouth Cook and Arthurs Pass and Table 8.4 summarises the date information.

Since the work of Whitehouse, the Roundtop debris avalanche near the Toaroha River has been recognised and described (Wright, 1994; Wright, 1996), and has subsequently been dated as part of this study. This debris avalanche has an estimated deposit

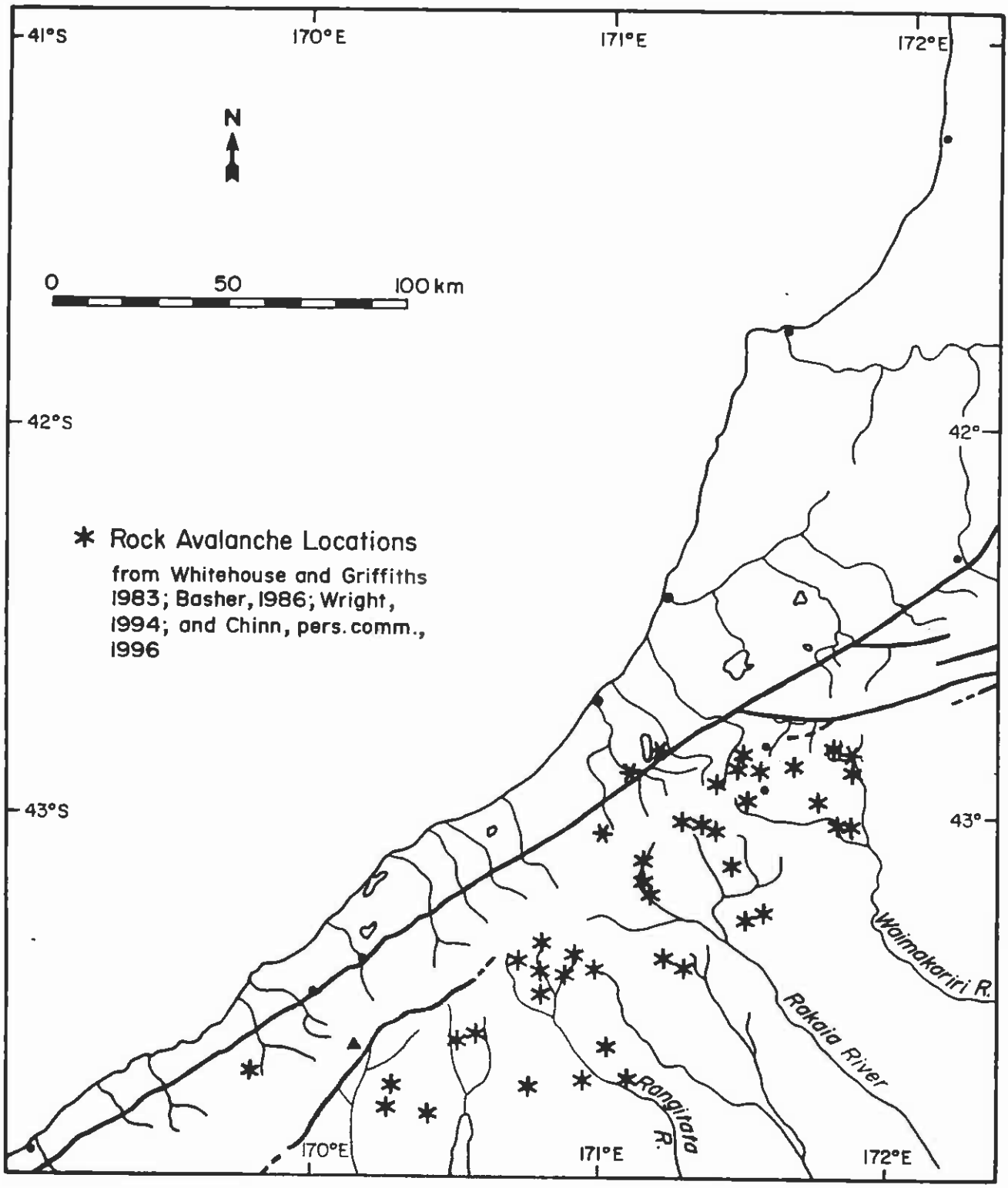

Figure 8.4 - All known rock avalanche locations in the Southern Alps and Westland between Mount Cook and Arthurs Pass. Information from Whitehouse (1983), Whitehouse and Griffiths (1983), and this study.

volume of 45 ± 28 million cubic metres and an extreme run out of approximately 3.5 km, measured from the base of the range front to the distal end of the deposit. Figures 8.5 and 8.6 show the source area on Roundtop and the runout material.

We obtained an intact section of broken kahikatea log from the abundant trees scattered among the basal debris exposed in a recent diversion of Cunninghams Creek (GR J33/535095). Radiocarbon dates were obtained for sections from both the sapwood, and wood closer to the heart, after first counting the rings bounding these. The possible calendric age is then restricted to the adjusted overlap in the respective calendric ranges and the error is substantially reduced. The age of the deposit is 950 ± 50 AD. Bull (1996) noted the clustering of eight rock avalanches ages approximately 1000 years ago (ie a mode of 963 AD). Could all of these avalanches been triggered by an Alpine Fault earthquake at this time as is suggested by Bull ? While the dating errors are so great that this cannot be categorically demonstrated it does appear to be very likely.

Locality	**Recalculated age in calendar years AD** (Nichols pers. comm, 1996)	**Possible Alpine Fault event**
Craigieburn Range	1700 AD ± 70	Toaroha River event
Clyde River	1626 AD ± 28	Crane Creek event
Havelock River	1620 AD ± 90	Crane Creek event
Cropp River (Basher, 1986)		Crane Creek event
McTaggart Creek		Crane Creek event
Lawrence River (Herm. Hut)	1365 AD ± 160	Geologists Creek event ?
Geologists Creek (Chinn, 1996)		Geologists Creek event
Lawrence River	1290 AD ± 180	Muriel Creek event ?
Cass River	1200 AD ± 200	Muriel Creek event
Roundtop Debris Avalanche	950 AD ± 50	Roundtop event
N. Ashburton River	960 AD ± 270	Roundtop event
Rangitata River (Lake Camp)	930 AD ± 270	Roundtop event
Rangitata River (Pudding Valley)	880 AD ± 270	Roundtop event
Havelock River (Fan Stream)	960 AD ± 270	Roundtop event
Rangitata River (Forest Creek)	960 AD ± 270	Roundtop event
Godley River (Bloody Point)	880 AD ± 270	Roundtop event
Jollie River (Arthurs Pass)	880 AD ± 270	Roundtop event
Mathias River (Boundary Ck)	1000 AD ± 270	Roundtop event

Table 8.4 : Possible correlation between the recalculated rock avalanche ages of Whitehouse & Griffiths (1986) and inferred Alpine Fault events. Recalibrated age estimates are provided by Nichols pers. comm. 1996.

Figure 8.5 - Roundtop on the left with the reforested scarp creating an obvious "hole" in the side of the hill. The run-out material from the debris avalanche forms the hummocky ground at the right and extends past the photo right margin to the banks of the current Kokatahi River (see also below).

Figure 8.6 - The avalanche debris near the Kokatahi River forming Lake Arthur and adjacent lakes. The very smooth surface of the debris under pasture is a result of bulldozer regrading.

Figure 8.7 shows the distribution of the rock avalanches from this time. They are exactly where we would expect them to be for an Alpine Fault earthquake based on the isoseismal patterns presented earlier. However this also corresponds to the steepest area of the country where the preconditions are most favourable for their occurrence.

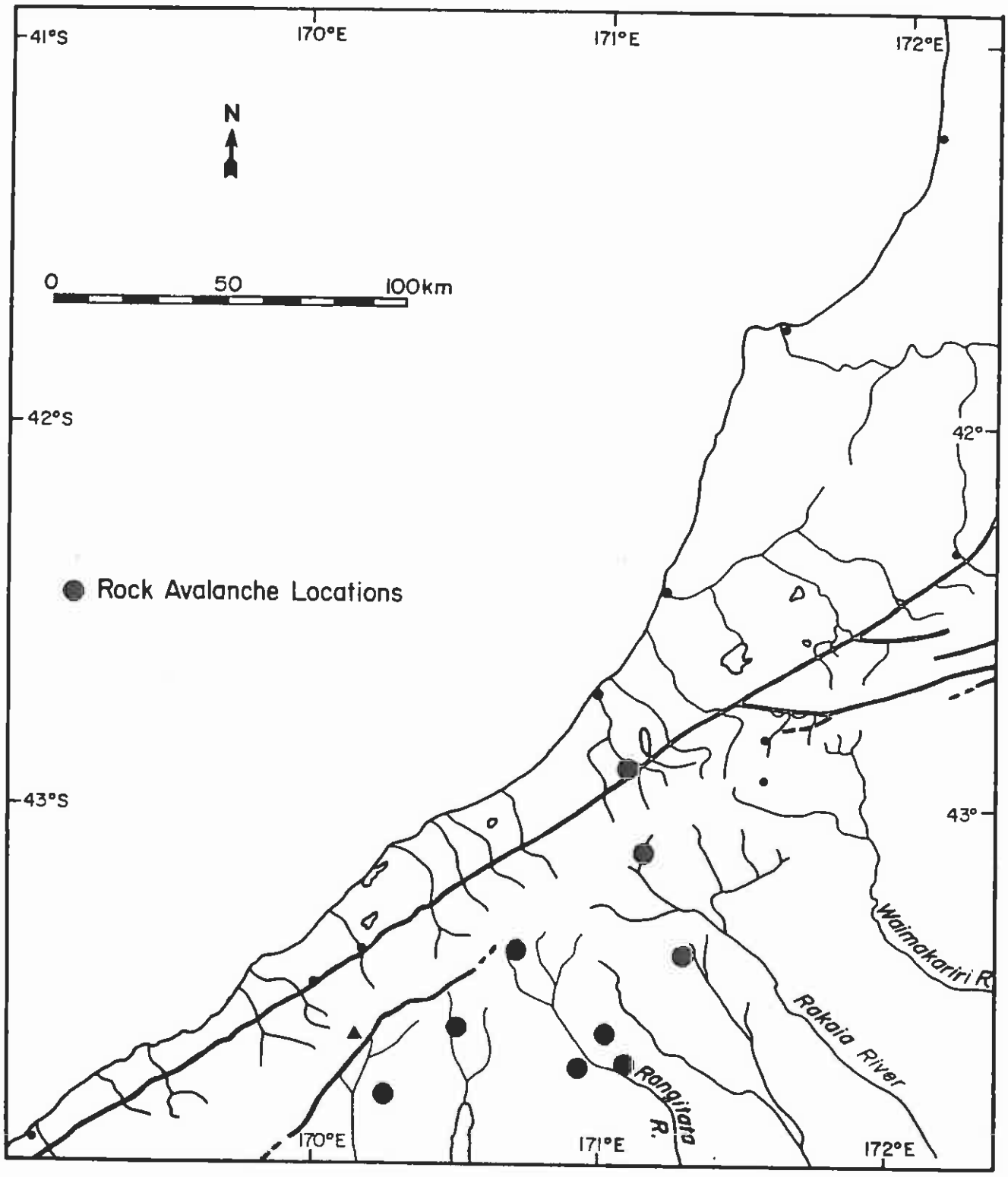

Figure 8.7 - Locations of known rock avalanches with ages matching the inferred Roundtop Alpine Fault earthquake event approximately 1000 years ago.

Other inferred Alpine Fault events may also be represented in the rock avalanche ages of Whitehouse and Griffiths. Table 8.4 indicates other possible matches. The most recent Toaroha River event appears to be poorly represented, but possible connection to this event is hampered by the large date error, relative to the short time interval, between this and the penultimate Crane Creek event.

The Crane Creek event has four possible matches. The Geologists Creek event, and the preceding poorly defined Muriel Creek event, each have two possible matches.

If these have been triggered by Alpine Fault earthquakes, and if the relative abundance of the deposits is a true reflection of shaking intensity, this would suggest the largest event of the four was the Roundtop event, which is strongly represented despite it also being the oldest. Conversely the smallest, at least in this area north of Mount Cook, appears to have been the Toaroha River event. This also matches the suggestions in the forest disturbance record.

However there are many assumptions in these inferences and both more data, and a higher dating precision, is required to seriously test these hypotheses.

The Roundtop debris avalanche does indicate the possible hazard which exists at the Southern Alps range front, particularly to property within 500 metres to 1 kilometre of the foot of the mountains. However, even in a large earthquake it is unlikely that many long run out landslides of this scale will occur right at the range front. It may not be practical or reasonable to exclude development along the entire range front just in case one does occur.

Areas most likely to be seriously affected by landslides

Various magnitude - distance relationships have been derived from landslides triggered in historical earthquakes to estimate the likely distance from the fault rupture that earthquake triggering can occur. The broadest classification is that of Keefer (Keefer, 1989; Keefer, 1984) which attempts to define the maximum distance landsliding will be triggered for a given magnitude of earthquake. A similar general relationship has been derived by Yasuda & Sugitana (1988), mainly from the extensive Japanese historical earthquake record. Both these general relationships suggest landslides will be triggered at distances as far away from the Alpine Fault epicentral region as 170 km (Akaroa). This also matches estimates which suggest triggering occurs at relatively low intensities of around MM 5 and 6 (Keefer, 1989).

While this may be correct at these most distant limits the number of landslides triggered will generally be very small. Of more practical application are the few studies in which the number and/or areal proportion of landslides have been assessed. Table 8.5 outlines predictions of the extent of landsliding at various locations based on Ishimara & Nakumura (1987), who studied the distribution of slopes which failed during the 1987 Equador earthquake on a percentage basis.

The towns included in Table 8.5 are not intended as a full list of those locations likely to be affected but provide a range of epicentral distances over which to establish the likely general pattern. Mora & Mora (1993) studied slope failures in Costa Rica

during 11 earthquakes from 1888 to 1991 and estimated the maximum distances from epicentres for two different categories: areas where more than 60% of slope failed, and areas where less than 15% of slopes failed but in which at least one slope per square kilometre failed. This latter category is still a large number of landslides but it marks the transition to areas where the impact of landslides becomes more minor.

Location	Distance (kms) *	Ishihara & Nakumura, 1987[1]	Mora & Mora, 1992[1]	ISSMFE, 1993	**Synthesis**
Otira	5	80 - 90 %	> 60 %	Destructive failures common	**Major Impact**
Franz Josef	10	80 - 90 %			
Arthurs Pass	10	80 - 90 %			
Main Divide	1- 20	50 - 80 %			
Mt Cook Village	20	50 - 60 %			
Hokitika	35	40 - 50 %		Failures occur but less serious	**Moderate Impact**
Greymouth	50	15 %			
Tekapo Village	60	<15 %	15 - 60 %		
Cant. Foothills	60 - 80	< 5 %	15 - 60 %		
Queenstown	75	Very few	< 15 %		**Low Impact**
Buller gorge	100	Very few	< 15 %		
Port Hills, ChCh	130	Very few	< 15 %		
Akaroa	170	Very few	Very few		

* Distance from the long axis of the maximum likely isoseismal
[1] Proportion of slopes which fail

Table 8 .5: Comparison of locations within the likely zone of slope failure triggering during an Alpine Fault earthquake, based on the most general relationships of Keefer (1989,1984) and Yasuda & Sugitana (1988). The relative abundance and impact of the landslides at indicative locations is then assessed by the more detailed methods noted in the right hand columns.

Because the Mora and Mora (1993) system has just two categories it is not easy to compare with Ishimara & Nakumura (1987). At moderate distances of around 30 - 50 kilometres, Mora and Mora appear to predict considerably more landslides. However the Mora and Mora (1993) approach has the advantage of being based on 11 earthquakes, not just one as for Ishimara & Nakumura. These 11 earthquakes span a range of pre-existing climatic conditions and geology and in general it is likely to be a more reliable estimate.

Climatic factors are important in applying these relationships. We noted in section 8.1 how the wet weather prior to the Buller earthquake was a factor which increased the landslide impact. I.S.S.M.F.E.(1993) also reviews existing relationships between epicentral distance and landslides and suggests a distinction be made between wet and dry areas. They adopt two categories; the most severe being "destructive slope failures" and a lesser category of simply "slope failures". This appears to be similar to the 60 % and < 15 % percent category of Mora and Mora (1993) but with a more subjective basis. In applying their method we have adopted a climate on the wet side

of average for areas west of the main divide and dry of average on the east. Table 8.5. shows these results and the two categories for our selection of locations.

It appears that no matter what method is used there is consistent agreement that the areas of slope within 30 km of the likely epicentral region of maximum shaking will experience major impact from slope failures. Fortunately the majority of the area likely to be worst affected by landslides, including the rock and debris avalanches discussed earlier, is the Southern Alps area which is largely uninhabited. The exceptions are the farms and small towns along SH 73 (Arthurs Pass), SH 6 (Kumara - Haast), and to a lesser extent SH 80 (Mt Cook). While none of towns listed in Table 8.5 in these areas are built directly on significant slopes many are close to the toe of some very high slopes. The risk at these locations is from debris inundation associated with run out from the landslides.

The larger towns are generally outside the most severe region and some (eg Hokitika and Greymouth) have only a small proportion of the town built on, or near, hill slopes. It is likely that landslides will also cause moderate to minor damage to slopes throughout the inland mountain basins (Mackenzie country, Castle Hill basin, etc) and also the foothill areas of Canterbury. Although the level of landslide damage on Banks Peninsula is likely to be low, and restricted mainly to minor property damage, the total number of properties affected may be large due to the high housing density.

Landslide Dams

Landslide dams have resulted from most large historical earthquakes in New Zealand including the 1855 Wairarapa earthquake, the 1929 Arthurs Pass earthquake, the 1931 Hawkes Bay earthquake, and the 1942 Masterton earthquake. Landslide dams have been created on the west coast by both of the large historical earthquakes this century. The Buller earthquake landslide dams have already been discussed in Section 8.1.

The 1968 Inangahua earthquake also triggered earthquakes in the Buller gorge area, one of which formed a large landslide dam. The 1968 landslide contained more than 4 million cubic metres of material which fell from a ridge 600m above the river, crossed the river, and rose 100m up the other side before falling back to form a dam 12m high (Adams, 1981; Johnson, 1974). In this case the ponding was not considered dangerous because the dam height was low and when the dam failed 21 hours later no damage was caused by the flood of 1.5 million cubic metres of water travelling at 5.4 m/sec (Sutherland, 1979).

Perrin & Hancox (1991) describe landslide dammed lakes which have survived in New Zealand, many of which are inferred to have been formed during earthquakes, with several examples from Westland and others from east of the main divide. However, most of the landslide dams which survive are the relatively small ones, with water volumes comparable to (or smaller than) that of the landslides which created them.

An Alpine Fault earthquake is very likely to create numerous landslide dams in the 25 - 30 major river valleys draining the western side of the Southern Alps. Most of these are likely to fail quickly due to the high rainfall (ie. days to weeks) but some may remain for longer periods. In general the steep river gradients will tend to reduce the

potential stored water volume for a given landslide dam height. However the combination of very narrow gorge sections of many of the rivers near the range front, and typical ridge to valley elevation differences in excess of 1000 metres, will generate at least some high dams and corresponding large volumes of ponded water.

Davies & Scott (1997) have modelled dam break flood hazard from landslide dams in the Callery River, a tributary of the Waiho River near Franz Josef. They conclude there is evidence for such events having occurred in the past and predict dam-break floods in the order of several thousand cubic metres. In their opinion the impact of such an event on Franz Josef would be severe and sufficient early warning to allow evacuation can not be guaranteed. The suggest the most realistic mitigation strategies involve restrictions on land-use.

No landslide dams have been reported during historical earthquakes in rivers east of the main divide with the exception of the 1929 Arthurs Pass earthquake. However an Alpine Fault earthquake is likely to cause these. The river gradients are generally less steep and it possible that although the landslide dams may be fewer in number the reservoir volumes could be relatively large. Fortunately many of the major river valleys are very wide in most places. However landslide dams may also form in the gorge sections of the major rivers close to the Canterbury Plains, with a corresponding flood hazard lower in the river. While it is statistically unlikely that an earthquake will coincide with heavy rain, the majority of later landslide dam failures do occur when the rainfall is extreme.

8.3.4 Liquefaction

Liquefaction results from the earthquake induced consolidation of loose saturated sediments which expel porewater at a rate faster than they can drain. As a result the porewater pressure exceeds the overburden weight and the sediment behaves as a liquid with no shear strength. Foundations sink into the soil and sloping ground tends to flow towards the lowest point (generally river and lagoon margins).

Preconditions favouring liquefaction are:

- young sediments (often poorly cemented and relatively unconsolidated)
- a low soil density and shear strength
- an abundance of sand and sandy silt as a soil matrix
- a high watertable (implying an elevation close to river and sea level and/or high rainfall).

The alluvial lower floodplains of most of the West coast rivers are locations which are vulnerable to liquefaction. The general exceptions are the higher river terraces and the coarser grained sediments of the upper catchments. These tend to have lower watertables and little or no sand matrix in the underlying gravels. Moraine, alluvial fans and colluvium slopes on bedrock are also unlikely sites for liquefaction.

The most at risk locations are close to the mouths of the major rivers, particularly the lagoonal and estuarine areas, and parts of the dune and beach area. Historically these river mouth sites offered potential for ports and river transport. As a result the largest west coast towns of Karamea, Westport, Greymouth and Hokitika all have geological conditions in at least some areas of the town which are typically susceptible to liquefaction.

Historical examples

Liquefaction has been a characteristic of all the significant west coast earthquakes this century, even the relatively small ones. Table 8.6 records the details of liquefaction recorded in 1913,1929, 1968 and 1991 in Karamea, Westport and Greymouth. To date this century these three towns have been the closest to the epicentres of the significant west coast earthquakes.

Earthquake and Magnitude	Summary of damage
1913 Westport M = 6 ?	Cracks in the ground and ejection of mud at Cape Foulwind.
1929 Buller M = 7.8	Fissures and subsidence and water spouts in Karamea, Westport, Greymouth, Inangahua and Greenstone.
1968 Inangahua M = 7.1	Sand boils, fissures and subsidence. Sand boils sufficient to lift and rotate one house in Westport on its foundations (Romilly Street).
1991 Westport M = 6	Minor liquefaction at Nine Mile Beach, Charleston causing subsidence and sand boils.

Table 8.6 Historical examples of liquefaction on the West coast in earthquakes this century (from Fairless & Berrill, 1984; Berrill et al, 1988 and Benn, 1992).

East coast South Island examples of liquefaction have been reported from the lower Wairau River (both the 1848 and 1855 earthquakes); Hanmer basin (1888 Amuri earthquake); Kaipoi, Hurunui River and Cheviot (1901 Cheviot earthquake); and Lake Sumner (1929 Arthurs Pass earthquake).

Likely extent of liquefaction in susceptible sediments

The furthest liquefaction has been recorded from an earthquake epicentre on the west coast is 122 km (Greenstone River, during the 1929 Buller earthquake; Benn, 1992). This compares with the maximum New Zealand recorded example of 193 km during the relatively small M = 7.1 Marlborough earthquake of 1848. The larger 1855 Wairapa earthquake induced liquefaction up to 160 km from the epicentre but the country was sparsely populated and other examples may not have been recognised (Fairless & Berrill, 1984).

Overseas examples of liquefaction have been analysed and a relationship derived between magnitude and epicentral distance. Kuribayashi & Tatsuoka (1975) considered 32 historic Japanese earthquakes and suggest a Magnitude 8 earthquake on average would produce liquefaction of susceptible sediments at distances of up to approximately 250 kilometres. Berrill & Fairless (1984) review the historical record of liquefaction in New Zealand and compare this with the relationship between earthquake magnitude and epicentral distance of Kuribayashi & Tutsaoka, 1975. In so doing they discount some of the most extreme New Zealand examples. They conclude that within the limited data set the relationship appears to hold for New Zealand conditions.

Ambraseys (1988) used an enlarged international data set and derived a relationship which extends the predicted distance over which liquefaction will occur to approximately 350 km for M = 8. More recently Wakumatsu (1993;1991) showed that at high magnitudes (such as M = 8) the Ambraseys relationship is appropriate for Japanese conditions only if minor signs of liquefaction are included. However if the data-set is restricted to cases of significant (or potentially damaging) liquefaction, then 250 km is the more appropriate limit.

Group	Towns & locations and distances*	Likely extent of liquefaction in susceptible sediments
Group one < 50 km	Locations such as Okuru (15 km); Paringa (15 km); Okarito (30 km); Kokatahi (20 km); Hokitika (30 km); Rotomanu (20 km); Iveagh Bay (20 km); Greymouth (50 km)	Extreme liquefaction in susceptible sediments. At the very closest distances some liquefaction in sediments not normally considered liquefiable.
Group two 75 - 150 km	Lakes Coleridge, Pukaki, Tekapo and Ohau (50 - 60 km); Inangahua valley (50 - 80 km); Queenstown (75 km); Westport (115 km); Kaipoi (115 km); Christchurch (115 - 130 km); Ashburton (110 km); Timaru (140 km).	Damaging liquefaction in the most susceptible sediments likely
Group three 150 - 250 km	Karamea (175 km); Dunedin (240 km); Blenhiem (250 km); Nelson (230 km).	Liquefaction in extremely susceptible sediments may occur at closest locations within this range but with limited impact and many susceptible sites unaffected

* distance as measured from the long axis of the likely maximum isoseismal

Table 8.7 : Locations where liquefaction may occur in susceptible sediments during a Magnitude 8 earthquake on the Alpine Fault.

It would appear that there is now broad agreement between the most recent analyses and 250 km is a reasonable general guide. Unfortunately no information exists on the percentage of susceptible sediments which are likely to liquefy at given distances but some reasonable inferences can still be made based on the historical record. If we consider the locations in the South Island of main interest in this report we can divide these into three groups based on their likely distance from the epicentral region (Table 8.7)

Defining susceptible soil

Liquefaction is a significant hazard at locations in the first two groups. Table 8.7 makes no assumptions that susceptible soils are present at the sites listed but these locations are in areas where this is definitely possible, and in most cases is likely. The list is not complete but includes typical examples from coastal areas; lake, swamp and river margins; and/or areas that have experienced liquefaction in previous earthquakes.

The only way to determine susceptibility is to carry out site specific subsurface investigation to determine soil size grading; density, and depth to watertable. To our knowledge Christchurch is the only large location where significant information has been gathered. The conclusions from analysis of some of this data confirms that liquefaction is likely in the most susceptible areas tested to date and details of this are included in reports prepared for the relevant Christchurch local authorities.

If liquefaction potential is recognised at a site the options are to pile the foundations, densify or replace soils prior to construction, lower the water table, or avoid the area. For many existing buildings it is frequently not practical to reduce the hazard but for critical structures (hospitals, police stations, and key utilities) remedial work may be justified.

8.3.5 Tsunami & Seiches

Tsunami are seismically generated sea waves produced by submarine faulting, uplift or landsliding. They travel very quickly in the open ocean with little surface expression, but gain in wave height near shore, particularly along gently shelving coastlines and within narrow embayments. The coastline of the west coast is relatively steep and no significant open bays exist, although there are many river mouth settlements. In general the Alpine Fault in central Westland is not expected to produce broad scale submarine uplift or deformation. It is still possible submarine or coastal landslides could be triggered which may produce local tsunami.

In Fiordland the fault continues offshore south of Milford, and rupture in this area, combined with the numerous narrow fiords could combine to create significant tsunami in Fiordland. However the fiords tend to be steep sided and only the head of the embayments would be vulnerable. This could affect the developed area of Milford Sound.

Strong seismic shaking also induces water in lakes to oscillate (or "slop") at a particular frequency controlled by lake size and depth. These oscillations are called seiches and were generated on the west coast during the 1929 Buller earthquake.

Benn (1992) quotes from the Greymouth Evening Star (20.6.1929) an account of damage to Lake Rotoroa and the Gowan River, which drains the west end of the lake:

"Lake Rotoroa rocked from side to side like a huge basin of water being tipped out. Half an hour after the main shake, the water receded from the hotel shore and exposed the lake bed for 50 yards. It then came back in a series of large waves. The bridge over the Gowan River at the lake was torn from its piles and the banks of the river and was hurled upstream. The wrecked structure was carried still further upstream by the Gowan waters, which were temporarily flowing back into the lake."

Lake Moana (Brunner) was also reported to have *"sank down in the middle then come up like a typhoon"* during this earthquake.

In general lake seiches are more likely to cause damage during an Alpine Fault earthquake than are tsunami. These lakes are closer to the area of strongest shaking and there are a large number on both sides of the main divide. On the west coast these include several small northern lakes (Haupiri, Lady Lake etc) but also include the much larger Lake Moana and Lake Kaniere, both with lake-shore settlements and dwellings. There are also numerous less populated lakes further south along SH 6 with generally less potential for material damage (Lake Mahinapua, Lake Ianthe, Lake Wahapo, Lake Mapourika, Lake Matheson; Lake Paringa, Lake Moeraki and Okarito Lagoon).

Of more concern than a shaking induced seiche for Lake Brunner and Lake Kaniere is the more remote possibility of a significant landslide falling into one of these lakes and creating a damaging wave. Both these lakes are very close to the fault trace (7 km and 500 m respectively) and both have steep peaks along their shorelines elevated more than 1000 metres above lake level (Mt Te Kinga, elevation 1204m and Mt Tuhua, elevation 1125m). Hawley (1984) and Benn (1992) also note this possibility.

East of the main divide are the large moraine dammed lakes of the Mackenzie Basin (Tekapo, Pukaki, Ohau) and Lake Benmore. All four are close to the likely epicentral region and seiches are likely to also be created in these. The larger southern lakes (Wanaka, Hawea and Wakatipu) are within 100 km of the fault trace and may also experience seiches although probably to a lesser extent.

8.4 Longer term effects

This section considers the likely longer term impacts which may follow an Alpine Fault earthquake. The time frame for these impacts extends from a matter of days following the main shock up to years or possibly tens of years.

8.4.1 Effects on forests and vegetation

Chapter 4 outlines the evidence preserved in the age structure and growth rings of the current forest which we interpret as indicating the impact of past Alpine Fault earthquakes. Vegetation in general will be killed or damaged immediately by strong shaking, landsliding, and liquefaction; and more slowly in the post seismic period by later rainfall triggered landsliding, aggradation, river channel avulsion and flooding.

Pearce & Watson (1986) document the burial of forest on valley floors by the Buller earthquake (refer again page 55). More recently Grapes & Downes (1997), quoting newspaper accounts from the time, note that the 1855 Wairapa earthquake removed nearly one third of the vegetation on the western face of the Rimutaka Range as viewed from Wellington. McKay (1901) describes landslides during this earthquake which "carried away hundreds of acres of bush, burying it and piling it in utter confusion ". Grapes (1988) looked in detail at the vegetation remaining on one large landslide from the 1855 earthquake and concluded only one pre-earthquake tree has survived.

Aquatic vegetation was also affected by seiches associated with this earthquake. Grapes and Downes (1997) outline reports of raupo, flax and toi toi torn up by the seiche wave action and left floating on the lakes.

8.4.2 Effects on rivers

In chapter 3 we outlined the typical impact of earthquake triggered landslides on river regime. In the longer term the impact of an Alpine Fault earthquake on the behaviour and character of rivers may prove to be one of the largest overall effects.

It is likely to induce a progressive "wave" of aggradation with associated channel avulsion, local bank erosion, and flooding which will move down through the river systems on both sides of the main divide. The greatest impact will be on the rivers draining the west coast because these have the largest flows, steepest catchments, and the largest current sediment budgets. The distance down river the aggradation will extend will vary from catchment to catchment and be controlled by the proportion of landslides in the upper catchment with respect to the average river flow.

In addition aggradation is normally most severe in the sections of river dominated by bedload, as opposed to suspended load. This is generally the steepest gravel dominated sections of river close to the main divide and the range front. Even relatively small streams which drain steep slopes, and which are within or near the epicentral region, are likely to experience rapid fan building and associated channel avulsion. The impact is likely to be the least in areas near the coast and relatively far from the mountains where river gradient is lowest and suspended load is the dominant transport process.

In general the rivers which give the greatest problems under the present conditions are also likely to be the most sensitive to the increased sediment budget. Obvious examples include the Waiho River, which is aggrading rapidly at present probably due to glacial fluctuation (Davies, pers. comm, 1997); the Waitangitaona River near Lake Wahapo (Griffiths & McSaveney, 1986); and possibly the Grey and Hokitika Rivers in sections where flooding has historically been a problem.

The Taramakua River could possibly shift channel at Inchbonnie during earthquake induced aggradation. At various times the river has flowed straight through to the Mitchells end of the Lake Moana and at other times around through the current Lake Poerua to the Te Kinga delta at Lake Moana and Iveagh Bay.

Figure 8.8 - The Waiho River at Franz Josef which has had a history of flooding and aggradation. The old bridge has had to be cut and lifted to maintain the waterway while a new temporary bridge has been put in immediately upstream for SH 6. This type of aggradation is likely in many other rivers draining the Southern Alps following an Alpine Fault earthquake.

Figure 8.9 - The Toaroha River immediately downstream of the Alpine Fault trace. Note the current bed level is such that coarse gravel bed load is currently being deposited on terrace surfaces previously only reached by suspended sediment. Locations such as this are extremely vulnerable to any future increase in bed levels.

Figure 8.10 - An aerial photo showing the Inchbonnie area and Lake Poerua with the current Taramakua River just visible turning left to Kumara. Note the old channels visible in the air photo heading to the right to the Mitchells end of Lake Brunner (Moana), and also back around into Lake Poerua. The white pointer shows the location of a buried grass sample 1.2 m below the current surface which returned a post 1700 AD date suggesting these channels may be very young. Reoccupation of the these channels following earthquake induced aggradation could result in floodwater from the Taramakua entering the flood prone Grey River catchment.

While looking over the Alpine Fault trace at Inchbonnie we collected a sample of buried grass from a 1.2 m excavation near the Inchbonnie Recreation Center (Figure 8.10). This building is on the Inchbonnie - Rotomanu road, which is north of the current Taramakua channel and in the old river route to Mitchells. This grass had been growing on the surface of coarse well rounded greywacke cobbles from the Taramakua River (the only source of greywacke amongst the nearby schist and granite slopes).

The grass had then be rapidly buried by over a metre of sandy silts typical of overbank flood material from a large river. This sample was radiocarbon dated (Wk 5509) as "modern" indicating major river flooding of this relatively low area since approximately 1700 AD. This matches accounts from old saw-millers who noted the really large trees were above the "terrace" (fault scarp) at Inchbonnie. The age and origin of the channels and surfaces in this area requires more detailed study.

The main consequence of water from the Taramakua River entering Lake Brunner (Moana) from either of the possible flood routes is that this water will then drain down the Arnold River and ultimately end up in the Grey River which has a history of flooding at Greymouth. While an Alpine Fault earthquake is unlikely to coincide with high river flows, and earthquake induced aggradation will probably take several weeks to impact, any abrupt change in channel is likely to occur during a flood event and this extra flow is likely to reach the Grey River when it is also high.

8.4.3 Effects on coasts

In general the coast line in Westland is likely to accrete rather than erode in response to the sediment pulse associated with an Alpine Fault earthquake. This will increase both the volume of material carried northward by littoral drift and sediment discharge from each individual main river mouth. River bars may tend to enlarge in response to this but the interaction is likely to be complex.

Hokitika has a history of cyclic coastal erosion of the area immediately north of the river mouth. Gibb (1987) noted that the erosion is controlled largely by the orientation of the river mouth within the coastal delta. If the river mouth and discharge is offset to the south there is generally erosion immediately to the north of the mouth which can affect the town. It is difficult to predict the influence an earthquake generated sediment pulse will have on river mouth alignment.

8.5 Summary

An Alpine Fault earthquake will have effects similar to the 1929 Buller earthquake but on a larger scale. Rupture will occur at the fault trace where is crosses State Highway 6 and several other more minor roads. Franz Josef is the only town through which the active fault trace passes.

Ground shaking will be very strong along the west coast and in the central Southern Alps. This shaking will cause direct structural damage to buildings and infrastructure. Strong to moderate shaking will occur in most South Island locations within 150

kilometres of the Alpine Fault. The shaking will trigger landslides over a very large area. The largest will occur in the central and western Southern Alps where it is likely some rock and debris avalanches will occur. Landslide dams will be formed in many valleys but most will fail relatively quickly.

Liquefaction in susceptible sediments will cause damage to buildings, services and transport routes up to 250 kilometres from the fault and liquefaction in these materials will be substantial within 150 kilometres. Susceptible sediments are known to exist in coastal locations such Westport, Greymouth and Christchurch but there will also be liquefaction along river, lake and swamp margins away from the coast.

Seiches (high waves) will be induced by the ground shaking on the many lakes in the general area, including the Southern Lakes and lakes in the Mackenzie basin. Longer term changes to river behaviour in response to the sediment overload from landslides will increase flood risk in many locations for a long time after the earthquake.

Chapter 9

Conclusions and Recommendations

9.1 Conclusions

1) The Alpine Fault is not "aseismic" and produces large earthquakes with associated liquefaction at the fault trace. This is demonstrated for the first time in the Kokatahi 2 trench excavated as part of this project.

2) Four independent lines of evidence are presented in this report that are consistent and indicate two major earthquakes in the last five hundred years.

3) The most unequivocal evidence comes from trenching of the fault. At two northern locations near the Ahaura River trenching indicates the last rupture event was between 1480 AD and 1645 AD. This wide date range is the inevitable consequence of the radiocarbon dating method.

4) At three locations further south trenching indicates a more recent rupture event which was post 1660 AD and probably between 1700 AD and 1750 AD. There is also evidence in one of these trenches for the earlier event noted above.

5) The landslide and aggradation terrace record, which in this type of steep terrain is likely to reflect the impact of large earthquakes, is consistent with the trench date ranges and also suggests two earthquakes at around 1600 AD and post 1700 AD.

6) The forest currently growing in Westland has several age modes consistent with common re-establishment following massive disturbance events. Earthquakes have been suggested independently by plant scientists as a possible explanation of the pattern. Earthquakes are known to cause landslides which can severely damage forests and the shaking and associated liquefaction often causes widespread treefall and branch damage. The inferred timing of the most recent disturbances at 1625 ± 15 years AD and 1715 ± 15 years AD matches the date ranges from the trenches and the landslide and aggradation terrace pattern.

7) Trees which have continued growing through these inferred earthquake events commonly exhibit abrupt fluctuations in tree ring width at dates which are again consistent with the trench date ranges, the landslide and terrace age modes, and the forest disturbance record. These tree ring chronologies are the best method to estimate the exact timing of these events.

8) We infer the most recent earthquake occurred in **1717 AD** and is referred to here as the **Toaroha River event**. The associated disturbance can be traced in cross matched tree ring chronologies from Lake Te Anau to Hokitika, a distance of more than 400 kilometres. The disturbance is absent from available tree ring chronologies further north at the Ahaura River and the Rahu Saddle, which is consistent with the evidence from trenches indicating the last rupture terminated slightly north of the Haupiri River.

9) The previous earthquake event is referred to here as the **Crane Creek event** and can be recognised in tree ring chronologies in the Copland Valley and Karangarua River (south of Mount Cook) and further south in the forest disturbance record near the Paringa River. We infer this earthquake occurred in **1620 AD ± 10 years** and had a minimum rupture length suggested by the forest disturbance record of more than 250 kilometres.

10) Other older events can also be inferred from the available data, including the preliminary results of other concurrent paleoseismic investigations at the Waitaha River in central Westland (Wright, pers. comm. 1998). The combined data suggests other earthquakes at around 1425 AD ± 15 yrs ; 1220 AD ± 50 yrs and 960 AD ± 50 yrs.

11) The timing of previous earthquakes can be used to estimate the probability of the next earthquake occurring in the central section of the fault using a range of methods. The most basic method assumes random earthquake occurrence and estimates 50 year probabilities of around 20 % and 100 year probabilities of around 40 %.

12) Other more realistic methods assume a seismic cycle of progressive stress accumulation with a steadily increasing probability of subsequent earthquake release. Methods which use only the inferred Alpine Fault recurrence sequence are hampered statistically by a lack of data, but suggest a higher 50 year probability of around 30% and a 100 year probability of approximately 70%.

13) The most realistic and reliable method assumes the Alpine Fault will resemble other plate boundary faults around the world and exhibit similar recurrence behaviour. While successive recurrence intervals will vary significantly about a mean enough intervals exist in this international database to statistically predict the probability of variation. This method applied to the Alpine Fault estimates a much higher **50 year probability of 65% ± 15 and a 100 year probability of 85 % ± 10**.

14) Mechanical considerations of crustal strength and observations of the high historical strain rates also suggest a finite limit to the possible future elapsed time of around 100 years.

15) The next Alpine Fault earthquake is likely to resemble the previous two and a range of shaking intensities can be predicted for the central South Island based on these earlier events. These suggest the highest likely Modified Mercalli intensities of 9 or greater will be experienced in the Southern Alps. Shaking will also be strong in most west coast towns (with the possible exceptions of Westport and Karamea) and in areas of the east coast foothills.

16) Recent revisions in attenuation relationships suggest the shaking in more distant locations such as Christchurch will not be as severe as some previous predictions. However the level of shaking in Christchurch is still likely to be the highest experienced in the last 100 years.

17) Landslides, including possible rock and debris avalanches, will be abundant in the Southern Alps and on nearby steep slopes. Analysis of the poorly dated record of previous rock and debris avalanches suggests many of these can be attributed to previous earthquakes on the Alpine Fault, in the particular the Roundtop event of around 960 AD. Landslides on the Port Hills and Banks Peninsula will be comparatively minor in comparison but may still affect a significant number of properties.

18) Landslide dams will be created in many river valleys on both sides of the main divide. While these may create a short term flood risk most will fail relatively quickly.

19) Based on previous New Zealand and international earthquakes liquefaction is predicted to occur in susceptible sediments as far away as 200 km from the epicentral region. The towns potentially most susceptible to liquefaction are Greymouth and Hokitika (both of which are within 50 km of the likely epicentral area) and the city of Christchurch.(130 km).

20) Large water waves (seiches) are likely to result from oscillation of water in lakes on both sides of the main divide in the areas of strongest shaking.

21) Vegetation damage following the Buller earthquake of 1929, and other overseas earthquakes in steep forested terrain, suggests that longer term landscape and vegetation impact on the large forests of the D.O.C. estate will be profound.

22) Aggradation and channel shifting following the earthquake is likely in the upper reaches of most of the rivers and streams near the epicentral area on both sides of the main divide. In some cases these impacts may extend progressively down river to affect populated areas at the river mouths.

23) More detailed considerations of the potential impacts of an Alpine Fault earthquake have been included as specific reports to local authorities and infrastructure providers.

9.2 General Recommendations

1) Potentially affected local authorities and infrastructure providers should incorporate the potential consequences of an Alpine Fault earthquake in their planning for the next 50 - 100 year time period.

2) This requires a short term immediate post earthquake contingency plan which will apply for the period of minutes and continue up to several days after the earthquake.

3) Assumptions to be made in the short term planning include:

- No vehicular access on SH 73 between Springfield and Kumara.
- No vehicular access on SH 6 between Ross and Haast.
- Possible loss of vehicular access between Lake Pukaki and Mount Cook Village.
- Loss of power and fixed telecommunications in this same general area.
- Disruption to utilities (water, power, sewer, telephone) and possibly to emergency service facilities in Hokitika and Greymouth.
- Liquefaction damage to Greymouth airport however Hokitika airport is more likely to remain serviceable.
- A short term flood hazard from breaching landslide dams on many west coast rivers (and possibly some gorges of large east coast rivers) immediately after the earthquake, and especially after the first rain.

4) Planning is also required to attempt to minimise the longer term impacts of the earthquake which are generally the most profound.

5) Such planning should allow for severely restricted vehicular access for at least several months following the earthquake.

6) There will also be only limited power generation capacity for several months on the west coast and disruption to the power transmission network on both sides of the main divide. The power generating capacity in the Mackenzie basin, upper Waitaki and also Lake Manaupori may also be disrupted (the later depends on the southern limit of rupture).

7) River behaviour is likely to change abruptly with aggradation of several metres in the upper reaches of most rivers draining both sides of the main divide. This will present a continued problem for bridges and land-use in these areas.

8) River behaviour may ultimately affect communities at river mouth locations as increased sediment load affects the lower reaches of the larger rivers.

9) Both the short term and long term impacts will be less severe in more distant locations away from the epicentral regions and these are outlined separately for the relevant authorities.

10) Profound short term economic impacts are likely for both Westland and Canterbury however in the long term the impact of post earthquake reconstruction and investment may be positive.

9. 3 Future Work Targets

1) To date Greymouth and Hokitika have had very little, if any, detailed investigation of foundation conditions at key emergency facilities such as hospitals, fire stations and police stations. This should include a structural engineering review of the likely building performance during a strong earthquake.

2) A lifelines study which reviews urban services and critical infrastructure, similar to those recently completed for Wellington and Christchurch, should also be considered for Greymouth and Hokitika. This may also be extended to the likely worst affected smaller towns (Arthurs Pass, Otira, Franz Josef, Fox etc).

3) We have noted earlier the importance of the northern section of the fault in relation to earthquake shaking at Christchurch, North Canterbury, Westport, and Karamea. There is potential for the fault to rupture as far north as the Nelson Lakes. More paleoseismic work in the area further north of the Ahaura River is required to investigate this possibility.

4) The area of alluvial fans and sediments at Inchbonnie where the Taramakua River currently flows south to Kumara is very young and there appear to be recent channels heading west to the Mitchells end of Lake Brunner which could be readily reoccupied. This would direct water from the large Taramakua River down to the flood prone Grey Valley. This area should be investigated to determine how recently this channel avulsion last occurred, what is the probability of this happening again, and how best the future risk of this occurring can be managed.

5) More investigation of the Alpine Fault in the area we have already examined and further south would always be desirable. However in relation to the best use of limited funds it is more appropriate for local authorities and infrastructure providers south of a line from Greymouth to Darfield to focus on earthquake preparedness. Further refinement of the past earthquake history on the Alpine Fault is unlikely to significantly reduce the perceived future hazard. Any investment in earthquake preparedness also has the added advantage of being of benefit during earthquakes on other faults and is often of benefit in other types of civil emergency.

Acknowledgments

A project of this size and duration depends on the support of many people and organisations for success. Funding and material support for the project have come from numerous organisations including the Earthquake Commission, the New Zealand Society of Earthquake Engineering, Canterbury Regional Council, Westland District Council, Grey District Council, Buller District Council, Selwyn District Council, Mackenzie District Council, Ashburton District Council, Timaru District Council, Queenstown & Lakes District Council, Hurunui District Council, Waimakariri District Council, Christchurch City Council, WestPower, Transit New Zealand, Electricorp and TransPower. We are extremely grateful to these organisations and the individuals within them for their support. Some of this work forms the basis on an ongoing PhD at the University of Canterbury assisted by the University of Canterbury geology department active tectonics programme and the University of Canterbury Doctoral scholarship programme.

A diverse group of geologists, farmers and artists provided vital help with the field work in frequently inhospitable weather and terrain. These include Howard Aschoff, Paul Eyles, Doug Johnson, Miles Reay, Phil Kelsey, Peter Kingsbury, Tim McMorran, Chris Chamberlain, Richard Wise, Helen Grant, and Ben Yetton. Discussion and practical field assistance also came from Dr Jarg Pettinga, Joc Campbell, and Dr John Berrill of the University of Canterbury. Andrew Wells, of the Plant Science Department at Lincoln University, contributed so much that he is acknowledged as a co-author of the report. Nick Traylen assisted at short notice with the probability assessments and is also included as a co-author. Warwick Smith (Seismological Observatory) acted as a sub consultant with the intensity modelling. Lee Leonard assisted with drafting of a high standard.

Don Elder provided useful discussion and encouragement. Bruce McFadgen (D.O.C.) helped with early analysis of some of the landslide and terrace age dates. Professor William Bull (University of Tucson) assisted in the field and with useful comments at various stages. Craig Wright made me welcome in his field area at the start of the project and has continued to keep me up to date with his work in the Waitaha River. Richard Norris and Alan Cooper allowed me to join the University of Otago fieldtrip along the Alpine Fault in 1996 which was of great benefit. Kelvin Berryman, Alan Hull and the late Sarah Beanland made files available from I.G.N.S. and provided early encouragement.

I would like to thank the many people of Westland we have met in a wide range of places for their unfailing interest and support of the project. In particular the farmers and contractors who provided access to their land and helped with the excavations. These include the Coates family of Ahaura and Gary Birchfield; Fervent Stedfast and other members of the Gloriavale Christian Community at the Haupiri River; Charlie Emerson & Terry Sheridan from the Kokatahi River; Bill Evans and Spike Jones at the Toaroha River; Nelson Cook at Lake Arthur; and Keith & Ruth Mackenzie at Poerua. John & Raylene Craig of Kopara and Marg Eadie (formally of Hokitika) made comfortable rented accommodation available. Finally I would like to thank my wife Lisa Yetton, and my children Ben and Renee, for helping in so many ways and putting up with my paleoseismic frenzy over the last three years.

REFERENCES

Adams, J. 1978: Late Cenozoic erosion in New Zealand. Unpublished Ph.D.thesis, lodged in the Library, Victoria University, Wellington, New Zealand. 108 pages.

Adams, J. 1980: Paleoseismicity of the Alpine Fault seismic gap. *Geology* 8: 72–76

Adams, J. 1981a: Earthquake-dammed lakes in New Zealand. *Geology* 9: 215–219

Adams, J. 1981b: Earthquakes, landslides, and large dams in New Zealand. *Bulletin of the New Zealand national society for earthquake engineering* 14: 93–95

Allen, R.B., Bellingham, P.J., & Wisser, S.K.(in press): An earthquakes role in the disturbance regime of a *Nothofagus* forest. Submitted to *Ecology*

Allis, R.G.; 1986: Mode of crustal shortening adjacent to the Alpine Fault, New Zealand. *Tectonics 5*: 15-32.

Allis, R.G.; Henley, R.E.; Carman, A.F. 1979: The thermal regime beneath the Southern Alps. In: *The Origin of the Southern Alps* (edited by Walcott, R.I.; Cresswell, M.M.). *Bulletin of the Royal Society of New Zealand 18*: 79-86.

Ambraseys, N.N. 1988: Engineering seismology. *Earthquake engineering and structural dynamics 17*: 1-105.

Anderson, H.; Webb, T. 1994: New Zealand seismicity: patterns revealed by the upgraded National Seismograph Network. *New Zealand journal of geology and geophysics 37*: 477-493.

Anderson, J.G.; Wesnousky, S.G.; Stirling, M.W. 1996: Earthquake size as a function of fault slip rate. *Bulletin of the Seismological Society of America* 86: 683-690.

Archuleta, R.J. 1982: Analysis of near-source static and dynamic measurements from the 1979 Imperial Valley earthquake. *Bulletin of the seismological society of America 72*: 1927-1956.

Bakun, W.; Lindh, A. 1985: The Parkfield, California, earthquake prediction equipment. *Science 229*: 619-24.

Barka, A.A.; Kadinsky - Cade, J. 1988: Strike slip fault geometry in Turkey and its influence on earthquake activity. *Tectonics* 7: 663 - 684.

Barosh, P.J. 1969: Use of seismic intensity data to predict the effects of earthquakes and underground nuclear explosions in various geologic settings. *Geological Survey Bulletin 1279*: 93 pp.

Basher, L. R. 1986: Pedogenesis and erosion history in a high rainfall, mountainous drainage basin - Cropp River, New Zealand. Unpublished Ph.D. thesis, lodged in the Library, Lincoln College, University of Canterbury, New Zealand.

Beanland, S. (comp.) 1987: Field Guide to Sites of Active Earth Deformation, South Island, New Zealand. *New Zealand Geological Survey record 19*.

Beck, S.L ; Christensen, D.H. 1991: Rupture process of the February 4, 1965, Rat Islands earthquake. *Journal of geophysical research 96*: 2205-2221.

Beck, S.L.; Ruff, L.J. 1987: Rupture process of the great 1963 Kurile Islands earthquake sequence: asperity interaction and multiple event rupture. *Journal of geophysical research 92*: 14123-14138.

Belich, J. 1996: Making peoples - a history of the New Zealanders. Auckland, Allen Lane Penguin Press.

Benn, J.L. 1990: A chronology of flooding on the West Coast, South Island, New Zealand, 1846 - 1990. Unpublished report, West Coast Regional Council, Greymouth, New Zealand. 159 p.

Benn, J.L. 1992: A review of earthquake hazards on the West Coast. Unpublished report, West Coast Regional Council, Greymouth, New Zealand. 61 p.

Berrill, J.B.; Bienveny, V.C.; Callaghan, M.W. 1988: Liquefaction in the Buller Region in the 1929 and 1968 Earthquakes. *Bulletin of the New Zealand national society for earthquake engineering 21, 3*: 174-189.

Berryman, K.R. 1979: Active faulting and derived PHS directions in the South Island, New Zealand. *Royal Society of New Zealand bulletin* 18: 29 - 34..

Berryman, K.R. 1980: Late Quaternary movement on the White Creek Fault, South Island, New Zealand. *New Zealand journal of geology and geophysics* 23: 93 - 101.

Berryman, K. R.; Beanland, S.; Cooper, A.F.; Cutten, H.N.; Norris, R.J.; Wood, P.R. 1992: The Alpine Fault, New Zealand: variation in Quaternary structural style and geomorphic expression. *Annales tectonicæ* VI: 126–163

Biasi, G.P.; Weldon, R. II. 1994b: Conditional probability of large earthquakes on the southern San Andreas fault from Paleoseismological evidence (submitted for publication).

Bonilla, M.G.; Buchanan, J.M. 1970: Interim Report on Worldwide Historic Surface Faulting. *United States Geological Survey* Open-File report. 32pp.

Bowen, F.E. 1957: Sheet S64 - Wanganui River bridge sites. Unpublished New Zealand Geological Survey immediate report, S64/ IR8. Institute of Geological and Nuclear Sciences, Kelburn, Lower Hutt, New Zealand.

Bull, W.B 1996: Prehistorical earthquakes on the Alpine fault, New Zealand. *Journal of geophysical research* 101: 6037–6050

Bull, W.B. and Cooper, A.F. 1986: Uplifted marine terraces along the Alpine Fault, New Zealand. *Science* 234: 1225 - 1228

Campbell, J.; Rose, R. 1996: Oblique tectonics and the restraining bend on the Alpine Fault. Geological Society of New Zealand miscellaneous publication 91A:40 Abstract only

Cave, M. 1987: Geology of Arthurs Pass National Park. National Parks scientific series number 7. Wellington, Department of Conservation.

Chinn, T.J.H 1981: Use of weathering rind thickness for Holocene absolute age dating in New Zealand. *Arctic alpine research 13*: 33–45.

Cooper, A.F.; Norris, R.J. 1990: Estimates for the timing of the last coseismic displacement on the Alpine Fault, northern Fiordland, New Zealand. *New Zealand journal of geology and geophysics* 33: 303–307

Cooper, A.F.; Norris, R.J. 1995: Displacement on the Alpine Fault at Haast River, south Westland. *New Zealand journal of geology and geophysics* 38: 509–514

Cowan, H.A. 1989: An evaluation of the Late Quaternary displacements and seismic hazard associated with the Hope and Kakapo faults, Amuri district, North Canterbury. Unpublished Msc Thesis, lodged in the Library, University of Canterbury, Christchurch, New Zealand.

Cowan, H.A. 1990: Late Quaternary displacements on the Hope fault at Glynn Wye, North Canterbury. *New Zealand journal of geology and geophysics* 33: 285–293

Cowan, H.A.; McGlone, M.S. 1991: Late Holocene displacements and characteristic earthquakes on the Hope River segment of the Hope fault at Glynn Wye, New Zealand. *Journal of the royal society of New Zealand* 21: 373–384

Cowan, H.A ; Nichol, A.; Tonkin, P. 1996: A comparison of historical and paleoseismicity in a newly formed fault zone and a mature fault, North Canterbury, New Zealand. *Journal of geophysical research* 101: 6021–6036

Cox, S.C.; Findlay, E.H. 1995: The Main Divide Fault Zone and its role in the formation of the Southern Alps, New Zealand. *New Zealand Journal of Geology and Geophysics 38*: 489-499.

Crespellani, T.; Vannuchi, G.; Zeng, X. 1991: Seismic hazard analysis, seismic hazard and site effects in the Florence area. Proceedings of the 10th Conference of the European society for soil mechanics and foundation engineering: 11-31.

Das, S.; Aki, K. 1997: Fault plane with barriers: a versatile earthquake model. *Journal of geophysical research 82*: 5658-5670.

Davies, T.R; Scott, B.K. 1997: Dambreak flood hazard from the Callery River, Westland, New Zealand. *Journal of Hydrology (NZ)* 36(1): 1-13.

DeMets, C.; Gordon, R.G.; Argus, D.F.; Stein S. 1990: Current plate motions. *Geophysical Journal International* 101: 425-478.

Dibble, R.R.; Ansell, J.H.; Berrill, J.B. 1983: Report on a study of seismic risk for B.P, New Zealand Ltd sites at Woolston and Lyttelton. Unpublished report to B.P. New Zealand Ltd.

Dowrick, D.J. 1991: A revision of attenuation relationships for Modified Mercalli intensity in New Zealand earthquakes. *Bulletin of the New Zealand national society for earthquake engineering* 24: 210-224.

Dowrick, D.J. 1992: Attenuation of Modified Mercalli intensity in New Zealand earthquakes. *Earthquake engineering and structural dynamics* 21: 181-196.

Dowrick, D.J. 1994: Damage and intensities in the magnitude 7.8 1929 Murchison, New Zealand, earthquake. *Bulletin of the New Zealand national society for earthquake engineering* 27: 190-204.

Downes, G.L. 1995: Atlas of Isoseismal Maps of New Zealand Earthquakes. *Institute of Geological and Nuclear Sciences monograph 11.*

Eberhart - Phillips, D. 1995: Examination of seismicity in the central Alpine Fault region, South Island, New Zealand. *New Zealand journal of geology and geophysics* 38: 571 - 578

Eiby, G.A. 1989: Earthquakes. Wellington, Heinemann Reed.

Elder, D.M; McCahon, I.F.; Yetton, M.D. 1991: The earthquake hazard in Christchurch: a detailed evaluation. Unpublished report to the Earthquake Commission, Wellington, New Zealand.

Fairless, G.J.; Berrill, J.B. 1984: Liquefaction during historic earthquakes in New Zealand. *Bulletin of the New Zealand national society for earthquake engineering* 17: 280-291.

Fumal, T.E.; Pezzopane, S.K.; Weldon, R.J. II; Schwartz, D.P. 1993: A 100-year average recurrence interval for the San Andreas fault at Wrightwood, California. *Science* 259: no. 5092, 199-203.

Geli, L.; Bard, P.Y.; Julien, B. 1988: The effect of topography on earthquake ground motion: a review and new results. *Bulletin of the seismological society of America* 78: 42 - 63.

Gibb, J.G. 1987: A coastal hazard management plan for Hokitika. Water and Soil technical publication 29.

Grapes, R.H. 1988: Geology and revegetation of an 1855 landslide, Ruamahanga River, Kopuaranga, Wairarapa. *Tuatara* 30: 77-83.

Griffiths, G.A.; McSaveney, M.J. 1986: Sedimentation and river containment on Waitangitaona alluvial fan - south westland, New Zealand. *Zeitschrift für geomorphologie N.F.* 30: 215 - 230

Hawley, J.G. 1984: Slope Stability in New Zealand. *In* Spenden, I., and Crozier, M.J. *(Eds)*, Natural Hazards in New Zealand. New Zealand Commission for U.N.E.S.O., 88-133.

Heaton, T.H. 1990: Evidence for and implications of self-healing pulses of slip in earthquake rupture. *Physics of the earth and planets interiors* 64: 1-20.

Henderson, J. 1937: West Nelson earthquake of 1929. *New Zealand Journal of Science and Technology* 19: 66-144.

Holm, D.K.; Norris, R.J.; Craw, D. 1989: Brittle/ductile deformation in a zone of rapid uplift: central Southern Alps, New Zealand. *Tectonics 8*: 153-168.

Hough, R. 1994: Captain James Cook - a biography. London, Hodder & Stoughton..

I.S.S.M.F.E. 1993: Manual for zonation of seismic geotechnical hazards. Technical Committee for earthquake geotechnical engineering, Publication TC4, International Society of Soil Mechanics and Foundation Engineering.

Ishihara, K.; Nakamura, S. 1987: Landslides in Mountain Slopes during the Ecuador Earthquake of March 5, 1987. US-Asia Conference on Engineering for Mitigating Natural Hazards Damages.

Jacoby, G.C. 1988: Irregular recurrence of large earthquakes along the San Andreas Fault: evidence from trees. *Science* 241:196 - 199

Jacoby, G. C. 1997: Application of tree ring analysis to paleoseismology. *Reviews of geophysics* 35: 109-124

Jibson, R.W. 1996: Use of landslides for paleoseismic analysis. *Engineering geology* 43: 291–323

Johnston, M.R. 1974: Major landslides in the Upper Buller Gorge, South-west Nelson. *New Zealand Institute of Engineers Transactions 1*: 239-244.

Keefer, D.K. 1984a: Landslides caused by earthquakes. *Geological society of America bulletin* 95: 406–421

Keefer, D.K. 1984b: Rock avalanches caused by earthquakes: source characteristics. *Science* 223: 1288–1290

Keefer, D.K. 1994: The importance of earthquake-induced landslides to long-term slope erosion and slope-failure hazards in seismically active regions. *Geomorphology* 10: 265–284

Keefer, D.K.; Watson, R.C. 1989: Predicting Earthquake-Induced Landslides with Emphasis on Arid and Semi-arid Environments. *Publications of the Inland Geological Society* 2: 118-149.

Khromovskikh, V.S. 1989: Determination of magnitudes of ancient earthquakes from dimensions of observed seismodislocations. *Tectonophysics* 166: 1-12.

Kitzberger, T.; Veblen, T.T.; Villalba, R. 1995: Tectonic influences on tree growth in northern Patagonia, Argentina: the roles of substrate stability and climatic variation. *Canadian journal of forest research* 25: 1684–1696

Koons, P.O. 1987: Some thermal and mechanical consequences of rapid uplift: an example from the Southern Alps, New Zealand. *Earth and planetary science letters* 86: 307-319.

Kuribayashi, E.; Tatsuoka, F. 1975: Brief review of soil liquefaction during earthquakes in Japan. *Soils and Foundations* 15, *4*: 81-92.

Lay, T.; Kanamori, H.; Ruff, L. 1982: The asperity model and the nature of large subduction zone earthquakes. *Earthquake prediction research* 1: 3-71.

Limin, Xiong. 1996: A dendroclimatic study of Libocedrus bidwillii Hook. f. (kaikawaka). Unpublished Ph.D. thesis, lodged in the Library, Lincoln University, Lincoln, New Zealand.

Lomnitz, C. 1996: Search of the worldwide catalogue for earthquakes triggered at intermediate distances. *Bulletin of the seismological society of America* 86: 293-299.

Mark, R.K.; Bonilla, M.G. 1977: Regression analysis of earthquake magnitude and surface fault length using the 1970 data of Bonilla and Buchanan. *U.S. Geol. survey.* Open-File report, 77-614. 8pp.

McCalpin, J.P. 1996: *Paleoseismology*. International Geophysics series No. 62, San Diego, Academic Press.

McKay, A. 1902: *Report on the Recent Seismic Disturbances within Cheviot County in Northern Canterbury and in the Amuri District of Nelson, New Zealand (November and December, 1901).* Government Printer, Wellington, New Zealand.

McNab, R. 1907: Murihiku and the southern islands. Invercargill, William Smith Printer.

McSaveney, M.J. 1992: A manual for weathering rind dating of grey sand-stones of the Torlesse Supergroup, New Zealand. *Institute of geological and nuclear science technical report* 92/4. 52 pp.

Mikumo, T.; Miyatake, T. 1978: Dynamical rupture process on a three-dimensional fault with non-uniform frictions and near-field seismic waves. *Geophysical journal of the Royal astronomical society* 54: 417-438.

Mora, S.; Mora, R. 1993: Landslides triggered by the Limon-Telire, Costa Rica Earthquake and comparison with other events in Costa Rica. *U.S. Geological Survey Professional Paper*, in press.

Munden, F. 1951: Notes of the Alpine Fault, Haupiri Valley, North Westland. *New Zealand Journal of science and technology* 33: 404 - 408.

Nishenko, S.P.; Buland, R. 1987: A generic recurrence interval distribution for earthquake forecasting. *Bulletin of the seismological society of America* 77: 1382-1399.

Norris, R.J.; Koons, P.O.; Cooper, A.F. 1990: The obliquely-convergent plate boundary in the South Island of New Zealand: implications for ancient collision zones. *Journal of Structural Geology 12*: 715-725.

Norris, R.J.; Cooper, A.F. 1995: Origin of small - scale segmentation and transpressional thrusting along the Alpine Fault, New Zealand. *Geological Society of America bulletin* 107: 231 - 240.

Norris, R.J ; Cooper, A.F. 1997: Erosional control on the structural evolution of range front faulting on the Alpine Fault. Geological Society of New Zealand miscellaneous publication 95A, p 136.

Norton, D.A. 1981: A dendroclimatic analysis of three indigenous tree species, South Island, New Zealand. Unpublished Ph.D. Thesis, lodged in the Library, University of Canterbury, Christchurch, New Zealand.

Norton, D.A. 1983a: Modern New Zealand tree ring chronologies I. Nothofagus solandri Tree-ring bulletin 43: 1-17

Norton, D.A. 1983b: Modern New Zealand tree ring chronologies II. Nothofagus menziesii Tree-ring bulletin 43: 39-49

Norton, D.A. 1986: Mauri Ora 13

Oelfke, J.G.; Butler, D.R. 1985: Lichenometric dating of calcareous landslide deposits, Glacier National Park, Montana. *Northwest Geology* 17: 7-10.

Officers of the Geological Survey, 1975: Earth deformation studies reconnaissance of the Alpine Fault. Unpublished report 30a & 30b of the earth deformation section of the former New Zealand Geological Survey, Institute of Geology and Nuclear Science, Gracefield, Lower Hutt.

Officers of the Geological Survey, 1985: Reconnaissance of the Alpine Fault and local geology of South Westland. Unpublished immediate report 85/4 of the earth deformation section of the former New Zealand Geological Survey, Institute of Geology and Nuclear Science, Gracefield, Lower Hutt.

Pain, C.F. 1972: Characteristics and geomorphic effects of earthquake-initiated landslides in the Adelbert Range, Papua New Guinea. *Engineering geology* 6: 261–274

Pain, C.F.; Bowler, J.M. 1973: Denudation following the November 1970 earthquake at Madang, Papua New Guinea. *Zeitschrift für geomorphologie N.F. supplement band* 18: 92–104

Pearce, A.J.; O'Loughlin, C.L. 1985: Landsliding during a M 7.7. earthquake: influence of geology and topography. *Geology* 13: 855–858

Pearce, A.J.; Watson, A.J. 1986: Effects of earthquake-induced landslides on sediment budget and transport over a 50-yr period. *Geology* 14: 52–55

Pearson, C.F.; Beavan, J; Darby, D.J.; Blick, G.H.; Walcott, R.I. (in prep.): Strain distribution across the Australian - Pacific Plate boundary in the central south island, New Zealand, from GPS and earlier terrestrial observations.

Perrin, N.D.; Hancox, G.T. 1992: Landslide-dammed lakes in New Zealand - preliminary studies on their distribution, causes and effects. In Bell, D.H. (Ed), Landslides: proceedings of the sixth international symposium, volume 2: 1457–1466

Potton, C. 1987: European settlement and discovery in South Westland. Franz Josef, Westland Publishing for Department of Conservation.

Reyners, M. 1987: Subcrustal earthquakes in the central South Island, New Zealand, and the root of the Southern Alps. *Geology* 15: 1168-1171.

Rikitake, T. 1976: Earthquake Prediction. Elsevier Scientific Publishing Company, Amsterdam. *Developments in Solid Earth Geophysics* 9: 357pp.

Robinson, R. 1979: Variation of energy release rate of occurrence and b-value of earthquakes in the main seismic region of New Zealand. *Physics of the earth and planetary interiors* 18: 209 - 220

Rydelek, P.A.; Sacks, I.S. 1996: Earthquake slip rise time and rupture propagation: Numerical results of the Quantum earthquake model. *Bulletin of the seismological society of America* 86: 567-574.

Savage, J.C. 1991: Criticism of some forecasts of the National Earthquake Prediction Evaluation Council. *Bulletin of the seismological society of America* 81: 862-881.

Savage, J.C. 1994: Empirical earthquake probabilities from observed recurrence intervals. *Bulletin of the seismological society of America* 84: 219-221.

Scholz, C.H. 1990: The mechanics of earthquakes and faulting. New York, Cambridge University Press.

Schuster, R.L.; Nieto, A.S.; O'Rourke, T.D.; Crespo, E.; Plaza-Nieto, G. 1996: Mass wasting triggered by the 5 March 1987 Ecuador earthquakes. *Engineering geology* 42: 1–23

Segall, P.; Du, Y. 1993: How similar were the 1934 and 1966 Parkfield earthquakes? *Journal of geophysical research* 98: 4527-4537.

Sheppard, P.R.; Jacoby, G.C. 1989: Application of tree-ring analysis to paleoseismology: two case studies. *Geology* 17: 226 -

Sheppard, P.R.; White, L.O. 1995: Tree ring response to the 1978 earthquake at Stephens Pass, northeastern California. *Geology* 23:109 - 112

Sibson, R.H.; White, S.H.; Atkinson, B.K. 1979: Fault rock distribution and structure within the Alpine fault zone: a preliminary account. In: *The Origin of the Southern Alps* (edited by Walcott, R.I.; Cresswell, M.M.). *Bulletin of the Royal Society of New Zealand* 18: 55-65.

Sieh, K.E. 1978: Prehistoric large earthquakes produced by slip on the San Andreas fault at Pallet Creek, California. *Journal of geophysical research* 83: 3907–3939

Sieh, K. 1984: Lateral offsets and revised dates of large prehistoric earthquakes at Pallett Creek, southern California. *Journal of geophysical research* 89: 7641-70.

Sieh, K. 1986: Slip rate across the San Andreas fault and prehistoric earthquakes at Indio, California. *ESO 67*: 1200.

Sieh, K.E.; Stuiver,M.; Brillinger, D. 1989: A more precise chronology of earthquakes produced by the San Andreas fault in southern California. *Journal of geophysical research* 94: 603 - 623

Simpson, G.D.H., Cooper, A.F. and Norris, R.J., 1994: Late Quaternary evolution of the Alpine fault zone at Paringa, South Westland, New Zealand . *New Zealand journal of geology and geophysics* 37: 49 - 58.

Sims, J.D.; Hamilton, J.C.; Arrowsmith, J.R. 1993: Geomorphic study of earthquake offsets and subsequent landform response along the San Andreas Fault, Carrizo Plain, California, (supplement). *ESO 74*: no. 43, 612.

Slemmons, D.B. 1982: Determination of design earthquake magnitude for microzonation. Proceedings of 3rd World Microzonation Conference, Seattle USA. pp. 213-221.

Smith, W.D. 1978: Spatial Distribution of Felt Intensities for New Zealand Earthquakes. *New Zealand journal of geology and geophysics* 21: 293-311.

Smith, W.D. 1995a: A development in the modelling of far-field intensities for New Zealand earthquakes. *Bulletin of the New Zealand national society of earthquake engineering* 28: 196-217.

Smith, W.D. 1995b: A Procedure for Modelling Near-Field Earthquake Intensities. *Bulletin of the New Zealand national society of earthquake engineering* 28: 218-223.

Smith, W.D.; Berryman, K. 1983: Revised estimates of earthquake hazard in New Zealand. *Bulletin of the New Zealand national society of earthquake engineering* 16: 259 - 272

Smith, W.D.; Berryman, K.R. 1986: Earthquake Hazard in New Zealand: Inferences from Seismology and Geology. *Royal Society of New Zealand bulletin* 24: 223-243.

Stern, T.; Melhuish, A; Harrison, T; Scherwath, M.; Kleffman, S. 1997: Crustal structure along the Mt.Cook profile of the South Island geophysical transect: - Onshore - offshore multichannel and refraction shooting. New Zealand geophysical society conference, Aug 1997. Abtract only.

Study Group of the New Zealand Society for Earthquake Engineering. 1992: A revision of the Modified Mercalli seismic intensity scales. *Bulletin of the New Zealand national society for earthquake engineering 25*: 345-356.

Stuiver, M.; Becker, B. 1993: High precision decadal calibration of the radiocarbon time scale, AD 1950–6000 BC. *Radiocarbon* 35: 35–65

Stuiver, M.; Reimer, P.J. 1993: Extended ^{14}C data base and revised CALIB 3.0 ^{14}C age calibration programme. *Radiocarbon* 35: 215–230

Suggate, R. P. 1968: The Paringa Formation, Westland, New Zealand. *New Zealand journal of geology and geophysics* 11: 345 - 355.

Suggate, R.P. 1963: The Alpine Fault. *Transactions of the Royal Society of New Zealand, geology, 2:* 105-129.

Sutherland, A.J. 1969: Some hydrological aspects of the Inangahua earthquake. *New Zealand journal of science 12*: 476-496.

Sutherland, R.; Norris, R.J. 1995: Late Quaternary displacement rate, paleoseismicity, and geomorphic evolution of the Alpine Fault: evidence from Hokuri Creek, South Westland, New Zealand. *New Zealand journal of geology and geophysics* 38: 419–430

Sykes, L.R.; Nishenko, S.P. 1984: Probabilities of occurrence of large plate rupturing earthquakes for the San Andreas, San Jacinto, and Imperial faults, California. *Journal of geophysical research* 89: 5905-27.

Thatcher, W.; Marshall, G.; Lisowski, M. 1997: Resolution of fault slip along the 470-km -long rupture of the great 1906 San Francisco earthquake and its implications. *Journal of geophysical research* 102: 5353-5367.

Tutton, M.A.; Browne, T.J. 1994: A review of damage caused by the Finisterre Range earthquakes, Papua New Guinea. *Proceedings of the 1994 Papua New Guinnea geology, exploration and mining conference*: 33–41

Van Dissen, R.J.; Yeats, R.S. 1991: Hope fault, Jordan thrust, and uplift of the Seaward Kaikoura Range, New Zealand. *Geology* 19: 393-396.

Veblen, T.T.; Ashton, D.H. 1978: Catastrophic influences on the vegetation of the Valdivian Andes, Chile. *Vegetation* 36: 149–167

Veblen, T.T.; Kitzberger, T.; Lara, A. 1992: Disturbance and forest dynamics along a transect from Andean rain forest to Patagonian shrubland. *Journal of vegetation science* 3: 507–520

Vogel, J.C.; Fuls, A.; Visser, E.; Becker, B. 1993: Pretoria calibration curve for short lived samples, 1930 - 3350 BC. *In* Stuiver, M.; Long, A.; Kra, R.S.; eds., Calibration 1993. *Radiocarbon* 35 (1): 73 - 85

Voight, B.; Pariseau, W.G. 1978: Rock-slides and avalanches: An introduction. *In* Voight, B. (ed.) Rockslides and avalanches 1. Developments in geotechnical engineering 14A. Amsterdam, Elsevier. 1-67.

Wakamatsu, K. 1991: Maps for Historic Liquefaction Site in Japan. Tokai University Press, Japan. 341pp. (in Japanese with English abstract)

Wakamatsu, K. 1993: History of Soil Liquefaction in Japan and Assessment of Liquefaction Potential Based on Geomorphology. A thesis in the Department of Architecture presented in partial fulfilment of the requirements for the Degree of Doctor of Engineering, Waseda University, Tokyo, Japan. 245pp.

Walcott, R.I. 1979: Plate motions and shear strains in the vicinity of the Southern Alps. *Royal Society of New Zealand bulletin* 18: 5 - 12.

Walcott, R.I. 1984: The kinematics of the plate boundary zone through New Zealand: a comparison of short- and long-term deformations. *Geophysical journal of the Royal astronomical society* 79: 613-633.

Wald, D.J.; Heaton, T.H. 1994: Spatial and temporal distribution of slip for the 1992 Landers, California, earthquake. *Bulletin of the seismological society of America* 84: 668-691.

Wallace, R.C. 1976. Partial fusion along the Alpine Fault Zone, New Zealand. *Geological society of America bulletin* 87: 1225-1228.

Ward, G. K.; Wilson, S.R. 1978: Procedures for comparing and combining radiocarbon age determinations: a critique. *Archaeometry* 20 (1): 19 - 31

Ward, G. K.; Wilson, S.R. 1981: Evaluation and clustering of radiocarbon age determinations: procedures and paradigms. *Archaeometry* 23 (1): 19 - 39

Warren, G. 1967: Sheet 17 Hokitika (1st Ed.) *Geological Map of New Zealand 1 : 250,000*. Department of Scientific and Industrial Research, Wellington, New Zealand.

Wellman, H.W. 1952: The Alpine Fault in Detail: River Terrace Displacement Maruia River. *New Zealand journal of science and technology* B33: 409–414.

Wellman, H.W. 1955a: New Zealand Quaternary Tectonics. *Geol. Rundsch. 43*: 248-257.

Wellman, H.W. 1955b: The Geology between Bruce Bay and Haast River, South Westland. *New Zealand geological survey bulletin* n.s. 48: (2nd Ed.).

Wellman, H.W. 1979: An uplift map for the South Island of New Zealand, and a model for uplift of the Southern Alps. *Royal Society of New Zealand bulletin* 18: 13 - 20..

Wells, A.; Stewart, G.H.; Duncan, R.P. (in press): Evidence of widespread, synchronous, disturbance-initiated forest establishment in Westland, New Zealand. *Journal of the royal society of New Zealand*

Wells, A; Yetton, M.D.; Stewart, G.H.; Duncan, R.P.(in prep.): Prehistoric dates of the most recent Alpine Fault earthquakes, New Zealand.

Wells, D.L.; Coppersmith, K.J. 1994: New empirical relationships among magnitude, rupture length, rupture width, rupture area, and surface displacement. *Bulletin of the seismological society of America* 84: 974 - 1002.

Wesnousky, S.G. 1989: Seismicity and the structural evolution of strike slip faults. In United States Geological Survey open file report 89 - 315: 409 - 431.

Wesnousky, S.G. 1990: Seismicity as a function of cumulative geologic offset: some observations from southern California. *Bulletin of the seismological society of America* 80: 1374-1381.

Whitehouse, I.E. 1983: Distribution of large rock avalanche deposits in the central Southern Alps, New Zealand. *New Zealand journal of geology and geophysics* 26: 271-279.

Whitehouse, I.E.; Griffiths, G.A 1983: Frequency and hazard of large rock avalanches in the central Southern Alps. *Geology* 11: 331–334

Wilson, D.; Eberhart-Phillips D. 1997: Estimating crustal thickness in the central South Island. Geological Society of New Zealand miscellaneous publication 95A. Abtract only. P 168.

Wilson, R.C.; Keefer, D.K. 1985: Predicting areal limits of earthquake-induced landsliding. *United States geological survey professional paper* 1360: 317–345

Wood, P.R.; Block, H.G. 1986: Some results of geodetic fault monitoring in South Island, New Zealand. *In* Recent Crustal Movements of the Pacific Region. Edited by: W.I. Reilley and B.E. Harford. *Royal Society of New Zealand Bulletin, 24*: 39-35.

Woodward, D.J. 1979: The crustal structure of the Southern Alps, New Zealand, as determined by gravity. In: *The Origin of the Southern Alps* (edited by Walcott, R.I.; Cresswell, M.M.). *Bulletin of the Royal Society of New Zealand* 18: 95-98.

Working Group on California Earthquake Probabilities. 1988: Probabilities of large earthquakes occurring in California on the San Andrea fault. *United States geological survey open file report* 88-398: 1-62.

Working Group on California Earthquake Probabilities. 1990: Probabilities of large earthquakes in the San Francisco Bay region, California. *United States geological survey circular* 1053: 1-51.

Working Group of California Earthquake Probabilities. 1995: Seismic hazards in southern California-Probable earthquakes, 1994-2024. *Bulletin of the seismological society of America. 85*: 379-525.

Wright, A.; Mella, A. 1963: Modifications to the soil pattern of south-central Chile resulting from seismic and associated phenomena during the period May to August 1960. *Bulletin of the seismological society of America* 53: 1367–1402

Wright, C.A. 1994: Alpine Fault and related geology of the Kokatahi Valley, Westland, New Zealand. Unpublished BSc(Hons) Thesis, lodged in the Library. University of Otago, Dunedin, New Zealand.

Wright, C.A. 1996: The long run-out Round Top debris avalanche, central Westland, New Zealand. Geological Society of New Zealand miscellaneous publication 91A Abstract only. P 179.

Wright, C.A. 1997: Paleoseismological potential of the Alpine Fault at Waitaha River, Westland. Geological Society of New Zealand miscellaneous publication 95A Abtract only. P 171.

Yang, J.S. 1992: Landslide mapping and major earthquakes on the Kakapo Fault, South Island, New Zealand. *Journal of the Royal society of New Zealand* 22: 205–212

Yasuda, S.; Sugitani, T. 1988: Case histories of slop failure during past earthquakes in Japan. *Proceedings of the 23rd conference of the Japanese society for soil mechanics and foundation engineering* 891-892. (in Japanese)

Yetton, M. D.; Nobes, D.C. (in prep.): Vertical offset and near surface structure of the Alpine Fault at the Toaroha River from ground penetrating radar profiling. Submitted to *New Zealand journal of geology and geophysics.*

Yetton, M.D. (in prep.): Progress in understanding the paleoseismicity of the central and northern Alpine Fault, Westland, New Zealand. Submitted to *New Zealand journal of geology and geophysics.*

Yetton, M.D.; Wells, A. (in prep.): Evidence of past Alpine Fault earthquakes from the terrace sequence and forest age in the Karangarua Valley, South Westland, New Zealand.

Appendix One

Calendric conversion of Radiocarbon dates.

As noted in the footnote on page 20 the relationship between radiocarbon "years" and calendric years is not linear and only roughly approximates to a 1:1 relationship. Radiocarbon dates (or conventional dates are they often referred to) are in radiocarbon years before 1950 when the testing of nuclear bombs first influenced the global levels of ^{14}C around the world. Figure A1 shows the calibration curve for the last 600 years from Stuiver & Becker (1993), which is the period of most interest in this project.

Note the "wiggles" in the curve in the last 450 years. It is these which result in separate possible date ranges for some of the samples plotted on page 53. Note also the wide fluctuations in the curve since around 1700 AD, which leads dating laboratories to simply quote "modern" in this time period

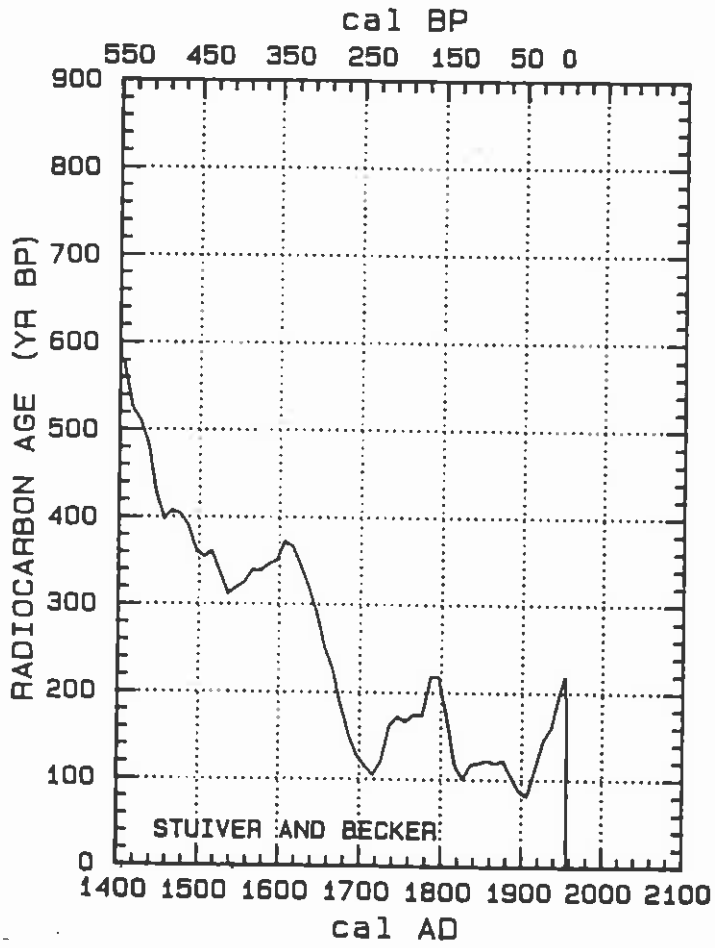

Figure A1- The decadal calibration curve of Stuiver and Becker (1993) for period since 1400 AD.

Southern Hemisphere offset

In addition the southern hemisphere calibration curve appears to be offset back in time from the curves derived in the northern hemisphere. Vogel *et al*, 1993 estimate this offset is 40 years and is constant through out the time range. It appears more likely that the offset is somewhat less than this and varies through time. Until the results of work by the University of Waikato radiocarbon dating laboratory, in conjunction with various northern hemisphere institutions, which is currently being undertaken is published we have adopted the Vogel *et al* offset. It makes little general difference to the calendric date ranges for the Toaroha River and Crane Creek events quoted here but any reduction from 40 years has the effect of moving both forward slightly while keeping approximately the same interval between them. Because the best earthquake date estimates have come from the forest age and tree rings any change in the southern hemisphere offset does not change our estimates of event timing.

Appendix Two

Probability assessment based on the method of Nishenko & Buland (1987)

Nishenko & Buland (1987) present a method for fitting a lognormal distribution to a consolidated set of data for earthquake recurrence periods gathered from rupture segments around the world.

The lognormal distribution is a function of an independant variable and two other parameters μ and σ which are the mean and standard deviation of the distribution and control it's shape. In their use of the lognormal distribution Nishenko & Buland set the independant variable to be (T/T_k), T being the data point return period and T_k being derived from $\ln(T_k)$ = average [ln(T)] for each earthquake segment K.

Into the distribution are also worked the errors associated with the derivation of the return periods, and also the natural variability of the recurrence periods. For each segment K, T_k is initially derived as described above. For events derived from carbon dating and similar methods with dating errors, errors are estimated and assigned as σ_{ik} (i denoting the individual data point within fault segment K).

An initial estimate of the natural overall variability of the return periods is also made, being σ_D, where $\sigma_D^2 = \text{var}[\ln T_{ik}]$. These two sources of error variability are then combined for each data point to give σ_{ik}^2 (for more details of this derivation readers are referred to Nishenko & Buland (1987) equations 10 and 11).

At this point in the analysis a least squares fitting method is used. For each data point a parameter τ is calculated ($\tau_j = T_{ik}/T_k$ - ie the return period normalised on the rupture segment T); all τ_j are collated in ascending order from j = 1 to N, and each event is assigned a probability level $F_{j,N} = (j - 1/2)/N$. The inverse lognormal function of each $F_{j,N}$ is then calculated, using initial estimates of μ_D and σ_D. The logarithm of the result is then subtracted from $\ln(\tau_j)$ and this is divided by a parameter σ_j^2 (this parameter is in turn derived from T_{ik}, T_k, σ_{ik}, and σ_d as described in Nishenko & Buland (1987) equations 10 and 11). The results of these calculations are summed for all the data points and then this sum is minimised by varying σ_d and μ_d.

Once the new values for μ_d and σ_d have been thus determined they are used to recalculate values for T_k (using Nishenko & Buland, 1987, equation 9), σ_k (using their equation 10) and σ_{ik} (their equation 12).

This leads into recalculation of the τ_j and consequent manipulations as described above, resulting in further iteration of the minimisation process to yield improved

estimates for σ_d and μ_d. This whole cycle is repeated until stable values of σ_d and μ_d. are arrived at, which also allows the calculation of final values for T_k.

These parameters (T_k, μ_d and σ_d) can be then be used to calculate expected recurrence intervals (Nishenko & Buland, 1987, equation 14) and conditional probabilities of events within given time periods (their equation 15).